

Chaos and time-reversal symmetry. Order and chaos in reversible dynamical systems

J.A.G. Roberts^{a,*} and G.R.W. Quispel^b

^a*Instituut voor Theoretische Fysica, Universiteit van Amsterdam, Valckenierstraat 65, 1018 XE Amsterdam, The Netherlands*

^b*Department of Mathematics, La Trobe University, Bundoora, Melbourne 3083, Australia*

Received August 1991; editor: E.G.D. Cohen

Contents:

1. Introduction and overview	66	4.1. Theory	112
1.1. Time-reversal symmetry and physics	66	4.2. Four classes of non measure-preserving reversible mappings	116
1.2. Time-reversal symmetry and chaos	66	4.3. Examples	122
1.3. Time-reversal symmetry and ordinary differential equations	67	5. Conservative behaviour in reversible mappings	126
1.4. Applications	70	5.1. KAM circles and their destruction	127
1.5. Time-reversal symmetry and mappings	73	5.2. Period doubling of symmetric fixed points	137
1.6. Outline of this report	77	6. Dissipative behaviour in reversible mappings	143
2. Review of some properties of mappings of the plane	79	6.1. Period doubling of asymmetric fixed points	145
2.1. Definitions and properties	80	6.2. Strange attractors	152
2.2. Measure preservation	86	7. Interplay of conservative and dissipative features of reversible mappings; a symmetry-breaking bifurcation	159
3. Reversibility and mappings of the plane	88	8. Concluding remarks and future directions	163
3.1. Some properties of reversible mappings	89	Appendix A. Integrable reversible mappings	166
3.2. Generating reversible mappings and involutions from symmetric second order difference equations	95	Appendix B. Nonlinear stability analysis for elliptic fixed points	169
3.3. Testing for reversibility and local reversibility	100	References	171
3.4. Area-preserving mappings that are not reversible	107		
4. Non measure-preserving reversible mappings with asymmetric fixed points	111		

Abstract:

Dynamical systems with independent (continuous or discrete) time variable t and phase space variable x are called reversible if they are invariant under the combination $\{t \rightarrow -t, x \rightarrow Gx\}$ where G is some transformation of phase space which is an involution ($G \circ G = \text{Identity}$). Reversible systems generalise classical mechanical systems possessing time-reversal symmetry and are found in ordinary differential equations, partial differential equations and diffeomorphisms (mappings) modelling many physical problems. This report is an introduction to some of the properties of reversible systems, with particular emphasis on reversible mappings of the plane which illustrate many of their basic features. Reversible dynamical systems are shown to be similar to Hamiltonian systems because they can possess KAM tori, yet they are different because they can also have attractors and repellers. We create and study examples of these hybrid dynamical systems and discuss the question of how to recognise whether a given dynamical system is reversible.

* Address from July 1992: Department of Mathematics, University of Melbourne, Parkville, Victoria 3052, Australia.

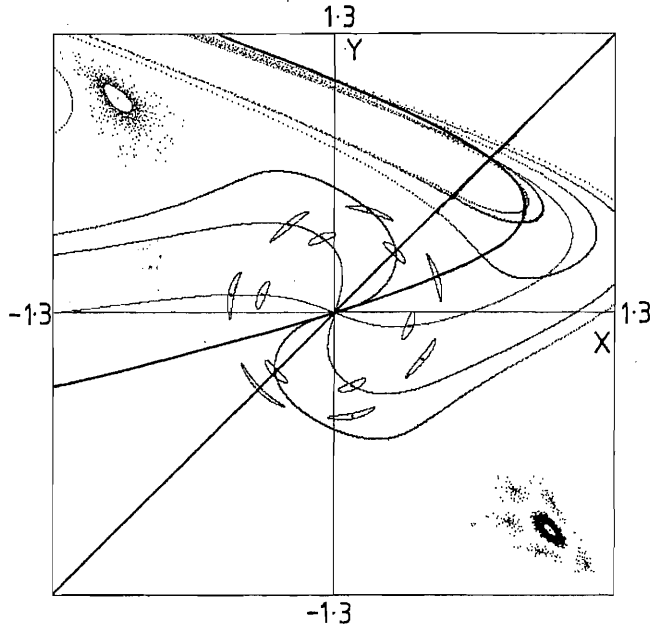


Fig. 3.1. Fig. 1.3 with many of the trajectories removed. The symmetry line $y = x$ of G is drawn in black together with the curved symmetry line of $H = L \circ G$. In colour are shown the first three iterates of the symmetry line of G under L , which are the symmetry lines of $L^2 \circ G$, $L^4 \circ G$ and $L^6 \circ G$ (cf. 3.14a). These are coloured green, red and blue, respectively. All symmetry lines pass through the symmetric fixed point at the origin and the other symmetric fixed point at the other intersection of the lines of G and H . The intersection of the symmetry lines of $L^6 \circ G$ and G accounts for the existence of the symmetric six-cycle. This cycle has two points on each of the symmetry lines of G and its iterates. The seven-cycle, being odd, has a point on the symmetry line of G and of H .

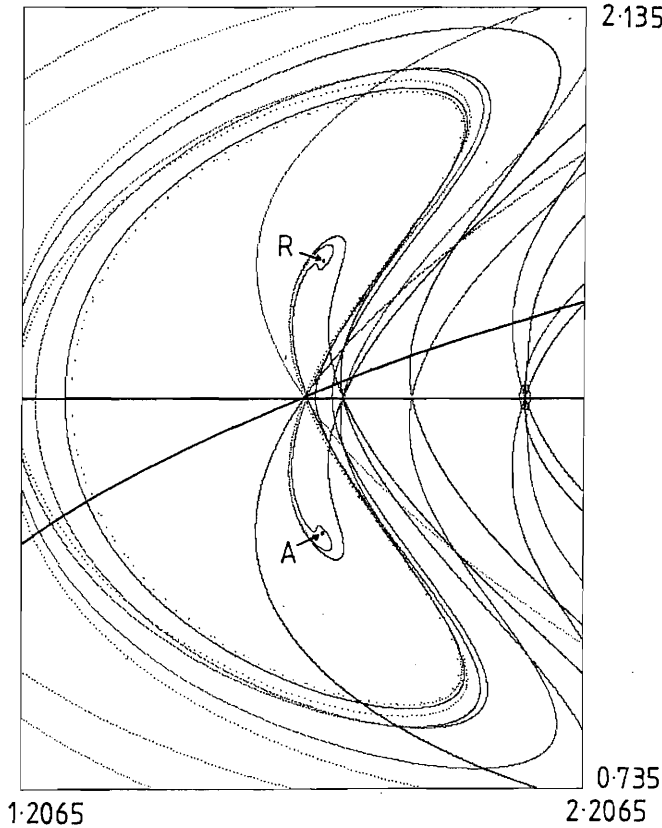


Fig. 6.2. Illustration of the behaviour of symmetry lines in the vicinity of attractors and repellers in reversible mappings. This picture is fig. 4.1b, a phase portrait of example 1 when $C = 2.87$, with the removal of some of the orbits shown there and the addition of some symmetry lines. The two innermost apparently closed curves from fig. 4.1b are reproduced here together with one of the small islands surrounding the symmetric eight-cycle (right-hand side). The symmetric fixed point at the centre of the picture is at the intersection of the (horizontal) symmetry line of G and the symmetry line of H , both of which are drawn in black. Two arrows mark the attracting asymmetric fixed point (A) in the bottom half of the picture and the repelling asymmetric fixed point (R) in the top half. The coloured lines are symmetry lines created by iterating the symmetry line of G . The colours dark blue, red and green correspond to two, eight and sixteen iterations of this line under the mapping example 1. The colours light blue, brown and purple correspond to 2, 8 and 16 iterations of the line under the inverse of example 1.

1. Introduction and overview

This report is a review of some of the properties of dynamical systems possessing time-reversal symmetry. In this report a system that is invariant under time reversal will be called *reversible*^{*}. The classical concept of time-reversal symmetry refers to the invariance of equations under the transformation $t \rightarrow -t$ (this definition will be generalised below). In this introductory chapter, we briefly discuss the place that time-reversal symmetry occupies in physics and look at the consequences that the possession of time-reversal symmetry has for nonlinear classical dynamical systems (cf. also Quispel [1992a]). We then describe reversible mappings, which have time-reversal symmetry where time is discrete. Our review will focus on such mappings.

1.1. Time-reversal symmetry and physics

Time-reversal symmetry has played, and still plays, an important role in physics (cf. Davies [1974], Sachs [1987], Thom [1980, 1990], Zocher and Török [1953]). Many of the differential equations of physics are time-reversible. This was first noticed by Loschmidt [1877] for particles moving in a velocity-independent force field. Boltzmann soon realized the importance of time-reversal symmetry and later showed that Maxwell's equations are reversible (if one also reverses the field $B \rightarrow -B$) [Boltzmann 1897 a, b, 1898]. Painlevé [1904] presented an early use of the time-reversal invariance of Newton's equations of motion for a free-falling body (cf. also Sachs [1987, chapter 2]). The Einstein equations of classical general relativity are reversible [Penrose 1979, 1989], as are the equations of, e.g., the famous three-body problem (cf. Marchal [1990]). Finally, Wigner has shown the importance of time-reversal symmetry in quantum mechanics [Wigner 1959; Doncel 1987].

In spite of the fact that physical laws may be invariant under time reversal, physical phenomena in general are not. This long-recognised (Loschmidt's) paradox is discussed in Penrose [1979]: "The local physical laws we know and understand are all symmetrical in time. Yet on a macroscopic level, time asymmetry is manifest. In fact, a number of apparently different such macroscopic arrows of time may be perceived." Penrose goes on to list seven apparently independent arrows of time as defined by the decay of the K^0 -meson, quantum mechanical observations, entropy increase, retardation of radiation, psychological time, expansion of the universe, and black holes versus white holes (cf. also Davies [1974], Hawking [1987, 1988], Coveney and Highfield [1990], Page [1992]). To these one might perhaps add the arrow defined by biological evolution. The usual explanation of the above-mentioned paradox is that although the laws of physics are invariant under time reversal, the initial conditions are such that the time evolution is not [Sachs 1987; Penrose 1989].

1.2. Time-reversal symmetry and chaos

In recent years "chaos" or, more properly, nonlinear dynamics has become an important area of research activity. A traditional division of classical nonlinear dynamical systems is into the class of

^{*} Note that dynamic reversibility, as defined here, is not necessarily equivalent to invertibility or to thermodynamic reversibility.

conservative systems and the class of dissipative systems. By “conservative” systems we mean Hamiltonian ordinary differential equations and symplectic mappings. Dissipative systems, on the other hand, are characterised by collapse of their motion after some transient time onto an attractor (for more details about conservative systems and dissipative systems, see for example MacKay and Meiss [1987], and Cvitanovic [1989], respectively).

In comparison, reversible dynamical systems have received far less attention and the treatment that they have received has tended to be less systematic. This has led to the situation where the literature on the subject is quite scattered, with some authors not being aware of the generality of the mathematical theory underlying their results. One of our motivations for writing this report is to try and remedy this situation. For the same reason we provide an extensive list of references on (nonconservative) reversible systems, both on their theory, and on their applications in such diverse fields as condensed matter physics, fluid dynamics, laser physics, molecular dynamics, quasicrystals, chemistry, biology etc. (for more references on reversible differential equations, see Sevryuk [1991b]).

Although this report concerns classical dynamical systems, we mention that reversibility plays an important role in “quantum chaology”, i.e., the study of semiclassical, but nonclassical, behaviour of systems whose classical motion exhibits chaos [Berry 1987]. In such quantum systems, reversibility manifests itself in the statistics of the spacing of energy levels (cf. Berry [1987], Ozorio de Almeida [1988], Keating [1990]). These statistics fall into universality classes. If the underlying classical system is integrable, the statistics of level spacings is that of a set of random numbers (i.e., Poissonian). If the classical system is chaotic and reversible, the level spacings obey the eigenvalue statistics of infinite random real symmetric matrices. If the classical system is chaotic and *not* reversible, the spacings have the same statistics as the spectra of random complex hermitian matrices. Thus time-reversal symmetry breaking induces a spectral phase transition (cf. Lenz and Haake [1990]).

1.3. Time-reversal symmetry and ordinary differential equations

Let us now be mathematically a bit more precise as regards a definition of reversibility. Traditionally, what springs to mind when one thinks of time-reversal symmetry is a system described by an equation of the form

$$\ddot{x} = F(x), \quad F: \mathbb{R} \rightarrow \mathbb{R} \quad (1.1)$$

(here the dot denotes d/dt). This equation describes, for example, the motion of a particle with unit mass moving along a line under the influence of a conservative force $F = F(x)$. This equation is reversible because it is invariant under time reversal: $t \rightarrow -t$ (and hence $d/dt \rightarrow -d/dt$). An immediate consequence of the reversibility of (1.1) is that if $x = \gamma(t)$ is a solution of the equation, then so is the time-reversed motion $\gamma(-t)$. The latter solution is what would be seen if a movie was made of $\gamma(t)$ and then played backwards.

It is easy to see that the following equations are also invariant under $t \rightarrow -t$,

$$\ddot{x} = F(x, \dot{x}^2), \quad F: \mathbb{R}^2 \rightarrow \mathbb{R}; \quad (1.2a)$$

$$\ddot{x} = F(x), \quad F: \mathbb{R}^m \rightarrow \mathbb{R}^m, \quad (1.2b)$$

for arbitrary (analytic) functions F . There is, however, one big difference between equation (1.1) on the

one hand and (1.2a, b) on the other. Equation (1.1) is conservative – it is derivable from the Hamiltonian

$$H(x, p) = \frac{1}{2} p^2 + V(x), \quad (1.3)$$

with $p = \dot{x}$ (recall mass = 1) and $F(x) = -dV/dx$, and the energy $E = H$ is conserved. Equations (1.2a, b) are in general not conservative.

This leads us to the main theme of this report: the similarities and differences between reversible and conservative systems. From the above examples, it is clear that there exist systems that are both reversible *and* conservative, and others that are reversible but *not* conservative. The actual situation is indicated in fig. 1.1. Region II represents systems that are both conservative *and* reversible. These systems are those where historically reversibility was first noticed and region II is the most studied region in the figure. It includes systems of the form (1.1), or equivalently (1.3), and more generally includes any system described by a Hamiltonian which is even in the momenta, i.e.,

$$H(x, p) = H(x, -p), \quad x, p \in \mathbb{R}^n. \quad (1.4)$$

Studies of Hamiltonian systems like these in which the time-reversal symmetry has been specifically studied or utilised in the analysis include investigations by de Vogelaere [1958], Meyer [1981], van der Schaft [1983], de Aguiar et al. [1987], de Aguiar and Malta [1988], Ozorio de Almeida and de Aguiar [1990], and Montaldi et al. [1990a, b]. Region I of fig. 1.1 represents systems that are reversible but *not* conservative. This includes systems of the form (1.2a, b). Finally, region III comprising systems that are conservative but *not* reversible is not empty, although examples are not as easy to find. An example given by Sevryuk [1992] is the system with Hamiltonian

$$H(x, p) = \prod_{i=1}^6 (a_i x + b_i p). \quad (1.5)$$

For general parameters a_i and b_i , the flow generated by this Hamiltonian is *not* reversible.

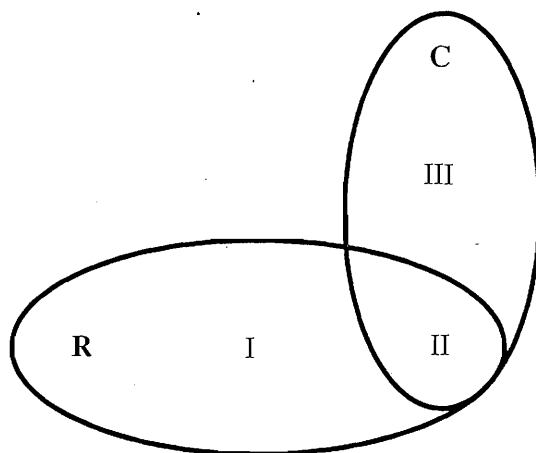


Fig. 1.1. Venn diagram showing the relation between reversible dynamical systems (set R) and conservative dynamical systems (set C).

The invariance under time reversal: $t \rightarrow -t$ of (1.1) shows up as invariance under $t \rightarrow -t$, $x \rightarrow x$, $p \rightarrow -p$ of the equivalent two first-order equations derivable from the Hamiltonian (1.3). Similarly, the equations of motion obtained from Hamiltonians with the property (1.4) are invariant under $t \rightarrow -t$, $x \rightarrow x$, $p \rightarrow -p$. Although not generally Hamiltonian, eq. (1.2a) can of course also be rewritten equivalently as a system of coupled first-order equations,

$$\dot{x} = y, \quad \dot{y} = F(x, y^2), \quad (1.6)$$

and the time-reversal invariance in this description manifests itself in a similar way to the Hamiltonian case. That is, eqs. (1.6) are invariant under $t \rightarrow -t$, $x \rightarrow x$, $y \rightarrow -y$; now in the two-dimensional phase space, if $(x(t), y(t))$ is a solution of the dynamics, then so is $(x(-t), -y(-t))$. The latter corresponds to flipping the trajectory $(x(t), y(t))$ via the transformation of phase space that leaves the coordinate unchanged and changes the sign of the velocity, and following the resulting trajectory in the opposite time sense. The drawback with this way of *defining* reversibility in phase space as invariance under $t \rightarrow -t$ accompanied by reversal of velocity $y \rightarrow -y$ (or momentum $p \rightarrow -p$) is that this definition is not coordinate-invariant. It is also too restrictive. The following definition remedies these defects [Devaney 1976]:

A dynamical system (not necessarily conservative) is reversible if there is an involution in phase space which reverses the direction of time.

This definition applies both to ordinary differential equations and also to mappings (see section 1.5). An ‘‘involution’’, which we will often denote by G , is a transformation that composed with itself yields the identity ($G \circ G = \text{Id}$).

Thus, a general system of first-order coupled ordinary differential equations,

$$dx/dt = F(x), \quad x \in \mathbb{R}^n, \quad (1.7)$$

is reversible if there is an involution G which reverses the direction of time, i.e.,

$$d(Gx)/dt = -F(Gx), \quad (1.8)$$

and hence

$$dG \cdot F = -F \circ G. \quad (1.9)$$

Here F and G are functions from \mathbb{R}^n to itself. The above definition means that under the transformation of the n -dimensional phase space by G , the system (1.7) transforms to that obtained by just putting $t \rightarrow -t$, so that under the combined action of the involution and time reversal the equations are invariant. An involution that achieves this is often called a (reversing) symmetry of the system. Trajectories that are left invariant by G are called *symmetric*; otherwise they are *asymmetric*. In the above examples (1.4) and (1.6) the involutions are $G: x \rightarrow x, p \rightarrow -p$ and $G: x \rightarrow x, y \rightarrow -y$, respectively. Note that this generalised definition of reversibility is no longer restricted to even-dimensional systems. Moreover in even $2m$ -dimensional systems, the set of fixed points of the involution G , which plays an important role in the dynamics, need not have dimension m .

Although at first sight it may not seem clear, this new definition of reversibility encapsulates exactly what one intuitively thinks of as time-reversal invariance – a consequence of it is that if $x(t)$ is a solution of (1.7) then so is $Gx(-t)$, which corresponds to a reflection of the trajectory $x(t)$ in the n -dimensional phase space followed in the opposite sense. Note that when the involution G is linear, the condition for the system (1.7) to be reversible [Moser 1973] is that G changes the sign of the vector field F , i.e.,

$$GF(x) = -F(Gx). \quad (1.10)$$

Reversible differential equations in which G is linear, feature prominently in physically relevant examples in the literature (see section 1.4 and references therein). The reason we allow in the general theory for an arbitrary (nonlinear) involution G is that, although simple linear involutions such as $G: x \rightarrow x, y \rightarrow -y$ can become very complicated under a coordinate transformation, they remain involutions. Being an involution is a coordinate-independent property.

Apart from generalising the definition, Devaney [1976] went on to show that there are very close similarities between the symmetric periodic orbits of a (generalised) reversible flow and the periodic orbits of a Hamiltonian flow (in particular symmetric periodic orbits in a large class of reversible flows come in one-parameter families, just as periodic orbits in Hamiltonian flows), cf. also Devaney [1977]. Earlier, Moser [1967, 1973] had shown that families of quasiperiodic motions or Kolmogorov–Arnol’d–Moser (KAM) tori, previously associated with Hamiltonian systems (cf. Arnol’d [1961], Moser [1968], Siegel and Moser [1971, section 36]), exist also in reversible systems, cf. also Bibikov [1979], Scheurle [1987], Iooss and Los [1990] and references therein. In particular, such KAM tori are found in the vicinity of linearly stable symmetric equilibrium points or symmetric periodic orbits. More recently, these similarities have been further emphasised by Arnol’d [1984], Arnol’d and Sevryuk [1986], and Sevryuk [1986, 1987, 1990, 1991a], who have extended some of the KAM results for general reversible differential equations. Further contributions towards establishing parallels between reversible systems and Hamiltonian systems include those by Vanderbauwhede [1986, 1990, 1992], Palmer [1977] and others (see the comprehensive bibliographies in Sevryuk [1991a, b]).

This is not to say that reversible systems have to be Hamiltonian. The above (generalised) definition of reversible systems explicitly includes systems that are not Hamiltonian (region I of fig. 1.1). Reversible systems in this region *can* have asymmetric periodic orbits that are attractors. Because of the time-reversal symmetry, the presence of an attractor A implies the presence of a repeller $R = GA$ given by the reflection of the attractor by the symmetry. This is illustrated by the so-called logistic differential equation $\dot{x} = x(1 - x)$. This equation is invariant under $t \rightarrow -t$, combined with the (one-dimensional) phase space involution $x \rightarrow 1 - x$. It is easy to verify that the fixed point $x(t) \equiv 1$ is attracting, and that its reflection $x(t) \equiv 0$ is repelling.

More generally, nonconservative reversible differential equations can display Hamiltonian-like behaviour near their symmetric cycles as well as behaviour typical of dissipative and expansive systems near their asymmetric cycles. This hybrid nature makes them interesting models in which to study within a single system the differences and crossover between conservative and dissipative behaviour.

1.4. Applications

To illustrate the range of problems that can be described by reversible systems that are not Hamiltonian, in this section we give some physically motivated examples of reversible differential equations belonging to region I of fig. 1.1.

(i) An externally injected class B laser (cf. *Arecchi [1987]*) can be described by three coupled nonlinear ordinary differential equations. When the damping rate associated with the field is much greater than that of the population, as in CO_2 lasers, *Politi et al. [1985, 1986a, b]* have shown that this system of equations is

$$\dot{x} = zx + y + C_1, \quad \dot{y} = zy - x, \quad \dot{z} = C_2 - x^2 - y^2. \quad (1.11)$$

Here C_1 and C_2 are parameters. The system (1.11) is reversible with respect to $G: (x, y, z) \rightarrow (-x, y, -z)$. However, the divergence of the vector field on the right is $2z$, illustrating that phase-space volume is not conserved. For realistic values of the physical parameters these equations were studied by *Politi et al.* They observed the coexistence of “dissipative-like structures”, i.e., periodic attractors and repellers, as well as KAM tori. Moreover the attractors and repellers arose from a symmetric periodic orbit via a symmetry-breaking bifurcation.

(ii) In nonequilibrium molecular dynamics simulations of a fluid or solid, Newton’s equations of motion are integrated numerically and thermodynamic quantities are related to long-time dynamical averages. Often the equations of motion are augmented by adding additional variables so as to achieve the constancy of some thermodynamic quantities like temperature or pressure throughout the dynamics, as can be realized experimentally. The resulting “extended” system of equations is often not derivable from a Hamiltonian, although still time-reversible [*Evans 1986*]. An example is provided by Nosé–Hoover dynamics [*Nosé 1984, 1986; Hoover 1985, 1986, 1988*] in which the additional variables are time-dependent “thermodynamic friction coefficients” which act so as to keep the average kinetic energy (temperature) constant whilst yielding the canonical ensemble in the “unextended” space of physical variables (cf. also *Jellinek [1988], Jellinek and Berry [1988, 1989], Hoover [1989], and Bulgac and Kusnezov [1990]*). A simple illustration of this Nosé–Hoover dynamics is provided by a particle with unit mass moving along a line under the influence of a periodic potential $\varepsilon(1 - \cos x)$ and fixed external force F [*Hoover et al. 1987*]. The particle has coordinate x and momentum y and its time-averaged kinetic energy is kept constant via a feedback mechanism involving a friction coefficient z . The equations of motion are

$$\dot{x} = y, \quad \dot{y} = F - \varepsilon \sin x - zy, \quad \dot{z} = \alpha(y^2 - 1), \quad (1.12)$$

where the parameter $\alpha > 0$ is called the thermostat strength. The friction coefficient z works so as to reduce the magnitude of the momentum y if the kinetic energy $y^2/2$ exceeds the equilibrium value $1/2$. On the other hand, if the kinetic energy is less than $1/2$, z decreases so that z can become negative, leading to an increase in the magnitude of y . Equations (1.12) are reversible with symmetry $G: (x, y, z) \rightarrow (x, -y, -z)$. Numerical investigations of these equations have revealed the presence of attracting limit cycles and fractal chaotic attractors in the 3D phase space. Numerical simulations of analogous reversible equations of motion for systems with several coupled oscillators have also revealed characteristic dissipative behaviour in the form of the phase space volume shrinking down to a strange attractor associated with steady-state trajectories (cf. *Holian et al. [1987], Hoover [1988]* and references therein).

(iii) The sedimentation of small spheres in a fluid, in the limit of infinite viscosity, has been studied by *Hocking [1964], Caffisch et al. [1988]* and *Golubitsky et al. [1991]*. Approximating the spheres by point particles, the equations of motion for n particles moving in a polygonal configuration are

$$\dot{r}_i = \sum_{k=1}^{n-2} [U(r_{i+1} + \dots + r_{i+k}) - U(r_{i-1} + \dots + r_{i-k})], \quad i = 1, 2, \dots, n; \quad U(r) = \frac{e_z}{|r|} + \frac{(e_z \cdot r)r}{|r|^3}, \quad (1.13)$$

where the indices are taken mod n . Here $r_1, \dots, r_n \in \mathbb{R}^3$ denote the consecutive edges of an n -sided polygon in \mathbb{R}^3 , and e_z is a unit vector in the z direction (in which gravity is acting). Equation (1.13) is reversible with symmetry $G: (x_1, y_1, z_1, x_2, y_2, z_2, \dots, x_n, y_n, z_n) \rightarrow (-x_1, y_1, z_1, -x_2, y_2, z_2, \dots, -x_n, y_n, z_n)$; this reversibility can be used to prove the existence of periodic and quasiperiodic solutions for the motion. [Note that the divergence of the right hand side of (1.13) is zero, i.e., (1.13) is volume-preserving, and hence possesses no attractors.]

(iv) Recently, Tsang et al. [1991a, b] have studied the following system of N coupled ordinary differential equations modelling electrical circuits comprising series arrays of Josephson junctions in parallel with a single resistor,

$$\dot{\theta}_k = \Omega + a \cos \theta_k + \frac{1}{N} \sum_{i=1}^N \cos \theta_i. \quad (1.14)$$

Here $k = 1, 2, \dots, N$, θ_k are phase angles, defined modulo 2π , and Ω and a are parameters. Equations (1.14) are invariant under $\theta_k \rightarrow -\theta_k$ with $t \rightarrow -t$. For $N = 2$, numerical investigations have shown, as in (i) above, coexistence of Hamiltonian-like behaviour with dissipation and expansion via the presence of a sink (attractor) and source (repeller). In other recent papers, Gonchar et al. [1991] study the interaction in reversible hydrodynamic equations between a sink-source pair of point-like vortices and a potential wave, and Kent and Elgin [1991a, b] consider a reversible system of three coupled ordinary differential equations relevant to travelling wave solutions of the Kuramoto-Sivashinsky equation, explaining some observed bifurcation behaviour of the periodic orbits of this system in terms of the reversibility.

We should remark at this point that in many applications one encounters reversible systems where the independent variable is a spatial variable, rather than a temporal one (e.g. MacKay [1987], Baesens and MacKay [1991]). In terms of the physical, or chemical, or biological interpretation this may make a difference, but mathematically, of course, the two symmetries are completely equivalent. For the sake of convenience we will always use the language of time reversal. Examples frequently arise in partial differential equations, and in partial differential-difference equations, when the stationary solutions satisfy reversible ordinary differential equations (e.g. Turing [1952], Eckmann and Procaccia [1991a, b]).

(v) The evolution of a gas flame front in the presence of an external stabilizing factor is described by a partial differential equation belonging to the class of equations of the form

$$\xi_t + \xi_{xxxx} + 2\alpha\xi_{xx} + \xi + \beta\xi^3 + \gamma\xi^2 + \delta\xi_x^2 = 0,$$

where $\xi = \xi(x, t)$ is the displacement of a flame point from its unperturbed position, x is the spatial coordinate, t is time and α, β, γ , and δ are parameters [Malomed and Tribelsky 1984]. The stationary solutions of this equation $\xi = \xi(x)$ are given by

$$\xi_{xxxx} + 2\alpha\xi_{xx} + \xi + \beta\xi^3 + \gamma\xi^2 + \delta\xi_x^2 = 0, \quad (1.15)$$

which also describes the stationary solutions of nonsteady laser evaporation of condensed matter. In the four-dimensional phase space of variables $(\xi, \xi_x, \xi_{xx}, \xi_{xxx})$, eq. (1.15) can be rewritten as a first order system of four coupled ordinary differential equations (in the usual way) and is invariant under the combined application of the involution $G: (\xi, \xi_x, \xi_{xx}, \xi_{xxx}) \rightarrow (\xi, -\xi_x, \xi_{xx}, -\xi_{xxx})$ and $x \rightarrow -x$. Thus it is reversible with x playing the role of “time”. This reversibility accounts for the existence of a one-parameter family of periodic solutions of (1.15) and some related stability results of these solutions [Arnol’d 1984; Arnol’d and Sevryuk 1986; Sevryuk 1986; Sevryuk 1989].

(vi) Other reversible partial differential equations have been studied by Kirchgässner [1982, 1983], Renardy [1982], Field et al. [1991], and van Saarloos and Hohenberg [1991]. The equations studied by Kirchgässner include ones that model permanent waves in density-stratified channels and viscous fluid flow between concentric cylinders. The equations studied by Renardy have applications to reaction–diffusion equations, describing, e.g., the Belousov–Zhabotinskii reaction. Vanderbauwhede [1986, 1990, 1992] has proved theorems showing the prevalence of bifurcations of subharmonic solutions in reversible ordinary differential equations which include the Mathieu equation. Some of these results have recently been illustrated in a computational study of a system of ordinary differential equations describing steady-state solutions of a system of two reaction–diffusion equations [Kazarinoff and Yan 1991].

1.5. Time-reversal symmetry and mappings

We turn our attention now to mappings (diffeomorphisms), on which we will concentrate in this report. In this section we will introduce reversible mappings, i.e., reversible dynamical systems with discrete time. Recall the definition of reversibility given in section 1.3. *A dynamical system is reversible if there is an involution in phase space which reverses the direction of time.*

Consider a mapping L that associates pairs of points of some space (e.g., \mathbb{R}^n) via

$$\mathbf{x}_{i+1} = L\mathbf{x}_i, \quad i \in \mathbb{Z}. \quad (1.16)$$

The set of points $\{\mathbf{x}_1, \mathbf{x}_2, \mathbf{x}_3, \dots\}$ formed by repeated application of the mapping to the point \mathbf{x}_0 constitutes its orbit, a discrete analogue of the continuous time trajectory of an initial condition of a differential equation. The mapping L is reversible if there exists an involution G such that

$$L \circ G\mathbf{x}_{i+1} = G\mathbf{x}_i, \quad (1.17)$$

where \circ denotes the composition of two mappings. Whereas in eq. (1.16) we have that \mathbf{x}_{i+1} is the successor of \mathbf{x}_i under L , eq. (1.17) shows that, under the transformation of phase space by G , we find $\mathbf{y}_{i+1} = G\mathbf{x}_{i+1}$ is now the predecessor of $\mathbf{y}_i = G\mathbf{x}_i$. That is, time evolution is reversed. From (1.17) and (1.16),

$$L \circ G\mathbf{x}_{i+1} = L \circ G \circ L\mathbf{x}_i = G\mathbf{x}_i. \quad (1.18)$$

Since this equation holds for arbitrary \mathbf{x}_i , we get the defining property of a reversible mapping

$$L \circ G \circ L = G, \quad G \circ G = \text{Id}, \quad (1.19a, b)$$

where Id is the identity mapping. G is called a (reversing) symmetry of L .

A reversible mapping can be written as the product (i.e., composition) of two involutions

$$L = H \circ G, \quad G \circ G = H \circ H = \text{Id}. \quad (1.20a, b)$$

This follows from (1.19a, b) with $H := L \circ G$ since

$$L = (L \circ G) \circ G = H \circ G, \quad H \circ H = (L \circ G) \circ (L \circ G) = \text{Id}. \quad (1.21a, b)$$

Conversely, any mapping that decomposes as a product of two involutions U and R , i.e., $L = U \circ R$, is reversible with, e.g., $G = U$ or $G = R$, so that (1.20a, b) is an equivalent way of defining a reversible mapping. One application of a reversible mapping then amounts to applying two reflections, one after another.

An important feature to note is that the definition of reversibility for mappings (1.19a, b) or the alternative definition (1.20a, b) is completely algebraic and does not rely on any differentiability properties of the mapping. This is the reason one can, for example, speak of cellular automata with time-reversal symmetry [Vichniac 1984; Margolus 1984; Pomeau 1984; Takesue 1987, 1989, 1990a, b; Toffoli and Margolus 1990; Ablowitz et al. 1991] (and references therein).

The major classes into which dynamical systems with continuous time are divided, and their distinguishing features, have close analogues in mappings. Moreover, the study of mappings has numerical and some conceptual advantages over the study of differential equations. It is now well recognised that even a two-dimensional mapping, a mapping of the plane, contains a wealth of exotic dynamical behaviour (cf. Helleman [1980], Hénon [1983], Lichtenberg and Lieberman [1983]). Therefore consider now the Venn diagram of fig. 1.1 in the context of mappings.

Hamiltonian ordinary differential equations have as their mapping analogue *symplectic* mappings. Both of these types of systems are combined in fig. 1.1 under the heading “conservative” dynamical systems. In two dimensions the only requirement for a map to be symplectic is that it is volume-preserving, i.e., *area-preserving*. Area-preserving mappings are widely discussed in the literature (cf. MacKay [1982], Hénon [1983], MacKay and Meiss [1987]). They can be obtained from the “surface of section” of a four-dimensional Hamiltonian system with motion on a three-dimensional energy surface (cf. Poincaré [1912], Hénon [1983], Lichtenberg and Lieberman [1983]). The possible motions in area-preserving mappings include periodic orbits, orbits that escape to infinity and, significantly, orbits that fill continuous curves in the plane. There is a KAM theorem that holds for area-preserving mappings [Moser 1973]. Under certain conditions it guarantees the presence of infinitely many closed invariant curves in the plane on which the motion is quasiperiodic. Between these curves are thin bands of chaotic orbits. Note that in higher dimensions, $D > 2$, volume preservation is no longer sufficient to make a mapping symplectic so that symplectic mappings are a strict subset of volume-preserving mappings.

A *reversible* mapping is an analogue of a reversible differential equation. The defining properties (1.19a, b) or (1.20a, b) given above guarantee that the application of a (reversing) symmetry G to an orbit of the mapping gives another orbit of the mapping when followed in the opposite sense, the essence of (continuous) time reversal as discussed in section 1.3 (cf. fig. 1.2 for an illustration of this in two dimensions). The “surface of section” mapping of a reversible differential equation is a reversible mapping (cf. de Vogelaere [1958]) and historically this is how they arose (cf. the study of Birkhoff [1915] of the restricted three-body problem, a Hamiltonian problem). The time-1 map of a reversible differential equation is also a reversible mapping. Reversible mappings can also arise from differential

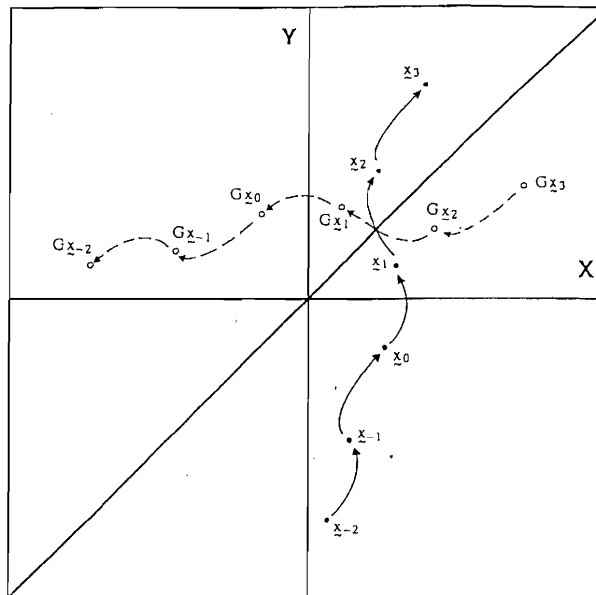


Fig. 1.2. Illustration of the nature of the motion in a reversible mapping L of the plane with symmetry $G: x \rightarrow y, y \rightarrow x$. Shown is part of the trajectory of a point x_0 with unbroken arrows indicating the action of L on each point. Reversibility implies that the trajectory of Gx_0 is found by reflecting the trajectory of x_0 by G . The forward and backward trajectories are interchanged on reflection as the broken arrows indicate.

equations in less obvious ways, e.g., in the theory of arbitrary (i.e., not necessarily reversible) discontinuous ordinary differential equations (cf. Teixeira [1981, 1990]). In such equations, which arise in control theory, economics and nonlinear oscillations, the vector field on the right-hand side of (1.7) is different in two different parts of phase space separated by a surface of discontinuity. In the neighbourhood of points on this surface, the surface-of-section mapping can be described as the composition of a pair of involutions.

Surface-of-section mappings and time-1 maps cannot usually be calculated explicitly from an underlying differential equation (a numerical integration scheme for reversible ordinary differential equations, which preserves time-reversal symmetry, is presented in Quispel [1992b]). Nevertheless, explicit mappings can be derived directly for various problems without the need to numerically integrate a differential equation. In particular, explicit reversible mappings can be analytically derived from some kicked reversible Hamiltonian systems (i.e., systems subjected to a regularly applied impulsive force) that occur as models in solid state physics (cf. Heagy and Yuan [1990] and references therein) and particle accelerator dynamics (cf. Helleman [1979, 1980]). Explicit reversible mappings also follow from problems modelled by symmetric difference equations, e.g.,

$$x_{i+1} + x_{i-1} = f(x_i); \tag{1.22a}$$

$$x_{i+2} + x_{i-1} = g(x_i, x_{i+1}); \quad g(x, y) = g(y, x), \tag{1.22b}$$

cf. section 3.2. These difference equations are symmetric because they propagate via the same formula in forward and backward time. Equations (1.22a, b) with appropriate identifications lead to two-dimensional and three-dimensional reversible mappings, e.g., respectively, $L: x_i = (x_{i-1}, x_i) \rightarrow x_{i+1} =$

(x_i, x_{i+1}) with symmetry $G: x_i = (x_{i-1}, x_i) \rightarrow x_{i+1} = (x_i, x_{i-1})$ and $L: x_i = (x_{i-1}, x_i, x_{i+1}) \rightarrow x_{i+1} = (x_i, x_{i+1}, x_{i+2})$ with symmetry $G: x_i = (x_{i-1}, x_i, x_{i+1}) \rightarrow x_{i+1} = (x_{i+1}, x_i, x_{i-1})$. Symmetric difference equations such as these (and hence reversible mappings) arise in, for example, models of the properties of one-dimensional crystals and quasicrystals [Janssen and Tjon 1983; Kohmoto 1987; Baake et al. 1992; Baake and Roberts 1992], spin chains [Belobrov et al. 1984; Roberts and Thompson 1988] and particle chains [Aubry 1983; Johannesson et al. 1988], and from looking at stationary states of differential-difference equations [Quispel et al. 1988, 1989; Lahiri and Ghosal 1987, 1988], and travelling wave solutions of partial difference soliton equations [Quispel et al. 1991, and references therein].

We now give examples of mappings in each of the three regions of fig. 1.1. The most studied systems are (again) those that are both reversible *and* symplectic (region II in fig. 1.1) see, e.g., MacKay [1983a, 1986], and Dewar and Meiss [1992] for area-preserving mappings of the plane and Hu and Mao [1987] and Kook and Meiss [1989] for higher-dimensional symplectic mappings (for studies of higher-dimensional reversible volume-preserving mappings, cf. de Vogelaere [1958], Hu and Mao [1987] and Mao [1988], and references therein). In two dimensions, a well known example from region II is the area-preserving Hénon mapping [Hénon 1969],

$$x' = y, \quad y' = -x + 2Cy + 2y^2 \quad (1.23)$$

[note that we depart from the subscript notation of (1.16) and hereafter use unprimed and primed variables for a point (x, y) and its image (x', y')]. This reversible mapping follows from the symmetric difference equation (1.22a) with $f(x_i) = 2Cx_i + 2x_i^2$ and the identification above. It can be written as the composition of two involutions $H \circ G$, with

$$H: \begin{cases} x' = x, \\ y' = -y + 2Cx + 2x^2, \end{cases} \quad G: \begin{cases} x' = y, \\ y' = x. \end{cases} \quad (1.24)$$

Another example of a reversible area-preserving mapping is the Chirikov-Taylor or standard mapping (cf. Taylor [1969], Froeschlé [1970], Chirikov [1979], Greene [1979]),

$$x' = x + y, \quad y' = y + (K/2\pi) \sin 2\pi x', \quad (1.25)$$

which arises from models of simple pendula and accelerator dynamics [Chirikov 1979, 1987] and ground states of the Frenkel-Kontorova model [Aubry 1983], and has been widely studied^{*}. It follows from (1.22a) with $f(x_i) = 2x_i + (K/2\pi) \sin 2\pi x_i$ and the identification $(x_i, x_{i+1} - x_i) \leftrightarrow (x, y)$, $(x_{i+1}, x_{i+2} - x_{i+1}) \leftrightarrow (x', y')$ [note that in this report we will often use - as in (1.25) - the compact notation of writing the primed variable of one of the defining mapping equations in the right-hand side of the other defining equation]. The standard mapping has the decomposition into involutions $H \circ G$ with

$$H: \begin{cases} x' = x, \\ y' = -y + (K/2\pi) \sin 2\pi x, \end{cases} \quad G: \begin{cases} x' = x + y, \\ y' = -y. \end{cases} \quad (1.26)$$

One of the practical benefits of studying area-preserving mappings that are also reversible is that in reversible systems many of the periodic orbits can be found by searching for a point of the orbit along

^{*} Note that eq. (1.25) looks slightly different to what most authors call the standard mapping but is in fact trivially related to it.

the fixed lines of the component involutions. Usually reversing symmetries possess such a line of fixed points [e.g., $y = x$ in the case of G in eq. (1.24)]. The periodic orbits found in this way are the symmetric periodic orbits.

As for differential equations, the reversibility property defined for mappings is independent of whether the mapping is conservative. Indeed, in a general reversible mapping parts of the phase space may be contracted whilst other parts may be expanded during the motion. It is only recently that nonconservative reversible mappings (region I of fig. 1.1) have received attention. Arnol'd and Sevryuk have proved KAM theorems for reversible mappings that need not be conservative [Arnol'd 1984; Arnol'd and Sevryuk 1986; Sevryuk 1986, 1990] (cf. also Sevryuk and Lahiri [1991] and Roy and Lahiri [1991] for results on Hopf-type bifurcations in four-dimensional reversible mappings, as well as Lahiri [1992]). In two dimensions the reversible mapping KAM theorems guarantee that under certain conditions the neighbourhood of a symmetric periodic orbit bears "striking similarities" [Arnol'd 1984] to the neighbourhood of a periodic orbit in an area-preserving mapping. That is, it contains a nested sequence of invariant curves, island chains and chaotic bands. A reversible mapping with both KAM curves and periodic attractors and repellers was discussed by Politi et al. [1985, 1986a, b]. It was not given explicitly but instead arose from taking a surface of section of the reversible system of three coupled ordinary differential equations listed in eq. (1.11) above. Bullett and coworkers [Bullett et al. 1986; Bullett 1988, 1991] have studied a class of reversible mappings in the complex plane containing attracting and repelling periodic orbits (cf. also Mestel and Osbaldestin [1989]).

An example of a reversible non area-preserving mapping (region I of fig. 1.1) is

$$x' = (C - y)[1 + (y' - 1)^2], \quad y' = x/[1 + (C - y - 1)^2]. \tag{1.27}$$

This mapping is composed of the two involutions (cf. chapter 4),

$$H: \begin{cases} x' = y[1 + (y' - 1)^2], \\ y' = x/[1 + (y - 1)^2], \end{cases} \quad G: \begin{cases} x' = x, \\ y' = C - y. \end{cases} \tag{1.28}$$

An example of an area-preserving nonreversible mapping (region III in fig. 1.1) is (cf. section 3.4),

$$x' = x - y^2(1 - y), \quad y' = y + Cx'^2(1 - x'), \quad C \neq 0, C \neq 1. \tag{1.29}$$

It will be shown in chapters 3 and 4 how one can construct both reversible and nonreversible mappings. Finally we note that there is no test for global reversibility. However, necessary conditions for a local form of reversibility are discussed in section 3.3.

1.6. Outline of this report

In this report we will study time-reversal symmetry in classical dynamical systems via a survey of the dynamics of reversible mappings of the plane. The reason for this restriction is that two-dimensional mappings are, in a sense, the simplest reversible systems capable of exhibiting both chaotic behaviour and ordered behaviour in different regions of phase space. The fact that area-preserving mappings of the plane possess some canonical features of conservative systems also allows us, at the level of two-dimensional mappings, to compare the relationship between conservative and reversible systems as depicted in fig. 1.1 (cf. also Roberts et al. [1991]).

We will to a large extent concentrate on nonconservative reversible systems (region I of fig. 1.1). The investigation of region I of fig. 1.1 is facilitated by the use of systematic methods for creating large classes of reversible nonconservative mappings with both attractors and repellers (cf. Quispel and Roberts [1988, 1989], Roberts [1990a, b]). The explicit reversible mappings thus obtained are much easier to study than ones defined by a surface of section. They graphically illustrate the fact that the phase portrait of a general reversible mapping typically contains both KAM tori, the distinguishing feature of area-preserving mappings, as well as attractors, the distinguishing feature of dissipative mappings (cf. fig. 1.3). The fact that most studies of reversible mappings to date have been restricted to area-preserving reversible mappings (region II) has tended to obscure this fact. To provide a complete survey of fig. 1.1, we also provide explicit examples of area-preserving mappings that are not reversible (region III) (cf. Roberts and Capel [1992a, b]).

We will be particularly interested in reviewing universality in reversible mappings with respect to two phenomena associated with the transition to chaos. The first phenomenon concerns the breaking up of KAM curves around a periodic orbit. Numerical studies on many (reversible) area-preserving mappings have indicated that this process is characterised by certain scaling numbers which are the same from one area-preserving mapping to the next (cf. Greene [1979], MacKay [1986]). It will be shown that the breakup of invariant curves around a symmetric periodic orbit of a general reversible mapping is characterised by the same scaling numbers.

The second phenomenon studied is the period-doubling route to chaos in reversible mappings. It is shown that symmetric periodic orbits period-double with the universal scaling numbers associated with period doubling in area-preserving mappings (cf. Benettin et al. [1980a, b], Bountis [1981], Greene et

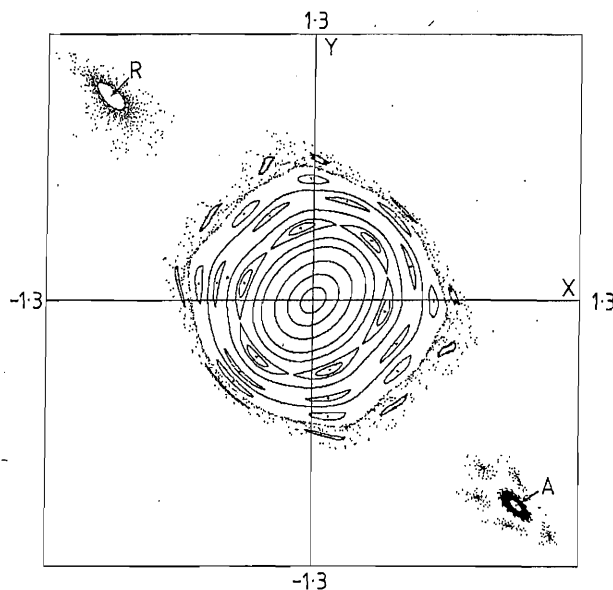


Fig. 1.3. Conservative and dissipative behaviour coexisting in a reversible dynamical system. Shown is the phase portrait of a non area-preserving reversible mapping L of the plane with symmetry $G: x' = y, y' = x$. The origin is an elliptic symmetric fixed point and is surrounded by invariant curves. These curves intersect the symmetry line $y = x$ and their symmetry with respect to reflection about this line is obvious. Also shown are elliptic symmetric six-, seven- and eight-cycles at the centres of the concentric "rings" of six, seven and eight islands. The KAM curves and islands are typically associated with conservative systems. Away from the origin, the fixed point A at $(1, -1)$ is attracting and its reflection $GA = R$ at $(-1, 1)$ is repelling. A trajectory that spirals in towards A is shown; its reflection by G spirals outwards from R . An attracting five-cycle is found near A and a trajectory that spirals towards it is also shown. The trajectories of many of the points not enclosed by curves around the origin or near A escape to infinity.

al. [1981]). This provides a quantitative similarity between the period doubling in the two classes of mappings. MacKay [1982] has previously indicated that qualitatively the period-doubling bifurcations of a periodic orbit in an area-preserving mapping and a symmetric periodic orbit in a reversible mapping are the same. The period doubling of (asymmetric) attractors in reversible mappings is also shown to be universal, with the same scalings as found in dissipative systems (cf. Cvitanovic [1989]). This period doubling can lead to the appearance of a strange attractor in reversible mappings. Because of reversibility, the period-doubling cascade of attractors is accompanied by a simultaneous period-doubling cascade of repellers and the appearance of a strange repeller.

Summarising the above, this report will show how the universal behaviour displayed in conservative mappings can be associated with universal behaviour of symmetric periodic orbits in reversible mappings, and how the universal behaviour found in dissipative mappings can be associated with universal behaviour of a reversible mapping's asymmetric periodic orbits. Although many interesting questions concerning general reversible mappings of the plane have yet to be answered, it seems timely to review and bring together what is known to date about reversible mappings. Moreover much of the new material presented here can be useful as a starting point for continuing their study.

The plan of this report is as follows. In chapter 2 we review in more technical detail than above the properties of area-preserving mappings (and their generalisation – measure-preserving mappings) as well as dissipative mappings. This is done as part of a general review of the properties of mappings of the plane. This discussion is included so that the report is largely self-contained and can be read with a minimum background in nonlinear dynamics. In chapter 3 we expand on the concept of reversibility for a mapping of the plane and discuss the consequences for the mapping's dynamics. We show how non area-preserving reversible mappings and non area-preserving involutions can be derived from certain second order difference equations. In the last two sections of the chapter some methods are presented for deciding whether a given mapping is not reversible. This leads to explicit examples of nonreversible area-preserving mappings given in section 3.4.

Large classes of non area-preserving reversible mappings with attractors and repellers are constructed in chapter 4. The methods provided are useful for creating reversible perturbations of reversible area-preserving mappings like the Hénon mapping (1.23) so that (asymmetric) dissipative and expansive dynamical features are introduced without the loss of the conservative-like behaviour associated with symmetric features. In chapter 5 we concentrate on the conservative features of these reversible mappings via a study of the breaking up of KAM curves and of symmetric period doubling, as discussed above. In chapter 6 we concentrate on the dissipative features, i.e. the attractors, in these reversible mappings.

In chapter 7 we discuss the interplay of the conservative and dissipative features of reversible nonconservative mappings via a symmetry-breaking bifurcation (cf. also Post et al. [1990a]). This bifurcation is a generalisation of a symmetry-breaking bifurcation studied in reversible conservative mappings by Rimmer [1978, 1983]. Finally, in chapter 8 we summarise the report and indicate some possible directions for future research. In appendix A, we give some integrable reversible mappings of the plane which complement the discussion in section 5.1. In appendix B, we discuss the nonlinear stability analysis for an elliptic fixed point which is used in section 6.1.

2. Review of some properties of mappings of the plane

The interest in studying mappings of the plane is to observe the types of possible dynamics that they can have. In this chapter we introduce some fundamental concepts associated with the dynamics of

mappings of the plane. Because we will be dealing in later chapters with mappings which have properties similar to conservative systems together with properties similar to dissipative systems, it is important to be familiar with the distinguishing dynamics of these two broad classes. At the same time it is important to know what properties a general mapping of the plane can have independently of how the area of a region is changed when the mapping is applied. This is because the reversible mappings of this report cannot be classified as either area-preserving or dissipative.

Section 2.1 reviews some technical notions used in the report and is provided to make it reasonably self-contained. This section can be passed over by those readers familiar with such things as invariant sets, classification of periodic orbits by linearisation, bifurcation of periodic orbits and Poincaré index, and conjugacy between mappings. General references for discussion on some or all of these topics include Arrowsmith and Place [1990], Devaney [1986], Guckenheimer and Holmes [1983], Hsu [1987] and Lichtenberg and Lieberman [1983]. Section 2.2 is a discussion of measure-preserving mappings.

2.1. Definitions and properties

A general mapping of the plane $L: \mathbb{R}^2 \rightarrow \mathbb{R}^2$ that assigns to a point $x = (x, y)$ an image point $x' = (x', y')$ can be written as

$$L: x' = f(x, y), \quad y' = g(x, y), \quad (2.1)$$

where f and g are arbitrary functions that may depend on one or more parameters. Most of the mappings in this report will be diffeomorphisms (i.e., differentiable bijections with differentiable inverses). A diffeomorphism (2.1) is C^k (more precisely, is of class C^k) if all the partial derivatives of f and g up to and including order k exist and are continuous. Many of the mappings in this report are in fact analytic, which implies that they are C^∞ . The domain of L may be the whole plane $\mathbb{R} \times \mathbb{R}$, or if one of x or y is an angle the domain may be the cylinder $\mathbb{R} \times (-\pi, \pi)$ as in the standard mapping (1.25). In this case, L is sometimes more specifically called a mapping of the cylinder. If both x and y are angular variables, L is a mapping of the torus: $[-\pi, \pi] \times [-\pi, \pi]$ with proper identifications.

The qualitative property of whether a planar mapping preserves, contracts or expands area is seen from the determinant of its Jacobian matrix,

$$dL(x, y) = \begin{pmatrix} \partial f / \partial x & \partial f / \partial y \\ \partial g / \partial x & \partial g / \partial y \end{pmatrix}. \quad (2.2)$$

This determinant, $\text{Det } dL(x, y)$, will be denoted by $J = J(x, y)$. As is well known, the absolute value of J gives the change in area of a small element after application of L . Mappings of the plane have been traditionally classified by J . When $J = \pm 1$ throughout the plane the mapping is area-preserving or conservative [e.g. (1.23) and (1.25)]. Area-preserving mappings have been studied well (see, for example, MacKay [1982], Hénon [1983], MacKay and Meiss [1987], Arrowsmith and Place [1990, chapter 6]). More generally, a conservative mapping is one for which we can write

$$J = m(x, y) / m(x', y'), \quad (2.3)$$

for some function $m(x, y)$. In this case the mapping L is called measure-preserving. Because in the literature conservative mappings are usually taken to be area-preserving, we will equate “conservative”

to area-preserving in this section. In section 2.2 we will discuss measure-preserving mappings and show that they possess most of the properties of area-preserving mappings.

Most mappings of the plane are not conservative. Nonconservative mappings include dissipative mappings which have $|J| < 1$ everywhere. On the other hand, when $|J| > 1$ everywhere, a mapping is called expansive. As an example, the two-parameter mapping

$$x' = By, \quad y' = -x + 2Cy + 2y^2, \tag{2.4}$$

or its equivalent forms, has been studied well. This mapping has $J = B$ and so is dissipative when $|B| < 1$ (e.g., cf. Hénon [1976], van der Weele et al. [1986], Cvitanovic et al. [1988], Grassberger et al. [1989]) and expansive for $|B| > 1$ (e.g., cf. Helleman [1980]). Most generally, mappings of the plane have a Jacobian determinant that varies throughout the plane and is locally contracting in some parts and locally expanding in other parts (cf. Chenciner [1983, 1987], Gumowski and Mira [1980]).

For diffeomorphisms, J is necessarily of constant sign throughout the plane because the Jacobian determinant of a diffeomorphism is never zero (if it were, the inverse mapping would not be differentiable at a point; this follows from differentiating $L \circ L^{-1} = \text{Id}$, where Id is the identity mapping). When a mapping has $J < 0$ or $J > 0$ everywhere, it is called, respectively, orientation-reversing or orientation-preserving [Buck 1978, chapter 8.4]. The property of orientation reversal has the following geometric consequence: if we map some points on a closed loop in the plane which are chosen in clockwise order then their image points will appear in counterclockwise order on the image of the loop. Orientation-preserving mappings preserve the order between the two sets of points.

From now on we consider only invertible mappings. The forward orbit, or forward trajectory, of a point $\mathbf{x}_0 = (x_0, y_0)$ under L is the set of points $F_L\{\mathbf{x}_0\} = \{\mathbf{x}_1, \mathbf{x}_2, \mathbf{x}_3, \dots\}$ such that $\mathbf{x}_{i+1} = L\mathbf{x}_i$ with $\mathbf{x}_i = (x_i, y_i)$. The backward orbit of a point \mathbf{x}_0 under L is the set of points $B_L\{\mathbf{x}_0\} = \{\mathbf{x}_{-1}, \mathbf{x}_{-2}, \mathbf{x}_{-3}, \dots\}$ that maps successively to \mathbf{x}_0 , i.e., $L\mathbf{x}_{-i} = \mathbf{x}_{-i+1}$. Thus $F_L\{\mathbf{x}_0\} = \{L^i\mathbf{x}_0, i \in \mathbb{Z}_+\}$ and $B_L\{\mathbf{x}_0\} = \{L^{-i}\mathbf{x}_0, i \in \mathbb{Z}_+\}$. Here L^i denotes L composed with itself i times, i.e. $L \circ L \circ \dots \circ L$, and L^{-i} is its inverse. The (full) orbit or trajectory of point \mathbf{x}_0 under L is the set of points $\{L^i\mathbf{x}_0, i \in \mathbb{Z}\}$.

When we iterate an initial point \mathbf{x}_0 forwards or backwards under a general mapping (2.1), some common possibilities are that *either*:

(i) we return to \mathbf{x}_0 after a finite number of iterations, generating along the way a finite set of distinct points (a zero-dimensional set);

(ii) the orbit of \mathbf{x}_0 is aperiodic and appears to fill a curve in the plane (a one-dimensional set);

(iii) the orbit of \mathbf{x}_0 is aperiodic but appears to densely fill a region of the plane – in this region two initially close starting points typically have exponentially diverging orbits and the orbits are called chaotic;

(iv) the orbit of \mathbf{x}_0 lies on a “strange attractor” (see below);

or the orbit of \mathbf{x}_0 is asymptotic to one of these possibilities. The orbit may also escape to infinity if the domain of the mapping is unbounded as when it is the whole plane or the cylinder.

A set of points Γ is called invariant under the mapping L if $L\Gamma = \Gamma$. An important example of an invariant set is a periodic trajectory, or n -cycle, which is a finite set of n points that is mapped to itself under L , i.e., a set of points $\mathbf{x}_i = \{L^i\mathbf{x}_0\}$, $i = 1, \dots, n$ with $L^n\mathbf{x}_0 = \mathbf{x}_0$ and $L^i\mathbf{x}_0 \neq \mathbf{x}_0$, $1 < i < n$. When $n = 1$, \mathbf{x}_0 is called a fixed point of L . Each point of an n -cycle, called a periodic point of period n , can be regarded as a fixed point of the mapping L^n . That is, a periodic point of period n is a solution of the equations

$$x_n(x, y) - x = 0, \quad y_n(x, y) - y = 0, \quad (2.5a, b)$$

where the functions x_n and y_n are the x and y components of the mapping L^n , formed by repeated composition of L with itself. It is important to realize that any result derived for a fixed point holds for a periodic point after taking a suitable power of the mapping. A second example of an invariant set is a curve C in the plane defined by the equation

$$I(x, y) = C, \text{ constant.} \quad (2.6)$$

If C satisfies $LC = C$, i.e.,

$$I(x', y') = C \quad (2.7)$$

whenever (x, y) satisfies (2.6), then it is called an invariant curve of the mapping.

A third example of an invariant set in a mapping is an attractor. There is no universally accepted definition of an attractor. An operational definition is that an attractor is a compact invariant set A to which neighbouring points evolve under forward iterates of L . As this working definition underlies computer experiments on attractors in mappings, in the spirit of this report, it will be adopted here. The definition can be made more mathematically precise in various ways (cf. Ruelle [1981, 1989], Eckmann and Ruelle [1985] and Milnor [1985]) with different emphasis; e.g., whether one requires *all* neighbouring points to converge to A or *almost all* points – computationally one can typically only get a feel for the second possibility. The set of all initial points x_0 in the plane that satisfy $L^i x_0 \rightarrow A$ as $i \rightarrow \infty$ is called the basin of attraction B of A so that $L^i B \rightarrow A$. We define a repeller R for a mapping L as a compact set satisfying the attractor definition with $L \leftrightarrow L^{-1}$ and $A \leftrightarrow R$. That is, a repeller is an attractor for the inverse mapping L^{-1} .

Because attractors and repellers involve, respectively, the contraction or expansion of an area in the plane, they cannot occur in area-preserving mappings. Attractors are the hallmark of dissipative mappings (e.g., Hénon [1976], Casdagli [1987, 1988], Schmidt [1988]) and commonly occur in various other nonconservative mappings (e.g., Chenciner [1983, 1987], Aronson et al. [1983], Lauwerier [1986], Gumowski and Mira [1980]). Attractors and repellers may take various forms; these are attracting (or repelling) periodic orbits, invariant curves and strange attractors. A *strange* attractor (or *strange* repeller) is an aperiodic attractor (repeller) which is characterised by the fact that the motion on it is chaotic, i.e., sensitively dependent on initial conditions which can be established via the existence of a positive Lyapunov exponent [Eckmann and Ruelle 1985]. This chaotic motion is often accompanied by the property that the attractor has a fractal geometric structure. Although most workers use the chaotic motion criterion to define “strangeness”, some others place greater emphasis on the self-similar geometry of the attractor [Grebogi et al. 1984; Holden and Muhamad 1986].

Any analysis of the dynamics of the mapping of the plane (2.1) usually starts by looking for its periodic orbits and studying their stability. A fixed point x_0 of a mapping L is said to be stable if for every small neighbourhood U of x_0 , there exists a neighbourhood W of x_0 such that all trajectories $L^i x$, $i > 0$, remain in U for $x \in W$. Therefore the idea is that one can remain as close as one likes to the point by choosing initial points close enough to the fixed point. The fixed point is called unstable if it is not stable. The *linear* stability of a fixed point is determined by the eigenvalues of the Jacobian matrix dL evaluated at the point. We call these the eigenvalues of the fixed point. Similarly, the linear stability of a periodic orbit of period $n > 1$ is found by evaluating the eigenvalues of dL^n , the Jacobian matrix

of the mapping L^n , at one point of the orbit. The matrix dL^n is called the return Jacobian of the orbit and is just the product of the mapping's Jacobian dL evaluated at each point of the orbit $[dL(x_1) \cdot dL(x_2) \cdot \dots \cdot dL(x_n)]$.

The eigenvalues λ of the matrix dL^n , $n \geq 1$, are given by

$$\lambda^2 - \text{Tr}(dL^n)\lambda + \text{Det}(dL^n) = 0, \quad (2.8)$$

which has the solutions

$$\lambda_{1,2} = \frac{1}{2} \{ \text{Tr}(dL^n) \pm [\text{Tr}^2(dL^n) - 4 \text{Det}(dL^n)]^{1/2} \}. \quad (2.9)$$

The sum of the two eigenvalues λ_1 and λ_2 is the trace $\text{Tr}(dL^n)$; their product is $\text{Det}(dL^n)$, which is called the return Jacobian determinant of the periodic orbit when $n > 1$. Since $\text{Det}(dL^n)$ and $\text{Tr}(dL^n)$ are real, the eigenvalues are real or complex conjugates. The classification of an n -cycle is based upon the nature of the eigenvalues of dL^n and various cases can be considered (cf. Lauwerier [1986], Hsu [1987]).

The cycle is termed *hyperbolic* if neither eigenvalue lies on the unit circle in the complex plane. In this event the local behaviour of the mapping near the orbit is similar to the linearised behaviour (the Hartman–Grobman theorem: the result holds if L^n is a C^1 diffeomorphism in a neighbourhood of the orbit, cf. Nitecki [1971]). In particular if $|\lambda_1| < 1$ and $|\lambda_2| < 1$ the periodic orbit is attracting. It is obviously stable by the definition given above and is more specifically termed asymptotically stable. The condition for the n -cycle to be attracting with $|\lambda_1| < 1$ and $|\lambda_2| < 1$ can be expressed in terms of $\text{Tr}(dL^n)$ and $\text{Det}(dL^n)$. We require

$$|\text{Det}(dL^n)| < 1, \quad |\text{Tr}(dL^n)| < 1 + \text{Det}(dL^n). \quad (2.10a, b)$$

If a hyperbolic cycle has at least one eigenvalue outside the unit circle, it is unstable. If $|\lambda_1| > 1$ and $|\lambda_2| > 1$ the orbit is repelling. Otherwise, λ_1 and λ_2 satisfy $|\lambda_1| > 1$ and $|\lambda_2| < 1$ or vice versa, and are necessarily real. A fixed point with such eigenvalues is usually called a saddle point. In the case of an n -cycle with such eigenvalues, each point of the cycle is a saddle point of L^n . It can be shown that each point of the n -cycle then has two smooth invariant curves passing through it. Points on one curve, called the stable manifold W^s , approach the point of the cycle under iteration of the mapping L^n whereas points on the other curve, called the unstable manifold W^u , approach the point of the cycle under iteration of the inverse mapping L^{-n} . The two curves may intersect transversally at a point, called a transverse homoclinic point (see Guckenheimer and Holmes [1983]). The orbit of such a homoclinic point is called a homoclinic orbit. The existence of these transverse homoclinic points leads to complex chaotic dynamics in their vicinity. Similar complexity is associated with transverse heteroclinic points which are the points of transverse intersection of the stable and unstable manifolds of two different saddle cycles.

When both the eigenvalues of a cycle lie on the unit circle in the complex plane and are not real (i.e., $\lambda_1 = e^{i\theta}$, $\lambda_2 = e^{-i\theta}$; $\theta \neq 0, \pi$), the cycle is called *elliptic* because in the linear approximation nearby trajectories move on ellipses encircling the points of the orbit. For a general mapping of the plane with an elliptic cycle, the nearby motion under the mapping L need not be the same as in the linear approximation. Instead, the nonlinear effects of L may cause the ellipses to degenerate into inward spirals or outward spirals in which case the cycle is an attractor or repeller. The situation is different for

orientation-preserving, area-preserving mappings where any periodic orbit with genuinely complex eigenvalues is necessarily elliptic since $\lambda_1 \lambda_2 = \text{Det}(dL^n) = 1$. In this case the KAM theorem for area-preserving mappings [Moser 1962, 1973] applies. It states that under some differentiability conditions and provided the eigenvalues are not 3rd or 4th roots of unity, then typically each point of the orbit is surrounded by infinitely many nested closed curves located arbitrarily close to the point and left invariant by the mapping L^n . On these so-called KAM curves, or KAM circles, the motion is quasiperiodic, i.e., essentially a rotation by an irrational multiple of 2π (for more details, cf. chapter 5). The effect in two dimensions of these closed invariant curves is to confine the dynamics of the mapping in the neighbourhood of the cycle. This is because the trajectory of a point which is inside a closed invariant curve surrounding a fixed point (each point of the n -cycle is a fixed point of L^n) must remain inside the curve by continuity. Consequently the cycle is stable. KAM curves around elliptic periodic orbits give area-preserving mappings their distinguishing phase portrait of nested islands within islands (such as also appear in the central part of fig. 1.3). Between these curves are thin bands of bounded chaotic orbits associated with transverse homoclinic points.

A third important case for the eigenvalues of a cycle occurs when they satisfy $\lambda_1 = \lambda_2 = \pm 1$. This can happen, for instance, in area-preserving mappings in which case the cycle is called *parabolic* (cf. Siegel and Moser [1971, section 31]). More generally, when $\lambda_1 = \pm 1$ or $\lambda_2 = \pm 1$, we have transition cases for the stability of a cycle. These cases feature prominently in an important aspect of the dynamics of mappings of the plane, whether area-preserving, dissipative or otherwise, concerned with the creation and destruction of periodic orbits as a mapping parameter is varied. The eigenvalues of a periodic orbit can be used to determine when such events can occur.

A fixed point is isolated from other fixed points or n -periodic points provided that neither of its eigenvalues is a root of unity. If this condition is satisfied at a particular value of the mapping parameter, it also guarantees that the fixed point persists (continues to exist) in a small parameter interval around this value. These results follow from applying the implicit function theorem to eqs. (2.5) (cf. Iooss and Joseph [1980, appendix V.1]). A fixed point $\mathbf{x}_0 = (x_0, y_0)$ is a solution of (2.5) for any $n \geq 1$. The implicit function theorem guarantees that if \mathbf{x}_0 satisfies (2.5) at the parameter value C_0 and the Jacobian matrix of the left-hand side of (2.5) has nonzero determinant at (x_0, y_0, C_0) , then there is a unique solution to (2.5) for some parameter interval around C_0 and box around (x_0, y_0) . The Jacobian determinant condition on (2.5) is equivalent to saying that at (x_0, y_0) and C_0

$$\text{Tr}(dL^n) \neq 1 + \text{Det}(dL^n). \quad (2.11)$$

It is only when the sides of (2.11) are equal that the persistence of the fixed point cannot be guaranteed and that the birth of an n -cycle from the fixed point may occur. The equality of the left-hand and right-hand sides of (2.11) implies that at least one of the eigenvalues of the fixed point is an n th root of unity. As mentioned above, important special cases are when $n = 1$ and $n = 2$. When a fixed point has an eigenvalue equal to $+1$ (the case $n = 1$), it can collide with other fixed points or give birth to them. In a *tangent* bifurcation, fixed points are born from a part of the plane where previously there were no fixed points. At birth these fixed points must have at least one eigenvalue equal to $+1$. When a fixed point has an eigenvalue equal to -1 (the case $n = 2$), a *period-doubling* bifurcation can occur and a two-cycle is created. The period-doubling bifurcations of fixed points in reversible mappings will be discussed in chapters 5 and 6. Note that in both of these cases, as the bifurcation occurs at a transition case for the stability of the fixed point, the bifurcations are associated with a change of stability.

A quantity that places some restriction on the sort of bifurcations that can occur in a mapping is the Poincaré index [Hsu 1980; Mira 1987, appendix A]. This is an integer, I , ascribed to an arbitrarily chosen closed curve in the plane and defined in terms of the number of revolutions made by the vector $v = Lx - x$ as x moves once around the closed curve. The sign given to this number in order to obtain the index is positive or negative depending on whether the rotation of the vector v and the traversal of the curve are in the same or opposite directions. The index of a fixed point is defined as the index of a closed curve enclosing this fixed point and not containing, or intersecting, any other fixed points. For a fixed point x_0 which is isolated from other fixed points [a sufficient condition is (2.11) above with $n = 1$], the index can be related to its linearisation, i.e.,

$$\text{Tr } dL(x_0) < 1 + \text{Det } dL(x_0) \Rightarrow I = +1, \quad \text{Tr } dL(x_0) > 1 + \text{Det } dL(x_0) \Rightarrow I = -1. \quad (2.12a, b)$$

For example, an elliptic fixed point has $I = +1$, as does an attracting fixed point with $0 < \lambda_1 < \lambda_2 < 1$. A saddle point with $0 < \lambda_1 < 1 < \lambda_2$ has index -1 . If a group of fixed points is encircled by a curve, the index of the curve is given by the sum of the indices of the fixed points within. Significantly, provided the closed curve does not intersect any fixed points, its index is constant. Therefore if a mapping parameter is varied and bifurcations of fixed points occur within a chosen closed curve, the only possible bifurcations are those for which the index of the curve before and after the bifurcations is the same. This can also be applied to bifurcations of cycles, as indices can be assigned to them and related to their linearisation in a similar way (cf. Hsu [1980]).

Finally, we say something about an important concept that arises in the study of mappings, namely that of conjugacy [Nitecki 1971]. Two mappings (diffeomorphisms) L and M are said to be conjugate if there exists an invertible mapping P such that

$$M = P \circ L \circ P^{-1}. \quad (2.13)$$

The conjugacy is classed as topological or differentiable accordingly as P is a homeomorphism (continuous bijection with a continuous inverse) or diffeomorphism. The process of rewriting the equations of a mapping under a coordinate transformation establishes a conjugacy between the mapping in the new and old coordinate systems. The Jacobian matrices in the new and old coordinates are related by

$$dM(x) = dP(L \circ P^{-1}(x)) dL(P^{-1}(x)) dP^{-1}(x). \quad (2.14)$$

The most important features of a mapping are those that are left unchanged under conjugacy. Nitecki [1971] lists some of the invariants of topological conjugacy. For example, if x_0 is a fixed point of L then Px_0 is a fixed point of M . For any x_0 , the forward and backward orbit of the point Px_0 under M is the image under P of the orbit of x_0 under L , i.e.,

$$B_M\{Px_0\} = P(B_L\{x_0\}), \quad F_M\{Px_0\} = P(F_L\{x_0\}). \quad (2.15a, b)$$

More generally if Γ is an invariant set for L then $P\Gamma$ is an invariant set for M , and if Γ is an attractor then so is $P\Gamma$. Consequently possession of an attractor is a conjugacy invariant. Another important conjugacy invariant is the linear stability of a fixed point (or periodic orbit) because eigenvalues of a fixed point (or periodic orbit) are preserved under differentiable conjugacy [eq. (2.14) becomes a

matrix conjugacy when \mathbf{x} is a fixed point of M]. It is not hard to show that orientation reversal and orientation preservation are also maintained under differentiable conjugacy. However, area preservation is in general not maintained under such a conjugacy unless the Jacobian determinant of the coordinate transformation is constant, i.e., independent of x and y .

In the study of mappings it is often useful to use coordinate transformations (conjugacies) to reduce a mapping to a simple or *normal* form. The idea is that the essential nature of the mapping is retained but that the study of the normal form is easier because some of the complexity associated with the terms of the original mapping is removed. For example, from the theory of (Jordan) normal forms for a real 2×2 matrix A , we know that there exists a real matrix T such that $A = TCT^{-1}$, where C assumes one of the forms:

$$\begin{pmatrix} \lambda & 0 \\ 0 & \mu \end{pmatrix}, \quad \begin{pmatrix} \lambda & b \\ 0 & \lambda \end{pmatrix}, \quad \begin{pmatrix} \alpha & -\beta \\ \beta & \alpha \end{pmatrix}. \quad (2.16a, b, c)$$

This result can be used when expanding a mapping (2.1) in a Taylor series around a fixed point. Assuming that it is sufficiently differentiable, the mapping can be written

$$\begin{aligned} x' &= Ax + By + F_{20}x^2 + F_{11}xy + F_{02}y^2 + F_{30}x^3 + F_{21}x^2y + F_{12}xy^2 + F_{03}y^3 + \dots, \\ y' &= Cx + Dy + G_{20}x^2 + G_{11}xy + G_{02}y^2 + G_{30}x^3 + G_{21}x^2y + G_{12}xy^2 + G_{03}y^3 + \dots, \end{aligned} \quad (2.17)$$

where the matrix $\begin{pmatrix} A & B \\ C & D \end{pmatrix}$ is the Jacobian matrix evaluated at the fixed point and this point has been shifted to the origin. The higher order coefficients are related to the partial derivatives of $f(x, y)$ and $g(x, y)$ at the point. Because of the above, the expansion can always be reduced via a linear transformation to a form

$$\begin{aligned} x' &= ax + by + f_{20}x^2 + f_{11}xy + f_{02}y^2 + f_{30}x^3 + f_{21}x^2y + f_{12}xy^2 + f_{03}y^3 + \dots, \\ y' &= cx + dy + g_{20}x^2 + g_{11}xy + g_{02}y^2 + g_{30}x^3 + g_{21}x^2y + g_{12}xy^2 + g_{03}y^3 + \dots, \end{aligned} \quad (2.18)$$

where its linear part (Jacobian matrix) is one of the three forms given. Now the eigenvalues of the fixed point are prominent – they can be read off the diagonal in (2.16a, b) and are complex conjugates $\alpha \pm i\beta$ in the case of (2.16c). The normal form (2.18), based upon the linear part of the mapping, is the simplest reduction we can perform on it. Some more powerful normal forms, based upon the use of nonlinear transformations to the original mapping, will be mentioned in chapter 3.

2.2. Measure preservation

In this section we consider measure-preserving mappings, a class of conservative mappings which are generalizations of area-preserving mappings. A mapping $L: \mathbf{x} = (x, y) \rightarrow \mathbf{x}' = (x', y')$ is called measure-preserving if there is a measure μ such that $\mu(S) = \mu(L^{-1}(S))$ for every measurable set S . Hence invertible mappings are measure-preserving if there is a function $m(x, y)$ such that

$$\int_D m(x, y) dx dy = \int_{L(D)} m(x', y') dx' dy' \quad (2.19)$$

for any region of the plane D . The function $m(x, y)$ is called a density. From the formula for change of variable in double integrals, (2.19) is equivalent to (2.3), which can be alternatively written using vector notation,

$$J = m(x)/m(Lx). \tag{2.20}$$

Measure-preserving mappings were studied, e.g., by Poincaré [1912] and Birkhoff [1913, 1920, 1927]. Area-preserving mappings satisfy (2.19) and (2.20) with $m(x, y) \equiv 1$. Mappings $L = P^{-1} \circ M \circ P$ that are conjugate to area-preserving mappings M are measure-preserving with density $m(x, y) = \text{Det } dP(x)$. Conversely, a measure-preserving mapping L with density $m(x, y)$ is conjugate to an area-preserving mapping if there exists a coordinate transformation $P: X = u(x, y), Y = v(x, y)$ with Jacobian determinant $(\partial u/\partial x) \partial v/\partial y - (\partial u/\partial y) \partial v/\partial x = m(x, y)$. A choice for the transformation P is [Moser 1965, Lemma 2]: $X = x, Y = \int m(x, t) dt$, which will be invertible in regions where $m(x, y)$ has constant sign, e.g., $m(x, y) > 0$. Consequently, the class of measure-preserving mappings can be thought of as essentially the class of area-preserving mappings and mappings conjugate to them, all with essentially the same conservative dynamics.*)

Unlike area preservation, measure preservation is maintained under (differentiable) conjugacy. However, whereas the composition of two area-preserving mappings is still area-preserving, measure preservation is not usually maintained under composition. Like the special case of area-preserving mappings, measure-preserving mappings cannot possess attractors. This follows because (2.19) in general implies that no proper subset V of the mapping domain can be such that it contains its image under the mapping i.e., $V \supset L(V)$. The existence of such a “trapping region” or shrinking neighbourhood is important in many definitions of an attractor (cf. Eckmann and Ruelle [1985], Ruelle [1981, 1989]).**)

Furthermore, all periodic orbits in any measure-preserving mapping have return Jacobian determinant ± 1 , which is a simple consequence of (2.20). In particular if we look at the expansion (2.17) around a fixed point of a measure-preserving mapping then this says that

$$AD - BC = \pm 1. \tag{2.21}$$

If the mapping is orientation-preserving, the right-hand side of (2.21) is $+1$. From (2.16a, b, c) it follows that in this case the expansion can be reduced to a normal form (2.18) with a linear part given by one of

$$\begin{pmatrix} \lambda & 0 \\ 0 & \lambda^{-1} \end{pmatrix}, \quad \begin{pmatrix} \pm 1 & b \\ 0 & \pm 1 \end{pmatrix}, \quad \begin{pmatrix} \cos \theta & -\sin \theta \\ \sin \theta & \cos \theta \end{pmatrix}. \tag{2.22}$$

In the first case the fixed point is hyperbolic (a saddle) and in the last case ($\theta \neq 0, \pi$) it is elliptic. The middle case corresponds to a transition case for stability; typically $b \neq 0$.

Measure preservation implies infinitely many relations between the coefficients of the terms of an expansion around a fixed point. This can be deduced from Birkhoff’s study of measure-preserving

*) Note that we will sometimes also call measure preserving a mapping with $\int_D m(x, y) dx dy = -\int_{L(D)} m(x', y') dx' dy'$ and $J = -m(x)/m(Lx)$.

**) Note that a “measure preserving” mapping in which the density is singular could have an attractor located at the singularity, e.g., $x' = px, y' = py$ with $0 < p < 1$ has density $(xy)^{-1}$ and an attracting fixed point at the origin whose basin of attraction is the whole plane. Such examples are not really in the spirit of measure preservation and perhaps should not even be classed as such (most of the measure-preserving mappings studied by Birkhoff were such that their density was everywhere positive).

Table 2.1

Necessary conditions for a mapping L to be locally measure-preserving around a fixed point. The conditions relate the coefficients of the expansion of L , given in (2.18), when its linear part has one of the typical canonical forms shown.

Linear part	Case	Second order	Third order
$\begin{pmatrix} \lambda & 0 \\ 0 & \lambda^{-1} \end{pmatrix}, \lambda \neq \pm 1$	1	no condition	$(\lambda - 1)(\lambda g_{12} + \lambda^{-1} f_{21} - f_{11} g_{11} - 2f_{02} g_{20}) + f_{20} f_{11} (\lambda^{-2} - 2\lambda^{-1}) + g_{11} g_{02} (2\lambda^2 - \lambda^3) = 0$
$\begin{pmatrix} 1 & b \\ 0 & 1 \end{pmatrix}, b \neq 0$	2	$g_{11} + 2f_{20} - 2bg_{20} = 0$	if $g_{20} = 0$ then $3b^2 g_{30} - bg_{21} - 3bf_{30} + 2f_{20} g_{02} + f_{20} f_{11} - 3bf_{20} g_{11} = 0$
$\begin{pmatrix} -1 & b \\ 0 & -1 \end{pmatrix}, b \neq 0$	3	no condition	$12bg_{30} + 4g_{21} + 12f_{30} + 2g_{11}^2 + 2f_{20} g_{11} + 22bf_{20} g_{20} + 10b^2 g_{20}^2 + 10f_{11} g_{20} + 11bg_{20} g_{11} + 4g_{20} g_{02} + 12f_{20}^2 = 0$

mappings in Birkhoff [1920]. Quispel and Capel [1989] have explicitly calculated some of these relations for an orientation-preserving measure-preserving mapping. They take the expansion of the mapping around the fixed point and write the Jacobian determinant J as a Taylor series with coefficients determined by the coefficients of the mapping expansion. They expand a possible density $m(x, y)$ likewise (assuming differentiability of m to some order) and substitute its series together with that for $J(x, y)$ into the definition (2.20), or equivalently

$$J(x, y)F(x, y) = F(x', y'), \quad F(x, y) = [m(x, y)]^{-1}, \quad (2.23)$$

where x' and y' are input from the mapping expansion. Equating both sides of (2.23) term by term leads to "formal" (i.e., without regard to convergence) necessary conditions on the coefficients of a mapping in order for a density to exist to some order. If a mapping satisfies these conditions to n th order then it is called locally measure-preserving to order n . The conditions up to third order are listed in table 2.1 for typical linear parts of the mapping expansion. Note that case 1 of table 2.1 yields the elliptic fixed-point case on the right-hand side of (2.22) in its complex form if we take $\lambda = e^{i\theta}$ ($\theta \neq 0, \pi$). The real mapping expansion $L: (x, y) \rightarrow (x', y')$ with real linear part around an elliptic fixed point is converted to a complex form $M: (X, Y) \rightarrow (X', Y')$ with complex linear part via $X = x + iy, Y = x - iy$.

3. Reversibility and mappings of the plane

In this chapter we formally introduce the property of reversibility for a mapping and discuss some of its consequences. As pointed out in the introduction, reversibility is a property that is quite independent of whether a mapping is measure-preserving or not and this gives reversible mappings the scope to incorporate a range of dynamical behaviours. The general features of reversible mappings are discussed in section 3.1, and in section 3.2 we give a simple method to create them. In the last two sections of the chapter we discuss the problem of how to recognise when a given mapping has the reversibility property and give some examples of mappings that are not reversible.

3.1. Some properties of reversible mappings

Recalling the definition given in section 1.5 of the introduction, we have that a mapping of the plane $L: \mathbb{R}^2 \rightarrow \mathbb{R}^2$ given by (2.1) is reversible [Sevryuk 1986] if there exists a mapping $G: \mathbb{R}^2 \rightarrow \mathbb{R}^2$ satisfying

$$L \circ G \circ L = G, \quad (3.1)$$

where G is an involution, i.e.,

$$G \circ G = \text{Id}, \quad (3.2)$$

and Id is the identity mapping. G is called a (reversing) symmetry of L . Equivalently, L can be written as the composition of two involutions

$$L = H \circ G, \quad H \circ H = G \circ G = \text{Id}. \quad (3.3a, b)$$

The reversibility property ensures that a mapping is invertible. In fact, from (3.1) and (3.2), the inverse mapping L^{-1} can be expressed as

$$L^{-1} = G \circ L \circ G^{-1} = G \circ H, \quad (3.4)$$

that is to say, the mapping and its inverse are conjugate, the conjugating transformation being the symmetry G cf. (2.13) with $M = L^{-1}$, $P = G$ and note $G^{-1} = G$. This conjugacy and the associated conjugacy invariants [Nitecki 1971] have important structural consequences for the dynamics of the mapping. In particular the reflection by G of the forward (backward) orbit of a point x_0 gives the backward (forward) orbit of the point Gx_0 [cf. eq. (2.15) with $M = L^{-1}$ and note $B_{L^{-1}}\{Gx_0\} = F_L\{Gx_0\}$ and $F_{L^{-1}}\{Gx_0\} = B_L\{Gx_0\}$]. This has been illustrated in fig. 1.2. Thus if the motion in one part of the plane is known, the motion in another part of the plane (i.e., in the region reflected by G) can be deduced. Note that the first equality in (3.4) expresses a conjugacy between L and its inverse independently of whether G is an involution. Mappings which satisfy (3.1) but do not require G to be an involution as in (3.2) are called *weakly* reversible and have been considered by Greene [1978], Arnol'd [1984], Arnol'd and Sevryuk [1986] and Sevryuk [1986], cf. also Lamb [1992]. Although we confine our discussion to reversible mappings, which have received much more attention than the superset of weakly reversible mappings, some of the properties below require only (3.1) instead of (3.1) and (3.2).

As stressed in section 1.5 the study of reversible mappings has been almost exclusively directed towards mappings that are also conservative. Nevertheless, the basic reversibility property (3.1) places no constraint on the Jacobian determinant of L in general and does not imply measure preservation of any sort [MacKay 1982]. It is true however that every differentiable involution is measure-preserving. This follows from differentiating (3.2) to give

$$dG(Gx) dG(x) = I, \quad (3.5)$$

where I is the identity matrix, whence

$$\text{Det } dG(x) = |\text{Det } dG(x)|^{1/2} |\text{Det } dG(Gx)|^{-1/2} \text{sgn}[\text{Det } dG(x)], \quad (3.6)$$

with the density given by $m(x, y) = |\text{Det } dG(x)|^{1/2}$ cf. (2.20). The product of two involutions, though, need not be measure-preserving because, as pointed out in section 2.2, measure preservation is not necessarily retained under composition. It is only recently that Arnol'd and Sevryuk have proved KAM theorems for general reversible diffeomorphisms which can possess attractors and repellers and so are not measure-preserving [Sevryuk 1986]. Explicit examples of reversible planar mappings with attractors and repellers will be given in the next chapter.

Various properties of reversible mappings will now be listed. Some of these were considered in the pioneering works of Birkhoff [Birkhoff 1915; Birkhoff and Lifshitz 1945]. Further discussion of the properties can be found in de Vogelaere [1958], Devaney [1976], Greene [1979], Greene et al. [1981], MacKay [1982], Arnol'd [1984], Arnol'd and Sevryuk [1986] and Sevryuk [1986]. These references however, have not considered attractors and repellers in reversible mappings, with the exception of Arnol'd and Sevryuk's limited qualitative discussion. Although our interest here is in reversible mappings in \mathbb{R}^2 , the majority of the properties carry over to any dimension (e.g., cf. Kook and Meiss [1989] for a discussion of reversibility in $2n$ -dimensional symplectic mappings).

The first point that can be made about a reversible mapping is that it has infinitely many symmetries. This follows because if G is a reversing symmetry for a mapping L , then it is easily verified that so are the mappings $L^i \circ G$ for i an integer. The letter G can be used indiscriminately to represent any symmetry. The set $\{L^i \circ G\}$ is called a family of symmetries of L and together with the set $\{L^i\}$ of powers of L it forms an infinite group [de Vogelaere 1958; Piña and Jiménez Lara 1987]. A mapping may possess more than one family of reversing symmetries, in which case it is called multiply reversible. For example, if a reversible mapping L with symmetry G commutes with a mapping M then $G \circ M$ and $M \circ G$ satisfy (3.1) because

$$L \circ (G \circ M) \circ L = (L \circ G \circ L) \circ M = G \circ M, \quad L \circ (M \circ G) \circ L = M \circ (L \circ G \circ L) = M \circ G. \quad (3.7a, b)$$

The mappings $G \circ M$ or $M \circ G$ are reversing symmetries of L if they are also involutions (more generally $G \circ M$ and $M \circ G$ are all examples of *weakly* reversing symmetries because they satisfy (3.1) but not necessarily (3.2) cf. Sevryuk [1986], Lamb [1992]). They are guaranteed to be involutions if M commutes with G as well as with L and if M is itself an involution. $G \circ M$ and $M \circ G$ are independent of the symmetry family generated by G provided that $M \neq L^i$, $i \in \mathbb{Z}$. An important case of doubly reversible mappings is reversible odd maps, for which $L(-x) = -L(x)$, i.e. L commutes with the mapping $M \equiv O$ where

$$O: x' = -x, \quad y' = -y. \quad (3.8)$$

Reversible odd maps have been discussed by Huiszoon [1983], MacKay [1984], Piña and Cantoral [1989] and Tanikawa and Yamaguchi [1989].

The reversibility property is preserved under conjugacy because

$$(P \circ L \circ P^{-1}) \circ (P \circ G \circ P^{-1}) \circ (P \circ L \circ P^{-1}) = P \circ G \circ P^{-1}, \quad (3.9)$$

which shows that $M = P \circ L \circ P^{-1}$ is reversible. Its symmetry $P \circ G \circ P^{-1}$ is conjugate to the symmetry of

L . Reversibility is not in general preserved by composition. However the composition (product) of two reversible mappings that share a symmetry is reversible. In particular any power of a reversible mapping is reversible with the same symmetries as the mapping, i.e.,

$$L^i \circ G \circ L^i = G, \quad i \in \mathbb{Z}. \tag{3.10}$$

This readily follows from (3.1) and has the consequence that

$$L^i \circ G = G \circ L^{-i}. \tag{3.11}$$

Powers of a reversible mapping provide examples of multiply reversible mappings. This is because the one family of symmetries for $L: \{L^i \circ G\}, i \in \mathbb{Z}$, divides into the k distinct symmetry families for $L^k: \{L^{ki+j} \circ G\} = \{L^{ki}(L^j \circ G)\}, j = 0, 1, \dots, k-1$. For example, if $k=2$ and L is reversible with symmetry G , then G and $L \circ G$ are both symmetries for L^2 but $L \circ G$ is not in the symmetry family $\{L^{2i} \circ G\}$ generated by G .

An important part of the structure that reversibility gives to a mapping derives from the set of fixed points of a symmetry G , denoted by $\text{Fix}(G)$. From (3.5) it follows that the linear part of any symmetry evaluated at one of its fixed points is a linear involution. In the commonly encountered case when G is orientation-reversing this means that dG has the form of the matrix

$$A = \begin{pmatrix} p & q \\ r & -p \end{pmatrix}, \quad p^2 + qr = 1. \tag{3.12}$$

An important result is that any involution is conjugate around one of its fixed points to its linear part (this holds in any dimension: ‘‘Bochner’s theorem’’, cf. Montgomery and Zippin [1955, section 5.2], Meyer [1981], Quispel and Capel [1989]). A simple way to see this follows from the following identity for any two involutions U and $R: (U + R) \circ U = R \circ (U + R)$. Taking $U = G$, and $R = dG$ evaluated at a fixed point $x_0: Gx_0 = x_0$, shows that $G = [G + dG(x_0)]^{-1} \circ dG(x_0) \circ [G + dG(x_0)]$ if $G + dG(x_0)$ is invertible. The latter is always invertible about x_0 if G is C^1 , via the inverse function theorem because its linear part $2dG(x_0)$ is nonsingular. Because the matrix A in (3.12) is similar to $\begin{pmatrix} 1 & 0 \\ 0 & -1 \end{pmatrix}$, it follows that around a fixed point of an orientation-reversing involution G we can write

$$G = P \circ V \circ P^{-1}; \quad V: x' = x, \quad y' = -y. \tag{3.13a, b}$$

Alternatively, at such a fixed point G is also conjugate to any linear involution which is conjugate to V . Meyer [1981] shows that if G in (3.13a) is area-preserving as well as orientation-reversing, then P can be taken as area-preserving.

Finn [1974] has shown that the fixed point set of a C^1 involution of the plane, whether orientation-preserving or orientation-reversing, is nonempty.*¹ For the case of an orientation-reversing involution G , application of the reduction (3.13a) about a fixed point, together with the fact that V in (3.13b) fixes the x -axis, then implies that G has a curve of fixed points in the plane which does not intersect itself or terminate (it is sufficient for G to be C^1 to obtain this result; Finn assumes analyticity of G and shows that the curve is also analytic). Such a curve of fixed points of G is called a symmetry line. Since

*¹This is not necessarily true for involutions on other manifolds.

virtually all of the involutions of reversible mappings studied to date, as well as those of the mappings of this report, are orientation-reversing, $\text{Fix}(G)$ below usually represents a symmetry line. On the other hand, if an involution is orientation preserving, its fixed points need not form lines, as the simple linear example $x' = -x$, $y' = -y$ illustrates. Because L , reversible, has infinitely many symmetries it also has infinitely many symmetry lines. The symmetry lines of the family $\{L^i \circ G\}$ can be obtained from those of G and $H = L \circ G$ by taking their images under powers of L because

$$L^i \{\text{Fix}(G)\} = \text{Fix}(L^{2i} \circ G), \quad L^i \{\text{Fix}(L \circ G)\} = \text{Fix}(L^{2i+1} \circ G), \quad i \in \mathbb{Z}. \quad (3.14a, b)$$

We now consider the effect that reversibility has on the invariant sets of a mapping. We will complement some of our discussion with references to the phase portrait fig. 1.3 of a non measure-preserving reversible mapping, and to fig. 3.1 which shows some of its symmetry lines. (A colour version of fig. 3.1 is found at the beginning of the report; a black and white copy is provided here.)

If Γ is an invariant set of a reversible mapping L then so is the set $G\Gamma$ since

$$G\Gamma = (L \circ G \circ L)\Gamma = L(G\Gamma). \quad (3.15)$$

For example, a point x_0 is a fixed point of a reversible mapping $L = H \circ G$ if and only if

$$Hx_0 = Gx_0, \quad (3.16)$$

and it is readily seen that if x_0 satisfies (3.16) then so does Gx_0 . As a further example, if the fixed point x_0 is a saddle point with stable and unstable invariant manifolds $W^s(x_0)$ and $W^u(x_0)$, then the images of these invariant sets under G are, respectively, the unstable and stable invariant manifolds of the fixed point Gx_0 , i.e., $G\{W^s(x_0)\} = W^u(Gx_0)$ and $G\{W^u(x_0)\} = W^s(Gx_0)$. Incidentally, this relationship makes it easier to prove the existence of homoclinic and heteroclinic points in reversible mappings than

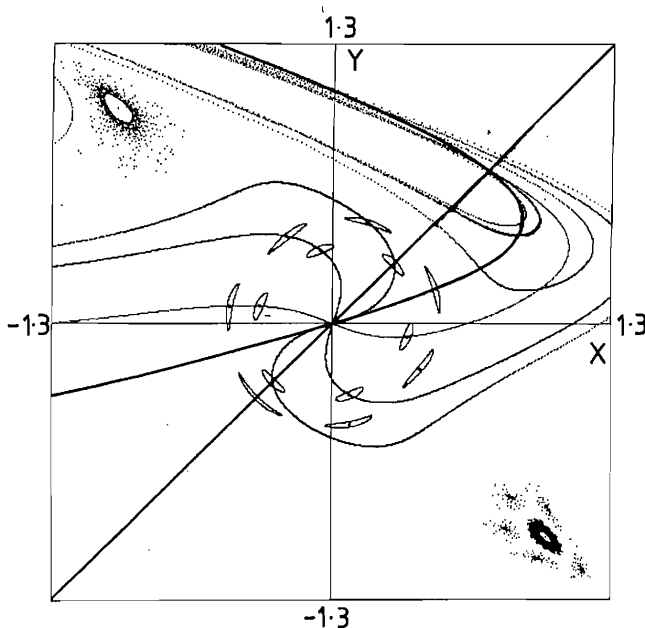


Fig. 3.1. Fig. 1.3 with many of the trajectories removed (a colour version of this figure is found at the beginning of the report). The symmetry line $y=x$ of G is drawn in black together with the curved symmetry line of $H=L \circ G$. In colour are shown the first three iterates of the symmetry line of G under L , which are the symmetry lines of $L^2 \circ G$, $L^4 \circ G$ and $L^6 \circ G$ (cf. 3.14a). These are coloured green, red and blue, respectively. All symmetry lines pass through the symmetric fixed point at the origin and the other symmetric fixed point at the other intersection of the lines of G and H . The intersection of the symmetry lines of $L^6 \circ G$ and G accounts for the existence of the symmetric six-cycle. This cycle has two points on each of the symmetry lines of G and its iterates. The seven-cycle, being odd, has a point on the symmetry line of G and of H .

in general, e.g., if $W^s(x_0)$ intersects $\text{Fix}(G)$, the point of intersection is a homoclinic or heteroclinic point accordingly as $x_0 = Gx_0$ or $x_0 \neq Gx_0$ [Devaney 1984, 1988; Fontich 1990; Heagy and Yuan 1990]. It also facilitates numerical calculation of the invariant manifolds, with application to transport problems [Rom-Kedar and Wiggins 1990, sections 6 and 7].

Since the image of an invariant set Γ under all the symmetries of the family $\{L^i \circ G\}$ is equal to $G\Gamma$, the invariant sets can be classified according to their invariance with respect to the symmetry G . An invariant set Γ of the mapping which is also invariant under the application of a symmetry (i.e., $G\Gamma = \Gamma$) is called symmetric. Symmetric sets, Γ_s , can include invariant curves of the mapping and trajectories (periodic or aperiodic), in which case we talk of symmetric trajectories. An attractor or repeller cannot be symmetric (see below). A symmetric trajectory intersects a symmetry line since for any $x \in \Gamma_s$,

$$Gx = L^i x \in \Gamma_s \quad \text{for some } i \in \mathbb{Z} \tag{3.17}$$

implies that

$$G(L^{i/2}x) = L^{i/2}x \quad \text{or} \quad L^{-1} \circ G(L^{(i-1)/2}x) = L^{(i-1)/2}x, \tag{3.18}$$

accordingly as i is even or odd [using eq. (3.11)]. Conversely, any trajectory that intersects the symmetry line of G (i.e., contains a point $y: Gy = y$) is symmetric with respect to G . This is because

$$L^i y = L^i(Gy) = G(L^{-i}y), \tag{3.19}$$

which shows that its forward orbit is the reflection by G of its backwards orbit. Moreover since the points of the forward and backwards orbits are iterations of $y \in \text{Fix}(G)$ by some positive or negative power of L , it follows from (3.14a) that every point of a symmetric trajectory lies on a symmetry line. This is consistent with the fact that the trajectory is symmetric with respect to the entire family of symmetries.

The symmetric periodic orbits are particularly important examples of symmetric trajectories. Every point of a symmetric periodic orbit not only lies on a symmetry line, but it lies at the intersection of a subfamily of symmetry lines, namely the lines of $L^{2in}G$, $i \in \mathbb{Z}$ if $L^n y = Gy = y$ [cf. eq. (3.14a)]. Conversely, the point of intersection of any two symmetry lines is necessarily a (symmetric) periodic point since

$$L^p \circ Gy = y \quad \text{and} \quad L^q \circ Gy = y \quad \Rightarrow \quad (L^p \circ G) \circ (L^q \circ G)y = L^{p-q}y = y, \tag{3.20}$$

after using (3.11). Consequently this is how symmetric periodic orbits arise (e.g., the six-cycle in fig. 3.1) and can be located (cf. Ichikawa et al. [1989], Jung and Richter [1990], Richter et al. [1990]). A special case of (3.20) occurs when $y \in \text{Fix}(G)$ (i.e., $p = 0$) and $y \in \text{Fix}(L^{-2r} \circ G)$ (i.e., $q = -2r$), with $L^r y \neq y$. This is equivalent to saying that y and $L^r y \neq y$ lie on the same symmetry line [cf. eq. (3.14a)], and (3.20) indicates that y is a periodic point of period $2r$. This implies that a symmetric trajectory can have at most two points on a given symmetry line, in which case it is a cycle of even period. It can be additionally checked that for any symmetric n -cycle, n even, with $Gy = y$ the halfway round point $L^{n/2}y$ lies on the same symmetry line [take $x = y$ in (3.17) and note that $Gy = y = L^n y$]. Therefore a symmetric periodic orbit has even period if and only if it contains two points on a symmetry line.

Another special case of (3.20) occurs when y and $L'y$ are, respectively, fixed points of $H = L \circ G$ and G . In this case y is a fixed point of L^{2r+1} and necessarily has odd period. Furthermore any symmetric cycle with odd period and with a point on the symmetry line of G has a point on the symmetry line of $H = L \circ G$ (e.g., the seven-cycle in fig. 3.1).

The fact that every point of a symmetric periodic orbit lies on a symmetry line and that the symmetry lines are smooth curves is very evident when one numerically finds and plots many periodic orbits of a reversible mapping (see, e.g., figures in Gumowski and Mira [1980]). Conversely, according to MacKay [1982, section 1.1.4.5], Greene has used the fact that periodic points of a perturbation of a reversible mapping did not appear to admit a smooth curve through them, to suggest that the perturbation is not reversible. Tanikawa and Yamaguchi [1987, 1989] have proved theorems about the ordering of symmetric periodic orbits of different periods on a symmetry line which are reminiscent of Sarkovskii's theorem for mappings of the interval (cf. also Andrews [1989]). The simplest case of a symmetric periodic orbit is a symmetric fixed point which is a point x_0 that satisfies (3.16) and has $Gx_0 = x_0$. It is also the general case as every point of a periodic orbit can be discussed as a fixed point of some power of L . From (3.14) it follows that every symmetry line of a family of symmetry lines passes through a symmetric fixed point. Thus symmetric fixed points act as a focus for the "web" that the symmetry lines form in the plane, cf. fig. 3.1 and Piña and Jiménez Lara [1987], Piña and Cantoral [1989].

Although the Jacobian determinant J of an arbitrary reversible mapping varies throughout the plane, symmetric periodic orbits are significant in that their return Jacobian determinant equals ± 1 . This follows from differentiating (3.10) with $i = n$ and using $L^n y = Gy = y$,

$$dL^n(GL^n y) dG(L^n y) dL^n(y) = dG(y) \Rightarrow \{\text{Det}[dL^n(y)]\}^2 = 1. \quad (3.21)$$

When the component involutions H and G of $L = H \circ G$ are orientation-reversing, the Jacobian determinant of L is necessarily positive (L is orientation-preserving) and the return Jacobian determinant of symmetric periodic orbits equals $+1$. This suggests some approximate area-preservation property after traversal of the periodic orbit, or equivalently a local "almost-area-preserving" environment around each point of an n -cycle when considered as a fixed point of L^n . Work done by Quispel and Capel [1989], which will be discussed in more depth in section 3.3, shows that this "almost-area-preserving" property associated with symmetric periodic orbits often extends to higher orders.

The *linear* stability analysis of symmetric periodic orbits in orientation-preserving reversible mappings (on which we concentrate in this report) is the same as for cycles in measure- or area-preserving mappings so that cycles are generically elliptic or hyperbolic with real reciprocal eigenvalues. The normal forms for the linear part of the return mapping L^n at a point of the n -cycle are the same as those for a measure-preserving mapping around a fixed point, e.g.,

$$\begin{pmatrix} \lambda & 0 \\ 0 & \lambda^{-1} \end{pmatrix}, \quad \begin{pmatrix} \pm 1 & b \\ 0 & \pm 1 \end{pmatrix}, \quad \begin{pmatrix} \cos \theta & -\sin \theta \\ \sin \theta & \cos \theta \end{pmatrix}. \quad (3.22)$$

The KAM theorems of Arnol'd and Sevryuk show that the *nonlinear* stability of symmetric elliptic periodic orbits is also the same as that in area-preserving mappings, i.e., a symmetric elliptic periodic orbit is in general stable because it is surrounded arbitrarily closely by nested closed invariant curves that are symmetric. This "conservative" behaviour of reversible mappings associated with symmetric sets will be discussed in chapter 5 and is very evident from the curves and islands shown in fig. 1.3.

When an invariant set Γ of a reversible mapping with symmetry G is not symmetric, there are two remaining possibilities: (i) $\Gamma \cap G\Gamma = \emptyset$, the empty set; or (ii) $\Gamma \cap G\Gamma = V$, V nonempty. In the first

case, we call the invariant set Γ asymmetric and denote it by Γ_a . In this case $G\Gamma_a$ is an invariant set distinct from Γ_a . In the second case, V is a strict subset of Γ and $G\Gamma$, and is a symmetric invariant set. Hence in this case the union of Γ and $G\Gamma$, which is also an invariant set, is composed of a symmetric invariant subset and a pair of asymmetric invariant subsets. In general then an invariant set of a reversible mapping is symmetric, asymmetric, or composed of symmetric invariant subsets and pairs of asymmetric invariant subsets. Periodic orbits are necessarily symmetric or asymmetric. Attractors, whether they be periodic orbits or not, are necessarily asymmetric so that an example of a Γ_a is an attractor A with basin of attraction B . Then it is not hard to show that GA is a repeller with basin of repulsion GB . This follows from the fact that L and L^{-1} are conjugate [cf. eq. (3.4)] and GA is therefore an attractor for L^{-1} because possession of an attractor is invariant under conjugacy.

Therefore, attractors and repellers come in pairs in reversible mappings, as shown by the attracting fixed point in fig. 1.3 and its reflection, which is a repelling fixed point. In the simple case of a periodic attractor A , this can also be understood by noting that the periodic orbit GA always has the opposite linear stability to A , i.e., the eigenvalues of its return Jacobian are the reciprocals of those of A . This property was stated in Politi et al. [1985, 1986a, b] and independently proved in Feingold et al. [1988]. At the level of fixed points it says that if x_0 is an asymmetric fixed point [i.e., it satisfies (3.16) with $Gx_0 \neq x_0$] and has eigenvalues λ and μ , then the fixed point Gx_0 has eigenvalues λ^{-1} and μ^{-1} . This follows because (3.4) is a differentiable conjugacy if G is a diffeomorphism, and thus the matrices $dL^{-1}(Gx_0)$ and $dL(x_0)$ share the same eigenvalues. But $dL^{-1}(Gx_0)$ is the inverse of the matrix $dL(Gx_0)$ and hence the eigenvalues of $dL(Gx_0)$ are reciprocals of those of $dL(x_0)$, i.e., λ^{-1} must be an eigenvalue of $dL(Gx_0)$ if λ is an eigenvalue of $dL(x_0)$.*) As usual the result for periodic orbits (n -cycles) follows by using the conjugacy between L^n and L^{-n} . Note however that asymmetric periodic orbits may have return Jacobian determinants equal to 1 and be linearly (elliptically) stable, and still be attracting or repelling – see chapter 4.

An attractor or repeller in a reversible mapping cannot intersect a symmetry line because this would imply that they are symmetric.***) Then $A = GA$, and A or GA would need to be an attractor and a repeller at the same time which is impossible. This explains why symmetric sets cannot be attractors or repellers. Symmetry lines in the vicinity of an attractor or a repeller line up parallel to one another in contrast to their behaviour near symmetric periodic orbits cf. fig. 3.1, and chapter 6 where the dissipative behaviour in reversible mappings associated with their asymmetric sets will be discussed.

3.2. *Generating reversible mappings and involutions from symmetric second order difference equations*

The previous section was largely theoretical in nature and gave an indication of the many properties that arise when a mapping L satisfies the reversibility condition (3.1). Of immediate practical interest is how difficult it is to find mappings that satisfy this property. Some reversible mappings arise naturally

*) This relation holds in any dimension for reversible mappings. Of course it also applies to symmetric fixed points $x_0 = Gx_0$ or symmetric periodic orbits and shows that their linear stability is similar to symplectic mappings in that eigenvalues must come in reciprocal pairs. For measure-preserving mappings, the restriction that the eigenvalues have a product of 1 is less severe. In higher dimensions, periodic orbits in measure-preserving systems are typically unstable. The importance of reversibility in these systems is that it can stabilise symmetric orbits, giving these systems their only stable orbits. Non measure-preserving systems, on the contrary, typically have attractors. The importance of reversibility in these systems is that it can give rise to the conservative behaviour associated with symmetric periodic orbits whilst still allowing coexisting dissipative and expansive behaviour.

**) Note that for an aperiodic attractor the proof (3.19) needs to be modified to account for the fact that the attractor is not the trajectory of some point. The proof can be done by assuming that there is a dense orbit on the attractor, i.e., an orbit of some point of the attractor which comes arbitrarily close to each other point of it.

from a physical problem (e.g., from a surface of section of a reversible differential equation). The point of this section is to show that many reversible mappings and their component involutions can be found by considering symmetric second order difference equations, using the fact that any second order difference equation can be rewritten as two coupled first order difference equations. The reversible mappings found in this way include the important forms of area-preserving mapping previously studied in the literature and some non measure-preserving mappings that will be discussed in later chapters.

A lot of the mappings of the plane that have been studied arise from second order difference equations,

$$H(x_{n+1}, x_{n-1}, x_n) = 0, \quad (3.23)$$

which have the property that they can be explicitly solved for x_{n+1} as a function of x_{n-1} and x_n , i.e.,

$$x_{n+1} = F(x_{n-1}, x_n). \quad (3.24)$$

By using the identification

$$(x_{n-1}, x_n) \leftrightarrow (x, y) = \mathbf{x}, \quad (x_n, x_{n+1}) \leftrightarrow (x', y') = \mathbf{x}', \quad (3.25a, b)$$

we can associate (3.24) with the mapping of the plane

$$L: x' = y, \quad y' = F(x, y). \quad (3.26)$$

(Note that some authors make the alternative identification $(x_{n-1}, x_n) \leftrightarrow (y, x)$; for higher order recurrence relations and their relation to mappings cf. Angenent [1990]). Conversely, many, but certainly not all, mappings of the plane $x' = f(x, y)$, $y' = g(x, y)$ can be written as a second order difference equation. Certainly a sufficient condition for this to be possible is for $x' = f(x, y)$ to be solvable explicitly for $y(x, x')$ or for $y' = g(x, y)$ to be solvable explicitly for $x(y, y')$, e.g., if $f(x, y)$ is linear in y or $g(x, y)$ is linear in x . A second order difference equation can then be created on substitution for the solved variable into the other equation of the mapping (with an appropriate identification).

One way to create *reversible* mappings of the plane is to consider second order difference equations that are symmetric, i.e.,

$$H(x_{n+1}, x_{n-1}, x_n) = H(x_{n-1}, x_{n+1}, x_n), \quad (3.27)$$

which ensures that (3.23) can be solved for x_{n-1} with the same dependence on x_{n+1} and x_n as x_{n+1} has on x_{n-1} and x_n (assuming still that we can explicitly solve for x_{n+1}), i.e.,

$$x_{n+1} = F(x_{n-1}, x_n) \Leftrightarrow x_{n-1} = F(x_{n+1}, x_n). \quad (3.28)$$

In this case the difference equation (3.23) is invertible (backward iterates are uniquely specified) and we can show that the mapping (3.26) derived from such a symmetric difference equation is reversible. Taking

$$S: x' = y, \quad y' = x, \quad (3.29)$$

we find that

$$L \circ S \circ L(x, y) = (y, F(F(x, y), y)). \quad (3.30)$$

From (3.28) with (3.25a, b) we have

$$F(F(x, y), y) = x, \quad (3.31)$$

and hence

$$L \circ S \circ L = S. \quad (3.32)$$

Since S is an involution, the mapping L is reversible [cf. eq. (3.32) with (3.1)]. It follows that $L \circ S$ is also an involution

$$L \circ S: x' = y, \quad y' = F(y, x). \quad (3.33)$$

This shows that if a mapping of the plane can be reduced to a second order difference equation that is symmetric, then it is reversible.

If, as well as being symmetric, the difference equation (3.23) is such that

$$H(-x_{n+1}, -x_{n-1}, -x_n) = \pm H(x_{n+1}, x_{n-1}, x_n), \quad (3.34)$$

then $F(-x_{n-1}, -x_n) = -F(x_{n-1}, x_n)$, and the derived mapping L in (3.26) is odd since it commutes with

$$O: x' = -x, \quad y' = -y. \quad (3.35)$$

Then the mapping $T = S \circ O = O \circ S$, i.e.,

$$T: x' = -y, \quad y' = -x, \quad (3.36)$$

is a symmetry of L distinct from the family generated by S [cf. (3.7a, b) with $G = S$, $M = O$ and note that T is an involution]. As a result $L \circ T$ is also an involution, where

$$L \circ T: x' = -x, \quad y' = -F(y, x). \quad (3.37)$$

We have used symmetric, and symmetric-odd, second order difference equations to create various involutions $L \circ S$ and $L \circ T$. We now present some examples of difference equations (ΔE) together with their associated reversible mappings of the plane L and involutions $L \circ S$ and $L \circ T$ (the conditions on the functions listed after $L \circ T$ guarantee that L is odd). All the involutions obtained are orientation-reversing.

Example 1

$$\Delta E: \quad H(x_{n+1}, x_{n-1}, x_n) = x_{n+1} + x_{n-1} - f(x_n) = 0.$$

$$\text{Mapping:} \quad L: x' = y, \quad y' = -x + f(y); \quad (3.38)$$

$$\text{Involution: } L \circ S: x' = x, \quad y' = -y + f(x); \quad (3.39)$$

$$\text{Involution: } L \circ T: x' = -x, \quad y' = y - f(x), \quad f \text{ odd}. \quad (3.40)$$

Example 2

$$\Delta E: H(x_{n+1}, x_{n-1}, x_n) = x_{n+1}x_{n-1}f_3(x_n) - (x_{n+1} + x_{n-1})f_2(x_n) + f_1(x_n) = 0.$$

$$\text{Mapping: } L: x' = y, \quad y' = \frac{f_1(y) - xf_2(y)}{f_2(y) - xf_3(y)}; \quad (3.41)$$

$$\text{Involution: } L \circ S: x' = x, \quad y' = \frac{f_1(x) - yf_2(x)}{f_2(x) - yf_3(x)}; \quad (3.42)$$

$$\text{Involution: } L \circ T: x' = -x, \quad y' = \frac{f_1(x) - yf_2(x)}{-f_2(x) + yf_3(x)},$$

$$f_1/f_2 \text{ odd}, \quad f_3/f_2 \text{ odd}. \quad (3.43)$$

Example 3

$$\Delta E: H(x_{n+1}, x_{n-1}, x_n) = (x_{n+1}^3 + x_{n-1}^3)f(x_n) + (x_{n+1}^2 + x_{n-1}^2)m(x_n)$$

$$+ (x_{n+1} + x_{n-1})g(x_n) + h(x_n) = 0, \quad m^2 - 3fg < 0. \text{*)}$$

Mapping:

$$L: \begin{cases} x' = y, \\ (y'^3 + x^3)f(x') + (y'^2 + x^2)m(x') + (y' + x)g(x') + h(x') = 0; \end{cases} \quad (3.44)$$

Involution:

$$L \circ S: \begin{cases} x' = x, \\ (y'^3 + y^3)f(x) + (y'^2 + y^2)m(x) + (y' + y)g(x) + h(x) = 0; \end{cases} \quad (3.45)$$

Involution:

$$L \circ T: \begin{cases} x' = -x, \\ (y'^3 - y^3)f(x') + (y'^2 + y^2)m(x') + (y' - y)g(x') + h(x') = 0; \\ f/h, g/h \text{ odd}, m/h \text{ even}. \end{cases} \quad (3.46)$$

The mapping L in example 1 is an area-preserving mapping and is in fact one of the standard forms for area-preserving reversible mappings. We will call the mapping form (3.38) the McMillan form (after McMillan [1971]). Equation (1.23) is the McMillan form of the Hénon mapping. Its phase portrait is shown in fig. 3.2.

*) The point of this condition is that it guarantees that there is a unique solution x_{n+1} to $H(x_{n+1}, x_{n-1}, x_n) = 0$ by ensuring that $H(x_{n+1}, x_{n-1}, x_n)$ is a monotonic cubic polynomial in x_{n+1} .

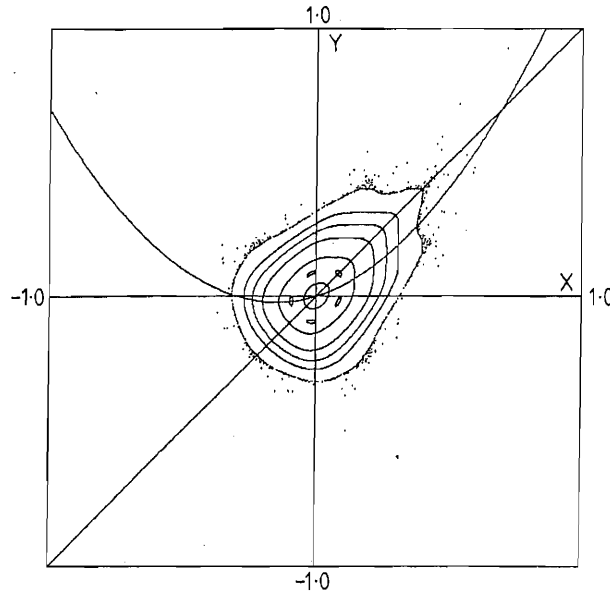


Fig. 3.2. Phase portrait of the Hénon mapping in McMillan form: $x' = y$, $y' = -x + 2Cy + 2y^2$, when $C = 0.3$. The symmetry lines $y = x$ and $y = Cx + x^2$ are shown. The origin is an elliptic symmetric fixed point. Another fixed point which is also symmetric, but hyperbolic, is at the other point of intersection of the symmetry lines, i.e., at $(1 - C, 1 - C) = (0.7, 0.7)$.

Table 3.1 presents, as well as the McMillan form, two other well known and well studied forms of area-preserving reversible mappings. The generalised standard form is the composition of one involution of the type (3.39) and one involution of the type (3.40). These involutions are orientation-reversing and area-preserving. The Chirikov–Taylor or standard mapping (1.25) is of generalised standard form with $f(y) = y$ and $g(x') = (K/2\pi) \sin 2\pi x'$. Because $f(y)$ and $g(x')$ are both odd, it can be decomposed

Table 3.1
Three classes of area-preserving reversible mappings $L = H \circ G$.

Class	Mapping L	Involutions		Fixed points
		H [symmetry line]	G [symmetry line]	
Generalised standard	$x' = f(y) + x$ $y' = g(x') + y$, g odd	$x' = -x$ $y' = y - g(x)$, g odd [$x = 0$]	$x' = -x - f(y)$ $y' = y$ [$x = -f(y)/2$]	$(x_0, y_0): g(x_0) = f(y_0) = 0$
Generalised standard	$x' = f(y) + x$, f odd $y' = g(x') + y$	$x' = x$ $y' = -y + g(x)$ [$y = g(x)/2$]	$x' = x + f(y)$, f odd $y' = -y$ [$y = 0$]	$(x_0, y_0): g(x_0) = f(y_0) = 0$
McMillan	$x' = y$ $y' = -x + f(y)$	$x' = x$ $y' = -y + f(x)$ [$y = f(x)/2$]	$x' = y$ $y' = x$ [$y = x$]	$(x_0, x_0): f(x_0) - 2x_0 = 0$
De Vogelaere	$x' = f(x) - y$ $y' = x - f(x')$	$x' = y + f(x)$ $y' = x - f(x')$ [$y = x - f(x)$]	$x' = x$ $y' = -y$ [$y = 0$]	$(x_0, 0): f(x_0) - x_0 = 0$

into the product of involutions in two ways [this double reversibility occurs because (1.25) commutes with (3.35) – cf. (3.7a, b)]. The generalised standard form is important because it includes the other two forms in table 3.1 via coordinate transformations. A mapping in McMillan form (3.38) can be written in generalised standard form by using the transformation $x \rightarrow x$, $y \rightarrow x - y$. Figure 3.3 shows a phase portrait of Hénon's mapping in generalised standard form. Mappings in de Vogelaere form can also be transformed to generalised standard form because they can be transformed to McMillan form via $x \rightarrow y$, $y \rightarrow x - f(y)$. Although it is not possible to convert an arbitrary mapping in generalised standard form into McMillan form, many mappings of physical interest can always be written in McMillan form so that it is practically a very important form (cf. Laslett [1978, 1986]).

The involutions of examples 2 and 3 above are not in general area-preserving. Their Jacobian determinants are given by $\pm \partial y' / \partial y$, which can be found by implicit differentiation in example 3. Since a reversible mapping is simply a combination of involutions, any non area-preserving involution can be coupled to another or to an area-preserving involution to form a non area-preserving reversible mapping. This approach will be used in the next chapter where mappings that are not area-preserving and *not* measure-preserving, like that depicted in fig. 1.3, will be constructed.

3.3. Testing for reversibility and local reversibility

In the previous sections we discussed reversibility and its consequences and then gave some examples of mappings that are reversible. In this and the next section we continue to explore the properties of reversibility but with a view to answering the question: how does one tell if a given mapping is reversible? Since reversibility gives a mapping a lot of dynamical structure, it is desirable to have a test for it and to explicitly find a reversing symmetry for the mapping.

Certainly some of the properties of reversibility can be used as necessary conditions to show that a

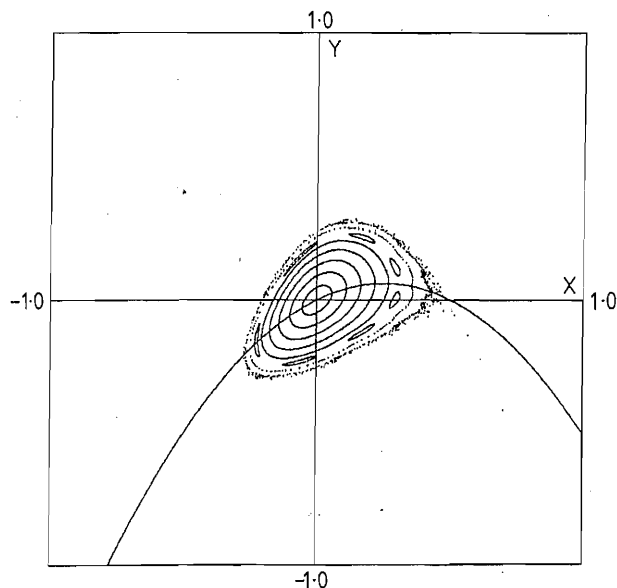


Fig. 3.3. Phase portrait of the Hénon mapping in generalised standard form: $x' = -y + x$, $y' = 2x'(1 - C - x') + y$, when $C = 0.5$. The symmetry lines are the x axis and the parabola $y = x(1 - C - x)$. The origin is an elliptic symmetric fixed point and $(1 - C, 0) = (0.5, 0)$ is a hyperbolic symmetric fixed point.

given mapping is *not* reversible. One of the most applicable is the reciprocal-eigenvalues property of pairs of asymmetric fixed points (or periodic orbits) in reversible mappings that was mentioned above in section 3.1. Firstly, consider a given non measure-preserving mapping; typically it has a fixed point at which $J \neq \pm 1$. If this mapping would be reversible, such a fixed point is necessarily asymmetric and so would have a partnering fixed point with reciprocal eigenvalues. If, in the given mapping, there is no such partner (which would be the typical case for an arbitrary mapping) then the non measure-preserving mapping can be declared not reversible. Consider now a measure- or area-preserving mapping which is also orientation-reversing. Now every fixed point has $J = -1$ and every odd-periodic orbit has a return Jacobian determinant of -1 . A possible symmetric fixed point in such a mapping must have eigenvalues $\{1, -1\}$ to be consistent with λ and λ^{-1} both being eigenvalues. Consequently, most fixed points in orientation-reversing conservative mappings can be ruled out as being possible symmetric fixed points, and then the mapping can be excluded as being reversible when possible asymmetric partners with reciprocal eigenvalues cannot be found for such points, cf. Roberts and Capel [1992b]. On the other hand, for an orientation-preserving measure- or area-preserving mapping, applying a reversibility test at the level of fixed points proves a lot less effective because every fixed point has $J = +1$. If a partner with reciprocal eigenvalues does not exist for a fixed point or periodic orbit, the most that can be concluded is that the fixed point or periodic orbit is necessarily symmetric if the mapping is reversible [in two dimensions all possible linearisations when $J = +1$ at a fixed point are consistent with it being a symmetric fixed point in a reversible mapping, cf. (2.22) and (3.22)]. Note that when $J = +1$, an asymmetric partner of a fixed point has the *same* eigenvalues as the fixed point because the eigenvalues of any fixed points are themselves reciprocals of one another.

An explicit example of an orientation-preserving area-preserving mapping that may not be reversible is

$$R: x' = x + y + 1 - \cos y, \quad y' = y - C \sin x' - C(1 - \cos x'). \quad (3.47)$$

This mapping was created by Rannou [1974]. Its form is similar to the generalised standard form of table 3.1 but here neither $f(y) = y + 1 - \cos y$ nor $g(x') = -C \sin x' - C(1 - \cos x')$ is odd, so that it is not known whether it is reversible. An exception occurs when $C = 0$ in which case $g(x') \equiv 0$ is odd trivially and the mapping is reversible. The mapping (3.47) is a mapping of the torus, $-\pi < x \leq \pi$ and $-\pi < y \leq \pi$, so that x and y are taken mod 2π . It has two fixed points at $(0, 0)$ and $(-\pi/2, 0)$ which are elliptic for $0 < C < 4$ and $-4 < C < 0$, respectively. Because these parameter intervals are different, the two points are not an asymmetric pair if the mapping is reversible and so can only be symmetric. A phase portrait of Rannou's mapping (cf. Rannou [1974]) shows no obvious global symmetry like that seen in the reversible mappings in figs. 3.1, 3.2 and 3.3, but this apparent lack of symmetry is also found in many reversible mappings that do not have a linear reversing symmetry (i.e., it is hard to "see" the effect of nonlinear reversing symmetries).

Although not studying reversibility as such, Rannou created (3.47) to avoid "hidden symmetries" obtained in numerical results on other mappings which were reversible.* No such symmetry in the results was observed for (3.47). This appears to be the reason that Rannou's mapping has been suggested in the literature as not being reversible (cf. Greene et al. [1981], MacKay [1983a]; also Grebogi and Kaufman [1981]). In this and the next section we describe a method for telling whether

* Rannou's interest was to study the effect of round-off errors in mappings of the plane. This was done by studying (3.47) on a lattice so that x and y took a finite number of values and the mapping could be defined on the integers (cf. Rannou [1974] and also Hénon [1983], section 9).

nonconservative mappings, as well as a special class of area-preserving mappings, are not reversible. The reversibility or nonreversibility of Rannou's mapping, however, remains an open question.

A mapping is called *locally* reversible by MacKay if it is reversible in some region of the plane (cf. MacKay [1982, section 1.1.4.5]). That is, the defining relation $L \circ G \circ L = G$ holds for some involution G in some region of the plane, or, equivalently, the mapping can be written as the composition of two involutions in some region. Obviously all reversible mappings as defined in section 3.1 (which might be called "globally" reversible mappings) are locally reversible everywhere. The converse need not be true.

The concept of local reversibility we use here is that of local reversibility to order n about a fixed point. It involves finding out whether a mapping is reversible in a Taylor expansion to order n about the fixed point. This idea was introduced in Quispel and Capel [1989] and we follow the treatment given there. The first step of this method is to identify a fixed point p of a given mapping L as necessarily symmetric if the mapping would be reversible by comparing its eigenvalues to those of other fixed points, as outlined above. This point is therefore a common fixed point of the mapping and any possible symmetry.

Assume then that the mapping L has a Taylor series expansion of order n in a neighbourhood of p – a sufficient condition is that L is C^k , $k > n$. This obviously includes mappings that are analytic in a neighbourhood of the point. Then consider mappings \tilde{G} which also have Taylor expansions of order n around the fixed point p and are involutory to order n in a neighbourhood of p , i.e., $\tilde{G} \circ \tilde{G} = \text{Id} + O_{n+1}$, where the O_{n+1} notation stands for terms of order $n+1$ and higher. The class of mappings \tilde{G} obviously includes all C^k involutions of the plane, $k > n$, and in particular analytic involutions. Substituting such a \tilde{G} into $L \circ \tilde{G} \circ L = \tilde{G}$ and equating both sides of this relation to order n leads to necessary conditions on the coefficients of the expansion of L up to order n in order for a \tilde{G} to exist. If these conditions are satisfied, and therefore to order n there exists a \tilde{G} , the mapping is called locally reversible to order n around the fixed point. On the other hand, if these conditions are not satisfied then local reversibility with respect to the class of mappings \tilde{G} is ruled out. Consequently, global reversibility of L with respect to all C^k involutions, $k > n$ (as well as all analytic involutions) is also ruled out. It is in this sense that we then call L *not* reversible.

Note that the necessary conditions for local reversibility derived in the way just described are precisely the same as those for reversibility of a "formal" diffeomorphism with respect to a "formal" reversing symmetry. Here "formal" refers to a mapping or involution defined by an infinite power series expansion about a fixed point, without regard to convergence of the series. Analytic mappings or involutions are a special case of formal ones when the series does indeed converge in a neighbourhood of the point (for some more discussion of "formal" properties of diffeomorphisms see, e.g., Broer and Takens [1989]). It is readily verified that local reversibility as described has many of the important properties of global reversibility discussed in section 3.1. For example, if L is locally reversible to order n with \tilde{G} being the reversing involution to order n , then we have:

- (i) $\{L^i \circ \tilde{G}\}$ are also reversing involutions to order n ;
- (ii) L^i is locally reversible to order n , with reversing involution \tilde{G} ;
- (iii) local reversibility is maintained under coordinate transformations, i.e., $P \circ L \circ P^{-1}$ is locally reversible to order n with $P \circ \tilde{G} \circ P^{-1}$ being the reversing involution to order n .

Furthermore, the various alternative ways of expressing the global reversibility property are also equivalent at the level of local reversibility to order n . For example, since a reversible mapping can be written

$$L = U \circ R, \tag{3.48}$$

where U and R are involutions, and since locally about a symmetric fixed point an orientation-reversing involution U can be written as

$$U = P \circ V \circ P^{-1}, \tag{3.49}$$

with V given by (3.13b), the following relation holds for a reversible mapping L about a symmetric fixed point:

$$P^{-1} \circ L = V \circ P^{-1} \circ R, \tag{3.50}$$

for some coordinate transformation P^{-1} and involution R . In the common case when L is orientation-preserving, R is necessarily orientation-reversing if U is orientation-reversing.

The formulation (3.50) can be used to investigate local reversibility conditions (cf. Brown [1991] for a different approach). Assume the (possibly symmetric) fixed point to be at the origin and expand L , R and P^{-1} “formally” around this point in Taylor series. The expansion for the mapping L , assumed orientation-preserving, can be chosen to be

$$\begin{aligned} x' &= ax + by + f_{20}x^2 + f_{11}xy + f_{02}y^2 + f_{30}x^3 + f_{21}x^2y + f_{12}xy^2 + f_{03}y^3 + \dots, \\ y' &= cx + dy + g_{20}x^2 + g_{11}xy + g_{02}y^2 + g_{30}x^3 + g_{21}x^2y + g_{12}xy^2 + g_{03}y^3 + \dots, \end{aligned} \tag{3.51}$$

with $ad - bc = 1$ and the linear part, which we will write as (a, b, c, d) , given by one of eqs. (3.22). The possible involution R is assumed to be orientation-reversing, in line with the common case that reversibility of mappings is with respect to orientation-reversing involutions. Consequently, the expansion for R must have a linear part of the form (3.12).

Following the general procedure described above, the expansions for L , R and P^{-1} are substituted into (3.50) and equating like terms on each side leads to relations connecting their coefficients. The coefficients for R and P^{-1} can be eliminated to give necessary conditions on the coefficients of the mapping L which ensure the existence of solutions for R and P^{-1} satisfying (3.50) up to n th order terms in x and y . If these conditions are satisfied, calculation of the R and P^{-1} which satisfy (3.50) to order n can be achieved. Typically, not all the coefficients of R and P^{-1} are completely determined so that some choice is available. Table 3.2 summarises the necessary conditions on the second and third order coefficients of the expansion of L for the most common forms of its linear part. In case 1 is included the case when the point is elliptic with complex-conjugate eigenvalues. As remarked in section 2.2, this complex linear part differs from the real linear part on the right hand side of (3.22) but the respective expansions can be related to one another via a linear transformation. Note that for the typical linear parts of an orientation-preserving mapping given in table 3.2, the only possible reversing symmetries are orientation-reversing in line with the assumption on R above (an orientation-preserving reversible mapping is either the product of two orientation-reversing involutions or two orientation-preserving involutions; the latter must have linear part equal to $-I$ (I is the identity matrix) about a symmetric fixed point, which implies that $dL = I$ at the point).

We illustrate the application of the local reversibility tests with the following example [Quispel and Capel 1989]:

$$L: x' = x + \omega(y) \pmod{1}, \quad y' = \frac{y + (K/2\pi) \sin(2\pi x')}{1 - yh(x')}. \tag{3.52}$$

Table 3.2

Necessary conditions for a mapping L to be locally reversible around a symmetric fixed point. The conditions relate the coefficients of the expansion of L , given in (3.51), when its linear part has one of the typical canonical forms shown.

Linear part	Case	Second order	Third order
$\begin{pmatrix} \lambda & 0 \\ 0 & \lambda^{-1} \end{pmatrix}, \lambda \neq \pm 1$	1	no condition	$(\lambda - 1)(\lambda g_{12} + \lambda^{-1} f_{21} - f_{11} g_{11} - 2f_{02} g_{20}) + f_{20} f_{11} (\lambda^{-2} - 2\lambda^{-1}) + g_{11} g_{02} (2\lambda^2 - \lambda^3) = 0$
$\begin{pmatrix} 1 & b \\ 0 & 1 \end{pmatrix}, b \neq 0$	2a ^{a)}	$g_{11} + 2f_{20} - 2bg_{20} = 0$	if $g_{20} = 0$ then $3b^2 g_{30} - bg_{21} - 3bf_{30} + 2f_{20} g_{02} + f_{20} f_{11} - 3bf_{20} g_{11} = 0$
	2b ^{b)}	$g_{20} = 0$	$6b^2 g_{30} - 2bg_{21} - 6bf_{30} + 2f_{20} g_{02} + bf_{20} g_{11} + 6bf_{20}^2 + 2bg_{11}^2 - f_{11} g_{11} - g_{11} g_{02} = 0$
$\begin{pmatrix} -1 & b \\ 0 & -1 \end{pmatrix}, b \neq 0$	3	no condition	$12bg_{30} + 4g_{21} + 12f_{30} + 2g_{11}^2 + 2f_{20} g_{11} + 22bf_{20} g_{20} + 10b^2 g_{20}^2 + 10f_{11} g_{20} + 11bg_{20} g_{11} + 4g_{20} g_{02} + 12f_{20}^2 = 0$

^{a)} If linear part of involution R is $\begin{pmatrix} 1 & b \\ 0 & -1 \end{pmatrix}$. ^{b)} If linear part of involution R is $\begin{pmatrix} -1 & b \\ 0 & 1 \end{pmatrix}$.

For $h(x') = 0$ and $\omega(y) = y$, this mapping reduces to the Chirikov–Taylor or standard mapping given by (1.25) which is area-preserving and reversible. Otherwise, if $h(x')$ is nonzero and also odd, or $\omega(y)$ is odd, then it can be shown that the mapping is also reversible [Quispel 1988]. It then belongs to a class of reversible non measure-preserving mappings that will be constructed in the following chapter (cf. class IV, section 4.2). We consider the case when ω and h are not odd functions but contain an even part via the modifications

$$\omega(y) = \omega_{\text{odd}}(y) + \omega_2 y^2, \quad h(x) = h_0 + h_{\text{odd}}(x), \quad (3.53)$$

where ω_{odd} and h_{odd} are arbitrary odd functions and ω_2 and h_0 are constants.

We want to know whether (3.52) with ω and h given by (3.53) is reversible, using the method of local reversibility. The fixed points (x_0, y_0) of the mapping (3.52) have to satisfy

$$\omega(y_0) \in \mathbb{Z}, \quad (K/2\pi) \sin(2\pi x_0) = -y_0^2 h(x_0).$$

For $y_0 = 0$, we have fixed points at $x_0 = 0$ and $x_0 = 1/2$. Expanding ω and h about 0,

$$\omega(y) = \omega_1 y + \omega_2 y^2 + \omega_3 y^3 + O_5, \quad h(x) = h_0 + h_1 x + O_3,$$

we find that the eigenvalues of dL at $(x_0, y_0) = (0, 0)$ are determined by

$$(1 - \lambda)^2 = K\lambda\omega_1, \quad (3.54)$$

from which it follows that $\text{Det } dL(0, 0) = 1$. The eigenvalues are different from those at $(x_0, y_0) = (1/2, 0)$ if $K\omega_1 \neq 0$, and are in general also different from the eigenvalues at possible fixed points with $y_0 \neq 0$. Therefore, the origin is a symmetric fixed point if (3.52) is reversible.

To investigate the local reversibility conditions around the origin, we expand the mapping to third order around this point. The result is

$$L: \begin{cases} x' = x + \omega_1 y + \omega_2 y^2 + \omega_3 y^3, \\ y' = Kx + \Omega y + (Kh_0)xy + (K\omega_2 + h_0\Omega)y^2 + g_3 x^3 + (3\omega_1 g_3 + Kh_1)x^2 y \\ \quad + (3\omega_1^2 g_3 + h_1\Omega + K\Psi)xy^2 + (K\omega_3 + \omega_1^3 g_3 + K\omega_2 h_0 + \Omega\Psi)y^3, \end{cases} \quad (3.55)$$

$$g_3 := -2\pi^2 K/3, \quad \Omega := 1 + K\omega_1, \quad \Psi := h_0^2 + \omega_1 h_1.$$

Applying to this expansion the linear transformation

$$X = (\lambda^{-1} - 1)x - \omega_1 y, \quad Y = (\lambda - 1)x - \omega_1 y, \quad (3.56)$$

together with (3.54), brings its linear part into the diagonal form $(\lambda, 0, 0, \lambda^{-1})$. The transformed second order and third order coefficients in the expansion are most easily found using an algebraic manipulation program. Substitution into the third order local reversibility condition for case 1 of table 3.2 yields

$$\frac{-2\omega_2 h_0 (\lambda - 1)\lambda}{\omega_1^3 (\lambda + 1)^2} = 0. \quad (3.57)$$

From (3.57), it follows that the mapping is not locally reversible at third order at the origin if $\omega_2 h_0 \neq 0$, i.e., when both $\omega(y)$ and $h(x')$ contain an even part. Consequently, the mapping is not globally reversible.

It is significant that the above mapping (3.52) was not measure-preserving. The results of applying the test to a measure-preserving mapping follow from comparison of table 3.2 with the necessary conditions for local measure preservation in table 2.1. It is seen that the conditions for cases 1, 2 and 3 of table 2.1 are identical to those for cases 1, 2a and 3 of table 3.2. Therefore, to third order the necessary conditions for local reversibility are immediately satisfied by measure-preserving mappings in all the cases of the linear parts shown. Consequently, this analysis to third order cannot be used to find measure-preserving mappings that are not reversible. In fact, this equivalence between local measure preservation and local reversibility extends to arbitrary order for measure-preserving mappings when the fixed point has a (normalised) Jacobian matrix given by the cases of table 3.2 (cf. Roberts and Capel [1992b]). This follows by observing that around such fixed points in measure-preserving mappings there is a formal transformation to a normal form which is locally reversible (cf. Birkhoff [1920], Moser [1956, 1968], Simó [1980]). Considering each case of table 3.2 in turn we have:

(i) *Case 1.* When the fixed point is hyperbolic (i.e., it is a saddle point) the normal form can be written

$$x' = xh(xy), \quad y' = y/h(xy) \quad (3.58)$$

with the function h uniquely determined and $h(0) = \lambda$. The mapping (3.58) can be verified to be reversible with symmetry $S: x' = y, y' = x$. Moser [1956] has actually shown that the transformation to this form is more than just formal because a coordinate transformation can be found which converges in a neighbourhood of the point. When the fixed point is elliptic, $\lambda = e^{+i\theta}$ and $\lambda^{-1} = e^{-i\theta}$, with $\theta/2\pi$ irrational, the normal form can be written

$$x' = x \cos \omega - y \sin \omega, \quad y' = x \sin \omega + y \cos \omega \quad (3.59)$$

with $\omega = \theta + S(r)$ where $S(r) = s_1(x^2 + y^2) + \dots$ is an infinite power series in $r = x^2 + y^2$. Equation (3.59) has the same form as the linear part of the mapping – rotation around the origin. It is reversible, again with symmetry $S: x' = y, y' = x$. In general the transformation taking the mapping to the form (3.59) is *only* formal; it does not converge in any neighbourhood of the fixed point. However, a convergent (area-preserving) transformation can always be found such that the transformed mapping agrees with the normal form (3.59) to any desired finite order [Siegel and Moser 1971, section 23]. Consequently, the mapping around the elliptic fixed point is locally reversible to any finite order.

(ii) *Case 2.* When the fixed point is parabolic with repeated eigenvalue $+1$ and its Jacobian has nondiagonal Jordan normal form (i.e., $b \neq 0$), it follows from Simó [1980] that the expansion around the point can be brought to the form

$$x' = x + y + O_{n+1}, \quad y' = y + F_n(x + y) + O_{n+1}, \quad (3.60)$$

where $F_n(x + y)$ is a polynomial in $(x + y)$ with terms of degree 2 to n , and n is an arbitrary integer. The expansion to order n is reversible with $G: x' = x + y, y' = -y$ (cf. the generalised standard form of table 3.1) which corresponds to local reversibility case 2a of table 3.2.

(iii) *Case 3.* When the fixed point is parabolic with repeated eigenvalue -1 and $b \neq 0$, it follows from a similar procedure to that used in case 2 (cf. Roberts and Capel [1992b]) that the normal form is

$$x' = -x - y + O_{n+1}, \quad y' = -y + F_n(x + y) + O_{n+1}, \quad (3.61)$$

where F_n is again a polynomial with terms of degree 2 to n , and n is an arbitrary integer. The expansion to order n is reversible with $G: x' = -x - y, y' = y$.

It appears that, even when a normal form is not instantly recognisable as locally reversible as above, normal forms can play an important role in local tests for reversibility, in the same way that they do in local stability analysis (cf. Mira [1987]). For example, around a nonresonant elliptic fixed point ($\lambda^q \neq 1$), a real analytic mapping which is not necessarily area- or measure-preserving can always be formally brought to the complex form (cf. Moser [1968], Arrowsmith and Place [1990]),

$$L: x' = \lambda x + \sum_{i+j=k \geq 3} f_{ij} x^i y^j, \quad y' = \lambda^{-1} y + \sum_{i+j=k \geq 3} f_{ij}^* x^i y^j, \quad (3.62a, b)$$

where $\lambda = e^{i\theta}$, $\theta/2\pi$ is irrational, $i - j = 1$, and the symbol $*$ denotes complex conjugation. Furthermore, the reduction to the form (3.62) to a desired finite order can be achieved by an analytic (polynomial) transformation. Using the nonresonant normal form to develop local reversibility conditions leads to simpler conditions. For example, local reversibility to third order leads to the simple condition

$$\lambda^{-1} f_{21} + \lambda f_{21}^* = 0. \quad (3.63)$$

This is the same as the condition for measure preservation of (3.62) to third order. When transformed back via the nonlinear transformation used to obtain (3.62), the third order condition (3.63) becomes that listed for case 1 of table 3.2.

When we are interested at a theoretical level in identifying whether there is a difference at some order between measure preservation and reversibility, it makes sense to remove as many terms as possible from the mapping expansion and so use normal forms. On the other hand, when applying reversibility tests to a specific mapping, as on (3.52) above, some work is needed to achieve a normal form because it involves using a nonlinear transformation. It is practically desirable to have necessary reversibility conditions that only require a linear transformation before they can be used, as summarised in table 3.2. It may still turn out (particularly in higher dimensions) that the derivation of these conditions is best done by finding the condition for a normal-form mapping and then transforming this simpler condition by a nonlinear transformation. For more about an approach that uses normal forms to derive reversibility conditions, and leads to reversible normal forms, see Lamb et al. [1992] (reversible forms are also obtained in, e.g., Sevryuk [1986] and Moser and Webster [1983]).

We conclude this section by asking when local reversibility is not consistent with local measure preservation. From the comparison of tables 3.2 and 2.1, it is seen that at a symmetric fixed point reversibility is usually consistent with measure preservation at the point, at least to the order worked to here. However, case 2b of table 3.2 is not in general consistent with measure preservation. In chapter 7 this case will be related to a symmetry-breaking bifurcation that produces an attracting fixed point and a repelling fixed point from the symmetric fixed point.

3.4. Area-preserving mappings that are not reversible

The normal forms listed above indicate that the only possibilities for a mapping that is locally area-preserving (and orientation-preserving) around a fixed point to *not* be locally reversible are that the fixed point is parabolic with linearisation given by the identity matrix $I = (1, 0, 0, 1)$, or that the fixed point is a resonant elliptic fixed point with eigenvalues $\lambda = e^{\pm i\theta}$ where $\theta = 2\pi p/q$ and p, q are coprime. In this section we follow Roberts and Capel [1992a, b] who have studied the former case and shown that area-preserving mappings possessing a fixed point where the linearisation is the identity matrix are generally not locally reversible about this point and so cannot be globally reversible. The case where the linear part of the mapping expansion equals I was not considered in the analysis of the previous section as it is atypical compared to those in table 3.2. This special case is included in the local reversibility analysis of Brown [1991].

Consider a mapping L with fixed point p which has been identified as necessarily symmetric if L is reversible. We transfer the point to the origin 0 and assume that the mapping expansion takes the form

$$L: x' = x + f_2(x, y) + f_3(x, y) + O_4, \quad y' = y + g_2(x, y) + g_3(x, y) + O_4, \quad (3.64a, b)$$

where the k th order terms of x' are given by

$$f_k(x, y) = \sum_{i+j=k} f_{ij} x^i y^j, \quad (3.65)$$

and similarly for $g_k(x, y)$ for $k = 2$ and 3 , and the O_4 notation stands for 4th and higher order terms in x and y .

Area preservation of L imposes conditions on some of the coefficients f_{ij} and g_{ij} . The Jacobian determinant $J(x, y)$ of (3.64) takes the form

$$J(x, y) = 1 + \left(\frac{\partial f_2}{\partial x} + \frac{\partial g_2}{\partial y} \right) + \left(\frac{\partial f_3}{\partial x} + \frac{\partial g_3}{\partial y} - \frac{\partial f_2}{\partial y} \frac{\partial g_2}{\partial x} \right) + O_3.$$

Equating the first bracketed term to 0 implies

$$g_{11} = -2f_{20}, \quad g_{02} = -\frac{1}{2}f_{11}, \quad (3.66a, b)$$

so that when (3.64) is area-preserving, the second order coefficients are specified by just $\{f_{20}, f_{11}, f_{02}, g_{20}\}$. Similarly, equating the second bracketed term to 0 implies

$$g_{21} = -3f_{30} - 2f_{20}g_{11} + 2g_{20}f_{11}, \quad g_{12} = -f_{21} + 2f_{02}g_{20} - 2f_{20}g_{02}, \quad (3.67a, b)$$

$$g_{03} = -\frac{1}{3}(f_{12} + 2f_{11}g_{02} - 2f_{02}g_{11}), \quad (3.67c)$$

so that the third order coefficients are specified by $\{f_{30}, f_{21}, f_{12}, f_{03}, g_{30}\}$.

Consider now the case of a possible (orientation-reversing) symmetry G of (3.64) whose expansion around $\mathbf{0}$ has linear part $(1, 0, 0, -1)$,

$$G: x' = x + l_2(x, y) + l_3(x, y) + O_4, \quad y' = -y + m_2(x, y) + m_3(x, y) + O_4. \quad (3.68a, b)$$

It can be shown that if one wants (3.64), when area-preserving to third order, to have such a reversing symmetry, then necessary conditions on the coefficients in the expansion of L are

$$f_{20} = f_{02} = 0, \quad f_{11}^2 - 4f_{12} = 0. \quad (3.69a, b)$$

The conditions (3.69a, b) are derived by finding the inverse L^{-1} of the expansion (3.64) to third order and imposing local reversibility with respect to G in (3.68) to third order about the origin in the form

$$L \circ G = G \circ L^{-1}. \quad (3.70)$$

In doing this it is also necessary to impose that (3.68) is an involution to second order. The analysis reveals that condition (3.69a) is found to be necessary for local reversibility at second order and condition (3.69b) is needed for local reversibility at third order.

Conditions (3.69a, b) give additional constraints on the coefficients of L , when consistent with area preservation, to be locally reversible with respect to just one possible involution (3.68). Nevertheless, they can be used to generate additional necessary conditions for local reversibility when the involution has the expansion

$$G: \begin{cases} x' = px + qy + l_2(x, y) + l_3(x, y) + O_4, & (3.71a) \\ y' = rx - py + m_2(x, y) + m_3(x, y) + O_4, & (3.71b) \end{cases}$$

where p, q and r are arbitrary real numbers satisfying

$$p^2 + qr = 1. \quad (3.72)$$

The linear part of (3.71), together with (3.72), is the general form of dG about a symmetric fixed point for G orientation reversing [cf. eq. (3.12)]. The analysis for the simple orientation-reversing involution (3.68) can be used to handle the general case because: (i) the general linear part of the orientation-reversing involution (3.71) can be reduced by a linear transformation to that of (3.68), i.e., to $(1, 0, 0, -1)$; (ii) any linear transformation leaves the form of (3.64) invariant, which is an essential point and true precisely because its linear part is the identity; (iii) local reversibility is maintained under coordinate transformation; and (iv) area preservation to a certain order is maintained under a linear coordinate transformation. Consequently, the mapping L in (3.64) is reversible with respect to (3.71) for given $\{p, q, r\}$ only if, after applying to L a linear transformation that takes $(p, q, r, -p)$ to $(1, 0, 0, -1)$, we obtain $\tilde{f}_{20} = \tilde{f}_{02} = 0$ and $\tilde{f}_{11}^2 - 4\tilde{f}_{12} = 0$ in the transformed mapping \tilde{L} . These conditions can be rewritten in terms of the original coefficients of the mapping L .

What emerges from this analysis is that the linear parts of possible orientation-reversing involutions of (3.64), that is, the values of $\{p, q, r\}$ in (3.71), are determined by the second order coefficients of the mapping expansion and are finite in number. A thorough knowledge of the possible involution linear parts for a given mapping allows its set of possible involutions to be narrowed down (it can also be shown that there is always at least one possible linear part). A third order local reversibility condition for each possible orientation-reversing involution with a linear part allowed by the second order coefficients can then be found via a linear transformation of the coefficients appearing in (3.69b). Because the linear part of (3.64) equals the identity matrix I , we need also derive third order reversibility conditions for possible reversing symmetries which are orientation-preserving, with linear part equal to $-I$ (cf. Brown [1991], Roberts and Capel [1992b]). A mapping which satisfies *none* of the necessary conditions so obtained from each of its possible involution linear parts can be declared *not* reversible.

This philosophy can be illustrated in a direct way on the generalised standard mapping

$$L: x' = x + f(y), \quad y' = y + g(x'). \tag{3.73a, b}$$

As pointed out in section 3.2, this mapping is area-preserving for any functions f and g , and known to be reversible when f or g is an odd function (cf. table 3.1). Assume that the origin $\mathbf{0}$ is a fixed point with linearisation equal to the identity matrix and that about $\mathbf{0}$ the mapping expansion takes the form

$$L: \begin{cases} x' = x + f_n y^n + f_{n+1} y^{n+1} + O_{n+2}, & (3.74a) \\ y' = y + g_n x'^n + g_{n+1} x'^{n+1} + O_{n+2}, \quad n \geq 2. & (3.74b) \end{cases}$$

Of course, the typical case in (3.74) will be for $n = 2$ [when it becomes a special case of (3.64)] but the analysis and results for $n > 2$ in this example follow in a similar fashion. Assume that the n th order coefficients f_n and g_n in (3.74) satisfy

$$f_n \neq 0, \quad g_n \neq 0. \tag{3.75}$$

Because of the particular form of (3.73) the expansion (3.74) is automatically area-preserving to all orders, i.e., no conditions need be imposed on the coefficients as in the more general expansion (3.64).

However, there are conditions on the coefficients of (3.74) in order for it to be locally reversible around the origin (assuming $\mathbf{0}$ to be also fixed under possible reversing symmetries). It is found that the

coefficients f_n and g_n select the possible involution linear parts, and these coefficients together with the coefficients f_{n+1} and g_{n+1} are involved in necessary conditions for local reversibility at order $n+1$. By choosing the coefficients $\{f_n, g_n, f_{n+1}, g_{n+1}\}$ in (3.74) appropriately, we can ensure that none of the necessary conditions is satisfied and so rule out local reversibility of the mapping expansion (3.74) with respect to orientation-reversing symmetry expansions around the fixed point. It can be shown that the choices of coefficients that rule out local reversibility of (3.74) and (3.75) with respect to orientation-reversing symmetry expansions suffice to also exclude local reversibility with respect to orientation-preserving symmetry expansions. Consequently, global reversibility can be ruled out. This analysis is summarised in the following result [Roberts and Capel 1992a]:

An area preserving mapping (3.73) with expansion (3.74) and (3.75) around a fixed point, and having no other fixed point with linearization equal to the identity matrix, is not reversible if $f_{n+1} \neq 0$ and $g_{n+1} \neq 0$ and $\{f_n, g_n, f_{n+1}, g_{n+1}\}$ do not satisfy the condition

$$(f_n)^{n+2}(g_{n+1})^{n+1} = -(g_n)^{n+2}(f_{n+1})^{n+1}. \quad (3.76)$$

If n in (3.74) is even, in particular $n=2$, the result can be extended; the mapping is also not reversible if just one of f_{n+1} and g_{n+1} is nonzero [in which case (3.76) is immediately violated]. An example from the class of nonreversible area-preserving mappings with expansion (3.74) in the typical case $n=2$ is provided by

$$M: x' = x - y^2(1 - y), \quad y' = y + Cx'^2(1 - x'). \quad (3.77a, b)$$

Here C is an arbitrary parameter. This polynomial mapping obviously has the expansion (3.74) about the fixed point at the origin with $f_2 = -1$, $f_3 = 1$, $g_2 = -g_3 = C$. From the above result, it is not reversible if $C \neq 0$ [cf. assumption (3.75)], and from (3.76), $C \neq 1$. When $C = 0$, M is reversible because $g(x') = 0$ is odd. When $C = 1$, M is reversible with reversing involution $G: x' = y, y' = x$ because (3.73) is always globally reversible with this involution whenever $g(y) = -f(y)$. If we restrict (3.77) to $C > 1$, we have a one-parameter nonreversible mapping of the plane. The mapping M has other fixed points at $(1, 0)$, $(0, 1)$ and $(1, 1)$. The fixed point at $(1, 1)$ has a linearisation dependent on the mapping parameter C , seen by evaluating the trace of the Jacobian matrix which equals $2 - C$ so that the point is elliptic for $0 < C < 4$. From a local analysis around the fixed point $(1, 1)$ the lack of reversibility of M is less transparent. In fact when the fixed point $(1, 1)$ is hyperbolic ($C > 4$), the mapping is locally reversible to all orders about this point because of the normal form (3.58), even though globally the mapping is not reversible.

Note that although (3.77) is defined over the entire xy plane; it is easy to create nonreversible area-preserving mappings of the cylinder or the torus by choosing one or both of $f(y)$ and $g(x')$ in (3.73) to be periodic functions. The way in which the lack of reversibility of mappings such as M manifests itself in their dynamical properties is yet to be investigated (cf. Robnik and Berry [1985, 1986] for a discussion of the consequences of breaking time-reversal symmetry in billiard dynamics).

The results of Roberts and Capel [1992a, b] show that quite generally an area-preserving mapping possessing a fixed point where the linearisation is the identity matrix is not reversible. In the case of the generalised standard mapping (3.73), we can look at the result stated directly above eq. (3.76) in the following way: if the functions f and g in the generalised standard mapping (3.73) are such that the

lowest order in both of their expansions around a fixed point is cubic, then, when we add an even term to both f and g , by virtue of nonzero quadratic terms or nonzero quartic terms the mapping is generically not reversible. It would be interesting to know whether this conclusion extends to the case when the expansions of f and g have linear parts and even terms are present by virtue of nonzero quadratic terms. Rannou's mapping (3.47) is an example where this occurs. About the fixed point at the origin, we find

$$f(y) = y + y^2/2 + O(y^4), \quad g(x') = -C(x' + \frac{1}{2}x'^2) + O(x'^3).$$

There is a relation between the mapping expansion (3.64) and the case of a resonant elliptic fixed point, in the sense that the q th power of the mapping expansion around a fixed point with eigenvalue λ satisfying $\lambda^q = 1$ has linear part $(1, 0, 0, 1)$. This would seem to suggest a program for testing local reversibility at a q resonance of an area preserving mapping: take the q th power of the mapping, analyse it as an example of (3.64) and check whether the local reversibility conditions derived for mappings of the form (3.64) are satisfied. The underlying idea is that if L^q can be shown not to be locally reversible, then it follows that L is not locally reversible because the property is preserved on taking powers. Preliminary investigations of this type have revealed that L^q for small q *does* satisfy the lowest order reversibility conditions derived for mappings like (3.64).

This can also be seen from a direct approach based upon nonlinear normal forms. At a resonance a real analytic mapping, not necessarily area- or measure-preserving, can always be formally brought via a nonlinear transformation to the complex form (3.62) where now $i - j = 1 \pmod{q}$. Furthermore, the reduction to this form to a desired finite order can be achieved by an analytic (polynomial) transformation. The fact that local measure preservation and local reversibility are maintained under the reduction to normal form can be exploited by studying the conditions under which the reduced mapping is measure-preserving and reversible. It is not hard to show that for small q (i.e., $q = 3, 4$), the expansion of L in this case is locally reversible at the first few orders of the expansion when it is locally measure-preserving, and vice versa. Further systematic investigation of the normal form is required to determine if local reversibility exists to all orders around a fixed point of an area-preserving mapping at a resonance.

4. Non measure-preserving reversible mappings with asymmetric fixed points

This chapter introduces some large classes of non measure-preserving reversible mappings. The basic features of some examples from these classes will be discussed here and they will be studied in more depth in chapters 5 and 6. It will be shown that their dynamics includes chaotic motion, attractors and repellers, as well as motion on invariant curves. It is not sufficient to make a mapping non area-preserving in order to introduce attractors or repellers. For example, a reversible mapping may have a Jacobian determinant that varies throughout the plane but it may in fact be conjugate to an area-preserving reversible mapping. Certainly this class of reversible measure-preserving mappings cannot have attractors or repellers.*)

What is necessary, therefore, in order to have attractors and repellers is that the mapping be non

*) This may explain the statements in Belobrov et al. [1984] that reversible mappings cannot have attractors – it seems that the reversible mappings studied there can be transformed to area-preserving forms.

measure-preserving. For the orientation-preserving reversible mappings discussed below, it will be shown analytically that they can possess fixed points at which the Jacobian determinant is not equal to one. These points are necessarily asymmetric from the discussion of section 3.1, and furthermore from section 2.2 it follows that these mappings *cannot* be measure-preserving. In fact, often these asymmetric fixed points in one-parameter families of reversible mappings are attractors or repellers in some range of the mapping parameter. This can be shown explicitly using linear stability analysis. In one of the reversible mappings below there also appear asymmetric fixed points at which $J = 1$. Computer studies suggest that these points can also be attracting or repelling in a range of the mapping parameter. This can be confirmed by higher order stability analysis.

Reversible mappings with attractors and repellers arose in the work of Politi et al. [1985, 1986a, b] and Bullett [1988, 1991]. In the former case a specific example of a nonconservative reversible flow arising from a physical example was studied, and the reversible mapping arose from a surface of section. In the latter case, a special class of mappings of part of the complex plane was studied and attracting and repelling periodic orbits arose in some cases. The discussion below will indicate how to explicitly and systematically construct large families of reversible mappings with attractors and repellers. These families allow a study of reversible systems without the need to take sections of flows, and are convenient for creating reversible non measure-preserving perturbations of reversible conservative mappings.

4.1. Theory

The construction of reversible mappings with attracting/repelling fixed points requires the construction of mappings which possess (i) asymmetric fixed points; and (ii) comprise at least one non area-preserving involution. Recall from (3.16) that a point x_0 is a fixed point of a reversible mapping $L = H \circ G$ if and only if

$$Hx_0 = Gx_0. \quad (4.1)$$

If $Gx_0 = x_0$ (and hence $Hx_0 = x_0$) then the fixed point is symmetric, has $J = 1$ (when L is orientation-preserving) and cannot be an attractor or repeller. If for a mapping there does exist a point satisfying (4.1) with $Gx_0 \neq x_0$, then the fixed point x_0 is asymmetric and the point Gx_0 is another fixed point of L .

It appears that the best "first principles" way of creating non area-preserving involutions is by conjugating area-preserving ones. This method was used by Pinnow [1986]. The involution thus created can be used to make a non measure-preserving reversible mapping (recall that although any involution is necessarily measure-preserving, the composition of two measure-preserving mappings need not be). To use Pinnow's method, take an area-preserving involution V and conjugate it with an arbitrary invertible coordinate transformation W ,

$$H := W \circ V \circ W^{-1}. \quad (4.2)$$

The resulting mapping H is an involution but it is in general not area-preserving if W is not area-preserving since

$$\text{Det } dH(x) = \pm \frac{\text{Det } dW^{-1}(x)}{\text{Det } dW^{-1}(Hx)}. \quad (4.3)$$

The + or - sign is taken accordingly as V (and therefore H) is orientation-preserving or orientation-reversing. The conjugacy of H to V ensures that if x_0 is a fixed point of V then Wx_0 is a fixed point of H . Hence the symmetry line of H is the image under W of the symmetry line of V .

When H is composed with another involution G we obtain a reversible mapping that is in general not area preserving,^{*} for example,

$$L = H \circ G = W \circ V \circ W^{-1} \circ G. \tag{4.4}$$

If G is area-preserving as well as V and they are both orientation-reversing (the case we usually consider), then the Jacobian determinant of L is

$$J(x) = \frac{\text{Det } dW^{-1}(Gx)}{\text{Det } dW^{-1}(Lx)}, \tag{4.5}$$

so that at a fixed point x_0 it is

$$J(x_0) = \frac{\text{Det } dW^{-1}(Gx_0)}{\text{Det } dW^{-1}(x_0)}. \tag{4.6}$$

If x_0 is asymmetric so that $x_0 \neq Gx_0$, then (4.6) shows that in general $J(x_0) \neq 1$ which means that L is not measure-preserving.

The above method can be illustrated with a simple example. Take

$$V: x' = y, \quad y' = x, \tag{4.7}$$

$$W: x' = x[1 + (y - 1)^2], \quad y' = y. \tag{4.8}$$

The transformation W would appear to be one of the simplest examples of an invertible transformation which is not area-preserving. With these choices we obtain for the non area-preserving involution H in (4.2),

$$H_1: x' = y[1 + (y' - 1)^2], \quad y' = x/[1 + (y - 1)^2], \tag{4.9}$$

which we compose with the simple one-parameter area-preserving involution

$$G_1: x' = x, \quad y' = C - y. \tag{4.10}$$

The result $H_1 \circ G_1$ is the reversible mapping

$$L_1: x' = (C - y)[1 + (y' - 1)^2], \quad y' = x/[1 + (C - y - 1)^2]. \tag{4.11}$$

One finds that for a substantial range of C this mapping has a symmetric fixed point and a pair of

^{*} As far as we are aware Pinnow did not create reversible mappings with asymmetric fixed points at which the Jacobian determinant was not equal to 1.

asymmetric fixed points, e.g., at $C=3$ these are readily calculated: the symmetric fixed point is at $(15/8, 3/2)$ and the asymmetric pair at $(2, 1)$ and $(2, 2)$. Furthermore the Jacobian determinant of (4.11) can be found using (4.8), to readily find W^{-1} , followed by (4.5),

$$J_1(\mathbf{x}) = [1 + (y' - 1)^2] / [1 + (C - y - 1)^2]. \quad (4.12)$$

So at the asymmetric fixed points when $C=3$, we find $J_1 = 0.5$ and $J_1 = 2$ respectively. Further calculation of the linearisation at these points reveals that they are in fact, respectively, attracting and repelling fixed points. Fuller details for the mapping L_1 will be given in section 4.3 (see example 1, table 4.1). In fig. 4.1a, b a part of the phase portrait of this mapping is shown. Figure 4.1c shows the variation of the Jacobian determinant over a portion of the plane.

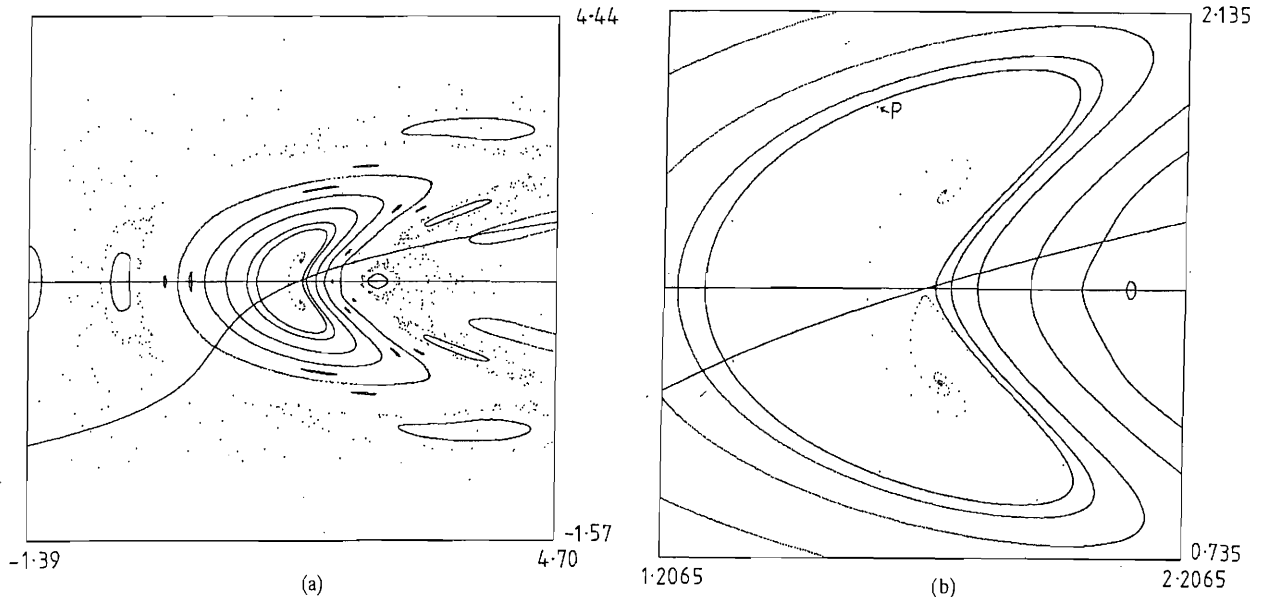


Fig. 4.1. (a) Phase portrait of the mapping L_1 in (4.11) when $C=2.87$ (see also example 1 of table 4.1 in section 4.3). For clarity the x and y axes are not drawn. At the centre of the picture is a symmetric fixed point which lies at the intersection of the symmetry line of G , which is $y = 1.435$, and the symmetry line of H , which is the monotonic increasing curve shown. The symmetric fixed point is hyperbolic (a saddle), and below and above it are two asymmetric fixed points that form a spiral attracting/repelling pair. A trajectory is shown that starts close to the repeller above the symmetry line of G and moves down over the line to spiral into the attracting fixed point. The attractor and repeller and the hyperbolic symmetric fixed point appear to be enclosed by invariant curves. Some elliptic symmetric cycles and their associated islands are also shown: a symmetric eight-cycle and a symmetric seven-cycle which lie, respectively, inside and outside, one of the curves, and an outer symmetric six-cycle which is surrounded by large islands. The three islands cut off by the border of the picture are part of the island chain surrounding a symmetric five-cycle. One chaotic orbit is also shown. (b) Enlargement around the centre of fig. 4.1a. The coordinates of the hyperbolic symmetric fixed point at the centre are $(1.7065\dots, 1.435)$. The attracting and repelling asymmetric fixed points below and above the horizontal symmetry line have, respectively, coordinates $(1.74, 1.1916\dots)$ and $(1.74, 1.6783\dots)$. We have added two trajectories not shown in a. The first appears to be quasiperiodic and produces the innermost apparently closed curve. The second additional trajectory is that of the point marked P which starts close to this curve and moves anti-clockwise around it towards the hyperbolic symmetric fixed point, before changing direction and spiralling in towards the attractor. There can be no invariant closed curves which enclose the symmetric and two asymmetric fixed points and which have P in their exterior. (c) Plot of the Jacobian determinant (4.12) of the mapping L_1 in (4.11) over the part of the plane shown in b. The top two pictures show the surface obtained by plotting $J(x, y)$ when viewed from two different perspectives. Over the region shown $J(x, y)$ varies from approximately 0.5 to 2.5, mostly increasing with increasing x and increasing y . In the bottom picture we show only the part of the surface where $J > 1$. The repelling fixed point which has $J = 1.408\dots$ is contained in the part of the plane beneath this part of the surface. The boundary of this part of the surface is the contour with $J = 1$, on which lies the symmetric fixed point. In reality this is a smooth curve but its jagged appearance here is an artefact of the graphics package.

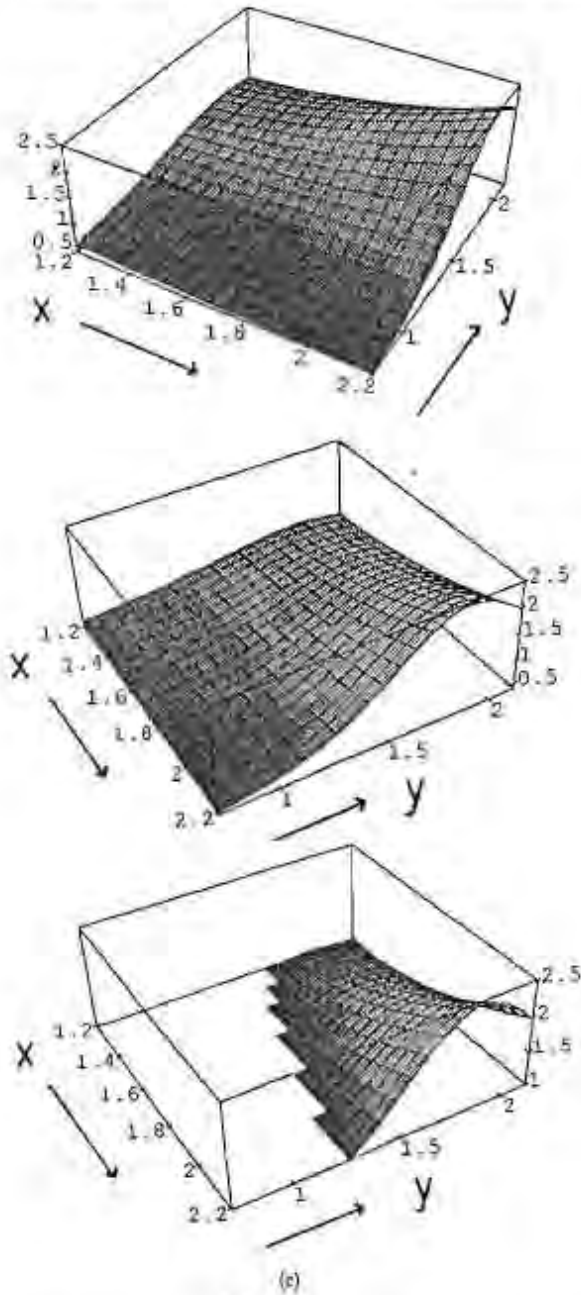


Fig. 4. (cont)

It appears that the method just described is the most systematic way of creating reversible non measure-preserving mappings. It is also very general because many invertible transformations can be used for W . In section 3.2 it was shown how involutions could be derived from symmetric second order difference equations. Some of these involutions were not area-preserving. It turns out that the involutions created by this method are in fact further examples of the Pinnow method because transformations can be found that reduce them to area-preserving form. Thus, for example, the

involution (3.45) can be written $W \circ V \circ W^{-1}$ with $V: x' = x, y' = -y$, and

$$W^{-1}: x' = x, \quad y' = y^3 f(x) + y^2 m(x) + yg(x) + h(x)/2. \quad (4.13)$$

The transformation W^{-1} is invertible because of the assumption $m^2 - 3fg < 0$.

4.2. Four classes of non measure-preserving reversible mappings

In this section we give four classes of non measure-preserving reversible mappings created in the way just outlined. These classes vary in the simplicity and analyticity of their mappings and the ease of finding fixed points, etc. Each class involves arbitrary functions which, with appropriate care, can be chosen to guarantee that the mappings have asymmetric fixed points where the Jacobian determinant is often not equal to 1. This will be illustrated in the next section by creating examples with simple choices for these functions. Here we list the basic form of the mapping in each class, its component orientation-reversing involutions, at least one of which is not area-preserving, and the mapping's Jacobian determinant. From this information such details as symmetry lines, fixed points [cf. eq. (4.1)] and the Jacobian determinant at fixed points are readily obtained. The reader may prefer to skip over this section and proceed straight to the specific examples of section 4.3, and in particular to table 4.1, where most of the salient features of some model mappings have been calculated. This section can be used for reference on the class to which each example belongs.

Classes I and II below are analytic mappings of the plane that are useful for perturbing reversible area-preserving mappings written in McMillan form (cf. table 3.1), which for ease of reference we rewrite here as

$$L_M: x' = y, \quad y' = -x + 2h(y), \quad (4.14)$$

with its involutions

$$H_M: x' = x, \quad y' = -y + 2h(x); \quad G_M: x' = y, \quad y' = x. \quad (4.15)$$

Class III also consists of analytic mappings but these mappings involve taking cube roots to get the image point (x', y') from (x, y) . Class IV mappings have singularity lines in the plane where they are not defined. Classes III and IV mappings are useful for perturbing reversible area-preserving mappings when they are in generalised standard form,

$$L_S: x' = f(y) + x, \quad y' = g(x') + y. \quad (4.16)$$

In the case that f is odd, the involutions are

$$H_S: x' = x, \quad y' = g(x) - y; \quad G_S: x' = f(y) + x, \quad y' = -y, \quad f \text{ odd}. \quad (4.17)$$

L_S in general can possess asymmetric fixed points. However since L_S is area-preserving, these asymmetric fixed points cannot be attractors. In the mappings of class III and class IV below, one or both of the involutions in (4.17) is replaced with a non area-preserving involution which allows asymmetric fixed points to be attracting or repelling. Classes III and IV can also be used to perturb

mappings in McMillan form (4.14) after first converting them to generalised standard form using the transformation $x \rightarrow x, y \rightarrow x - y$.

4.2.1. Class I

This class of mappings takes the McMillan mapping (4.14) and (4.15) and conjugates its second involution to give

$$L_I \equiv \check{H}_M \circ W \circ G_M \circ W^{-1}. \tag{4.18}$$

The transformation chosen for W is

$$W: x' = xf(y), \quad y' = y. \tag{4.19}$$

The function $f(y)$ is taken strictly positive or negative so that the inverse W^{-1} is everywhere defined. The mapping L_I is therefore the product of the involutions $H_I \equiv H_M$ and

$$G_I \equiv W \circ G_M \circ W^{-1}: x' = yf(y'), \quad y' = x/f(y). \tag{4.20}$$

Observe that the transformation W in (4.19) generalises the W in (4.8) and that, since G_M is equal to V in (4.7), the involution G_I generalises the involution H_1 in (4.9). The explicit form of $L_I = H_I \circ G_I$ is

$$L_I: x' = yf(x/f(y)), \quad y' = -x/f(y) + 2h(x'). \tag{4.21a, b}$$

Its Jacobian determinant is given by the right-hand side of (4.3), with the + sign and $H \rightarrow G_I$, because in (4.18) the conjugated involution is after the area-preserving one,

$$J_I(x, y) = f(-y' + 2h(x'))/f(y), \tag{4.22}$$

with $x'(x, y)$ and $y'(x, y)$ obtained from (4.21). When $f \equiv 1$, the transformations W and W^{-1} become the identity transformation and the mapping L_I is the area-preserving McMillan mapping L_M .

4.2.2. Class II

This class is again derived from the McMillan mapping (4.14) and (4.15) but in this case the first involution is conjugated to give

$$L_{II} = W \circ H_M \circ W^{-1} \circ G_M. \tag{4.23}$$

Here we take

$$W: x' = [x - q(y')]/p(y'), \quad y' = y - r(x), \tag{4.24}$$

$$p(y) > 0, \text{ even}; \quad q(y) \text{ odd}; \quad r(x) \text{ not odd}, \quad r(0) = 0. \tag{4.25}$$

This transformation has Jacobian determinant $1/p(y')$. From (4.23), together with (4.15) and (4.24), the explicit form for L_{II} can be derived,

$$L_{II}: x' = [\mu - q(y')]/p(y'), \quad y' = -x + 2h(\mu) - 2r(\mu), \quad (4.26a, b)$$

$$\mu = yp(x) + q(x). \quad (4.27)$$

Here the variable μ is an auxiliary variable introduced to make L_{II} neater to write down. To calculate (x', y') one first evaluates μ and substitutes it and x into (4.26b) to find y' . The values of μ and y' are then used in (4.26a) in order to find x' .

The reversible mapping (4.26) is the product of the involutions

$$H_{II} \equiv W \circ H_M \circ W^{-1}: x' = [\nu - q(y')]/p(y'), \quad y' = -y + 2h(\nu) - 2r(\nu), \quad (4.28)$$

$$\nu = xp(y) + q(y), \quad (4.29)$$

where ν is another auxiliary variable and $G_{II} \equiv G_M$. The Jacobian determinant of L_{II} follows from (4.5) and the Jacobian determinant $p(y)$ of W^{-1} ,

$$J_{II}(x, y) = p(x)/p(y'), \quad (4.30)$$

with $y'(x, y)$ given by (4.26b). It is always defined and positive because $p(y) > 0$.

The reason for the particular choice of W in (4.24) and (4.25) is that it ensures that L_{II} has the pair of fixed points

$$(x_0, y_0) = \{(x_0, -x_0), (-x_0, x_0)\}, \quad x_0 p(x_0) - q(x_0) = 0. \quad (4.31)$$

This holds provided $h(0) = 0$, i.e., provided that the original McMillan mapping has the origin as a fixed point [cf. (4.14)], which is equivalent to it possessing any fixed point. The above pair of fixed points of L_{II} are in general asymmetric because when $x_0 \neq 0$ they do not lie on the symmetry line $y = x$ of G_{II} . Moreover L_{II} does not have the symmetry line $y = -x$ because it cannot be odd if $r(x)$ is not an odd function. From (4.30), the Jacobian determinant J_{II} at the pair of fixed points is equal to $+1$ because p is an even function. Despite this, in the cases that we have investigated numerically (e.g., see example 2, section 4.3) we find that these points form a spirally attracting/repelling pair when they are elliptic. This suggests that they are genuinely asymmetric. This is confirmed by higher order stability analysis around the points which is discussed in chapter 6. Note also that by construction [cf. (4.25)] the origin is certainly always a symmetric fixed point of L_{II} . Other symmetric fixed points may certainly exist but are harder to find analytically.

4.2.3. Class III

The third class of non measure-preserving reversible mappings takes the form

$$L_{III}: x' = p(y) + x, \quad (y'^3 - y^3)q(x') + (y'^2 + y^2)r(x') + (y' - y)s(x') + t(x') = 0. \quad (4.32)$$

In (4.32), t is a completely arbitrary function and p is an arbitrary odd function. The functions q , r and s must satisfy

$$r^2(v) - 3q(v)s(v) < 0, \quad \text{all } v, \quad (4.33)$$

so that q and s are necessarily both everywhere positive or both everywhere negative. With these mild restrictions, (4.32) is reversible and assigns a unique image point (x', y') to a given point (x, y) . This is because the left hand side of the second equation in (4.32) is a monotonic cubic function for y' as a function of x' and y [as a result of (4.33)] and hence has only one real zero. The explicit expression for this unique value of y' follows from standard formulae for the root of a cubic (cf. Abramowitz and Stegun [1972, section 3.8.2]). These formulae are needed for computational work with the mapping.

The non-area-preserving involution H_{III} in this class of mappings is

$$H_{III}: x' = x, \quad (y'^3 + y^3)q(x) + (y'^2 + y^2)r(x) + (y' + y)s(x) + t(x) = 0. \quad (4.34)$$

This involution is obtained from a second order symmetric difference equation [cf. (3.45)] but, as remarked above, is conjugate to a simple area-preserving involution via (4.13). The area-preserving involution G_{III} is of the form of G_S in (4.17) with $f \rightarrow p$. The mapping $L_{III} = H_{III} \circ G_{III}$ is in general a non area-preserving mapping with

$$J_{III}(x, y) = \frac{3y^2q(x') - 2yr(x') + s(x')}{3y'^2q(x') + 2y'r(x') + s(x')}. \quad (4.35)$$

In (4.35), $x'(x, y)$ and $y'(x, y)$ are calculated from (4.32). The mapping L_{III} can be used for reversible non area-preserving perturbations of the generalised standard mapping (4.16). It reduces to an area-preserving mapping of this form when $q = r \equiv 0$. If the functions p, q, r, s and t are analytic and satisfy the conditions above, then L_{III} is an analytic diffeomorphism.

4.2.4. Class IV

In this class we consider mappings given by

$$L_{IV}: x' = \frac{f_1(y) + x}{1 - xf_3(y)}, \quad y' = \frac{g_1(x') + y}{1 - yg_3(x')}, \quad (4.36a, b)$$

where g_1 and g_3 are completely arbitrary functions and f_1 and f_3 are arbitrary odd functions. The functions f_1, f_3, g_1 and g_3 can be chosen to be analytic (e.g., polynomial or rational) and to depend on one or more mapping parameters.

The mapping L_{IV} is the product of the involutions

$$H_{IV}: x' = x, \quad y' = \frac{g_1(x) - y}{1 + yg_3(x)}; \quad (4.37a)$$

$$G_{IV}: x' = \frac{f_1(y) + x}{1 - xf_3(y)}, \quad y' = -y. \quad (4.37b)$$

The involution H_{IV} is of the form (3.42) with f_2 in (3.42) taken equal to $+1$ and the obvious replacements. G_{IV} is of the form (3.43) with $x \leftrightarrow y$ and f_2 there taken equal to -1 . When $f_3 = g_3 \equiv 0$, H_{IV} and G_{IV} become equal to H_S and G_S in (4.17) and this class reduces to the area-preserving generalised standard mapping (4.16). However, H_{IV} and G_{IV} are not in general area-preserving. The Jacobian determinant of L_{IV} is

Table 4.1
Some examples of non measure-preserving reversible mappings $L = H \circ G$

	Mapping L [Jacobian determinant J]	Involutions	
		H [Symmetry line]	G [Symmetry line]
Example 1 [Class I]	$x' = (C - y)(y'^2 - 2y' + 2)$ $y' = \frac{x}{1 + (C - y - 1)^2}$ $\left[J = \frac{y'^2 - 2y' + 2}{1 + (C - y - 1)^2} \right]$	$x' = y(y'^2 - 2y' + 2)$ $y' = \frac{x}{1 + (y - 1)^2}$ $[x = y(1 + (y - 1)^2)]$	$x' = x$ $y' = C - y$ $[y = C/2]$
Example 2 [Class II]	$x' = \frac{\mu - 2\epsilon^2 y'^3}{1 + \epsilon^2 y'^2}$ $y' = -x + 2C\mu + 2\mu^2$ $(\mu = y + \epsilon^2 x^2 y + 2\epsilon^2 x^3)$ $\left[J = \frac{1 + \epsilon^2 x^2}{1 + \epsilon^2 y'^2} \right]$	$x' = \frac{\nu - 2\epsilon^2 y'^3}{1 + \epsilon^2 y'^2}$ $y' = -y + 2C\nu + 2\nu^2$ $(\nu = x + \epsilon^2 y^2 x + 2\epsilon^2 y^3)$ $\left[x = \frac{-(4\epsilon^2 y^3 + C) \pm \sqrt{4y + C^2}}{2(1 + \epsilon^2 y^2)} \right]$	$x' = y$ $y' = x$ $[y = x]$
Example 3 [Class III]	$x' = -y + \epsilon^2 y^3 + x$ $(y'^3 - y^3)\epsilon^2 - (y'^2 + y^2)\epsilon$ $+ (y' - y) - 2x'(1 - C - x') = 0$ ^{a)} $\left[J = \frac{3\epsilon^2 y^2 + 2\epsilon y + 1}{3\epsilon^2 y'^2 - 2\epsilon y' + 1} \right]$	$x' = x$ $(y'^3 + y^3)\epsilon^2 - (y'^2 + y^2)\epsilon$ $+ (y' + y) - 2x(1 - C - x) = 0$ $[\epsilon^2 y^3 - \epsilon y^2 + y + Cx + x^2 - x' = 0]$	$x' = -y + \epsilon^2 y^3 + x$ $y' = -y$ $[y = 0]$
Example 4 [Class IV]	$x' = \frac{-y/(1 + \epsilon^2 y^2) + x}{1 - xy^3/(1 + y^2/\epsilon^2)}$ ^{a)} $y' = 2x'(1 - C - x') + y$ $\left[J = \frac{(1 + y^2/\epsilon^2)(1 + \epsilon^2 y^2 + y^2/\epsilon^2)}{(1 + \epsilon^2 y^2)(1 + y^2/\epsilon^2 - xy^3)^2} \right]$	$x' = x$ $y' = 2x(1 - C - x) - y$ $[y = x(1 - C - x)]$ ^{b)}	$x' = \frac{-y/(1 + \epsilon^2 y^2) + x}{1 - xy^3/(1 + y^2/\epsilon^2)}$ $y' = -y$ $[y = 0]$ ^{b)}

^{a)} Asymmetric fixed points exist only when $|C| > 2\sqrt{2}$ and bifurcate from symmetric fixed point when $C = \pm 2\sqrt{2}$.

^{b)} Another symmetric fixed point exists as shown in fig. 4.2a.

^{c)} Position of asymmetric fixed points listed is independent of C ; linear stability of asymmetric fixed points listed is independent of ϵ . The point $(1/\epsilon, -1/\epsilon)$ has $J = 1$ and for $\epsilon > 0$ is apparently spirally attracting when it is elliptic. Note that other asymmetric fixed points can be found computationally, cf. chapter 6, section 6.1.1.

$$J_{IV}(x, y) = \frac{[1 + g_1(x')g_3(x')][1 + f_1(y)f_3(y)]}{[1 - yg_3(x')]^2[1 - xf_3(y)]^2}, \quad (4.38)$$

with $x'(x, y)$ calculated from (4.36a). Clearly it varies throughout the plane.

An obvious feature of the mappings of this class is that they possess singularities, i.e., curves in the

Table 4.1 (cont.).

Symmetric fixed points ($J = 1$ at these points)	Asymmetric fixed points (given in pairs)	ϵ
$(\frac{1}{2}C[1 + (1 - \frac{1}{2}C)^2], \frac{1}{2}C)$; $\text{trace} = \frac{C(C-2)}{1 + (1 - \frac{1}{2}C)^2}$; $2 - \sqrt{8} \leq \text{trace} \leq 2 + \sqrt{8}$, elliptic for $-2\sqrt{2} < C < 2\sqrt{2}$	(i) $(x, y_{\pm}) = (2(C-2), \frac{1}{2}(C \pm \sqrt{C^2-8}))$ $J_{\pm} = \frac{C \pm \sqrt{C^2-8}}{C \mp \sqrt{C^2-8}}$, $\text{trace}_{\pm} = \frac{(4-C)(C \pm \sqrt{C^2-8})}{2(C-2)}$ (x, y_-) and (x, y_+) are attractor/repeller pair for all $C > 2\sqrt{2}$ ^{a)} (x, y_+) and (x, y_-) are attractor/repeller pair for all $C < -2\sqrt{2}$ ^{a)}	-
$(0, 0)$ ^{b)} ; $\text{trace} = 2C$ elliptic for $-1 < C < 1$	(i) ^{c)} $(\pm 1/\epsilon, \mp 1/\epsilon)$; $J = 1$; elliptic for $\frac{1}{2} < C < \frac{3}{2}$	1.1
$(0, 0)$; $\text{trace} = 2C$ elliptic for $-1 < C < 1$	(i) ^{e)} $(\frac{1-C + \sqrt{(1-C)^2 + 4/\epsilon}}{2}, \pm \frac{1}{\epsilon})$; $J = \frac{1}{3}, 3$ for $y = \frac{-1}{\epsilon}, \frac{1}{\epsilon}$ attractor/repeller pair for $0 < (1-C)^2 + 4/\epsilon < 16$	
$(1-C, 0)$; $\text{trace} = 2(2-C)$ elliptic for $1 < C < 3$	(ii) ^{e)} $(\frac{1-C - \sqrt{(1-C)^2 + 4/\epsilon}}{2}, \pm \frac{1}{\epsilon})$; $J = \frac{1}{3}, 3$ for $y = \frac{-1}{\epsilon}, \frac{1}{\epsilon}$ this pair of points always saddle points	1.0
$(0, 0)$; $\text{trace} = 2C$ elliptic for $-1 < C < 1$ $(1-C, 0)$; $\text{trace} = 2(2-C)$ elliptic for $1 < C < 3$	(i) $(1-C, \pm y_1)$, $y_1 > 0$: $\epsilon^4(1-C)^2 y_1^4 + (\epsilon^2(1-C)^2 - 1)y_1^2 - \epsilon^2 = 0$ (there is a positive solution $y_1^2 \forall C \neq 1, \epsilon \neq 0$) $(1-C, \pm y_1)$ often attractor/repeller pair for fixed ϵ and some range of C , e.g., for $\epsilon = 0.02$, $(1-C, -y_1)$ is attracting for $-12.943 \dots < C < 1$	0.02

^{d)} To calculate y' in this mapping use the formula for the root of a cubic polynomial.

^{e)} If $\epsilon < 0$, asymmetric fixed points do not exist for all C ; two pairs arise by tangent bifurcation when $(1-C)^2 + 4/\epsilon = 0$.

^{f)} Singularity line of mapping: $x = 1/y^3 + 1/\epsilon^2 y$. Note that $1 + f_1(y)f_3(y) > 0 \forall y, \epsilon$ so unique inverse for every point, cf. (4.39).

^{g)} Symmetry lines are the same as in Hénon map.

plane where the denominators appearing in the mappings and their derivatives vanish. The appearance of the singularities in both the mapping $L_{IV} = H_{IV} \circ G_{IV}$ and its inverse $L_{IV}^{-1} = G_{IV} \circ H_{IV}$ can be regarded as due to the presence of singularities in the component involutions H_{IV} and G_{IV} . The effect of such singularities is that some points in the plane possess only backwards orbits while others possess only forward orbits. It is also possible for a curve of points to all have the same image point under L_{IV} .

However this loss of injectivity can be removed by ensuring that f_1, f_3, g_1 and g_3 satisfy

$$1 + g_1(v)g_3(v) > 0, \quad 1 + f_1(v)f_3(v) > 0, \quad \text{all } v. \quad (4.39)$$

This condition also ensures that the symmetry line of H_{IV} , which is typically double-valued if $g_3(x) \neq 0$, extends throughout the plane and does not terminate. Note that some area-preserving mappings have been studied which have singularities (e.g., Devaney [1981], McMillan [1971]) or non-unique backwards orbits associated with points (cf. G umowski and Mira [1980, chapter 3.9]). Finally, like the generalized standard mappings, if g_1 and g_3 in (4.36) are odd instead of (or together with) f_1 and f_3 , then the mapping L_{IV} can be written as the product of $-H_{IV}$ and $-G_{IV}$. The basic properties of this form resemble those described above.

4.3. Examples

We now present some specific examples of mappings in the four classes discussed above. These examples and some of their details are listed in table 4.1. They illustrate specifically many of the

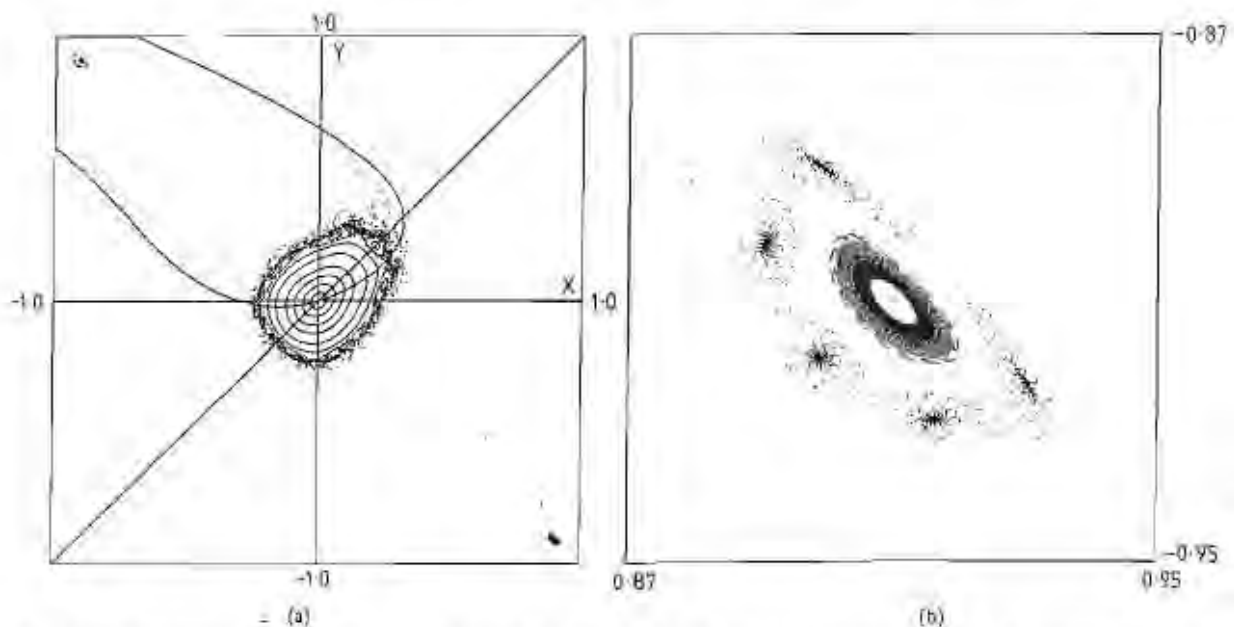


Fig. 4.2. (a) Phase portrait of the mapping example 2 of table 4.1 when $C=0.3$. The line $y=x$ and the curve passing through the origin are the symmetry lines of G and H respectively. The origin is an elliptic symmetric fixed point and so is surrounded by invariant KAM curves. The other point of intersection of the symmetry lines is a hyperbolic symmetric fixed point. The asymmetric fixed point at $(-0.909 \dots, 0.909 \dots)$ is observed to be spirally repelling. Its reflection is the asymmetric fixed point at $(0.909 \dots, -0.909 \dots)$ which is observed to be spirally attracting as shown in b. (b) Enlargement of the bottom right hand corner of a showing the spirally attracting fixed point $(0.909 \dots, -0.909 \dots)$ at the centre. Also shown is a spirally attracting five-cycle. (c) Plot of the Jacobian determinant of example 2 over the part of the plane shown in a. Over this region $J(x, y)$ ranges from close to 0 to greater than 2. The top two pictures show the surface obtained by plotting the Jacobian determinant when viewed from two different perspectives. The surface is humped in the general $y = -x$ direction and falls away sharply from this direction. The bottom picture shows the part of the surface with $J > 1$. In this example the symmetric and two asymmetric fixed points all have $J = 1$ and so lie in the plane beneath the boundary of this part of the surface. Note that quite near to the spirally attracting fixed point at $(0.909 \dots, -0.909 \dots)$ are regions where $J(x, y)$ is greatest.

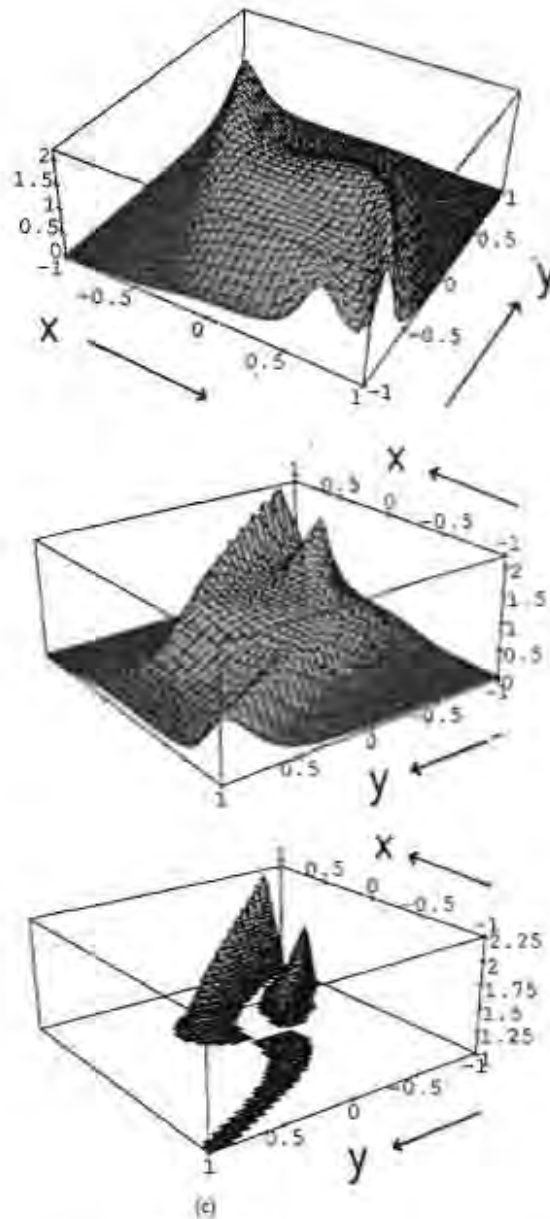


Fig. 4.2 (cont.)

properties of a non measure-preserving reversible mapping that were previously discussed in general terms in section 3.1. Example 1 is the simple example introduced in section 4.1. It depends on one parameter C . It is composed of two involutions of the type presented in class I of the previous section except that it has the conjugated involution in front of the area-preserving one. Nevertheless we consider it as a very simple mapping of this type. Examples 2–4 depend on two parameters C and ϵ . The parameters are used in the following way; we fix ϵ and study the resulting one-parameter family of mappings parametrised by C . The value of ϵ adopted for numerical study of each mapping is listed in

table 4.1. It will be shown in chapters 5 and 6 that for these fixed values of ε , the one-parameter families of mappings exhibit both qualitatively and quantitatively conservative and dissipative behaviour.

Unless otherwise noted, when we refer to examples 2–4 we mean the examples with the values of ε given in table 4.1. It is worth pointing out however that there is nothing particularly special about the values of ε chosen. As indicated in table 4.1, these mappings are reversible and non area-preserving with asymmetric fixed points for almost all values of C and ε . The linear stability of the symmetric fixed points is constructed so that it is independent of ε (because $J = 1$ at these fixed points, the linear stability is completely determined by the *trace* of the Jacobian matrix). The linear stability of the asymmetric fixed points usually depends on ε and C , and for each ε there is often a range of the parameter C (which usually depends on ε) for which the points are attracting or repelling. [The range of parameter C for which a fixed point is attracting can be deduced analytically in many cases by using eqs. (2.10a, b) with $n = 1$.] Of course (from section 3.1) if the stability of one point of an asymmetric pair of fixed points is known, then the stability of the other point is also known because of their reciprocal eigenvalues.

The parameter ε in examples 2–4 is in fact a perturbation parameter because these examples are derived from the area-preserving Hénon mapping. The area-preserving Hénon mapping has been chosen as the basis for examples 2–4 because of its pre-eminence as a numerically and analytically studied mapping of the plane. These examples illustrate how the mappings of classes II, III and IV can be used to introduce dissipative and expansive dynamical features into conservative systems.

Example 2 (class II) derives from the area-preserving Hénon mapping in McMillan form, (4.14) with $h(y) = Cy + y^2$. The symmetry lines of the area-preserving Hénon mapping in this form are $y = Cx + x^2$ and $y = x$. The mapping has two fixed points which are both symmetric. The point $(0, 0)$ is elliptic when $-1 < C < 1$ and the point $(1 - C, 1 - C)$ is elliptic when $1 < C < 3$. The mapping of example 2 reduces to this area-preserving mapping when $\varepsilon = 0$. When $\varepsilon \neq 0$, example 2 has asymmetric fixed points with Jacobian determinant equal to unity, which are born at infinity and move in to the origin along the line $y = -x$ with increasing ε . Numerically they are found to be a spiral attracting/repelling pair when their linearisation is elliptic. In figs. 4.2a–c we show the phase portrait of example 2 and its Jacobian determinant. Figure 4.2a should be contrasted with the phase portrait of the Hénon mapping shown in fig. 3.2. [If in example 2 one applies the scaling transformation $x \rightarrow x/\varepsilon$ and $y \rightarrow y/\varepsilon$, the asymmetric fixed points are at $(1, -1)$ and $(-1, 1)$ for all ε and C ; figs. 1.3 and 3.1 show this transformed mapping when $\varepsilon = 20$ and $C = 0.3$.]

Examples 3 and 4 are derived from the area-preserving Hénon mapping in generalised standard form, (4.16) with $f(y) = -y$ and $g(x') = 2x'(1 - C - x')$. In this form the symmetry lines of the Hénon mapping are $y = x(1 - C - x)$ and $y = 0$ and its (symmetric) fixed points are $(0, 0)$ and $(1 - C, 0)$. Their stability is the same as in the McMillan form. Examples 3 and 4 possess the same symmetric fixed points with the same stability as the fixed points of the Hénon mapping, independently of ε . Example 3 is a particularly simple example from class III of the previous section. Its phase portrait and Jacobian determinant are shown in fig. 4.3a, b (compare fig 4.3a with the phase portrait of the Hénon mapping shown in fig. 3.3). Example 4 is from class IV and is perhaps a less satisfactory example of a nonconservative reversible mapping, from the mathematical point of view, because it has lines in the plane where it and its Jacobian determinant are not defined. Despite this, the regions around both its symmetric and asymmetric fixed points display similar dynamical features to those portrayed together in figs. 4.1–4.3, although the two sets of fixed points are more separated here because of the smallness of the perturbation strength ε (the asymmetric fixed points are again “born” from infinity at $\varepsilon = 0$).

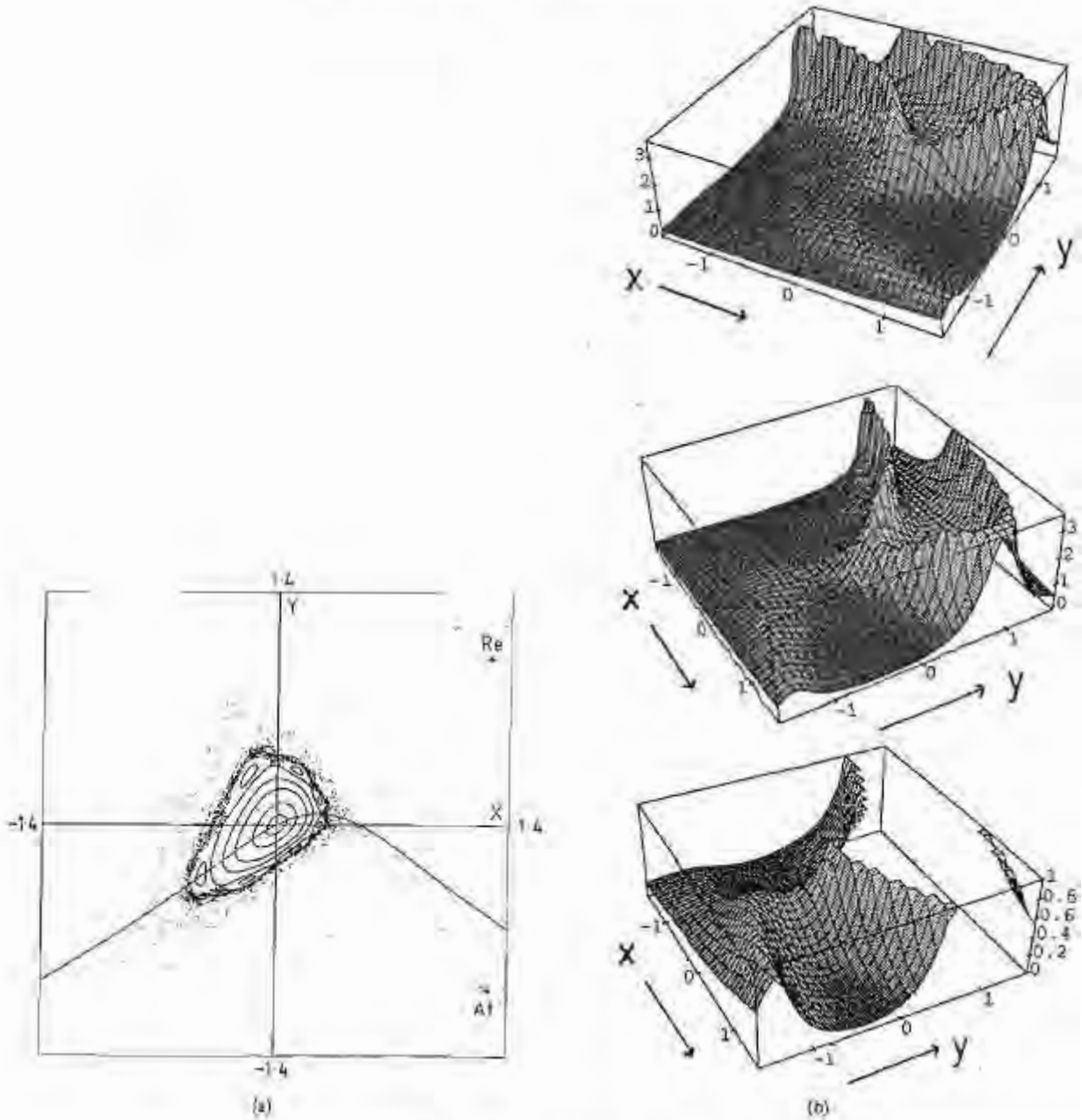


Fig. 4.3. (a) Phase portrait of the mapping example 3 of table 4.1 when $C = 0.5$. The symmetry line of H is the humped curve shown and the symmetry line of G is the x axis. The symmetric fixed point at the origin is elliptic and surrounded by KAM curves. The attracting (At) and repelling (Re) asymmetric fixed points are marked with crosses. External to the KAM curves and island chain are shown two trajectories that eventually converge to the attracting fixed point. (b) Plot of the Jacobian determinant of example 3 over the part of the plane shown in a (actually the domain here is $[-1.5, 1.6] \times [-1.6, 1.6]$). Over this region $J(x, y)$ ranges from close to 0 to greater than 3. The top two pictures show the surface obtained by plotting the Jacobian determinant when viewed from two different perspectives. It has a trough near the attracting asymmetric fixed point at $(1.2807, \dots, -1)$ and is much higher around the repelling asymmetric fixed point at $(1.2807, \dots, +1)$. In the bottom picture we show only the part of the surface where $J < 1$ (note the expanded scale on the J axis). The symmetric fixed points at $(0, 0)$ and $(0.5, 0)$, which have $J = 1$, are points on the projection of the boundary of this part of the surface onto the plane.

Between them, the four examples in table 4.1 display a range of features and phenomena. These examples will be used in chapters 5 and 6 to illustrate via numerical and pictorial investigations some of the properties of general (i.e., non measure-preserving) reversible mappings. Attention will tend to focus on examples 1–3 because, unlike example 4, they are “far” from area-preserving reversible mappings, and moreover they are analytic throughout the plane without the complication of having singularity lines.

5. Conservative behaviour in reversible mappings

In this chapter, phenomena associated with the symmetric periodic orbits of reversible mappings will be studied. We review the work done on area-preserving reversible mappings and present results for the non measure-preserving reversible mappings of table 4.1. As previously remarked, the neighbourhood of an elliptic symmetric fixed point in the examples of table 4.1 appears indistinguishable to the eye from that of an elliptic fixed point in an area-preserving mapping (cf. fig. 4.2a around the origin with fig. 3.2). What is obviously different between area-preserving mappings and the mappings of table 4.1 is that, although the Jacobian determinant at an elliptic symmetric fixed point in the latter equals 1, it is not equal to 1 around the fixed point, but varies in a range of values on either side of 1 (cf. the Jacobian determinant plots in the previous chapter).

Here we investigate whether there are any quantitative effects due to this lack of area preservation around symmetric fixed points or symmetric cycles in a general reversible mapping. In section 5.1 we study the breaking of the KAM curves, or circles, around elliptic symmetric fixed points by studying symmetric periodic orbits that lie close to these curves. In section 5.2 we study the period-doubling cascade that can arise after symmetric periodic orbits turn from being elliptic to hyperbolic. Critical exponents associated with these two processes involving symmetric periodic orbits are shown to be the same as those previously associated with conservative mappings (cf. also Quispel and Roberts [1988, 1989]).

Because the phenomena discussed here involve the study of symmetric periodic orbits in one-parameter reversible mappings, it is important to realise that an isolated symmetric periodic orbit stays symmetric as a mapping parameter is varied. The argument for this has been given by MacKay [1982] and relies on the Poincaré index (cf. section 2.1). If the periodic orbit has length n , then take L^n so that each periodic point is a fixed point (of L^n). A symmetric fixed point x_0 has $J = \text{Det } dL(x_0) = 1$ for L orientation-preserving, so that its index is $+1$ or -1 accordingly as $\text{Tr } dL(x_0) < 2$ or $\text{Tr } dL(x_0) > 2$ [cf. (2.12a, b)]. If the fixed point were to become asymmetric at any stage by moving off the symmetry line, then this event would be accompanied by the birth of an asymmetric partnering fixed point. It is easy to check that these two asymmetric points (which most generally have $J \neq 1$) have the same index because their eigenvalues are reciprocals of one another [cf. (2.12); if (2.12a) is true for one point, it is true for the other point and similarly with (2.12b)]. The two asymmetric fixed points therefore have a combined index of $+2$ or -2 which is different to the total index of $+1$ or -1 before the symmetric fixed point left the symmetry line, contradicting the conservation of Poincaré index.

Although numerically the problem of finding periodic orbits of an arbitrary mapping of the plane L in general requires a two-dimensional (2D) search for solutions of eqs. (2.5), the search for symmetric periodic orbits in a reversible mapping $L = H \circ G$ is a 1D search. We look along a curve in the plane, namely a symmetry line, and our trial points for the search are parametrised by one coordinate. If, for example, the symmetry line has the equation $y = h(x)$ then only one independent variable x appears in

the trial point $(x, h(x))$. A point of a symmetric n -cycle on the symmetry line can be calculated by, for example, repeated applications of the secant method. By fully exploiting the benefits of reversibility (cf. section 3.1), symmetric n -cycles can be located without the need to traverse the entire cycle. Even n -cycles can be found by going halfway around the orbit and using the condition that $y_{n/2} = h(x_{n/2})$, i.e., the halfway round point is necessarily on the same symmetry line as the initial point. Odd n -cycles can be more economically found by noting, for instance, that $(x_{(n+1)/2}, y_{(n+1)/2})$ lies on the symmetry line of H if the initial point is on the symmetry line of G . It is a further consequence of the properties of section 3.1 that although a reversible mapping can be written in many different ways as the composition of involutions by using different symmetries from a family [e.g., $L = (L^{i+1} \circ G) \circ (G \circ L^{-i})$], we can expect to find any symmetric periodic orbit by searching upon the two symmetry lines of the two involutions that provide a nice decomposition for L , like those listed in table 4.1.

5.1. KAM circles and their destruction

The outline of this section is as follows. We first review the KAM theorems for area-preserving mappings and for reversible mappings (section 5.1.1). This leads to a discussion of the (irrational) rotation number of invariant KAM circles and its approximation by a sequence of rational convergents. We then describe a quantitative technique that uses symmetric periodic orbits with rotation numbers equal to these rational convergents to study a given KAM circle (section 5.1.2). This technique, Greene's residue criterion (cf. Greene [1979], MacKay [1992]), was originally developed for area-preserving reversible mappings but we discuss the application of this technique to non measure-preserving reversible mappings and present some numerical results.

5.1.1. Conservative and reversible KAM theorems

The most ordered of dynamical systems are the integrable systems because they do not have any chaotic motion. Their dynamics typically consists of periodic and quasiperiodic motion. The canonical integrable mapping of the plane is the integrable twist mapping

$$r' = r, \quad \theta' = \theta + \omega(r). \quad (5.1)$$

This mapping in polar coordinates leaves invariant all circles centred on the origin so that the radius r is an integral or "constant of the motion". The quantity $\rho(r) = \omega(r)/2\pi \in (0, 1)$, is called the rotation number of a given circle and most generally varies from circle to circle. It completely describes the dynamics on the circle of radius $r = r_0$. When $\rho(r_0) = p/q$ for p, q relatively prime, the orbit of every point on the circle is periodic of length q and involves p complete revolutions around the origin. On the other hand, if $\rho(r_0)$ is irrational, the orbit of each point densely fills the circle and is quasiperiodic. The integrable twist mapping has the distinguishing property that it has sets of closed invariant curves whose rotation numbers completely fill some interval. There are no gaps at the rational rotation numbers and these correspond to invariant curves of non-isolated periodic points.

The mapping (5.1) is area-preserving. It is also reversible with respect to the involution $r' = r, \theta' = -\theta$. Indeed, (5.1) is simply the polar form of the formal normal form (3.59) around an elliptic fixed point of a measure-preserving mapping. Integrable mappings like (5.1) are special and rare – see appendix A for some other examples of integrable reversible mappings. Their significance is nonetheless assured by the KAM theorems that state that systems close to integrable retain some of the important properties of integrable mappings.

The starting point of the KAM theorems for mappings of the plane arises from a consideration of what happens to the dynamics when (5.1) is slightly perturbed by the addition of small functions of period 2π in θ to give the mapping

$$r' = r + a(r, \theta), \quad \theta' = \theta + \omega(r) + b(r, \theta). \quad (5.2)$$

The result when the perturbing functions in (5.2) are such that the perturbed mapping is still area-preserving, have been known for a long time [Moser 1962, 1968; Siegel and Moser 1971]. In this case the invariant circles of (5.1) with rational rotation number $\rho = p/q$ typically break up to leave just two cycles with that rotation number (typically a mapping of the plane is not integrable and so does not have an infinity of cycles of a certain length, cf. Moser [1968]). These are the so-called Poincaré–Birkhoff cycles and they have opposite stability. Some of the invariant circles of (5.1) with irrational rotation number remain for the perturbed mapping, though they are deformed into closed invariant curves homeomorphic to circles. The motion on these deformed circles is still quasiperiodic with the same rotation number as in the unperturbed mapping. In fact, the set of deformed invariant circles has finite measure and covers an increasing fraction of the area around the fixed point at the origin if one considers smaller and smaller neighbourhoods around this point.

Other invariant circles with irrational rotation number do break up on perturbation; and the larger the perturbation, the smaller the measure of invariant curves that remain. The criterion that determines whether a circle breaks or not under perturbation, and when it breaks (as a function of the size of the perturbation), is the “degree of irrationality” of its rotation number. This will be discussed below.

Originally the above result, which we will call the global KAM theorem for area-preserving mappings, had the mathematical requirements: (i) that the functions $a(r, \theta)$ and $b(r, \theta)$ be real and analytic; and (ii) that $\omega(r)$ be analytic and monotonic increasing so that the unperturbed mapping (5.1) bent a given radius vector uniformly in the one direction (it was a monotone twist mapping). The domain of the mapping (5.2) could either be a disc centred on the origin or the annulus $c \leq r \leq d$ (not necessarily mapped into itself). Later work has relaxed the differentiability conditions on the functions a and b so that the result still holds (i.e., invariant curves still persist) if these functions are only C^3 , which is in fact the minimum possible differentiability requirement on them for which the theorem still holds [Herman 1983].

Significantly, the global KAM theorem has wide applicability to very many area-preserving mappings, not necessarily those that are slight perturbations of the integrable mapping (5.1). This is because in the neighbourhood of a “typical” elliptic fixed point of an area-preserving mapping, the mapping takes the form (5.2). Here “typical” means, for a mapping that is at least C^4 differentiable, that the eigenvalues of the fixed point are not first, second, third or fourth roots of unity [Siegel and Moser 1971; Moser 1968, 1973]. This application of the global result, which we call the local KAM theorem, implies that an elliptic fixed point of an area-preserving mapping is surrounded by invariant curves as well as island chains associated with elliptic Poincaré–Birkhoff cycles. Interspersed between these curves are chaotic bands associated with the transverse homoclinic intersections of the stable and unstable manifolds of hyperbolic Poincaré–Birkhoff cycles.

The recent KAM theorems of Arnol'd and Sevryuk for reversible mappings also exist in both global and local versions [Arnol'd 1984; Arnol'd and Sevryuk 1986; Sevryuk 1986]. The global theorem considers the perturbed twist mapping (5.2) when $a(r, \theta)$ and $b(r, \theta)$ are chosen so that the perturbed mapping remains reversible though not necessarily area-preserving. It requires the perturbing functions

to be analytic. The conclusion is much the same as in the area-preserving case^{*)}; a large proportion (a finite measure) of the invariant curves of an integrable reversible mapping persist under a small reversible perturbation. This result is illustrated in fig. 5.1 with an integrable reversible mapping taken from Quispel et al. [1989]. According to Arnol'd and Sevryuk, the rational circles of (5.1) break up to still leave at least two cycles with each rational rotation number. These cycles are symmetric (cf. Sevryuk [1986, chapter 5]) and they constitute the Poincaré–Birkhoff cycles for the (reversible) perturbed mapping.^{**)}

The local KAM theorem for reversible mappings, with which we will be more concerned, guarantees the existence of infinitely many nested closed invariant curves around a nonresonant elliptic symmetric fixed point. Moreover these curves are invariant under the symmetry G as well as under the mapping L . Again the local result follows from the global one by noting that close to an elliptic symmetric fixed point the motion is locally conjugate to a perturbation of integrable motion.

The determining factor in the (reversible or conservative) KAM theorems to establish whether a particular invariant curve of (5.1) persists under perturbation is its rotation number. The “robustness” of a given curve is directly related to how irrational its rotation number is. The circles of (5.1) that do persist under sufficiently small (reversible or conservative) perturbations (5.2) are those circles with “sufficiently irrational” rotation number ρ satisfying relations of the form

$$|\rho - p/q| \geq K/(q^{2+\tau}), \tag{5.3}$$

for all integers p and $q > 0$ and for some positive constants K and τ .

A large fraction of invariant circles remain because of the number-theoretic properties of irrational numbers. The condition (5.3) is an example of a Diophantine condition and is satisfied by most irrational numbers (for small K). It is a statement of how well the irrational number ρ can be approximated by nearby rationals. It is known that any irrational number ρ can be best approximated by the sequence of rationals $\rho_n = p_n/q_n$, called the convergents of ρ , which are obtained as the n th level truncations of its continued fraction expansion (CFE),

$$\frac{1}{n_1 + \frac{1}{n_2 + \frac{1}{n_3 + \dots}}} =: [n_1, n_2, n_3, \dots], \tag{5.4}$$

where n_i are positive integers. Every irrational $\rho \in (0, 1)$ has a unique representation as such a continued fraction – see Niven [1956] for a discussion and the method for generating the CFE. The irrational number lies between any two successive truncations, so that the convergents approximate it

^{*)} The KAM theorem proved by Moser [1962] is typically applied to area-preserving mappings but in fact the theorem holds if the perturbed mapping (5.2) is presumed instead to have the self-intersection property, which says that it maps any closed curve in the annulus domain in such a way that the curve intersects its image (see Siegel and Moser [1971, sections 32–34]). Although in general reversibility does not imply this intersection property, Sevryuk [1986, p. 57] states that he does not know of any reversible mapping arbitrarily close to the twist mapping (5.1) that does not possess the property (see also Sevryuk [1986, p. 154]).

^{**)} Very few theorems exist concerning the number and arrangement of symmetric cycles along symmetry lines in non area-preserving reversible mappings. One exception, from Tanikawa and Yamaguchi [1987], says that between the two points of a symmetric $2j$ -cycle on a symmetry line lies a periodic point of period j .

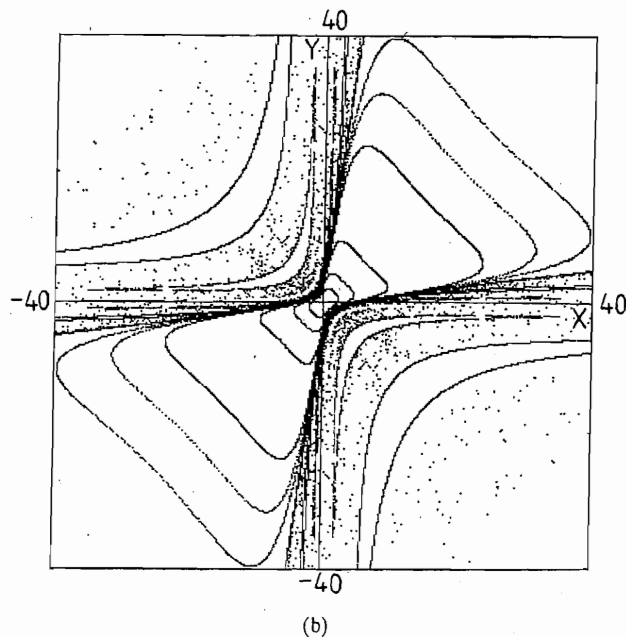
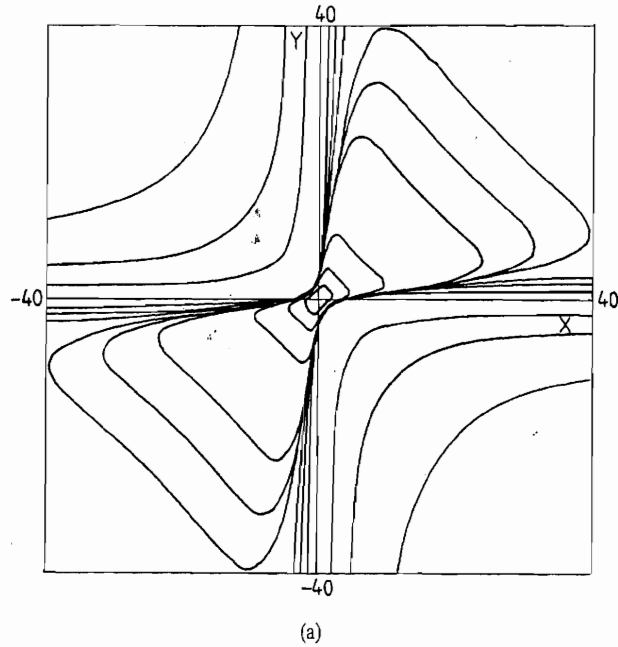


Fig. 5.1. (a) Phase portrait of the mapping $x' = y$, $y' = [2\lambda y - x(1 - \lambda^2 y^2)] / (1 - \lambda^2 y^2 + 2\lambda xy)$ with $\lambda = 0.25$. This mapping is an integrable reversible mapping (cf. Quispel et al. [1989]). The "bow-tie" shaped closed curves are all invariant under the mapping, as are sets of two pairs of the unclosed curves that are symmetric about $y = x$. (b) Phase portrait of the mapping $x' = y$, $y' = [2\lambda y + py^3 - x(1 - \lambda^2 y^2)] / (1 - \lambda^2 y^2 + 2\lambda xy)$, for $p = 0.0005$. This mapping is a nonintegrable reversible perturbation of the integrable mapping shown in a. It still appears to have invariant curves.

from either side. Furthermore successive convergents p_n/q_n and p_{n+1}/q_{n+1} are neighbouring rationals, i.e.,

$$p_n q_{n+1} - p_{n+1} q_n = \pm 1. \tag{5.5}$$

The “most irrational” irrationals, those that are poorly approximated (relatively speaking) by their rational convergents, are called the “noble numbers” (cf. Series [1985] for a readable discussion). The noble numbers have CFE’s ending in 1, 1, 1, The canonical example of a noble number in the interval (0, 1) is the number

$$\gamma^{-1} = \frac{1}{2}(\sqrt{5} - 1), \tag{5.6}$$

which is the reciprocal of the golden mean,

$$\gamma = \frac{1}{2}(\sqrt{5} + 1). \tag{5.7}$$

The number (5.6) has a CFE (5.4) that consists entirely of 1’s. One finds by successively truncating its CFE that its rational convergents are given by F_n/F_{n+1} where F_n are the Fibonacci numbers: 1, 1, 2, 3, 5, 8, 13, 21, . . . given by $F_{n+2} = F_{n+1} + F_n$.

In the interval $(p/q, p'/q')$, where p/q and p'/q' are any neighbouring rationals with $q' > q$, the number

$$(p + \gamma p')/(q + \gamma q') \tag{5.8}$$

is noble. Its rational approximants are

$$p_0/q_0 = p/q, \quad p_1/q_1 = p'/q', \quad p_2/q_2 = (p_0 + p_1)/(q_0 + q_1), \tag{5.9}$$

and in general

$$p_{n+1}/q_{n+1} = (p_{n-1} + p_n)/(q_{n-1} + q_n). \tag{5.10}$$

Thus the approximants are generated by a Farey tree construction.

5.1.2. Breakup of KAM circles; the residue criterion

Invariant curves with noble rotation number, being the curves on which the rotation number is most strongly irrational, certainly survive the small perturbations from integrability allowed in the conservative and reversible KAM theorems. In addition however, they figure prominently in numerical studies of KAM curve breakup when the size of the perturbation exceeds the realm of the analytical theory. This is because Greene [1979] found numerically, for reversible area-preserving mappings, that often the invariant curves with noble rotation numbers are the most robust; if an invariant curve of some non-noble frequency exists, then there is also a noble invariant curve (cf. Schmidt and Bialek [1982]). An approximate renormalisation scheme also leads to this conclusion [Escande 1982]. It has been conjectured (cf. MacKay [1986]) and recently proved under some conditions (cf. MacKay and Stark [1991]) that for typical one-parameter area-preserving mappings, the last invariant curve to break in an

interval of rotation number $(p/q, p'/q')$, where p/q and p'/q' are neighbouring rationals with $q' > q$ and the interval is short, is the curve with rotation number (5.8). The interval of rotation number $(p/q, p'/q')$ can be translated into an appropriate region of phase space by locating two periodic orbits with rotation numbers p/q and p'/q' , respectively.

The numerical method developed by Greene conjectures a relationship between the linear stability of symmetric periodic orbits nearby a KAM curve of an area-preserving mapping and the existence or non-existence of the invariant curve. The periodic orbits used are precisely those (Poincaré–Birkhoff) cycles with rotation numbers $\rho_n = p_n/q_n$ equal to the convergents of the irrational rotation number ρ of the curve. We will variously call these particular periodic orbits the (noble) *approximating*, or *approximant*, (periodic) orbits or cycles. The method is called the *residue criterion*, where the residue, R , of a periodic orbit with period q_n is given by

$$R = \frac{1}{4}(2 - \text{Tr}[dL^{q_n}]). \quad (5.11)$$

When $0 < R < 1$ the orbit is elliptic, and when $R < 0$ or $R > 1$ the orbit is hyperbolic or more specifically a saddle, so it is unstable. The transition cases $R = 0$ and $R = 1$ correspond respectively to a pair of eigenvalues at $+1$ and a pair of eigenvalues at -1 . The two Poincaré–Birkhoff cycles for each rational rotation number are such that one has positive residue and the other negative residue.

Denote by R_n the positive residues of the symmetric cycles with rotation numbers $\rho_n = p_n/q_n \rightarrow \rho$ at a given value of a mapping parameter C . Then Greene's conjecture based upon observations for area-preserving reversible mappings is that as $n \rightarrow \infty$ one of the following occurs:

$$R_n \rightarrow 0^+ \text{ and there is a smooth invariant curve with rotation number } \rho \text{ at } C; \quad (5.12a)$$

$$R_n \rightarrow +\infty \text{ and there is no curve with rotation number } \rho \text{ at } C; \quad (5.12b)$$

$$R_n \rightarrow R_{\text{KAM}}, 0 < R_{\text{KAM}} < 1 \text{ at } C = C_{\text{KAM}} \text{ and there is a non-smooth invariant curve with rotation number } \rho. \quad (5.12c)$$

In case (5.12b) the nearby symmetric periodic orbits all have $R_n > 1$ beyond some n , or equivalently beyond some orbit length q_n , and so are unstable. Case (5.12c) is the critical (transition) case, in the sense that (5.12a) occurs on one side of C_{KAM} and (5.12b) occurs on the other. The interpretation given to this behaviour of the residues, evidence for which includes carefully assembled pictorial investigations [Greene 1979; Shenker and Kadanoff 1982], is that in case (5.12a) the successive approximating periodic cycles appear to lie on smooth curves that converge from either side to a smooth KAM curve. In case (5.12b), the approximating orbits are on jagged curves that seem to preclude the existence of a KAM curve between them – the KAM curve has broken up by developing infinitely many gaps in it and has self-similar structure like a Cantor set (dubbed a cantorus, cf. Percival [1979])^{*}. At the intermediate critical stage (5.12c) when $C = C_{\text{KAM}}$, the approximating orbits of longer and longer periods appear to lie upon curves with self-similar features upon magnification. [Note that C_{KAM} can also be identified by studying the negative-residue Poincaré–Birkhoff cycles with rotation numbers ρ_n ; their residues R_n^- behave analogously to that listed in (5.12a–c), with, respectively, $0^+ \rightarrow 0^-$, $+\infty \rightarrow -\infty$

^{*} We remark that recent work of Hu et al. [1991] shows that in nonanalytic (C^1) twist maps a KAM curve can reappear after it has broken up; they also report different residue behaviour in some cases from that listed in (5.12).

and $R_{\text{KAM}}, 0 < R_{\text{KAM}} < 1 \rightarrow R_{\text{KAM}}^-, -1 < R_{\text{KAM}}^- < 0$. Very recently, some aspects of the relationship between the residues and the existence of the KAM curve have been made rigorous (cf. MacKay [1992]).

The existence of a local KAM theorem for reversible mappings as described in section 5.1.1 above makes it natural to study the residue criterion in reversible (non measure-preserving) mappings (cf. Quispel and Roberts [1988, 1989]). We have studied the destruction of an invariant noble curve around the elliptic symmetric fixed point at the origin in example 3 of table 4.1, and at $(1 - C, 0)$ in example 4. The chosen noble rotation number is the reciprocal of the square of the golden mean,

$$\rho_{\text{KAM}} = \gamma^{-2} = \frac{1}{2}(3 - \sqrt{5}) = 0.381\,966\,011\dots, \tag{5.13}$$

which has the CFE $[2, 1, 1, 1, \dots]$. This number is of the form (5.8) with $p/q = 1/2$ and $p'/q' = 1/3$. Its rational approximants from (5.9) and (5.10) turn out to be ratios of second successive Fibonacci numbers, i.e.,

$$\rho_n = p_n/q_n = F_n/F_{n+2}. \tag{5.14}$$

As in studies of area-preserving reversible mappings, we locate the positive-residue symmetric Poincaré–Birkhoff periodic orbits with rotation numbers (5.14) and “plot” their residues as the parameter C is varied. Of course, without area preservation, the return Jacobian determinant of these orbits still equals 1 because of their symmetry and (5.11) still completely describes their stability. The best way to locate these orbits is to start searching for the shortest approximant orbits [e.g., $1/3, 2/5, 3/8, 5/13$ for $\rho_{\text{KAM}} = (3 - \sqrt{5})/2$] on the symmetry lines of H and G . The position and rotation number of these smaller period approximant orbits can be used to give good initial guesses for the positions of successively longer approximant orbits. This is because the rotation number is found to be locally monotonic as a function of position along the symmetry lines so that at each value of the parameter the position of an approximant periodic orbit can be estimated by linearly interpolating between the positions found for the previous two approximants (note that the rotation number of each approximant orbit lies between those of the two previous approximants).

In area-preserving mappings it has been observed numerically that it is always possible to consider the symmetry lines of G and H which intersect at the symmetric fixed point as four half-lines, and to find one point of every approximating positive-residue orbit on just one of these half-lines (cf. Greene [1979], MacKay [1986], Meiss [1986]); sometimes this is only possible for the orbits beyond some length (cf. Ketoja and MacKay [1989]). That this should always be possible is called the “dominant reversor conjecture” for the residue criterion. We find that it appears to hold in non measure-preserving, reversible mappings as well.

Once the approximant periodic orbits are located for one value of the mapping parameter C , the parameter can be incremented and the motion of the orbits on the symmetry line can be followed. Calculation of the residue of the orbit for each parameter value is done by multiplying the Jacobian matrices evaluated at each point of the orbit to give the return Jacobian matrix and then by using the definition (5.11). In such a way, the residue curve as a function of parameter for the particular periodic orbit is constructed, cf. fig. 5.2. The qualitative behaviour of the residues in fig. 5.2 is consistent with Greene’s observations described in (5.12a)–(5.12c) above. Quantitative comparisons with the results for area-preserving mappings can also be made. A numerical study of the break up of noble curves in several one-parameter families of area-preserving reversible mappings has revealed some universal

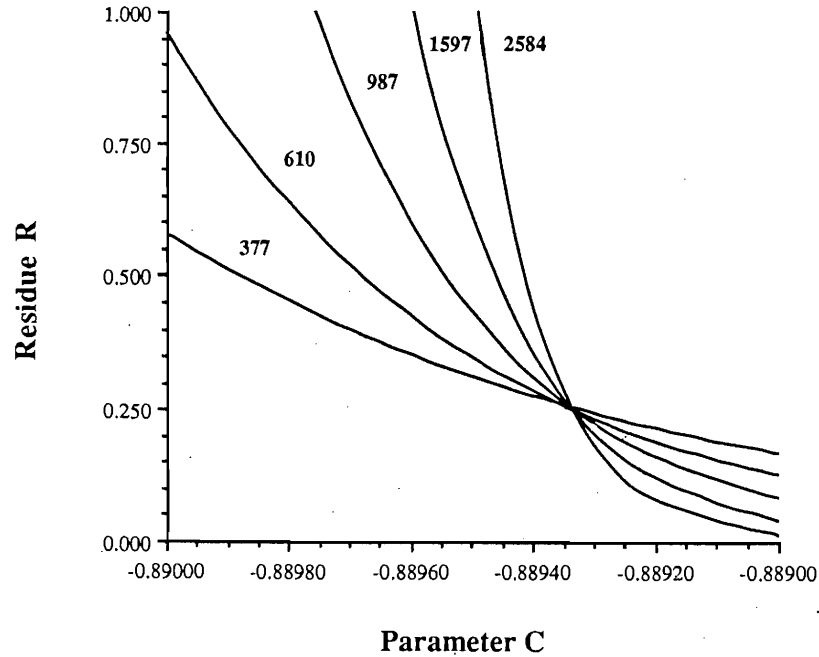


Fig. 5.2. Residue curves for symmetric cycles surrounding the origin in example 3 of table 4.1 with periods 377, 610, 987, 1597 and 2584. The rotation numbers of these cycles are respectively $144/377$, $233/610$, $377/987$, $610/1597$ and $987/2584$. This sequence of rational numbers converges from either side to the noble irrational number $(3 - \sqrt{5})/2$.

quantitative behaviour and asymptotic scaling [MacKay 1986]. We find identical behaviour for the non measure-preserving reversible mappings of chapter 4, in particular:

(i) The value of R_{KAM} in (5.12c) is the same for each of these mappings with value

$$R_{\text{KAM}} = 0.250\,08\dots \quad (5.15)$$

This value can be obtained as the limit of the residues at the points of intersection of the residue curves $R_n(C)$ and $R_{n+1}(C)$ of successive pairs of rational convergents. Denote the sequence of these intersection residues by R_n^{int} . Then the convergence of R_n^{int} is asymptotically geometric, i.e.,^{*)}

$$\delta_{R_n} = \frac{R_n^{\text{int}} - R_{n-1}^{\text{int}}}{R_{n+1}^{\text{int}} - R_n^{\text{int}}} \rightarrow \delta_{R,\text{KAM}} = -1.637\dots \quad (5.16)$$

The negative value of $\delta_{R,\text{KAM}}$ indicates that R_{n+1}^{int} lies between R_{n-1}^{int} and R_n^{int} . This is illustrated in fig. 5.3.

(ii) The value of C_{KAM} can be found from the sequence of parameter values C_n^{int} at the points of intersection of the residue curves $R_n(C)$ and $R_{n+1}(C)$. This sequence converges to a value C_{KAM} asymptotically geometrically with a universal ratio so that

^{*)}We adopt the common convention of saying that something converges geometrically but quoting the inverse of the geometric ratio. This inverse is a number greater than one in absolute value.

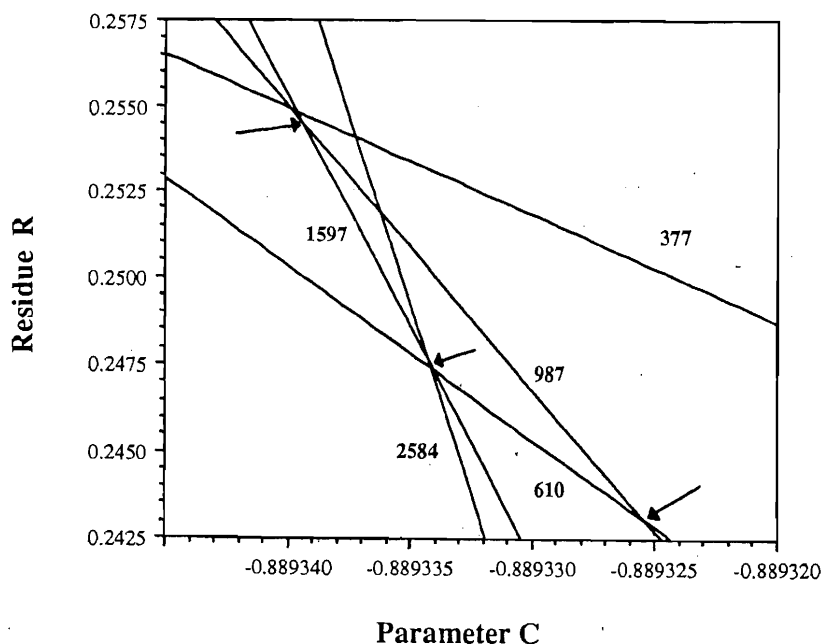


Fig. 5.3. Enlargement of fig. 5.2 around the area in which the residue curves appear to all intersect. In fact this is not the case, but we can look at intersections between the curves of successive approximant cycles. Here we indicate by arrows the intersection of the residue curves of periods 610 and 987 (right-hand arrow), 987 and 1597 (left-hand arrow) and 1597 and 2584 (middle arrow). This illustrates the pattern that the parameter value and residue value at an intersection of the residue curves of two successive approximants are contained between those values at the previous two intersections.

$$\delta_{C_n} = \frac{C_n^{\text{int}} - C_{n-1}^{\text{int}}}{C_{n+1}^{\text{int}} - C_n^{\text{int}}} \rightarrow \delta_{C, \text{KAM}} = -2.665 \dots \quad (5.17)$$

Note that these scalings could have been obtained by alternative methods as detailed by MacKay [1986]. Some residue behaviour different to that described above will be discussed at the end of this section.

To specifically illustrate the determination of the quantities (5.15)–(5.17), table 5.1 presents numerical results for the break up of the curve with rotation number γ^{-2} given by (5.13) in example 3 of table 4.1. Listed are the sequences R_n^{int} and C_n^{int} for successive rational approximant periodic orbits (5.14) [note: rotation number for these orbits = (revolutions around the origin)/period], as well as the position of one of the points of each approximant orbit on a symmetry line (the number of figures quoted for the coordinate reflects confidence in agreement with the true value). For each triple of consecutive C_n^{int} values we calculate the value δ_{C_n} defined by (5.17). The number δ_{R_n} on each line is calculated similarly, substituting the R_n^{int} value from the line together with the values from the lines immediately above and below into (5.16). The sequences of values δ_{R_n} and δ_{C_n} indicate that the values of R_n^{int} and C_n^{int} appear to converge asymptotically geometrically, respectively, from above and below to a value R_{KAM} , and from left and right to a value C_{KAM} . We estimate these limiting values by superconverging each sequence (using Aitken's method, cf. Abramowitz and Stegun [1972, section 3.9.7]).

These limiting values are listed in table 5.2, together with the values of $\delta_{C, \text{KAM}}$ and $\delta_{R, \text{KAM}}$ obtained from the sequences δ_{C_n} and δ_{R_n} , again by superconverging. Also shown are the figures obtained from

Table 5.1

Intersections of residue curves of periodic orbits around the symmetric fixed point (0, 0) of example 3 of table 4.1. The parameter value C_n^{int} should give agreement between the residues of each pair of orbits shown to at least the number of figures in R_n^{int} .

Period	Revolution	Coordinate ^{a)}	Sym ^{a)}	C_n^{int}	δ_{C_n}	R_n^{int}	δ_{R_n}
377	144	0.104 587 420 634 ...	1				
610	233	0.104 586 361 402 ...	1	-0.889 362 553 666 079 0		0.262 010 8 ...	
610	233	0.104 577 979 034 ...	1				
987	377	0.104 578 328 862 ...	1	-0.889 325 434 858 058 5	-2.665 957 8 ...	0.243 081 ...	-1.662 ...
987	377	0.104 581 471 16 ...	1				
1 597	610	0.104 581 357 98 ...	1	-0.889 339 358 111 869 0	-2.665 211 1 ...	0.254 471 ...	-1.622 ...
1 597	610	0.104 580 178 58 ...	1				
2 584	987	0.104 580 215 66 ...	1	-0.889 334 134 040 381 3	-2.676 184 8 ...	0.247 449 ...	-1.655 ...
2 584	987	0.104 580 656 28 ...	1				
4 181	1 597	0.104 580 644 2 ...	1	-0.889 336 086 099 661 9	-2.788 162 4 ...	0.251 69 ...	-1.703 ...
4 181	1 597	0.104 580 486 18 ...	1				
6 765	2 584	0.104 580 490 12 ...	1	-0.889 335 385 975 720 7		0.249 2 ...	

^{a)} "Sym" = 1 corresponds to $y^3 - y^2 + y + Cx + x^2 - x = 0$ and "coordinate" is the x coordinate on this line.

Table 5.2

Numerical results for residue scalings associated with noble KAM curves in reversible mappings.

	Non measure-preserving reversible mappings ^{a)}		Area-preserving reversible mappings ^{b)}
	Example 3	Example 4	
R_{KAM}	0.2501 ...	0.250 08 ...	0.250 088 8 ...
$\delta_{R, \text{KAM}}$	-1.6 ...	-1.637 ...	-1.637 116 1 ...
$\delta_{C, \text{KAM}}$	-2.6 ...	-2.665 ...	-2.665 142 9 ...
C_{KAM}	-0.889 335 55 ...	2.841 404 026 ...	

^{a)} These results are obtained from double-precision calculations.

^{b)} These results are taken from MacKay [1986] and are the result of quadruple-precision calculations.

similar calculations for example 4 of table 4.1, as well as the results found for area-preserving mappings. From table 5.2 we conclude that the value R_{KAM} and the scalings $\delta_{R, \text{KAM}}$ and $\delta_{C, \text{KAM}}$ associated with noble KAM curves in non measure-preserving, reversible mappings are universal, and moreover the same as those universal values previously found for area-preserving, reversible mappings. The values of C_{KAM} are of course peculiar to the mapping and not universal.

We conjecture that the behaviour observed carries over to relating the behaviour of the residues to the existence of the noble curve as done by Greene [1979]. This is based upon the qualitative similarities shown in fig. 5.2 and the quantitative agreement shown in table 5.2, and on the fact that Greene's conjecture would seem to rely on the topological property of how well the approximant orbits fit the KAM curve, which would not appear to be affected by the local Jacobian determinant environment.

Finally we come to the theoretical explanation of the universal behaviour associated with noble KAM curve destruction, at least for area-preserving mappings, for which such theory has been developed. The theoretical explanation is in terms of renormalisation group theory. This topic for area-preserving mappings has already been thoroughly covered – see Shenker and Kadanoff [1982], MacKay [1982, 1983b, 1986, 1988], Escande [1985], Greene [1986] and references therein – so we mention it only briefly.

In the renormalisation picture, the existence of KAM curves with noble rotation number in area-preserving reversible mappings is explained by the presence of a simple attracting fixed point of a certain renormalisation operator in the space of (pairs of) area-preserving mappings. The simple fixed point mapping is integrable like (5.1) and possesses an invariant circle with noble rotation number. The question of whether a given (nonintegrable) mapping possesses a noble circle amounts to whether this mapping lies in the basin of attraction of the simple fixed point. Mappings attracted to this fixed point have noble approximant periodic orbits with residues $R_n \rightarrow 0$. Part of the boundary of the basin of attraction of the simple fixed point comprises the stable manifold of another fixed point of the renormalisation operator, the so-called critical fixed point, which has a critical noble circle. Mappings attracted to this fixed point along its stable manifold have noble approximant periodic orbits with residues $R_n \rightarrow R_{\text{KAM}} = 0.250\,088\dots$. The critical residue scalings $\delta_{\text{C,KAM}}$ and $\delta_{\text{R,KAM}}$ given in table 5.2 above are related to the eigenvalues of the linearised renormalisation operator around this critical fixed point.

Recent work has concentrated on further defining the basin boundary of the simple fixed point mapping. This has led to the discovery of other area-preserving mappings that are fixed points or periodic orbits of the renormalisation operator [Greene et al. 1987; Johannesson et al. 1988; Ketoja and MacKay 1989; Greene and Mao 1990; Greene 1990; Wilbrink 1990]. Mappings on the stable manifolds of such other fixed points or cycles have different residue behaviour to that listed above. For instance, the sequence of residues R_n of noble approximant periodic orbits may converge to a three-cycle of values, none equal to $0.250\,088\dots$, corresponding to a three-cycle of the renormalisation operator [Greene and Mao 1990; Wilbrink 1990]. Such behaviour appears when the mapping has additional symmetry, or equivalently, commutes with a nontrivial mapping [MacKay 1984], for example if the mapping is odd so that $L(-\mathbf{x}) = -L(\mathbf{x})$ (e.g., Huiszoon [1983]). When the mapping is reversible, the existence of nontrivial commuting maps often leads to it being multiply reversible (cf. 3.7a, b) with consequently more reversing symmetries and symmetry lines (cf. Wilbrink [1990]).

It would be desirable to extend the renormalisation group treatment to encompass the above results for reversible mappings that are not area-preserving (cf. also Khanin and Sinai [1986]).

5.2. Period doubling of symmetric fixed points

The points of transition between a symmetric fixed point being hyperbolic or elliptic occur when its eigenvalues are both $+1$ or both -1 . These two cases correspond to the trace of the (Jacobian matrix at the) fixed point equalling $+2$ or -2 . In the present section we discuss the case where both eigenvalues of a symmetric fixed point of a one-parameter reversible mapping (symmetric with respect to G , say) pass through -1 (i.e., its trace is -2) and the point turns hyperbolic. For every example in table 4.1 it is observed that a symmetric two-cycle is born at this stage (cf. fig. 5.4). The eigenvalues of the two-cycle at creation are both $+1$ as required by continuity (the eigenvalues of the fixed point at

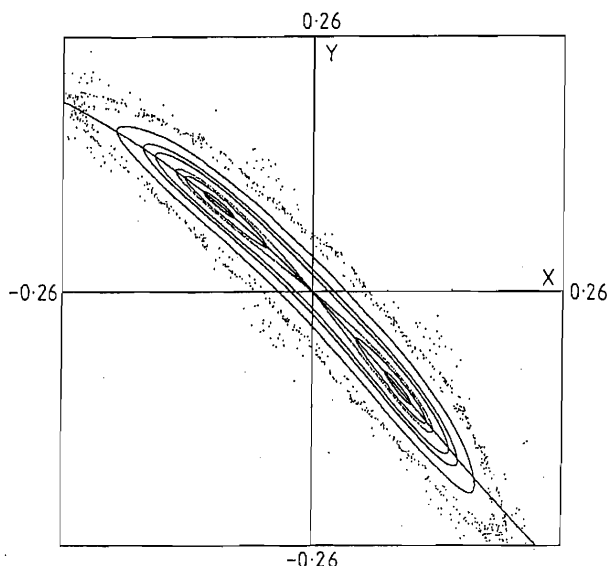


Fig. 5.4. Region around the origin in example 2 of table 4.1 at $C = -1.02$, soon after the symmetric fixed point there has turned hyperbolic and given birth to a symmetric two-cycle lying on the symmetry line of H . The two-cycle is elliptic and so is surrounded by its own invariant curves (the nested double islands). Some of the outer invariant curves that enclosed the origin when it was elliptic appear to still exist even though the point is now hyperbolic.

bifurcation are $+1$ when it is considered as a fixed point of L^2 rather than of L .)^{*} The two-cycle is found to have both of its points on the symmetry line of G or on the symmetry line of $H = L \circ G$.

With the continuous variation of the mapping parameter C we find that, after it is born (with trace equal to 2), the eigenvalues of the two-cycle become complex so that the two-cycle is elliptic. They then typically traverse the unit circle in the complex plane, passing through the so-called superstable point (trace equal to 0) where they are $\pm i$, and coinciding again when they are both -1 (trace equal to -2). At this time, the two-cycle turns hyperbolic and gives birth to a symmetric four-cycle. The four-cycle has two points on the same symmetry line as the two-cycle. These two points are born along this symmetry line from one point of the two-cycle; the other point of the two-cycle bifurcates across this symmetry line to produce the other two points of the four-cycle.

We wish to study here the numerical observation that this process can apparently in some cases continue ad infinitum. That is, by continuously varying the map parameter, successive symmetric period doublings continue with a symmetric 2^n -cycle giving birth to a symmetric 2^{n+1} -cycle when its eigenvalues are both -1 . In this way, a cascade of even symmetric cycles is formed. The most recent cycle is elliptic with $-2 < \text{trace} < 2$ and so is surrounded by KAM curves; the previous cycles in the cascade are hyperbolic with both eigenvalues being negative (cf. fig. 5.5).

These qualitative observations are explained by the analysis of MacKay [1982] who has shown that a symmetric fixed point in a reversible (area-preserving or non area-preserving) mapping L generically period-doubles to give a symmetric two-cycle on the symmetry line of G or of $L \circ G$. Each point of the symmetric two-cycle is itself a symmetric fixed point of the reversible mapping L^2 . Consequently if the

^{*} From our discussion below (2.11) of section 2.1, we know that the only time when a two-cycle could be born from a fixed point with $J = 1$ is when the trace of the fixed point equals -2 .

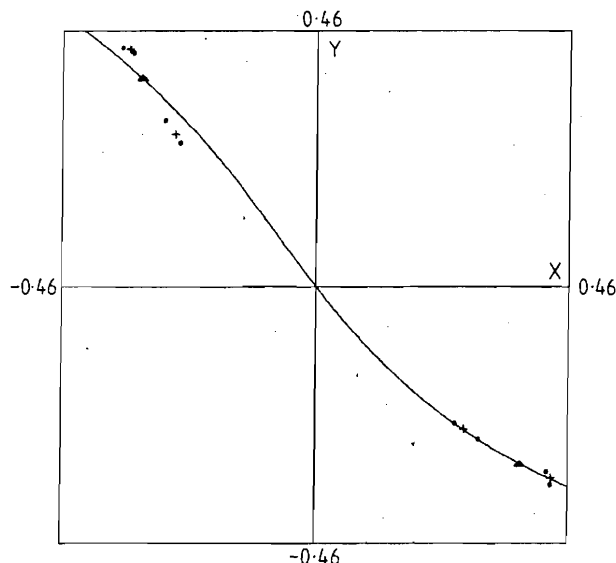


Fig. 5.5. Phase portrait of example 2 of table 4.1 at $C = -1.27294 \dots$, further along the symmetric period doubling cascade arising from the origin. Now there exists a two-cycle (\blacktriangle), a four-cycle ($+$) and an eight-cycle (\bullet). The eight-cycle is elliptic but its invariant curves are too small to see. It is just about to turn hyperbolic and bifurcate to a 16-cycle. The two-cycle and four-cycle are already hyperbolic but still remain symmetric. The period doubling occurs along and across the symmetry line of H with each cycle having two points on this line. Note the x - y symmetry of each cycle.

two-cycle then period-doubles, one point of it must bifurcate along the symmetry line of G and the other point must bifurcate along the symmetry line of $L^2 \circ G$, because we know that a symmetric cycle can have at most two points on the one symmetry line and does so only when even. The continued application of this result gives the symmetric period doubling cascade that is observed.

After MacKay, the symmetry line on which each orbit of the period doubling cascade has two points is called the dominant symmetry line. The point of each cycle that period-doubles along the line is called the “good” point. The point that bifurcates across the line is called the “bad” point and is halfway around the periodic orbit from the good point. The dominant symmetry line is not unique because if the most recent cycle of the cascade has period 2^j , and it and the previous cycles all have two points on the symmetry line of G , say, then all cycles have the same two points on the symmetry line of $L^k \circ G$ where k is any multiple of 2^j .

For many one-parameter families of area-preserving, reversible mappings the symmetric period doubling process has been quantitatively followed along a dominant symmetry line and universal self-similar behaviour has been observed [Bountis 1981; Greene et al. 1981; MacKay 1982, 1983a]. Our investigation of symmetric period doubling in non measure-preserving, reversible mappings reveals the same scaling behaviour. Our results can be summarised as follows:

(i) Define C_n as the parameter value at which the 2^n -cycle becomes unstable and bifurcates (in a slight abuse of notation we will use the subscript n to mean 2^n , i.e., the period of the cycle). Then the sequence of successive parameter values C_n converges to a value $C_{PD,SYM}$.

(ii) The convergence of the parameter values C_n is asymptotically geometric, i.e.,

$$\delta_{C_n} = \frac{C_n - C_{n-1}}{C_{n+1} - C_n} \rightarrow \delta_{PD,SYM} = 8.72109 \dots, \tag{5.18}$$

where $\delta_{\text{PD,SYM}}$ has a universal value independent of the mapping. Actually, (5.18) is equally well obtained by using the C_n values at which each cycle in the cascade is superstable (has trace = 0). We differentiate between the two sequences C_n of parameter values by using C_n^{bif} and C_n^{sup} .

(iii) The successive distances $d_{\alpha,n}$ between the good and bad points of each cycle on the dominant symmetry line measured at C_n also form asymptotically a geometric progression, i.e.,

$$\alpha_n = d_{\alpha,n}/d_{\alpha,n+1} \rightarrow \alpha_{\text{PD,SYM}} = 4.018 \dots, \quad (5.19)$$

where $\alpha_{\text{PD,SYM}}$ is another universal constant. It is observed that between consecutive cycles the good point alternates being the left-most or right-most point of the two points of each cycle on the dominant symmetry line (cf. fig. 5.6 where this is shown in example 2).

(iv) The distances between the points one-quarter and three-quarters the way around each 2^n -cycle ($n \geq 2$) from the good point form an asymptotically geometric progression with universal ratio $\beta_{\text{PD,SYM}}$, i.e.,

$$\beta_n = d_{\beta,n}/d_{\beta,n+1} \rightarrow \beta_{\text{PD,SYM}} = 16.363 \dots \quad (5.20)$$

Because the good point lies on the dominant symmetry line, the two points used to calculate the distance $d_{\beta,n}$ are reflections of one another by the dominant symmetry. These two points are the ones born across the symmetry line from the bad point of the preceding orbit.

The observations (iii) and (iv) correspond to self-similar scaling along and across the dominant symmetry line (for area-preserving mappings, the scaling has been extended to other distances within the 2^n -cycle in Gunaratne and Feigenbaum [1985]). An alternative way to define the distances $d_{\alpha,n}$ and

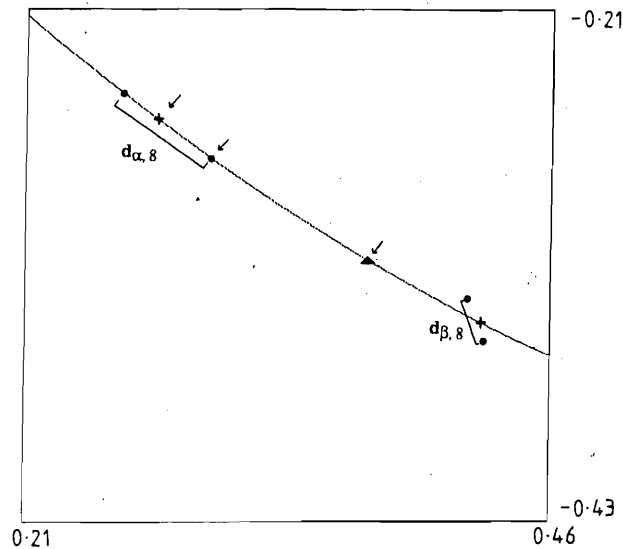


Fig. 5.6. Enlargement of the lower right hand corner of fig. 5.5 which contains half the points of the period doubling cascade. We have marked the respective good points of the two-cycle, four-cycle and eight-cycle with arrows. These are the points of the cycle on the symmetry line of H that bifurcated along this line or, in the case of the eight-cycle, will bifurcate along this line. The good points of successive cycles alternate between being the leftmost and rightmost points of the two points of the cycle on the symmetry line of H . The distances $d_{\alpha,8}$ and $d_{\beta,8}$ are distances for the eight-cycle used to calculate the scalings along and across the symmetry line.

$d_{\beta,n}$ is in terms of maximal “half distances” [Benettin et al. 1980a, b; Collet et al. 1981b; van der Weele et al. 1986]. A half distance is the distance between a point and the point halfway around the periodic orbit from the point. The maximal half distance is the largest half distance around the orbit. The distances $d_{\alpha,n}$ and $d_{\beta,n}$ defined above are examples of “half distances” for the symmetric periodic orbit (we know for instance that in any even symmetric cycle the two points on the same symmetry line are halfway around the cycle from one another). We can just define $d_{\alpha,n}$ to be the maximal half distance on the orbit and $d_{\beta,n}$ to be the half distance one quarter of the cycle around from $d_{\alpha,n}$. This definition is a generalisation of the definition used in one-dimensional and higher-dimensional dissipative period doubling (cf. chapter 6). There is good numerical evidence to suggest that the maximal half distance definition selects the distances along and across the symmetry line in any event. Note that the maximal half distance (and any other distance between points of the orbit) may not be unique. Since a symmetric orbit is its own reflection by an entire family of symmetries, every distance may occur twice if a symmetry preserves distances (e.g., $G: x' = y, y' = x$). The distance $d_{\alpha,n}$ will occur elsewhere in the orbit if such a distance-preserving symmetry exists and is not dominant (see, e.g., van der Weele et al. [1986]).

The scalings (5.18)–(5.20) are derived from studies of the symmetric period doubling of the origin in examples 2, 3 and 4 of table 4.1 for the ε values shown there – the explicit numerical results for example 2 are shown in table 5.3. In these three examples, the origin turns hyperbolic at $C = -1$. The subsequent symmetric period doubling cascade is followed to periods 1024 in examples 2 and 3, which are large perturbations of the area-preserving Hénon mapping, and to period 256 in example 4 which is a small perturbation. The period doubling occurs over a small range of the parameter C with accumulation values ranging from $C_{\text{PD,SYM}} = -1.266\,807\dots$ in example 4 to $C_{\text{PD,SYM}} = -1.473\,315\dots$ in example 3. For these three examples, we follow the symmetric period doubling along the symmetry line of their involution H which in all cases we find to be the dominant symmetry line. This is not surprising as these examples are directly (example 2) or indirectly (examples 3, 4) related to the McMillan form of the Hénon mapping (1.23) and the simple symmetry $G: x' = y, y' = x$ of McMillan mappings (4.14) and (4.15) can be shown not to be dominant [MacKay 1982, section 3.1.1]. We took the definition of $d_{\alpha,n}$ and $d_{\beta,n}$ in terms of distance along and across the dominant symmetry line as defined in (iii) and (iv) above. However we checked that the distance $d_{\alpha,n}$ was maximal for the orbit. In example 2, which has a distance-preserving symmetry, this distance occurred twice.

Table 5.4 summarises in table form the period doubling results for examples 2, 3 and 4, and those obtained from area-preserving, reversible mappings. It also includes period doubling results for example 1 of table 4.1. For this example the symmetric fixed point does not period-double because its trace is bounded from below by $2 - \sqrt{8} = -0.828\,4\dots$. Instead the symmetric period doubling of one of its five-cycles is studied. Since this cycle is odd it has one point on the symmetry line of H and one point on the symmetry line of G . It turns out that the point on the symmetry line of H bifurcates along this line to produce a symmetric ten-cycle (this point of the five-cycle is inside the “chopped off” island straddling the symmetry line of H on the right hand border of fig. 4.1a). Following the continuing cascade to period 2560 gives similar scalings to those of the fixed points in examples 2, 3 and 4. Of course if we consider the mapping L_1^5 we are again studying the period doubling of a symmetric fixed point.

The results summarised in table 5.4 suggest that symmetric period doubling in non area-preserving and area-preserving reversible mappings belong to the same universality classes. The numbers are consistent with the quadruple-precision figures available for area-preserving mappings (those shown in table 5.4) and compare well with those from double-precision studies on them [Benettin et al. 1980a, b;

Table 5.3
Period doubling of the symmetric fixed point (0, 0) of example 2 of table 4.1.

Period	Revo- lution	Coordinate ^{a)}	C_n^{sup}	δ_{c_n}	$d_{e,n}$	α_n	$d_{\beta,n}$	β_n
1	-	0.000 000 000 000 000	0.000 000 000 000 000					
2	1	-0.202 706 538 626 633 4	-1.111 539 932 305 716	8.149 955 ...	0.623 590 594 447 986 5	5.471 15 ...		
4	2	-0.267 307 468 473 189 ...	-1.247 925 948 662 615	6.070 633 ...	0.113 977 981 480 334 ... ^{b)}	3.203 49 ...	0.113 977 981 480 334 ... ^{b)}	8.289 ...
8	4	-0.269 584 259 190 999 ...	-1.270 392 470 857 283	7.853 132 ...	0.035 579 289 588 183 ...	4.142 72 ...	0.013 750 803 434 939 ...	19.313 ...
16	8	-0.272 018 266 046 65 ...	-1.273 253 306 784 571	8.596 060 ...	0.008 588 389 363 25 ...	3.974 88 ...	0.000 711 991 329 63 ...	15.491 ...
32	16	-0.271 766 934 514 4 ...	-1.273 586 114 595 625	8.705 485 ...	0.002 160 668 477 2 ...	4.027 35 ...	0.000 045 960 953 1 ...	16.569 ...
64	32	-0.271 870 880 513 5 ...	-1.273 624 344 261 287	8.719 337 ...	0.000 536 498 254 4 ...	4.015 62 ...	0.000 002 773 943 2 ...	16.311 ...
128	64	-0.271 849 747 521 ...	-1.273 628 728 730 196	8.720 886 ...	0.000 133 602 713 ...	4.018 67 ...	0.000 000 170 065 ...	16.378 ...
256	128	-0.271 855 550 28 ...	-1.273 629 231 485 162	8.721 080 ...	0.000 033 245 52 ...	4.017 94 ...	0.000 000 010 384 ...	16.379 ...
512	256	-0.271 854 168 381 ...	-1.273 629 289 133 403	8.721 072 ...	0.000 008 274 262 ...	4.018 19 ...	0.000 000 000 634 ...	
1024	512	-0.271 854 519 4 ...	-1.273 629 295 743 627		0.000 002 059 2 ...			

^{a)} This is the y coordinate of the point of the periodic orbit on the left (-) branch of the symmetry line $x = (-4\epsilon^2 y^3 - C \pm \sqrt{4y + C^2}) / (2 + 2\epsilon^2 y^2)$, with $\epsilon = 1.1$, at superstability; this point eventually bifurcates along this symmetry line.

^{b)} For the four-cycle the distances $d_{e,n}$ and $d_{\beta,n}$ are the same because of the x-y symmetry.

^{c)} For the 1024-cycle the distance $d_{\beta,n}$ is 0 to the accuracy obtainable for the cycle.

Table 5.4
Numerical results for symmetric period doubling in reversible mappings.

	Non measure-preserving reversible mappings ^{a)}				Area-preserving reversible mappings ^{b)}
	Example 1	Example 2	Example 3	Example 4	
$\delta_{PD,SYM}$	8.721 0 ...	8.721 0 ...	8.721 0 ...	8.721 09 ...	8.721 097 200 ...
$\alpha_{PD,SYM}$	4.018 ...	4.018 ...	4.018 ...	4.018 ...	4.018 076 704 ...
$\beta_{PD,SYM}$	16.3 ...	16.37 ...	16.36 ...	16.363 8 ...	16.363 896 879 ...
$C_{PD,SYM}$	3.390 191 684 068 ...	-1.273 629 296 599 ...	-1.473 315 452 618 ...	-1.266 807 948 37 ...	

^{a)} These results are obtained from double-precision calculations.

^{b)} These results are taken from MacKay [1982, 1983a] and are the result of quadruple-precision calculations.

Bountis 1981]. In non measure-preserving reversible mappings, the presence of attractors and repellers in other regions of the plane during the range of parameter in which the symmetric period doubling occurs does not seem to affect the local behaviour being quantitatively conservative-like.

The explanation for the scalings (5.18)–(5.20) in area-preserving reversible mappings is again in terms of renormalisation group analysis [Collet et al. 1981b; MacKay 1982; Widom and Kadanoff 1982; Eckmann et al. 1984]. It is shown that in the space of these mappings there is a universal mapping which is a hyperbolic fixed point under the action of a doubling operator, and whose presence determines the period-doubling behaviour in typical one-parameter families of mappings. Again it would be interesting to see if this renormalisation group argument could be extended to account for the results given here.

6. Dissipative behaviour in reversible mappings

In this chapter we study attractors and repellers in non measure-preserving reversible mappings. Attractors and repellers are necessarily asymmetric features of reversible mappings as pointed out in the general discussion of reversible systems in section 3.1. Here we will mainly concentrate on attractors because their influence on the dynamics of the mapping is more transparent than that of repellers. Attractors are common in dissipative systems as discussed in section 2.1. To investigate the dissipative features of reversible planar mappings quantitatively, the period doubling of attracting asymmetric fixed points in some of the examples of table 4.1 above has been studied.

It is very well known from the study of dissipative systems that they too have period doubling cascades like conservative systems (in fact historically period doubling was recognised first in dissipative systems). However there are significant qualitative and quantitative differences between the cascades in the two systems. Period doubling of simple attractors in dissipative mappings provides a universal route to chaos [Feigenbaum 1980]. The chaotic attracting structures that result often have a self-similar or fractal nature. For mappings of the plane the canonical example of this process is Hénon's dissipative mapping

$$x' = -0.3y, \quad y' = -x + 2Cy + 2y^2. \tag{6.1}$$

This orientation-reversing mapping has $J = -0.3$ throughout the plane. It has two fixed points and is not reversible because the eigenvalues of these two points are not reciprocals (the points could only possibly be asymmetric if the mapping were to be reversible because $J \neq -1$). Hénon [1976] showed that as the

mapping parameter is varied, an attracting fixed point becomes unstable and bifurcates to an attracting two-cycle which in turn loses stability and bifurcates to an attracting four-cycle etc.*) As the mapping parameter C is further varied, the period doubling process continues, resulting in a cascade of infinitely many bifurcations with the values C_n^{bif} at which successive bifurcations occur accumulating at some value. Beyond this value Hénon found an apparently aperiodic (strange) attractor which has the nature of a direct product of a line with a Cantor set.

The successive bifurcation parameter values C_n^{bif} for the mapping (6.1) were shown to converge asymptotically geometrically, i.e.,

$$\delta_{C_n} = \frac{C_n - C_{n-1}}{C_{n+1} - C_n} \rightarrow \delta_{\text{PD,DISS}}, \quad (6.2)$$

where $\delta_{\text{PD,DISS}} = 4.669\dots$ [Derrida et al. 1979]. This value is significantly different to the value for area-preserving period doubling [cf. eq. (5.18)]. This same δ_{PD} characterises period doubling in one-dimensional systems [Feigenbaum 1978, 1979], where it has been calculated to many places, e.g., $\delta_{\text{PD,DISS}} = 4.669\,201\,609\,1\dots$. It also characterises period doubling in higher-dimensional dissipative systems [Collet et al. 1981a].

More generally, the behaviour described above is observed in mappings of the form (6.1) with -0.3 replaced by a parameter B , i.e.,

$$x' = By, \quad y' = -x + 2Cy + 2y^2. \quad (6.3)$$

When the value of B satisfies $|B| < 1$, these mappings are dissipative – we collectively call them Hénon's dissipative mapping [note that when $B = 1$ (6.3) is the reversible area-preserving Hénon mapping in McMillan form]. Since the Jacobian determinant of the mappings (6.3) is constant ($J = B$) the return Jacobian determinant of a 2^n -cycle is B^{2^n} . Apart from $\delta_{\text{PD,DISS}}$, the period doubling in these mappings is also characterised quantitatively by one orbit scaling factor $\alpha_{\text{PD,DISS}}$ which measures the ratio of maximal half distances of successive orbits in the period doubling process [cf. eq. (5.19) where $d_{\alpha,n}$ now means the biggest distance within the cycle between a point and the point halfway around the cycle from that point]. The limiting value of this ratio for dissipative systems is also significantly different to that found in conservative systems (cf. table 6.2 below). Furthermore there is now no second orbit scaling factor β_{PD} as there is for conservative systems.

The universality of the constants $\delta_{\text{PD,DISS}}$ and $\alpha_{\text{PD,DISS}}$ (i.e., their appearance in many dissipative mappings of the plane) has been explained in terms of the renormalisation group and the fact that locally around a fixed point many dissipative mappings reduce to Hénon's dissipative mapping. The approach of the δ_{C_n} to $\delta_{\text{PD,DISS}}$ in the mappings (6.3) as a function of the return Jacobian determinant of the 2^n -cycle has also been shown to be universal [Zisook 1981; Quispel 1985; van der Weele et al. 1985, 1986].

In this chapter it is shown that asymmetric fixed points in reversible mappings that are not measure-preserving commonly period-double and that this process repeats itself, leading to a cascade of 2^n -cycles. This asymmetric period doubling is characterised by universal scaling exponents that are the same as those found in dissipative mappings (cf. also Quispel and Roberts [1989]). The approach to these exponents as a function of the return Jacobian determinants of the cycles also appears to be the

*) Actually Hénon studied the mapping $x' = y + 1 - ax^2$, $y' = 0.3x$ which is simply related to (6.1) cf. Note 35 in Helleman [1983].

same as in dissipative mappings (section 6.1). Furthermore, beyond the accumulation point of the period doubling, attractors are observed that are very reminiscent of Hénon's strange attractor (section 6.2). Heuristically, these results are expected because the period doubling of an initially attracting, asymmetric fixed point typically occurs in a region of phase space where the Jacobian determinant is smaller than 1 (cf. the Jacobian plots in chapter 4), as in a dissipative mapping.

It is worth remembering in this chapter that because the mappings studied are reversible, the presence of an attractor implies the presence of a repeller. Consequently every period doubling sequence of attractors in one part of the plane is accompanied by a mirror period doubling sequence of repellers in another part of the plane, and every strange attractor is accompanied by a strange repeller.

Finally, a numerical note about finding asymmetric periodic orbits. Without the benefits of symmetry, a 1D search along symmetry lines can no longer be conducted as in chapter 5. A search for asymmetric n -cycles involves a genuinely 2D search for solutions of eqs. (2.5). A satisfactory technique for finding these solutions is via repeated applications of a two-dimensional Newton's method (cf. Buck [1978, chapter 10]).

6.1. Period doubling of asymmetric fixed points

A fixed point of a mapping of the plane can only be attracting if neither of the eigenvalues of its linearisation are outside the unit circle of the complex plane. Generically an attracting fixed point period-doubles when one of the eigenvalues crosses the unit circle at -1 and it ceases to be attracting (cf. section 2.1). The reversible mappings in table 4.1 are orientation-preserving throughout the plane. The attracting asymmetric fixed points (x_0, y_0) of examples 1–4 divide into two classes: those with a Jacobian determinant $J = J(x_0, y_0)$ such that $0 < J < 1$, which typically varies as C is changed, or those with $J = 1$ independent of C . We now present period doubling results for these two classes.

6.1.1. Asymmetric fixed points with $0 < J < 1$

The typical behaviour of the eigenvalues λ_1 and λ_2 of such an asymmetric fixed point prior to, during, and after period doubling is reasonably well described by that of a fixed point in a one-parameter dissipative mapping of the plane (6.3) with $J = \lambda_1 \lambda_2 = B$, constant, and $0 < B < 1$.

A description of the behaviour in this last case was given, for example, in van der Weele et al. [1986]. As a mapping parameter C is varied in one direction, the eigenvalues move from both being on the positive real axis to both being on the negative real axis via intermediate traversal of the circle in the complex plane with radius $B^{1/2}$. They coincide on the negative real axis when $\lambda_1 = \lambda_2 = -B^{1/2}$, and when $\lambda_1 = -1$, $\lambda_2 = -B$ the attracting fixed point loses its stability and a two-cycle is born. At this point of bifurcation the trace of the linearisation of the fixed point, denoted Tr_1^{bif} satisfies

$$\text{Tr}_1^{\text{bif}} = -(1 + B). \quad (6.4)$$

The eigenvalues of the two-cycle when it is created are, by continuity, 1 and B^2 . Its return Jacobian determinant is therefore B^2 . The above description with $B \rightarrow B^2$ then describes the motion of the eigenvalues of the return Jacobian of the two-cycle as C is varied. It bifurcates to a four-cycle when its eigenvalues are -1 and $-B^2$. More generally, the 2^n -cycle bifurcates when

$$\text{Tr}_{2^n}^{\text{bif}} = -(1 + B^{2^n}). \quad (6.5)$$

The return Jacobian determinant B^{2^n} of the 2^n -cycle decreases with the length of the cycle and tends to 0 for $n \rightarrow \infty$.

In a mapping with nonconstant Jacobian, the 2^n -cycle in a period-doubling sequence bifurcates at a C value when

$$\text{Tr}_{2^n}^{\text{bif}} = \text{Tr}(dL^{2^n}) = -[1 + \text{Det}(dL^{2^n})], \quad (6.6)$$

which is a generalisation of (6.5). The C value at which (6.6) is satisfied is the only value at which the implicit function theorem fails to guarantee the isolation of the 2^n -cycle from cycles of twice its length, cf. the discussion above and below (2.11) in section 2.1. Equation (6.6) applies to the asymmetric attracting fixed points and cycles in reversible mappings, where the (return) Jacobian determinant J , typically changes with C . Consequently the eigenvalues, when they are complex, do not move on a circle but on a deformed circle whose radius varies with the polar angle. Because the windows of stability of successive cycles in the period-doubling cascade become smaller and smaller, the description above for constant J becomes asymptotically correct as $2^n \rightarrow \infty$.

Asymmetric period doubling has been followed in examples 2, 3 and 4 of table 4.1. In example 3, we study the period doubling of the asymmetric fixed point $(\frac{1}{2}[1 - C + \sqrt{(1 - C)^2 + 4}], -1)$ which turns unstable when $C = 1 - 2\sqrt{3} = -2.46 \dots$. At this stage its x coordinate is $2 + \sqrt{3} = 3.73 \dots$ and its Jacobian determinant is $\frac{1}{3}$. In example 4, the period-doubling cascade arising from the asymmetric fixed point $(1 - C, -y_1)$ is followed. This fixed point turns unstable at $C = -12.943 \dots$ when its coordinates are $(13.943 \dots, -175.5 \dots)$ and the value of its Jacobian determinant is approximately 0.02. The results for example 2 are not obtained from the asymmetric fixed points at $(0.909 \dots, -0.909 \dots)$ and $(-0.909 \dots, 0.909 \dots)$ because the Jacobian determinant at these points is always equal to 1 (their period doubling is discussed in section 6.1.2 below). Instead we study the period doubling of another asymmetric fixed point P that becomes attracting below $C = 1/6 = 0.166 \dots$, after colliding with the point $(-0.909 \dots, 0.909 \dots)$. This interaction of the two points is depicted in fig. 6.1 and is called a transcritical bifurcation (cf. Guckenheimer and Holmes [1983, p. 149]; also Post et al. [1990a], who give a discussion of such bifurcations in reversible and nonreversible mappings). At $C = -0.21014 \dots$, the fixed point P turns unstable and period doubles, with coordinates $(-0.826 \dots, 0.956 \dots)$ and Jacobian determinant 0.866 \dots . Tabulation of the period-doubling cascade arising from P is presented in table 6.1 [note that the parameter values shown are the so-called *superstable* values C_n^{sup} defined by $\text{Tr}(dL^{2^n}) = 0$].

The critical exponents $\delta_{\text{PD,ASYM}}$ and $\alpha_{\text{PD,ASYM}}$ and accumulation parameter value $C_{\text{PD,ASYM}}$ that result from tabulations like that in table 6.1 are shown in the left hand column of table 6.2. Table 6.2 confirms that asymmetric period doubling in non measure-preserving, reversible mappings shares the same universality class as period doubling in quadratic dissipative mappings of the plane like (6.1).

We cannot study the period doubling of the asymmetric fixed points in example 1 because these points do not period-double. However we use these points to illustrate the behaviour of the symmetry lines around simple attractors and repellers in reversible mappings. Symmetry lines cannot intersect in the basin of attraction of an attractor or the basin of repulsion of a repeller. This is because the point of intersection of any two symmetry lines is always a symmetric periodic point and the corresponding symmetric periodic orbit cannot be attracted to something. Example 1 provides a good illustration of this because we have the two asymmetric fixed points close to the symmetric fixed point soon after they are born from it. Moreover as indicated in figs. 4.1a and b, there appear to be closed curves enclosing these three points. A coarse-grained sampling of the points within the innermost of these curves

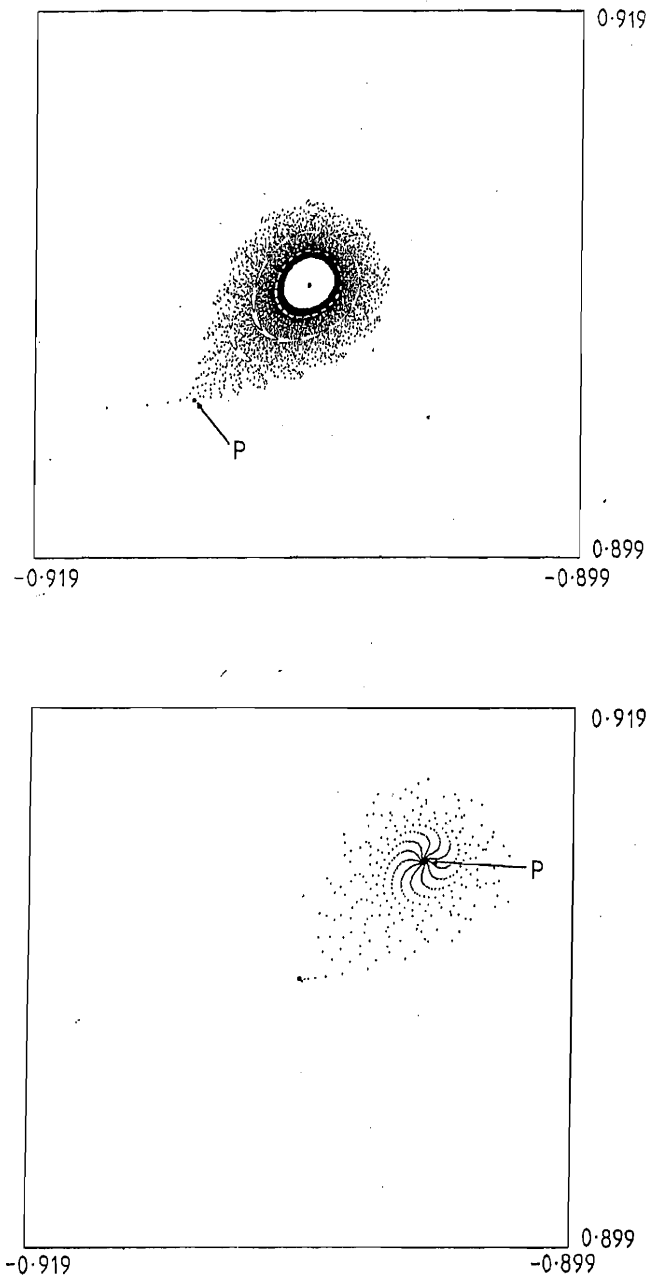


Fig. 6.1. Transcritical bifurcation involving the asymmetric fixed point $(-0.9090\dots, 0.9090\dots)$ in example 2 of table 4.1. This point, which has these same coordinates and $J = 1$ for all C , is at the centre of each picture. It is elliptic for $0.166\dots < C < 0.5$, in which range it is found to be spirally repelling. In the top picture, $C = 0.192$ and we show one orbit winding out from it. Numerically we find another fixed point P at $(-0.9132\dots, 0.9048\dots)$ which has $J = 1.0093\dots$ and is a saddle. In the bottom picture $C = 0.140$. The point P has moved to $(-0.9045\dots, 0.9134\dots)$ and is now attracting with $J = 0.9903\dots$, as shown with one orbit spiralling into it. The fixed point at the centre is now a saddle (with $J = 1$). In the intervening range of C , the point P has moved up and to the right, passing through the fixed point at the centre at $C = 0.166\dots$, which is when it becomes attracting and the fixed point at the centre turns hyperbolic.

Table 6.1
Period doubling of the asymmetric fixed point P (depicted in fig. 6.1) of example 2 of table 4.1.

Period	Revo- lution	Coordinates ^{a)}				C_n^{sup}	δ_{C_n}	$d_{e,n}$	α_n	Return Jacobian determinant
		x	y							
1	-	-0.877 087 625 050 966	0.934 694 678 557 998		-0.004 332 085 107 125 7					0.938 608 661 766 ...
2	1	-0.771 205 168 902 497	0.922 634 130 746 345		-0.244 479 315 076 440 5	4.809 545 ...	0.114 470 548 572 577	5.437 35 ...		0.733 883 497 089 ...
4	2	-0.731 638 488 931 127	0.909 617 043 695 664		-0.294 410 688 757 753 8	6.160 333 ...	0.021 052 627 210 910	2.943 85 ...		0.500 228 238 139 ...
8	4	-0.726 850 147 249 158	0.909 419 194 436 750		-0.302 515 992 552 113 8	7.206 330 ...	0.007 151 399 792 093	3.534 05 ...		0.243 407 091 286 ...
16	8	-0.725 731 456 315 34 ...	0.908 970 211 678 54 ...		-0.303 640 740 301 551 9	6.195 975 ...	0.002 023 568 391 63 ...	2.749 25 ...		0.058 797 056 065 ...
32	16	-0.725 625 916 998 6 ...	0.908 969 328 904 0 ...		-0.303 822 269 067 725 2	5.032 977 ...	0.000 736 042 769 9 ...	2.566 59 ...		0.003 448 493 360 ...
64	32	-0.725 597 016 167 8 ...	0.908 961 702 484 5 ...		-0.303 858 336 938 830 6	4.681 560 ...	0.000 286 778 035 5 ...	2.498 23 ...		0.000 011 880 398 ...
128	64	-0.725 591 114 816 ...	0.908 960 331 389 ...		-0.303 866 041 179 491 4	4.664 364 ...	0.000 114 792 106 ...	2.507 20 ...		0.000 000 000 149 ...
256	128	-0.725 589 849 340 3 ...	0.908 960 037 222 4 ...		-0.303 867 692 903 209 4	4.667 507 ...	0.000 045 784 903 2 ...	2.501 53 ...	b)	
512	256	-0.725 589 578 243 1 ...	0.908 959 974 226 0 ...		-0.303 868 046 780 233 4	4.668 825 ...	0.000 018 302 757 7 ...	2.503 48 ...	b)	
1024	512	-0.725 589 520 18 ...	0.908 959 960 74 ...		-0.303 868 122 575 962 0	4.669 135 ...	0.000 007 310 92 ...	2.502 63 ...	b)	
2048	1024	-0.725 589 507 71 ...	0.908 959 957 82 ...		-0.303 868 138 809 315 7		0.000 002 921 29 ...		b)	

^{a)} This is one of the two points of the periodic orbit at an end of the orbit's maximal half distance; when the orbit period doubles, the two new points born from the point given will form the maximal half distance for the new orbit.

^{b)} For these cycles the return Jacobian determinant is 0 to the accuracy obtainable for the cycle.

Table 6.2

Numerical results for asymmetric period doubling in non measure-preserving reversible mappings and comparative results for period doubling in dissipative mappings.

	Non measure-preserving reversible mappings ^{a)}			Dissipative mappings ^{b)}
	Example 2	Example 3	Example 4	
$\delta_{PD,ASYM}$	4.669 ...	4.669 2 ...	4.669 2 ...	$\delta_{PD,DISS} = 4.669\ 201\ 609\ 1 \dots$
$\alpha_{PD,ASYM}$	2.502 ...	2.502 9 ...	2.502 ...	$\alpha_{PD,DISS} = 2.502\ 907\ 875\ 0 \dots$
$C_{PD,ASYM}$	-0.303 868 143 2 ...	-3.179 095 339 68 ...	-14.426 680 618 8 ...	

^{a)} These results are obtained from double-precision calculations.

^{b)} These results are taken from Feigenbaum [1980] and are the results for one-dimensional dissipative systems.

indicates that most of the points appear to be attracted to the attracting fixed point below the symmetry line of G : $y = C/2 = 1.435$.

In fig. 6.2 we reproduce fig. 4.1b with only the two innermost (apparently, closed) curves shown (the colour version of fig. 6.2 appears at the front of the report; a black and white copy is printed here). The symmetry lines of the involutions H and G of example 1 are shown in black, and drawn in colour are the results of iterating a portion of the symmetry line of G by the mapping example 1 for two (dark blue), eight (red) and 16 (green) iterations. We also show the results of iterating this portion of the symmetry line of G by the inverse of the mapping example 1 for two (light blue), eight (brown) and 16 (purple) iterations of the line under the inverse of example 1.

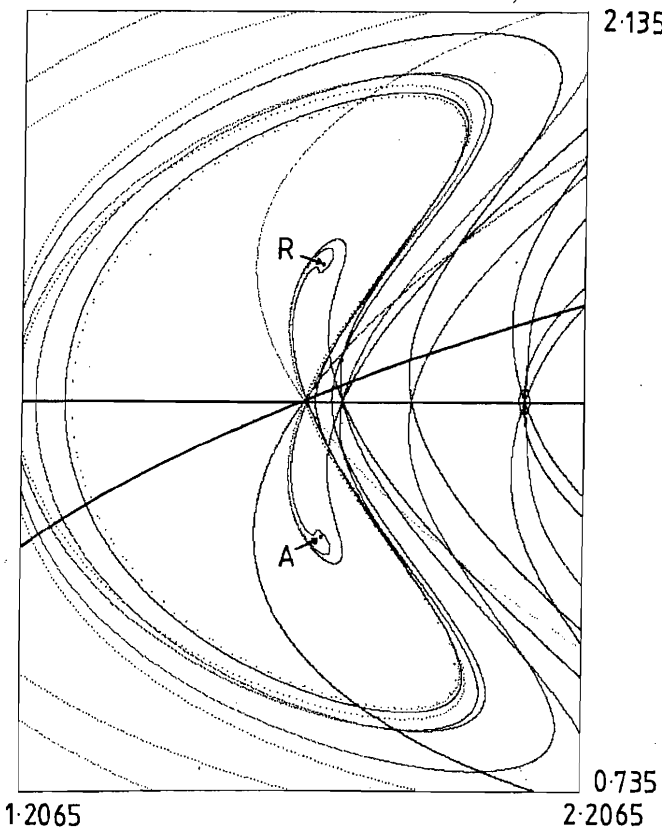


Fig. 6.2. Illustration of the behaviour of symmetry lines in the vicinity of attractors and repellers in reversible mappings (a colour version of this figure is found at the beginning of the report). This picture is fig. 4.1b, a phase portrait of example 1 when $C = 2.87$, with the removal of some of the orbits shown there and the addition of some symmetry lines. The two innermost apparently closed curves from fig. 4.1b are reproduced here together with one of the small islands surrounding the symmetric eight-cycle (right-hand side). The symmetric fixed point at the centre of the picture is at the intersection of the (horizontal) symmetry line of G and the symmetry line of H , both of which are drawn in black. Two arrows mark the attracting asymmetric fixed point (A) in the bottom half of the picture and the repelling asymmetric fixed point (R) in the top half. The coloured lines are symmetry lines created by iterating the symmetry line of G . The colours dark blue, red and green correspond to two, eight and 16 iterations of this line under the mapping example 1. The colours light blue, brown and purple correspond to 2, 8 and 16 iterations of the line under the inverse of example 1.

(purple) iterations. It follows from (3.14a) with $i = \pm 2, \pm 8, \pm 16$ that these coloured curves are also symmetry lines for the mapping example 1. Moreover $\text{Fix}(L^{2i} \circ G) = G\{\text{Fix}(L^{-2i} \circ G)\}$, which is obvious from the symmetry of the positive and negative iterates via reflection in the line $y = C/2$. It is immediately apparent that these symmetry lines appear to have hardly any intersections within the innermost curve but an abundance of intersections outside of it (the rightmost intersection of the red line with the horizontal symmetry line of G results in a periodic point of period 8 encircled by the small island shown). One obvious point of intersection contained within the innermost curve that cannot be in the basin of attraction is the symmetric fixed point which “anchors” the symmetry lines as they must all pass through it.

The behaviour of the symmetry lines within the innermost curve is consistent with their being in the basin of attraction. The second (dark blue) iterate of the part of the horizontal symmetry line of G to the left of the symmetric fixed point is bent anticlockwise to avoid the parts of $\text{Fix}(G)$ and $\text{Fix}(H)$. Successive iterations (red, green curves) of the part of the second iterate within the innermost closed curve move closer to the attracting fixed point and wrap around it, nesting themselves according to the number of their iteration. Thus although the points of an attractor cannot lie arbitrarily close to any given symmetry line, because then the attractor would be symmetric, a sequence of symmetry lines can converge to it. In this way, *some* symmetry line can be found within an arbitrarily small neighbourhood of the attractor but a *given* symmetry line cannot. Moreover, because of reversibility, if $y \in \text{Fix}(G)$ and the sequence $L^n y$ converges to an attractor A , then $GL^n y = L^{-n} G y = L^{-n} y$ converges to GA , a repeller. Consequently, the points on the part of a symmetry line within a basin of attraction of an attractor in a reversible mapping are also in the basin of repulsion of the repeller, that is, the asymmetric partner of the attractor. These points come arbitrarily close to the repeller under backwards iteration and arbitrarily close to the attractor under forwards iteration. In fig. 6.2, for example, the points on the purple line close to the repeller R iterate to points on the green line near the attractor A after 32 iterations. Thus the trajectories of these points link the attractors and repellers in reversible mappings. It seems highly unlikely though that the basins of attraction and basins of repulsion are one and the same set.

6.1.2. Asymmetric fixed points with $J = 1$

In example 2 of table 4.1 ($\varepsilon = 1.1$) the pair of asymmetric fixed points $(0.909 \dots, -0.909 \dots)$ and $(-0.909 \dots, 0.909 \dots)$ have $J = 1$, independently of C . In the range of C when these points are elliptic, it is found numerically that the first point is spirally attracting as indicated in fig. 4.2b, and that the second point is spirally repelling. Because the modulus of the eigenvalues of these fixed points equals 1, the attraction (repulsion) of these points is weak and convergence to (divergence from) these points is slower the closer one is to them. Such attractors and repellers are not usually discussed in the context of dissipative or expansive systems because typically these systems are taken by definition to have $|J| < 1$ or $|J| > 1$ everywhere.

More generally, consider example 2 of table 4.1 for arbitrary ε . The fixed point $(1/\varepsilon, -1/\varepsilon)$ has $J = 1$ for all C and all ε and, for any ε , is an elliptic fixed point when C is in the range $\frac{1}{\varepsilon} < C < \frac{1}{2}$. When it is an elliptic fixed point, it is stable in the linear approximation. Since $J = 1$, we can say that it is measure-preserving to first order. Since $J = 1$, it also passes the first order test for possibly being a symmetric fixed point (in fact the Jacobian determinant around this point is similar to that around a symmetric fixed point, varying from $J < 1$ on one side of the point to $J > 1$ on the other side, as in fig. 4.1c, cf. also fig. 4.2c). To analytically see why $(1/\varepsilon, -1/\varepsilon)$ of example 2 is attracting, we use higher order (i.e., nonlinear) stability analysis as described in appendix B. We calculate the quantity G_1 ,

involving the coefficients of second and third order terms in the expansion around the point to obtain

$$G_1 = 2[\varepsilon(2C - 1)(8C - 1)(6C - 1)^2]^{-1}. \tag{6.7}$$

Since $G_1 < 0$ when $\frac{1}{6} < C < \frac{1}{2}$ and ε is positive, the fixed point $(1/\varepsilon, -1/\varepsilon)$ is an attracting fixed point. In general, $G_1 \neq 0$ for a fixed point with $J = 1$ violates third order local measure preservation and local reversibility conditions (cf. appendix B), i.e., the point fails to be measure-preserving or symmetric at the third order.

It is found that when an asymmetric attracting fixed point with $J = 1$ period-doubles, its offspring has a return Jacobian determinant unequal to 1 and the ensuing cascade belongs to the dissipative regime discussed in section 6.1.1 above. This is to be expected because, *without* the benefits of the fixed point being symmetric or the mapping being measure-preserving, an asymmetric fixed point with $J = 1$ in a reversible non measure-preserving mapping cannot typically sustain a conservative Jacobian determinant throughout the cycles of its period-doubling cascade.

Thus in example 2, when $C = 0.5$ and the attracting fixed point $(0.909\dots, -0.909\dots)$ turns hyperbolic with both eigenvalues at -1 , the two-cycle born from it quickly assumes a return Jacobian determinant value slightly less than 1 (e.g., $0.9993\dots$ at $C = 0.502$) and is attracting. The behaviour of the eigenvalues of the 2^n -cycles, $n \geq 1$, of the period-doubling cascade is qualitatively similar to the behaviour of the eigenvalues of the fixed points and cycles with $0 < J < 1$ described above. However because the return Jacobian determinant of the two-cycle is so close to 1, the decrease in the return Jacobian determinant of later cycles is slow (the value for the 2^{n+1} -cycle is approximately the square of the value for the 2^n -cycle). Associated with this is a slow decrease in the successive δ_{C_n} values in the period doubling cascade [defined in (6.2)]. Despite this slowness it seems that the period doubling is again characterised by the dissipative exponents, e.g., the δ_{C_n} value formed from the 1024, 2048 and 4096-cycles is $4.678\dots$ and the α_n value calculated from the 1024 and 2048-cycles is $2.517\dots$. One would expect to see more accurate convergence to the dissipative values if it were possible to obtain good numerical results for enough periods of the cascade.

In fig. 6.3, the decrease of the δ_{C_n} in example 2 is illustrated by plotting their values against the return Jacobian determinants of the 2^n -cycle evaluated at superstability. The 2^n -cycle is the middle cycle of the 2^{n-1} -, 2^n -, 2^{n+1} -cycle triplet whose superstable C_n values are used to calculate δ_{C_n} . The data points from example 2 are supplemented by those from another reversible non measure-preserving mapping with an asymmetric fixed point with $J = 1$ (cf. example 1 in Quispel and Roberts [1988]; the fixed point $(0, -20\sqrt{2})$ of this example gives rise to a “dissipative” period-doubling cascade).

In dissipative mappings of the plane with constant Jacobian determinant $J = B < 1$, the values of δ_{C_n} in the period-doubling process regarded as a function of the effective Jacobian $B_e \equiv B^{2^n}$ (which is the return Jacobian determinant of the 2^n -cycle) fall on a universal curve. This is due to the relation $\delta_{C_{n+1}}(B) \approx \delta_{C_n}(B^2)$, which holds increasingly well as $B \rightarrow 0$. Therefore not only are the values of δ_{p_D} for the conservative ($B = 1$) case and the dissipative ($B < 1$) case universal numbers, but for weak dissipation (i.e., $B \approx 1$) the successive values of δ_{C_n} descend (“crossover”) from the first to the second with increasing n in a universal fashion. This follows from numerical results and renormalisation arguments [Zisook 1981; Quispel 1985; van der Weele et al. 1985, 1986]. To illustrate this crossover, the universal crossover curve for the Hénon dissipative mapping (6.3) is also plotted on fig. 6.3. This curve is obtained from the best fit to δ_{C_n} versus $B_e \equiv B^{2^n}$ data points for the period doubling of the fixed point at the origin in (6.3) for $B = 0.99$ and $B = 0.5$. The conclusion from fig. 6.3 is that the period doubling of $J = 1$ asymmetric fixed points in reversible mappings follows the universal crossover behaviour

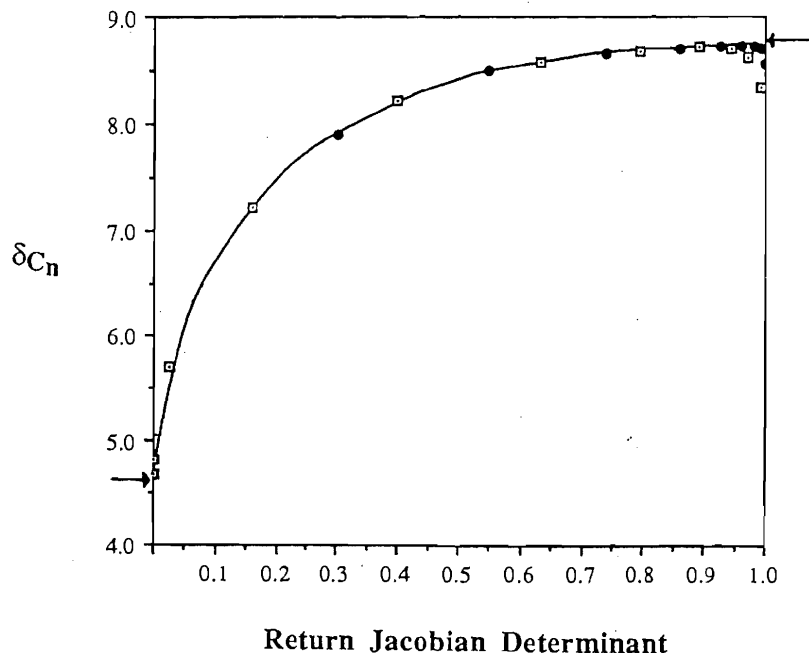


Fig. 6.3. Crossover-type behaviour in the period doubling of $J = 1$ asymmetric fixed points in non measure-preserving reversible mappings. Shown are the δ_{C_n} for the period doubling cascade arising from such a point in example 2 (\square), plotted as a function of the return Jacobian determinant of the 2^n -cycle. Also plotted are data points (\bullet) from example 1 of Quispel and Roberts [1988]. The curve drawn on the figure is the crossover curve for the Hénon dissipative mapping. The arrow on the left hand vertical axis marks the dissipative $\delta_{PD} = 4.6692\dots$, and the arrow on the right hand vertical axis marks the conservative $\delta_{PD} = 8.7210\dots$

previously found in the dissipative mappings (6.3) (note that the points where $B \approx 1$ are not terribly significant as the universality holds for $B \rightarrow 0$). This agreement might be expected because locally the return Jacobian determinant of cycles becomes constant in C as higher and higher cycles are considered.

Although the curve for the Hénon dissipative mapping in fig. 6.3 appears to decrease monotonically, it has in fact been shown to have a dip at a small value of $B \approx 10^{-7}$ where $\delta_{\min} \approx 4.6635$ [Quispel 1985; van der Weele et al. 1985, 1986]. For the $J = 1$ asymmetric fixed points it is not possible to numerically follow the period-doubling cascade until periodic orbits have negligible Jacobian determinants. However this is possible for the fixed points with $0 < J < 1$ discussed in section 6.1.1 above. In these cases, the period-doubling data each show a decrease in the δ_{C_n} to at least one value below $\delta_{PD,DISS} = 4.6692\dots$ and then an approach to this value from below, as shown for example in table 6.1.

6.2. Strange attractors

The combined results of sections 5.2 and 6.1 suggest that conservative and dissipative period-doubling processes can occur in different parts of the plane in a one-parameter reversible mapping. They are identified as such by their scaling exponents δ_{PD} and α_{PD} , and β_{PD} (for symmetric period doubling). For the examples in table 4.1, the ranges in parameter in which these two period-doubling processes occur overlap to varying degrees.

In example 4 of table 4.1, for instance, the point $(1 - C, -y_1) = (2.266, -1102.132\dots)$ is "just" attracting at $C = -1.266$ - its eigenvalues are 0.9907 and 5.188×10^{-4} . At this C value the symmetric

period doubling has reached a stage where an elliptic 8-cycle exists about the origin. As C is decreased the eigenvalues of the point $(1 - C, -y_1)$ move towards the (superstable) point at $C = -9.950 \dots$ where their sum equals 0. This is well beyond the accumulation point of the symmetric period doubling at $C_{PD,SYM} = -1.266 807 \dots$. Thus the symmetric period doubling accumulates at a parameter value such that the asymmetric period doubling of the attracting point $(1 - C, -y_1)$ has not even begun. The same behaviour arises in example 3 – the parameter intervals for the existence of stable asymmetric and symmetric cycles in their respective period-doubling cascades are shown in fig. 6.4a.

In example 2, the situation is reversed. Here the parameter values for the period-doubling cascade arising from the asymmetric fixed point P , which becomes attracting after it passes through the point $(-0.909 \dots, 0.909 \dots)$ at $C = \frac{1}{6}$, accumulate at $C_{PD,ASYM} = -0.303 868 1 \dots$, which is well within the range $-1 < C < 1$ in which the origin is elliptic and surrounded by KAM curves – see fig. 6.4b. The origin does not symmetrically period-double until $C = -1$. Note that the period-doubling cascade of the fixed point $(-0.909 \dots, 0.909 \dots)$ also accumulates well within the range $-1 < C < 1$ although it proceeds with increasing C after this fixed point period-doubles at $C = 0.5$. The parameter windows for this period-doubling cascade are not shown in fig. 6.4b.

In dissipative systems, period doubling can accumulate with the appearance of an aperiodic attractor (the “Feigenbaum Scenario”, cf. Eckmann [1981]). This attractor typically has many pieces which often recombine via “inverse bifurcations” as a parameter is varied (e.g., Schmidt [1988]). The aperiodic attractor often disappears for denumerably many windows in the parameter, being replaced by an attracting periodic orbit which again period-doubles, etc. In the Hénon dissipative mapping (6.3) aperiodic attractors and their evolution have been well studied (cf. e.g., Hénon [1976], Simó [1979], Feit [1978] and Cvitanovic et al. [1988]). The attractors are described as being “strange” by most authors because the motion induced on them is chaotic; in addition they possess self-similar structure on all scales. Very recently, it has been analytically proven that the mapping (6.3) does indeed have a strange attractor for a range of parameter values B and C (cf. Benedicks and Carleson [1989, 1991]). However, this range covers only very small values of B and does not include the value $B = -0.3$ studied by Hénon [1976] and many subsequent workers.

In all cases of period doubling of asymmetric ($0 < J < 1$) fixed points that we have studied in reversible mappings we have observed the formation of an apparently aperiodic attractor for many parameter values beyond $C_{PD,ASYM}$.*) Consider, for instance, example 3 for which $C_{PD,ASYM} =$

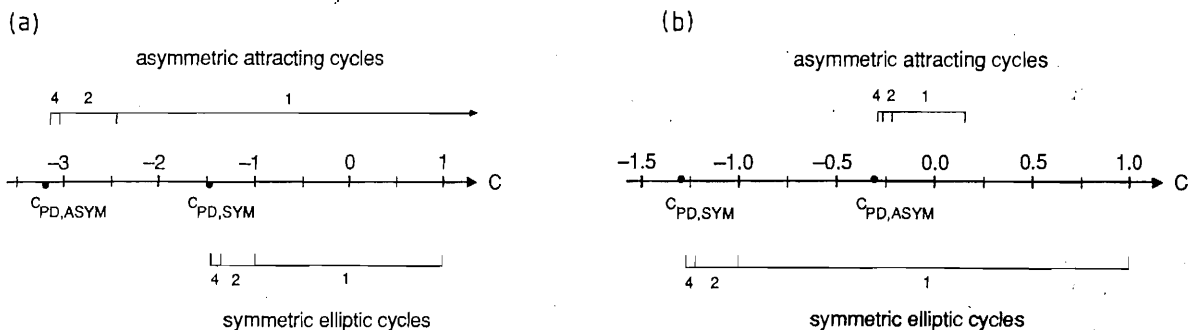


Fig. 6.4. Intervals in the parameter C for the existence of (asymmetric) attracting cycles and (symmetric) elliptic cycles in (a) example 3, and (b) example 2. The numbers 1, 2 and 4 label the windows of existence of cycles with these periods in the asymmetric and symmetric period doubling.

*) Such an attractor may also arise in the case of asymmetric ($J = 1$) period doubling but the slower convergence of the C_n makes it more difficult to investigate.

$-3.179\,095\dots$ We identify a four-piece aperiodic attractor at $C = -3.19$. Points attracted to it cycle around the four pieces. These four pieces merge to give two pieces for $-3.23 < C < -3.20$ and one piece for $-3.301 \leq C \leq -3.23$. The attractor does not appear to exist for $C = -3.302$. Like Hénon's attractor, self-similarity and an apparently endless series of folds are seen in this attractor. This is illustrated in fig. 6.5 where we show the attractor in 6.5a and some magnifications of it in 6.5b–d. In fig. 6.6 a further illustration is provided of the behaviour of symmetry lines around attractors. Here the attractor has more structure and “occupies” more space than the attracting fixed point in fig. 6.2. Again it is found that successive iterations of a part of a symmetry line in the basin of attraction come closer to the attractor. In the present case, they fold over to mimic the shape of the attractor. In the basin of attraction, the iterations are nested parallel to one another and to the attractor so that they do not intersect each other or cut the attractor itself.

Similar qualitative results are found in examples 4 and 2. For example 4 at $C = -14.8$ the aperiodic attractor is a large parabolic shaped “curve”. Its basin of attraction is very large: points that are attracted to it include $(-5, 1)$, $(30, 3)$ and $(0, 6.798)$. It appears to be the main dynamical feature of the mapping, as points not attracted to it apparently escape to infinity. The shape of this attractor is again reminiscent of that in Hénon's dissipative mapping.

The aperiodic attractor obtained in example 2 beyond $C_{\text{PD,ASYM}} = -0.303\,868\,1\dots$ comprises eight small pieces and has a very small basin of attraction. Significantly the attractor is not the main dynamical feature of the mapping. It *coexists* over the range of C in which it exists with the KAM region around the origin, which is an elliptic fixed point. This is shown in fig. 6.7 for $C = -0.303\,978\,5$. Therefore the mapping in this range of C has two types of bounded motion: the motion on and inside the regular region formed by the KAM curves around $(0, 0)$; and the motion towards and on the attractor. Figure 6.8 shows in more detail some of the pieces of the attractor. The magnification of any one of the pieces is again suggestive of fractal nature like fig. 6.5. The attractor seemingly ceases to exist for C a little less than $C = -0.303\,978\,5$ (e.g., the initial condition used to generate fig. 6.8 escapes to infinity at $C = -0.303\,979\,0$), and at destruction it still seems to comprise eight pieces (note that attractors with pieces arise in many physical examples, e.g., Short and Yorke [1984]).

It appears that the aperiodic attractors found in these non measure-preserving reversible mappings are good candidates for being labelled strange attractors à la Hénon – attractors on which the dynamics is chaotic and that have a geometric fractal nature. Qualitatively the pictures in fig. 6.5 suggest the geometric property; watching the generation of points on the attractor on a computer screen suggests the dynamical property. Quantitatively, the motion on the attractors in examples 2 and 3 is verified to be chaotic from the existence of a positive Lyapunov exponent μ_1 . We calculate both exponents μ_1 and μ_2 for each of the examples according to the standard procedure (cf. Eckmann and Ruelle [1985], Lichtenberg and Lieberman [1983], Mayer-Kress [1986], Young [1983]). That is, we follow an initially orthonormal pair of vectors around the attractor and at each iteration of the mapping, apply the linearised mapping (the Jacobian matrix) to the vector pair and re-orthonormalise them. The length rescaling factors $\chi_1(i)$ for the first vector and $\chi_2(i)$ for the second vector at the i th iteration are collected together to define μ_1 and μ_2 via $\mu_j = \lim[(1/n) \sum_{i=1}^n \log \chi_j(i)]$, for $j = 1, 2$, where the limit is as $n \rightarrow \infty$. It is found that $\mu_1 \approx 0.38$ and $\mu_2 \approx -0.98$ for the attractor of example 3 depicted in figs. 6.5–6.6. The fact that μ_1 is positive indicates exponential divergence of initially close points on the attractor; the average area change per iteration is by a factor $\exp(\mu_1 + \mu_2) \approx 0.55$. For the attractor of example 2 depicted in figs. 6.7–6.8, the results are $\mu_1 \approx 0.05$ and $\mu_2 \approx -0.23$ so that $\exp(\mu_1 + \mu_2) \approx 0.84$. The average area reductions in both cases emphasise again the similarity in these regions of the phase space between the reversible mapping and a dissipative mapping.

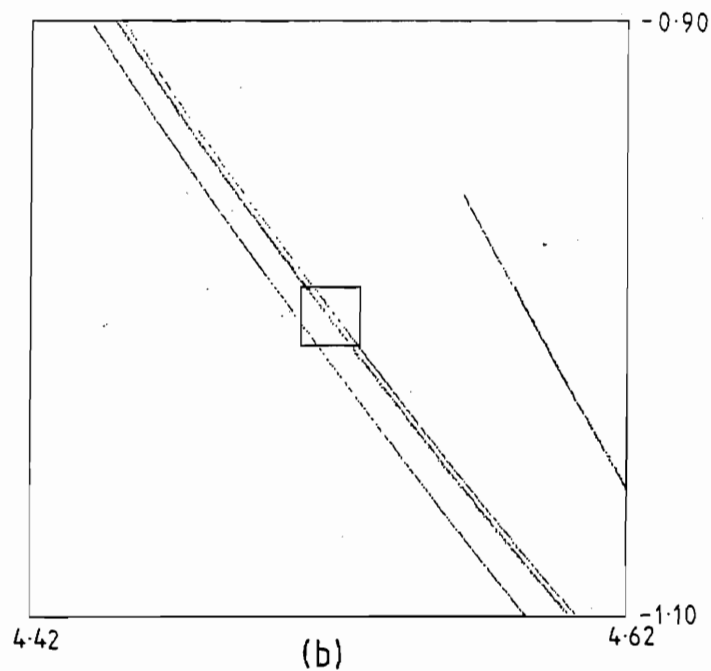
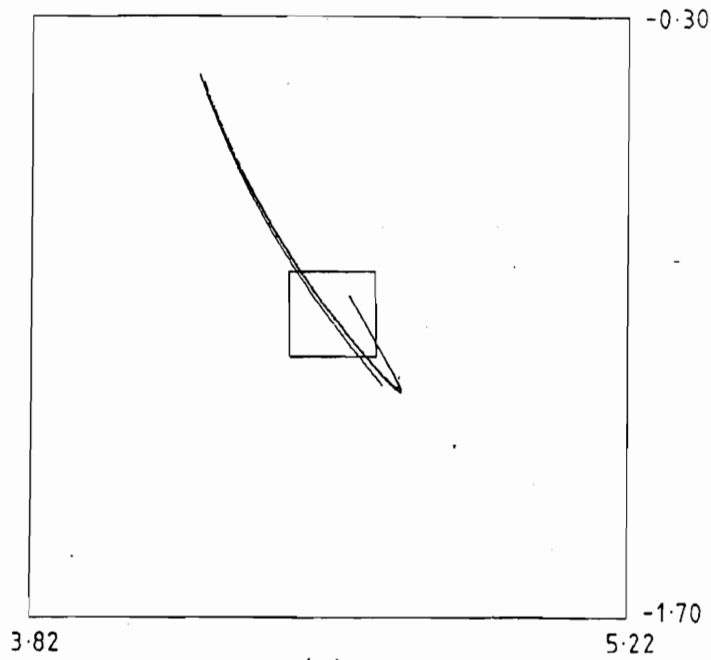


Fig. 6.5. Aperiodic attractor in the mapping example 3 for $C = -3.300$, and successive magnifications [(b) magnification of the boxed region in a, etc.]. At the centre of each picture is the hyperbolic fixed point $((1 - C + \sqrt{(1 - C)^2 + 4})/2, -1) = (4.52118\dots, -1)$ which was originally attracting. The attractor is generated by iterating the point $(4.5, -1.1)$, for up to 5 million iterations in the case of d, without plotting the first 2000 iterates.

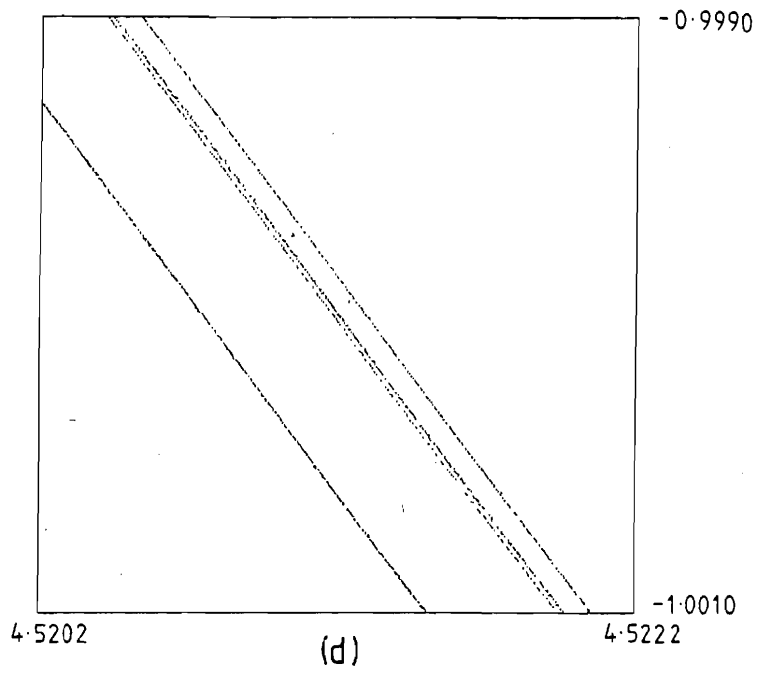
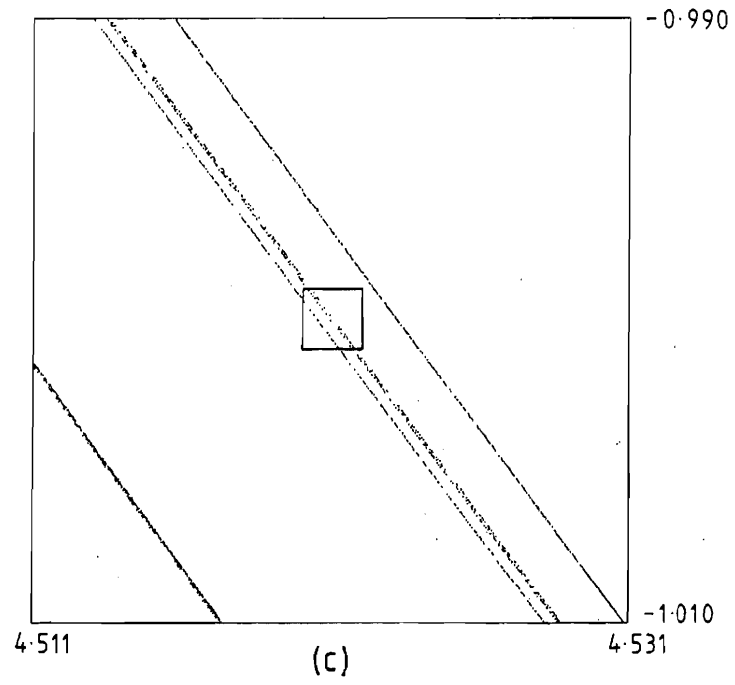


Fig. 6.5 (cont.).

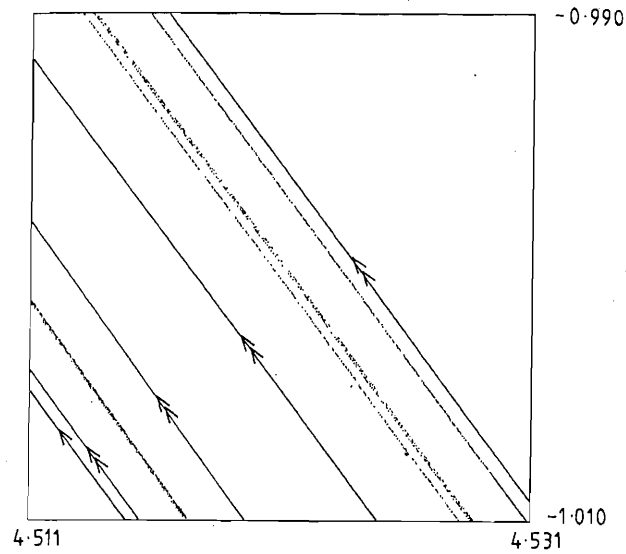


Fig. 6.6. Figure 6.5c with the addition of some parts of the symmetry lines of L^3G (single arrow) and L^7G (double arrows), where L is the mapping example 3. These lines are obtained by taking the second and third iterates under L of the symmetry line of H for example 3.

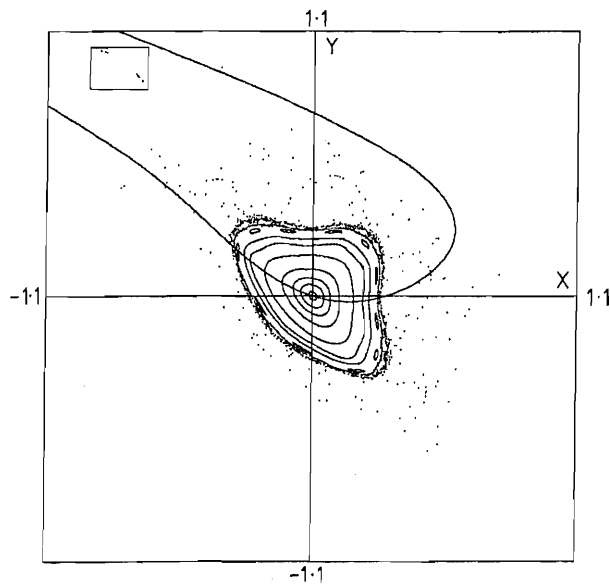


Fig. 6.7. Phase portrait of example 2 when $C = -0.3039785$. Note the KAM region around the origin and the boxed eight-piece aperiodic attractor in the top left corner. The symmetry line of H is also shown but the symmetry line of G , $y = x$, is omitted.

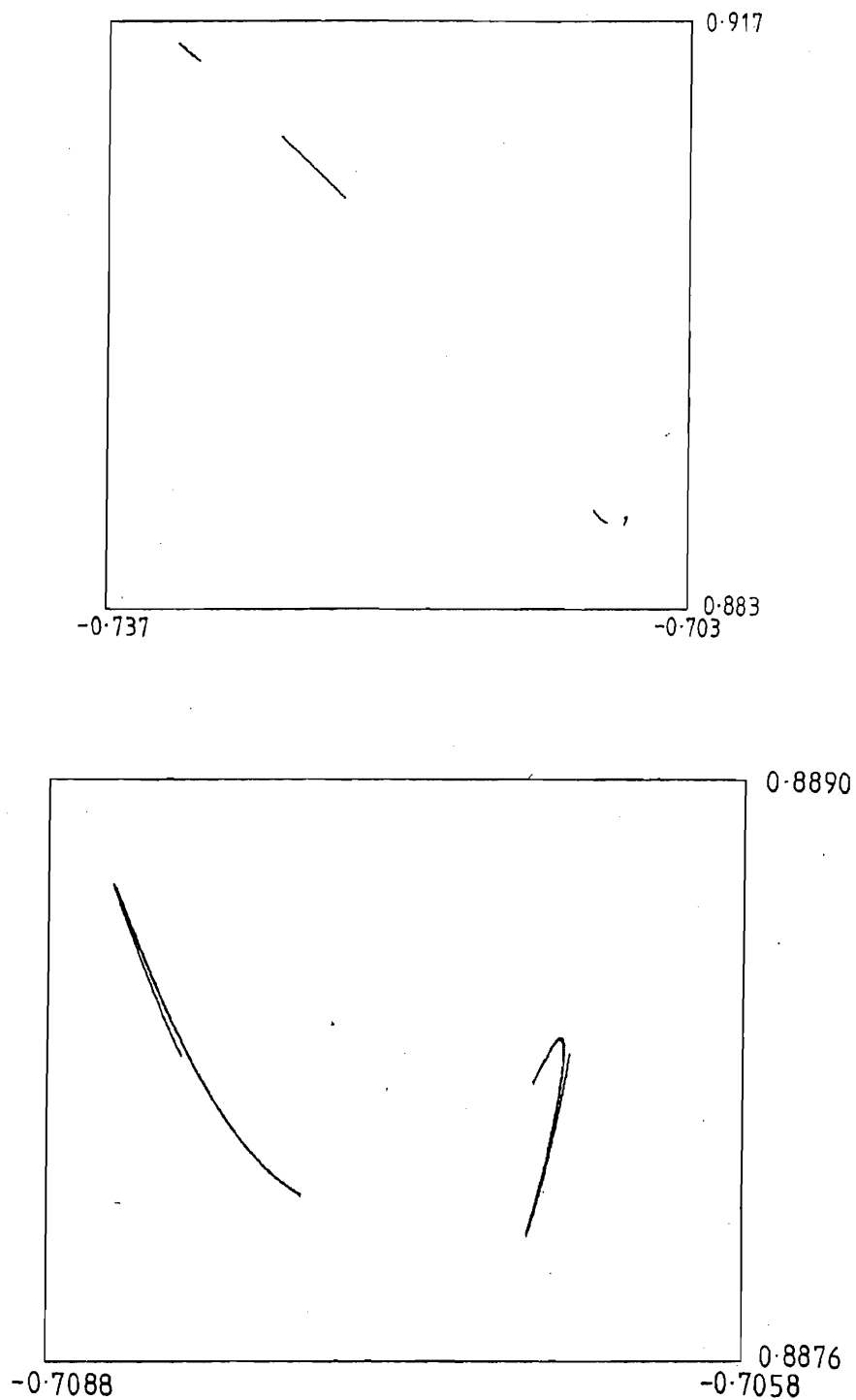


Fig. 6.8. Enlargement of the eight-piece attractor of fig. 6.7. The top picture shows the four rightmost pieces of the attractor and the bottom picture shows the two rightmost pieces of the top picture. The attractor is generated by iterating the point $(-0.883\ 039, 1.018\ 43)$ 20 000 times and plotting only the last 10 000 iterates.

7. Interplay of conservative and dissipative features of reversible mappings; a symmetry-breaking bifurcation

The combined results of the preceding two chapters indicate that non measure-preserving, reversible mappings provide a unique opportunity to study the interaction of conservative and dissipative features (e.g., KAM curves and attractors) within the one mapping, because of the identification of these features with, respectively, symmetric and asymmetric sets. In this short chapter, we concentrate on one aspect of this interplay, namely a symmetry-breaking bifurcation in which two asymmetric periodic orbits bifurcate from a symmetric conservative-like periodic orbit.

This symmetry-breaking bifurcation is seen immediately at the level of fixed points in example 1 of table 4.1, when two asymmetric fixed points, one attracting with $J < 1$ and one repelling with $J > 1$, are born from the symmetric fixed point at parameter value $C = \pm 2\sqrt{2}$. This bifurcation has also been observed in other non measure-preserving, reversible mappings by Politi et al. [1985, 1986a, b], Bullett [1988], Roberts [1990a] and Post et al. [1990a] (the latter reference also discusses other bifurcations in reversible mappings of the plane). The symmetry-breaking bifurcation is shown schematically in fig. 7.1a, with another possibility in fig. 7.1b. The analysis in Post et al. [1990a] suggests that such symmetry-breaking bifurcations should occur quite frequently in non measure-preserving, reversible mappings. In other (nonreversible) mappings similar bifurcations of two fixed points with, respectively, $J < 1$ and $J > 1$ from a fixed point with $J = 1$ are expected if a second order condition on the mapping expansion is satisfied. This condition is precisely the second order reversibility condition “case 2b” of

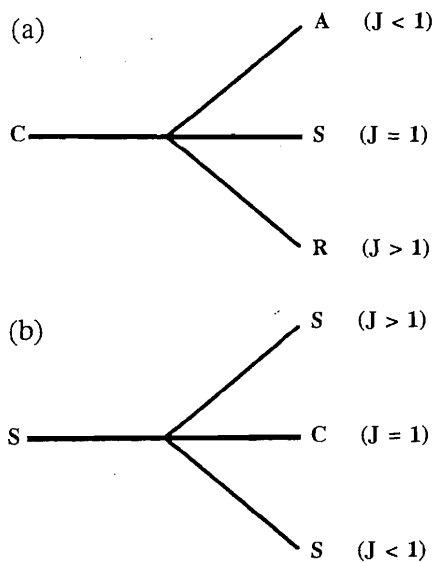


Fig. 7.1. Schematic representations of symmetry-breaking bifurcations in a non measure-preserving reversible mapping: (a) a symmetric fixed point with $J = 1$ (horizontal line) changes from being elliptic (a centre C) to hyperbolic (a saddle S) as the map parameter is varied, spawning an asymmetric attracting fixed point A with $J < 1$ and an asymmetric repelling fixed point R with $J > 1$; (b) a symmetric fixed point with $J = 1$ changes from being a saddle S to a centre C and emits two saddles, one with $J > 1$ and one with $J < 1$.

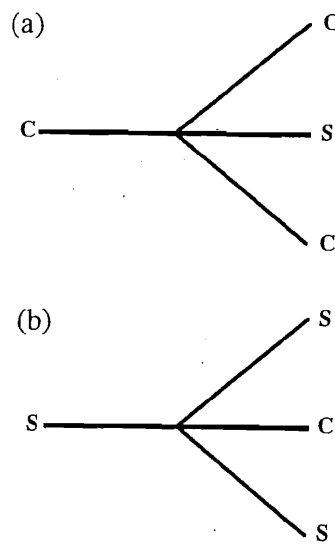


Fig. 7.2. Schematic representations of symmetry-breaking bifurcations in an area-preserving reversible mapping. Now all fixed points have $J = 1$. (a) a symmetric fixed point changes from a centre to a saddle and emits two asymmetric centres; (b) a symmetric fixed point changes from a saddle to a centre and emits two asymmetric saddles.

table 3.2; the other second order reversibility condition at “case 2a” of table 3.2, which is also the second order condition for local measure preservation (cf. “case 2”, table 2.1), need not be, and typically is not, satisfied.

In one-parameter, area-preserving, reversible mappings, a symmetry-breaking bifurcation was found by Rimmer [1978, 1983]. In this case there cannot be attracting and repelling fixed points and $J = 1$ everywhere. It is found that there can be two possibilities when a symmetric fixed point has repeated eigenvalue $+1$ and the parameter is varied: (a) the symmetric fixed point changes from being a centre to a saddle; and two asymmetric fixed points, which are centres each with the same eigenvalues, are born (fig. 7.2a); or (b) the symmetric fixed point changes from a saddle into a centre and emits two asymmetric saddles with identical eigenvalues (fig. 7.2b). The bifurcations in fig. 7.1a, b can be regarded as non measure-preserving versions of the Rimmer bifurcations in fig. 7.2a, b.

Rimmer showed that the symmetry-breaking bifurcation is a generic one for area-preserving reversible mappings. Previously, Meyer [1970] had considered the generic bifurcations in area-preserving mappings – in this wider class of mappings, such pitchfork bifurcations as in fig. 7.2 are not generic. MacKay [1982] showed that the area-preserving and reversible Hénon mapping first has asymmetric cycles at the level of six-cycles when two asymmetric six-cycles arise via a Rimmer bifurcation from a symmetric six-cycle. Schmidt and Wang [1983] find the bifurcation depicted in fig. 7.2a in their study of possible bifurcation scenarios in mappings of de Vogelaere form (cf. table 3.1). Beerens [1990] and Post et al. [1990b] have followed the period doubling of the asymmetric cycles produced by a Rimmer bifurcation in an area-preserving mapping and found the scaling $\delta_{PD,ASYM}$ to be $8.721\dots$. De Aguiar et al. [1987] give some examples of symmetry-breaking bifurcations in the vein of Rimmer in the two-dimensional surface of section of Hamiltonian systems with time-reversal symmetry (cf. also the discussion in Ozorio de Almeida and de Aguiar [1990]). Kook and Meiss [1989] discuss Rimmer bifurcations in four-dimensional symplectic reversible mappings.

Although the non measure-preserving, symmetry-breaking bifurcation is not seen among the other examples of table 4.1 at the level of their fixed points, it appears often in these other examples if we look at n -cycles, $n > 1$ (see fig. 7.3). In particular, the symmetry-breaking bifurcations often occur so as to interrupt the symmetric period doubling process. For example, the symmetric four-cycle shown in fig. 7.3 arises from two successive period doublings of the symmetric fixed point at the origin in example 3 (note the different ε value to that shown in the last column of table 4.1 and used in section 5.2). As the parameter C is lowered, the trace of the return Jacobian of this four-cycle decreases from the value $+2$ which it initially has when it is born from its parent symmetric two-cycle. However, the trace “turns around” at a value ≈ 1.88 when $C = -1.6090\dots$ and then increases through $+2$, which is when the symmetry-breaking bifurcation occurs.

For some time after the symmetry-breaking bifurcation in example 1 of table 4.1, the three fixed points are apparently enclosed by closed curves which are similar to the KAM curves surrounding the elliptic symmetric fixed point before it bifurcates (cf. figs. 4.1a, b). A similar situation is seen with the four-cycles in fig. 7.3. We now investigate whether the curves seen in figs. 4.1a, b and 7.3 are actually closed. This is suggested by numerical evidence as we do not see the curves fatten or degenerate after following them for many iterations. This contrasts with some examples of mappings in Post et al. [1990a] in which reversibility is only satisfied locally to some order around a fixed point (cf. section 3.3) and in which it is shown that the KAM tori change into slowly spiralling curves enclosing the attractor and repeller (heuristically, the higher the degree of local reversibility, the slower the discernable departure from a closed curve to a slow spiral).

Since example 1 is a fairly simple mapping that is reversible to all orders and the symmetry-breaking

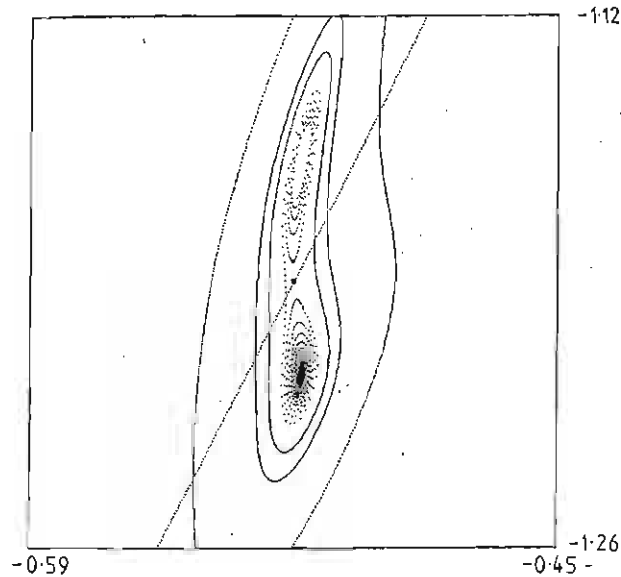


Fig. 7.3. Phase portrait of example 3 with $\varepsilon = 0.252$ when $C = -1.64755$. A symmetry-breaking bifurcation has occurred at $C = -1.64459\dots$. At the centre of the picture is a hyperbolic point of a symmetric four-cycle lying on a monotonic part of the symmetry line of H which is also shown. Above and below the point of the symmetric four-cycle are, respectively, one point of a repelling four-cycle and one point of an attracting four-cycle. A trajectory that winds out from the repeller to the attractor is shown.

bifurcation involves fixed points, we will study it. We have looked for a curve between the symmetric seven-cycle and the symmetric eight-cycle shown in fig. 4.1a. The rotation numbers of these cycles are respectively $1/7$ and $1/8$, i.e., it requires one anticlockwise revolution around the symmetric fixed point to visit every point of each cycle. In section 5.1.2 it was mentioned that in area-preserving mappings the last KAM curve expected to break up between cycles with neighbouring rotation numbers p/q and p'/q' has the rotation number (cf. also MacKay and Stark [1991]),

$$(p + \gamma p') / (q + \gamma q'), \quad \gamma = (\sqrt{5} + 1) / 2. \tag{7.1}$$

We investigate the existence of a curve with rotation number

$$(1 + \gamma) / (7 + 8\gamma), \tag{7.2}$$

using the residue behaviour of the symmetric periodic orbits with rotation numbers approximating (7.2), as described in section 5.1.2.

The rational approximants to (7.2), which is noble with CFE $[7, 1, 1, 1, \dots]$, are easily obtained by a Farey tree construction [cf. eqs. (5.9)–(5.10)]. The first few approximants are

$$\left\{ \frac{1}{7}, \frac{1}{8}, \frac{2}{15}, \frac{3}{23}, \frac{5}{38} \right\}. \tag{7.3}$$

Later approximants are found from table 7.1 (given by revolution/period) which lists the intersections of the residue curves of successive approximant periodic orbits. We are able to locate these (positive-residue) approximants all on the symmetry line $y = C/2$ of the involution G for example 1, providing

Table 7.1

Intersections of residue curves of periodic orbits around the symmetric fixed point of example 1 of table 4.1. The parameter value C_n^{int} should give agreement between the residues of each pair of orbits shown to at least the number of figures in R_n^{int} .

Period	Revo- lution	Coordinate ^{a)}	Sym ^{a)}	C_n^{int}	δ_{C_n}	R_n^{int}	δ_{R_n}
61	8	0.346 785 047 656 7 ...	1				
99	13	0.345 482 991 541 ...	1	2.877 593 007 458 568		0.238 462 674 5 ...	
99	13	0.344 204 379 987 ...	1				
160	21	0.344 623 077 653 ...	1	2.877 959 592 569 219	-2.791 032 ...	0.257 133 500 3 ...	-1.688 8 ...
160	21	0.345 083 619 910 ...	1				
259	34	0.344 946 020 861 ...	1	2.877 828 248 670 725	-2.767 324 ...	0.246 078 025 ...	-1.715 1 ...
259	34	0.344 780 070 8 ...	1				
419	55	0.344 824 732 83 ...	1	2.877 875 711 077 100	-2.715 285 ...	0.252 524 1 ...	-1.659 4 ...
419	55	0.344 885 942 26 ...	1				
678	89	0.344 871 340 38 ...	1	2.877 858 231 362 837	-2.703 593 ...	0.248 639 6 ...	-1.665 8 ...
678	89	0.344 848 718 57 ...	1				
109 7	144	0.344 853 472 06 ...	1	2.877 864 696 727 028	-2.685 86 ...	0.250 971 4 ...	-1.646 2 ...
109 7	144	0.344 861 898 219 ...	1				
177 5	233	0.344 860 346 78 ...	1	2.877 862 289 543 272		0.249 555 ...	

^{a)} "Sym" = 1 corresponds to $y = C/2$ and "coordinate" is the x coordinate on this line.

further evidence that the "dominant reverser conjecture" for reversible area-preserving mappings holds in more general reversible mappings (cf. our discussion in section 5.1.2).

From table 7.1, the following critical exponents for the noble curve with rotation number (7.2) are calculated, using superconvergence in the case of R_{KAM} : $R_{\text{KAM}} = 0.250 09 \dots$, $\delta_{R_{\text{KAM}}} = -1.6 \dots$, $\delta_{C_{\text{KAM}}} = -2.6 \dots$. We also find $C_{\text{KAM}} = 2.877 862 9 \dots$. These results agree well with those tabulated in table 5.2 for other non measure-preserving, reversible mappings as well as those for area-preserving, reversible mappings (considering that we do not continue to very long approximant orbits as in section 5.1.2).

The residues of the approximating orbits to (7.2) increase with increasing parameter C , becoming unbounded for $C > C_{\text{KAM}}$. For $C < C_{\text{KAM}}$ they tend to 0 from above. In area-preserving mappings, the behaviour of the residues has been used as a practical test for deciding whether there are invariant circles of a mapping in an interval of rotation number specified by two periodic orbits, cf. Greene et al. [1986]. Assuming that the most robust circle in the interval is a noble (cf. MacKay and Stark [1991]), one checks the residue of periodic orbits at the ends of the interval. If the residues are significantly larger than 0.25 (0.25 is approximately R_{KAM}), then one expects there is no noble circle between the periodic orbits and hence no invariant circles between them; if the residues are between 0 and 0.25, one expects that there are KAM circles between them. If the residue criterion or conjecture summarised by (5.12a)–(5.12c) is assumed to hold in the present case, we have that for $C < C_{\text{KAM}}$ there exists a smooth invariant circle with rotation number (7.2), whereas for $C > C_{\text{KAM}}$ there does not. As pointed out in section 5.1.2, we believe that, based on our numerical evidence, the residue conjecture does hold. As a result, it would seem that there can be closed invariant curves encircling symmetric, hyperbolic periodic orbits and their attracting and repelling offspring after a symmetry-breaking bifurcation.

8. Concluding remarks and future directions

Let us briefly summarise the work already presented and conclude with some possible directions for future research. In this report we have reviewed the dynamics of systems possessing time-reversal invariance. We have not restricted the discussion to conservative reversible systems, and so have been able to compare and contrast a general reversible system with a conservative system. We have concentrated in particular on reversible mappings of the plane. We have reviewed the properties of these mappings in broad terms in section 3.1 indicating that, in their full generality, reversible mappings combine the properties of conservative and dissipative mappings which were reviewed in chapter 2. We have discussed how to create reversible mappings in section 3.2 and talked about the problem of testing arbitrary mappings for reversibility in section 3.3. Some conservative nonreversible mappings were given in section 3.4.

Chapter 4 presented examples of nonconservative reversible mappings. These mappings can have attractors and repellers. We gave systematic methods for creating large classes of such mappings. We used these examples to survey some of the features of non measure-preserving, reversible mappings in chapters 5, 6 and 7. Chapter 5 has shown that if we take a non measure-preserving, reversible mapping and study phenomena associated with its symmetric periodic orbits, we find behaviour reminiscent of conservative reversible systems, which is reflected quantitatively in the critical exponents for the breakup of KAM circles and symmetric period doubling. Chapter 6 has shown that if we take the same mapping and study phenomena associated with asymmetric periodic orbits we find behaviour previously associated with dissipative systems, which is reflected quantitatively in the critical exponents for asymmetric period doubling. As remarked in section 6.2 and shown in fig. 6.4, the two different period doubling processes can occur at the same time in different parts of the plane. These results expand each of the universality classes of mappings with dissipative critical exponents and mappings with conservative exponents, at the same time showing that the two sets of exponents can be found in one and the same (reversible) mapping. Finally, chapter 7 illustrates some of the interplay between the conservative and dissipative features of reversible mappings.

The report has shown that reversible dynamical systems can qualitatively and quantitatively “bridge the gap” between the traditional “textbook” division of classical dynamical systems into conservative and dissipative systems: We conclude by listing various problems that we consider interesting for the future, some of which are already being explored:

(i) The local reversibility tests of sections 3.3 and 3.4 allow us to identify some area-preserving mappings like (3.77) that are not reversible. We have followed period doubling in such one-parameter, nonreversible, area-preserving mappings. We find the parameter sequence of successive period doublings is characterised by the exponent $\delta = 8.721 \dots$. Together with the results of chapter 5, this suggests $\delta_{AP} = \delta_{AP,R} = \delta_R = 8.721 \dots$, where the subscripts stand, respectively, for area-preserving, nonreversible mappings; area-preserving, reversible mappings; and non area-preserving, reversible mappings (symmetric period doubling in the last case). The number $\delta = 8.721 \dots$ therefore characterises a large period doubling universality class among mappings of the plane.

It would nevertheless be interesting to see if and how the lack of reversibility of area-preserving mappings like (3.77) could be detected in the geometry of the phase plane of the mapping. This may lead to an independent geometric test or criterion for identifying reversible mappings, which concentrates more on their global reversibility than on their local reversibility. As pointed out in section 3.4, the following is still an open question: is Rannou’s mapping,

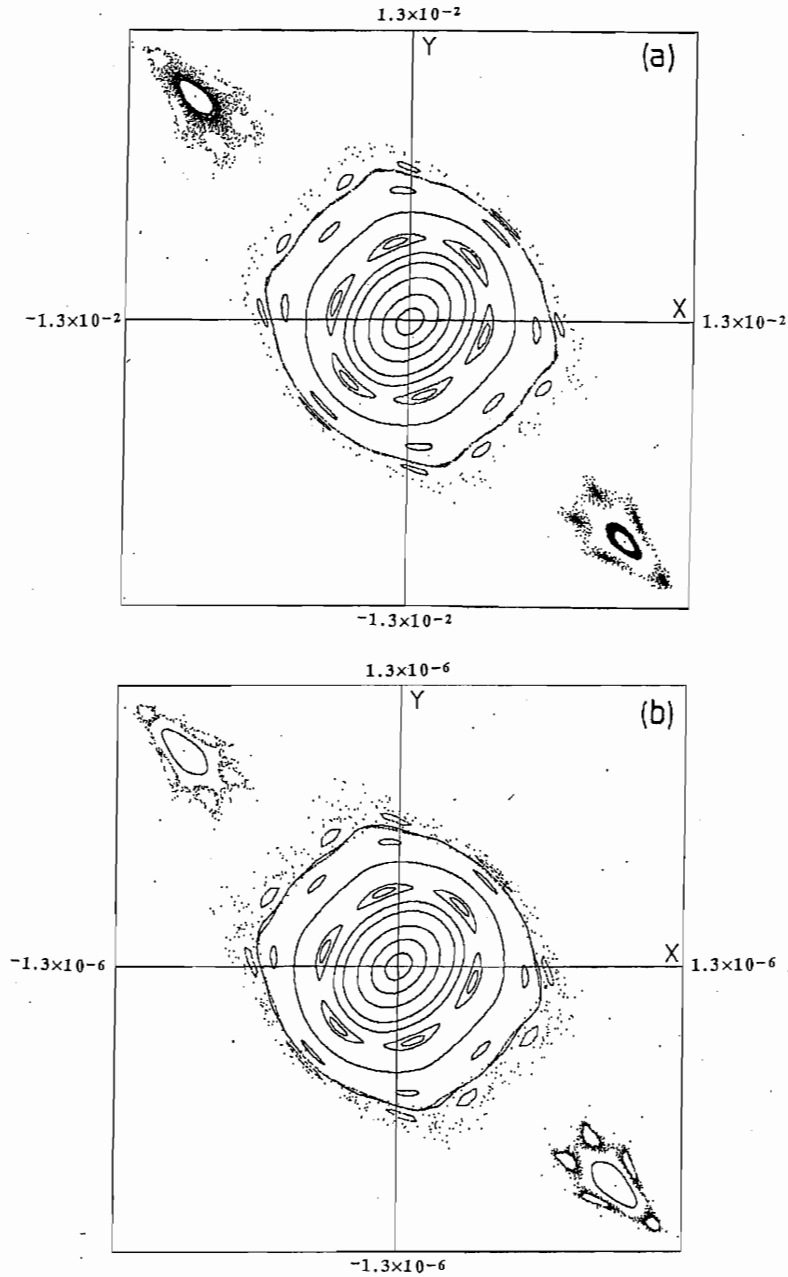


Fig. 8.1. Phase portraits of example 2 of table 4.1 with $C=0.3$ and: (a) $\varepsilon = 10^2$; (b) $\varepsilon = 10^6$. The origin is an elliptic fixed point when $C=0.3$ for all ε . The asymmetric fixed points are at $(1/\varepsilon, -1/\varepsilon)$ and $(-1/\varepsilon, 1/\varepsilon)$.

$$R: x' = x + y + 1 - \cos y, \quad y' = y - C \sin x' - C(1 - \cos x')$$

a reversible mapping of the plane?

(ii) It would be pleasing to extend the study of reversibility to higher-dimensional mappings. For

example, Feingold et al. [1988] give the following example of a three-dimensional volume-preserving mapping derived from the *ABC* flow in fluid dynamics,

$$L_{ABC}: \begin{cases} x' = x + A \sin z + C \cos y, \\ y' = y + B \sin x' + A \cos z, \\ z' = z + C \sin y' + B \cos x', \end{cases}$$

which is reversible in the case $A = B$ (see also Turner and Quispel [1992]).

(iii) Phase portraits like fig. 1.3 and figs. 4.1b or 6.2 make one wonder about the boundary in phase space between the conservative and dissipative (and expansive) regions in reversible mappings. In figs. 4.1b or 6.2 this boundary is provided by the innermost KAM curve, whereas in fig. 1.3 it is less clear where one region ends and the other begins. In fig. 8.1a, b we show an attempt to bring the attracting asymmetric fixed point $(1/\varepsilon, -1/\varepsilon)$ in example 2 close to the KAM curves around the origin by taking $\varepsilon \rightarrow \infty$ [from appendix B when $\frac{1}{6} < C < \frac{1}{2}$ and ε is positive, the fixed point $(1/\varepsilon, -1/\varepsilon)$ is an attracting fixed point and, moreover, the origin is stable]. We find that the KAM region contracts around the origin in proportion to the proximity of the attractor, producing an appealing self-similarity. It would be interesting to investigate the properties of the boundary between the two features.

(iv) In broader terms, the similarities between the dynamics in Hamiltonian systems and the dynamics associated with symmetric periodic orbits of reversible systems leads to asking if all the important "conservative" theorems and results go through to reversible systems under suitable conditions; e.g., at the level of mappings, is there a reversible Aubry–Mather theorem to mirror the area-preserving theorem (cf. Arrowsmith and Place [1990] for discussion of the area-preserving case). Some thoughts about the possible construction of a unified theory of Hamiltonian and reversible dynamical systems are given by Sevryuk [1986, p. 293], who also lists some further extensions and generalisations that could be made to the theory of reversible systems (see also conjectures and discussion in Sevryuk [1991a]). These include relaxing the analyticity assumptions in the reversible KAM theorem (Sevryuk [1991a] states that the C^∞ and finite differentiability versions are expected to hold), developing an infinite-dimensional reversible KAM theory and studying Arnol'd diffusion in reversible systems. Other possibilities include the study of reversible systems on other manifolds and topological (i.e. nondifferentiable) reversible systems. It appears that reversible partial differential equations are important for physical applications and so should also be well treated from the theoretical point of view.

Acknowledgements

This report is based upon the Ph.D. thesis of the first author at Melbourne University, Australia (cf. Roberts [1990a]). We are grateful to Colin Thompson and Hans Capel for their support and many useful suggestions. We have greatly benefitted from reading the significant contributions of Greene, MacKay and coworkers to the study of reversible, conservative systems. We thank M.B. Sevryuk for ongoing correspondence, including a useful bibliography on reversible systems compiled by him (cf. Sevryuk [1991b]). J.A.G.R. is grateful to the Stichting voor Fundamenteel Onderzoek der Materie (FOM) for financial support.

Appendix A. Integrable reversible mappings

In this appendix we give some examples from a special class of reversible mappings of the plane, namely the integrable reversible mappings. The twist mapping (5.1) is the canonical example of an integrable mapping, with integral $I = r$, the radius. By analogy, our working definition of "integrable" for a more general mapping of the plane $L: (x, y) \rightarrow (x', y')$ is that the mapping be measure-preserving (cf. section 2.2) and possess an integral $I(x, y)$ defined by

$$I(x', y') = I(x, y) \quad (\text{A.1})$$

for all (x, y) in the mapping's domain. I is evidently a constant of the (mapping's) motion. It follows that the orbits of all points in the plane lie on the level curves given by

$$I(x, y) = C, \quad (\text{A.2})$$

where C for any orbit is determined from the initial condition, i.e., $C = I(x_0, y_0)$. There are no chaotic orbits. Another way of expressing this is that the phase space of an integrable mapping (i.e., the plane) is foliated by invariant curves (A.2) [cf. (2.6) and (2.7) for the definition of an invariant curve], and that the motion on any invariant curve is regular, i.e., periodic or quasiperiodic, as in the canonical example of the integrable twist mapping given in (5.1). This working definition then mirrors the properties of an integrable Hamiltonian system with n degrees of freedom (cf. Whittaker [1927], Goldstein [1950], Percival [1986], Arnol'd [1988]), which has n independent constants of motion that are in involution, and linear motion on the n -dimensional level set defined by these constants. Commonly, the level set is equivalent to an n -torus and the motion is periodic or quasiperiodic on the torus.

One of the first people to study integrable mappings was McMillan [1971]. He introduced the mapping

$$L_1: x' = y, \quad y' = -x - \frac{\beta y^2 + \varepsilon y}{\alpha y^2 + \beta y + \gamma}, \quad (\text{A.3})$$

where α, β, γ and ε are arbitrary constants. This mapping is area-preserving and is reversible with involution $x' = y, y' = x$ (cf. table 3.1). It is also integrable because it preserves the following integral:

$$I_1(x, y) = \alpha x^2 y^2 + \beta(x^2 y + x y^2) + \gamma(x^2 + y^2) + \varepsilon x y. \quad (\text{A.4})$$

It follows that the one-parameter family of symmetric biquadratic curves $I_1(x, y) = C$, parametrised by C , foliates the phase plane of (A.3). Each curve in this family is symmetric about $y = x$ and double-valued.

A more general area-preserving and reversible integrable mapping is given by^{*}

$$L_2: x' = -x - \frac{\delta y^2 + \varepsilon y + \xi}{\alpha y^2 + \beta y + \gamma}, \quad y' = -y - \frac{\beta x'^2 + \varepsilon x' + \lambda}{\alpha x'^2 + \delta x' + \kappa}. \quad (\text{A.5})$$

^{*}This mapping can also be quantized, while retaining its integrability [Quispel and Nijhoff 1992].

The map L_2 can be written as the composition of two involutions, i.e., $L_2 = H_2 \circ G_2$ with

$$H_2: \begin{cases} x' = x, \\ y' = -y - \frac{\beta x^2 + \epsilon x + \lambda}{\alpha x^2 + \delta x + \kappa}; \end{cases} \quad G_2: \begin{cases} x' = -x - \frac{\delta y^2 + \epsilon y + \xi}{\alpha y^2 + \beta y + \gamma}, \\ y' = y. \end{cases} \quad (A.6)$$

The mapping L_2 has the following integral:

$$I_2(x, y) = \alpha x^2 y^2 + \beta x^2 y + \gamma x^2 + \delta x y^2 + \epsilon x y + \xi x + \kappa y^2 + \lambda y. \quad (A.7)$$

Each of the component involutions of L_2 also preserves the integral (A.7). The one-parameter family of biquadratic curves $I_2(x, y) = C$ that foliates the plane are now not in general symmetric about $y = x$. This is illustrated in fig. A.1 which is a phase portrait of a typical mapping of the form (A.5).

Finally, the most general integrable reversible mapping of the plane found to date is given by Quispel et al. [1988, 1989],

$$L_3: x' = \frac{f_1(y) - x f_2(y)}{f_2(y) - x f_3(y)}, \quad y' = \frac{g_1(x') - y g_2(x')}{g_2(x') - y g_3(x')}, \quad (A.8)$$

where the functions f_i and g_i are in general quartic polynomials defined by

$$f(x) = (f_1(x), f_2(x), f_3(x)) = (A_0 X) \times (A_1 X), \quad (A.9a)$$

$$g(x) = (g_1(x), g_2(x), g_3(x)) = (A_0^T X) \times (A_1^T X), \quad (A.9b)$$

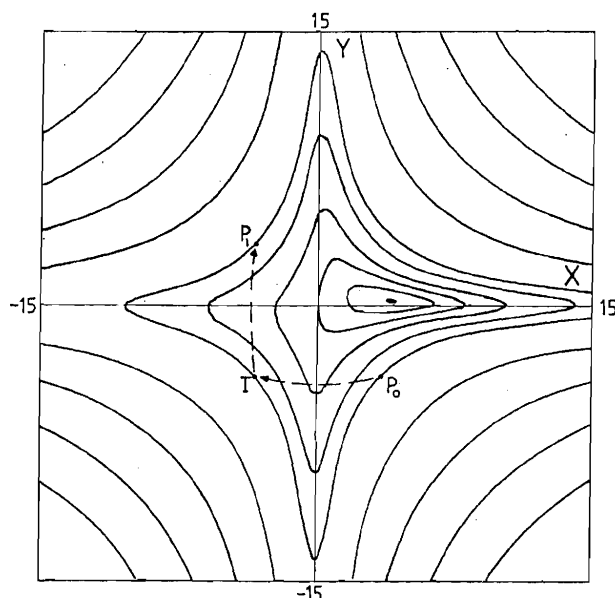


Fig. A.1. Typical invariant curves of the asymmetric integrable mapping (A.5) with $\alpha = \gamma = \kappa = 1$, $\beta = \delta = 0$, $\epsilon = -2$, $\lambda = -0.2$, $\xi = -8$. This mapping has an elliptic fixed point at about (4.01, 0.24). All of its invariant curves are closed. A representative initial point P_0 on a curve with $I = I_0$ is taken to the intermediate point T by the involution G_2 . The point T is then taken by H_2 to the point P_1 , which is the image of P_0 under the mapping (A.5) ($L_2 = H_2 \circ G_2$). For typical I_0 , successive iterates of P_0 fill out the entire curve $I = I_0$.

$$X := \begin{pmatrix} x^2 \\ x \\ 1 \end{pmatrix}, \quad Y := \begin{pmatrix} y^2 \\ y \\ 1 \end{pmatrix}, \quad (\text{A.10})$$

$$A_i := \begin{pmatrix} \alpha_i & \beta_i & \gamma_i \\ \delta_i & \varepsilon_i & \xi_i \\ \kappa_i & \lambda_i & \mu_i \end{pmatrix}, \quad (\text{A.11})$$

where $\alpha_i, \beta_i, \gamma_i, \delta_i, \varepsilon_i, \xi_i, \kappa_i, \lambda_i, \mu_i$ ($i=0,1$) are 18 arbitrary parameters. The mapping (A.8) is reversible since it can be written as the composition of two involutions, i.e., $L_3 = H_3 \circ G_3$ with

$$H_3: \begin{cases} x' = x, \\ y' = \frac{g_1(x) - yg_2(x)}{g_2(x) - yg_3(x)}; \end{cases} \quad (\text{A.12})$$

$$G_3: \begin{cases} x' = \frac{f_1(y) - xf_2(y)}{f_2(y) - xf_3(y)}, \\ y' = y. \end{cases}$$

The mapping L_3 has the following integral:

$$I_3(x, y) = \frac{\alpha_0 x^2 y^2 + \beta_0 x^2 y + \gamma_0 x^2 + \delta_0 x y^2 + \varepsilon_0 x y + \xi_0 x + \kappa_0 y^2 + \lambda_0 y + \mu_0}{\alpha_1 x^2 y^2 + \beta_1 x^2 y + \gamma_1 x^2 + \delta_1 x y^2 + \varepsilon_1 x y + \xi_1 x + \kappa_1 y^2 + \lambda_1 y + \mu_1} \\ = (X \cdot A_0 Y) / (X \cdot A_1 Y).$$

The mapping L_3 is not area-preserving, but it is measure-preserving (cf. section 2.2) with a density

$$m_3(x, y) = (\alpha_1 x^2 y^2 + \beta_1 x^2 y + \gamma_1 x^2 + \delta_1 x y^2 + \varepsilon_1 x y + \xi_1 x + \kappa_1 y^2 + \lambda_1 y + \mu_1)^{-1} \\ = (X \cdot A_1 Y)^{-1}.$$

A way of proving this measure preservation is to utilize the decomposition of L_3 as a product of involutions, remembering that any involution is measure-preserving [cf. eq. (3.6)]. Although we know that the composition of two measure-preserving mappings is not necessarily measure-preserving, we can use the fact that the involutions H_3 and G_3 also have the integral $I_3(x, y)$ to show that they share the same density, which guarantees that their composition L_3 is measure-preserving with this density as well. In this regard, it is easy to prove that if a measure-preserving mapping with density $m(x, y)$ is also integrable with invariant $I(x, y)$, then any function of $I(x, y)$ multiplied by $m(x, y)$ is another density for the mapping. Using this property, a common density for both of the component involutions of L_3 can be found [Roberts 1990a, 1992]. It should be noted above that the mapping L_2 is a special case of the mapping L_3 , and that in turn the mapping L_1 is (for all intents and purposes) a special case of L_2 .

Up to now we have not commented on the motion on the invariant biquadratic curves of these integrable mappings. On the closed biquadratics, it is in fact quasiperiodic, or else periodic with the curve comprising an infinity of adjacent n -cycles. On unbounded biquadratics, the motion typically diverges linearly to infinity. The dynamics on the biquadratics can be deduced from the fact that a biquadratic curve can be parametrised in terms of Jacobian elliptic functions [Roberts 1990a]. Very recently, measure-preserving, reversible integrable mappings of \mathbb{R}^n have been discovered (cf. Papageor-

giou et al. [1990], Quispel et al. [1991]; see also Capel et al. [1991] and references therein for other recent developments in the field of integrable mappings; also cf. Bellon et al. [1991a, b, c] for reversible mappings that possess algebraic integrals and arise from integrable statistical-mechanical models). (Note that the definition of integrability of mappings of \mathbb{R}^n is still under discussion.)

Appendix B. Nonlinear stability analysis for elliptic fixed points

In this appendix, we give a quantity that can be calculated from the expansion to third order around an elliptic fixed point and helps to decide the fixed point's stability. An example of the evaluation of this quantity is provided for example 2 of table 4.1. When a fixed point x_0 of a mapping is elliptic, it has a Jacobian determinant $J(x_0) = 1$ and the eigenvalues of the Jacobian evaluated at x_0 are $e^{\pm i\theta}$ with $\theta \neq 0, \pi$. In this case the point is linearly stable. The actual stability of the point can sometimes be determined by studying the higher order nonlinear terms of the expansion around the fixed point. Quantities involving successively higher degree coefficients of this expansion can be calculated to determine whether the point is stable or not (cf. Bernussou [1977, chapter II.4.1] and Mira [1987, chapter 5.7]). Here we give the first such quantity, denoted by G_1 , which involves coefficients of second and third degree terms of the expansion.

Assume that the mapping around the fixed point x_0 has been taken to the form

$$\begin{aligned} x' &= e^{i\theta}x + f_{20}x^2 + f_{11}xy + f_{02}y^2 + f_{30}x^3 + f_{21}x^2y + f_{12}xy^2 + f_{03}y^3 + \dots, \\ y' &= e^{-i\theta}y + f_{02}^*x^2 + f_{11}^*xy + f_{20}^*y^2 + f_{03}^*x^3 + f_{12}^*x^2y + f_{21}^*xy^2 + f_{30}^*y^3 + \dots, \end{aligned} \tag{B.1}$$

where * denotes complex-conjugate (the way to obtain this complex form of the mapping expansion from the real form is described at the end of section 2.2). Then define

$$G_1 = f_{21}^* e^{i\theta} + f_{21} e^{-i\theta} - 2f_{02}f_{02}^* - f_{11}f_{11}^* + f_{20}^*f_{11}^* \left(\frac{e^{3i\theta}}{1 - e^{i\theta}} + \frac{2e^{i\theta}}{1 - e^{-i\theta}} \right) + f_{20}f_{11} \left(\frac{2e^{-i\theta}}{1 - e^{i\theta}} + \frac{e^{-3i\theta}}{1 - e^{-i\theta}} \right). \tag{B.2}$$

This quantity is obviously real. Then provided $\theta \neq 2k\pi/3, k = 1, 2$, and $\theta \neq 2k\pi/4, k = 1, 3$, (as well as the original assumption $\theta \neq 0, \pi$) we have (cf. Mira [1987, proposition 5.7])

- (i) if $G_1 < 0$, the fixed point x_0 is spirally attracting,
- (ii) if $G_1 > 0$, the fixed point x_0 is spirally repelling,
- (iii) if $G_1 = 0$, the stability of the fixed point is undetermined.

In the last case, (iii), one may try and use other quantities $G_i, i > 1$, which involve higher degree coefficients (and so become very complicated) to determine stability in a similar way. If we write out the third order condition for the mapping expansion (B.1) to be measure-preserving (via table 2.1), which is equivalent to the third order condition that it be the expansion of a reversible mapping around a symmetric fixed point (via table 3.2), we find that the condition is equivalent to $G_1 = 0$. This is to be expected because a fixed point of a measure-preserving mapping, or a symmetric fixed point of a reversible mapping, cannot be attracting or repelling – the case $G_1 \neq 0$.

We use the quantity G_1 to investigate the stability of the fixed point $(1/\epsilon, -1/\epsilon)$ of the mapping example 2 of table 4.1,

$$x' = \frac{\mu - 2\varepsilon^2 y'^3}{1 + \varepsilon^2 y'^2}, \quad y' = -x + 2C\mu + 2\mu^2 \quad (\mu = y + \varepsilon^2 x^2 y + 2\varepsilon^2 x^3). \quad (\text{B.3})$$

This point has $J = 1$ for all C and all ε and, for any ε , is elliptic when C is in the range $\frac{1}{6} < C < \frac{1}{2}$. When it is elliptic, it is stable in the linear approximation. We have numerically studied this example when $\varepsilon = 1.1$ and found $(1/\varepsilon, -1/\varepsilon) = (0.9090\dots, -0.9090\dots)$ to be spirally attracting when it is elliptic (when $\varepsilon = 20$ we find the same behaviour, as shown in fig. 1.3).

Instead of using (B.3) in the analysis, consider the mapping obtained from it via the transformation $x \rightarrow x/\varepsilon, y \rightarrow y/\varepsilon$

$$x' = \frac{\mu - 2y'^3}{1 + y'^2}, \quad y' = -x + 2C\mu + 2\mu^2/\varepsilon \quad (\mu = y + x^2 y + 2x^3). \quad (\text{B.4})$$

In this form of the mapping, the fixed point $(1/\varepsilon, -1/\varepsilon)$ is taken to $(1, -1)$ for all ε and C . Its stability is unaffected because stability is a conjugacy-invariant. The expansion of (B.4) around the fixed point $(1, -1)$ to third order is

$$\begin{aligned} x' &= 4(1 - 4C)x + (1 - 8C)y + F_{20}x^2 + F_{11}xy + F_{02}y^2 + F_{30}x^3 + F_{21}x^2y + F_{12}xy^2 + F_{03}y^3, \\ y' &= (8C - 1)x + 4Cy + G_{20}x^2 + G_{11}xy + G_{02}y^2 + G_{30}x^3 + G_{21}x^2y + G_{12}xy^2 + G_{03}y^3, \end{aligned} \quad (\text{B.5})$$

where the second order coefficients are

$$\begin{aligned} F_{20} &= 32C^2 - 12C - 64/\varepsilon + 1, & G_{20} &= 2(5C + 16/\varepsilon), \\ F_{11} &= 4(8C^2 + C - 16/\varepsilon), & G_{11} &= 4(C + 8/\varepsilon), \\ F_{02} &= 4(2C^2 + C - 4/\varepsilon), & G_{02} &= 8/\varepsilon, \end{aligned}$$

and the third order coefficients are

$$\begin{aligned} F_{30} &= 256C^3 + 48C^2 + 18C + 256C/\varepsilon - 128/\varepsilon - 1, & G_{30} &= 4(C + 20/\varepsilon), \\ F_{21} &= 2(192C^3 + 36C^2 + 9C + 192C/\varepsilon - 40/\varepsilon), & G_{21} &= 2(C + 36/\varepsilon), \\ F_{12} &= 4(48C^3 + 10C^2 + 48C/\varepsilon + C + 2/\varepsilon), & G_{12} &= 16/\varepsilon, \\ F_{03} &= 8(4C^3 + C^2 + 4C/\varepsilon + 1/\varepsilon), & G_{03} &= 0. \end{aligned}$$

From the linear part of this expansion it is seen that $J(1, -1) = 1$ and $\text{Tr}(1, -1) = 4 - 12C$ so that $(1, -1)$ is elliptic for $-2 < 4 - 12C < 2$, which gives the range $\frac{1}{6} < C < \frac{1}{2}$ quoted above. With C in this range, apply to (B.5) the linear transformation

$$\begin{aligned} X &= (\lambda^{-1} - A)x - By, & Y &= (\lambda - A)x - By \\ A &= 4(1 - 4C), & B &= (1 - 8C), & \lambda &= e^{i\theta}: \quad \lambda^2 - (4 - 12C)\lambda + 1 = 0. \end{aligned}$$

This brings it into the complex form (B.1). Calculating G_1 we find

$$G_1 = 2[\varepsilon(2C - 1)(8C - 1)(6C - 1)^2]^{-1}. \quad (\text{B.6})$$

Since $G_1 < 0$ when $\frac{1}{6} < C < \frac{1}{2}$ and ε is positive, the fixed point $(1/\varepsilon, -1/\varepsilon)$ is an attracting fixed point in example 2.

References

- Ablowitz, M.J., J.M. Keiser and L.A. Takhtajan, 1991, Class of stable multistate time-reversible cellular automata with rich particle content, *Phys. Rev. A* 44, 6909–6912.
- Abramowitz, M. and I.A. Stegun, 1972, *Handbook of Mathematical Functions* (Dover Publ., New York).
- Andrews, B., 1989, Reversible dynamical systems, Honours Thesis, Department of Mathematics, Australian National University.
- Angenent, S.B., 1990, Monotone recurrence relations, their Birkhoff orbits and topological entropy, *Ergod. Th. Dynam. Sys.* 10, 15–41.
- Arecchi, F.T., 1987, The physics of laser chaos, *Nucl. Phys. B (Proc. Suppl.)* 2, 13–24.
- Arnol'd, V.I., 1961, The stability of the equilibrium position of a Hamiltonian system of ordinary differential equations in the general elliptic case, *Dokl. Akad. Nauk SSSR* 137, 255–257.
- Arnol'd, V.I., 1984, Reversible Systems, in: *Nonlinear and Turbulent Processes in Physics*, Vol. 3, ed. R.Z. Sagdeev (Harwood, Chur) pp. 1161–1174.
- Arnol'd, V.I., 1988, Integrable systems and integration methods, chapter 4, in: *Dynamical Systems III*, ed. V.I. Arnol'd (Springer, Berlin) pp. 107–137.
- Arnol'd, V.I. and M.B. Sevryuk, 1986, Oscillations and bifurcations in reversible systems, in: *Nonlinear Phenomena in Plasma Physics and Hydrodynamics*, ed. R.Z. Sagdeev (Mir, Moscow) pp. 31–64.
- Aronson, D.G., M.A. Chory, G.R. Hall and R.P. McGehee, 1983, Resonance phenomena for two-parameter families of maps of the plane: uniqueness and nonuniqueness of rotation numbers, in: *Nonlinear Dynamics and Turbulence*, eds G.I. Barenblatt, G. Iooss and D.D. Joseph (Pitman, Boston) pp. 35–47.
- Arrowsmith, D.K. and C.M. Place, 1990, *An Introduction to Dynamical Systems* (Cambridge Univ. Press, Cambridge).
- Aubry, S., 1983, The Twist Map, the Extended Frenkel – Kontorova Model and the Devil's Staircase, *Physica D* 7, 240–258; reprinted in MacKay and Meiss [1987, pp. 746–764].
- Baake, M. and J.A.G. Roberts, 1992, Trace maps as reversible dynamical systems, in preparation.
- Baake, M., D. Joseph and P. Kramer, 1992, Periodic clustering in the spectrum of quasiperiodic Kronig–Penney models, Preprint, Institute for Theoretical Physics, University of Tübingen.
- Baesens, C. and R.S. MacKay, 1991, Uniformly travelling water waves from a dynamical systems viewpoint: some insights into bifurcations from the Stokes family, preprint, Mathematics Institute, University of Warwick.
- Beerens, S.P., 1990, Period-doubling bifurcations in reversible mappings, Master's Thesis, Institute for Theoretical Physics, University of Amsterdam.
- Bellon, M.P., J.-M. Maillard and C.-M. Viallet, 1991a, Integrable Coxeter groups, *Phys. Lett. A* 159, 221–232.
- Bellon, M.P., J.-M. Maillard and C.-M. Viallet, 1991b, Higher dimensional mappings, *Phys. Lett. A* 159, 233–244.
- Bellon, M.P., J.-M. Maillard and C.-M. Viallet, 1991c, Rational mappings, Arborescent iterations, and the symmetries of integrability, *Phys. Rev. Lett.* 67, 1373–1376.
- Belobrov, P.I., V.V. Beloshapkin, G.M. Zaslavsky and A.G. Tretyakov, 1984, Order and Chaos in Classical Models of Spin Chains, *Sov. Phys. - JETP* 60, 180–186.
- Benedicks, M. and L. Carleson, 1989, On the Hénon attractor, in: *Proc. IXth Inter. Congress on Mathematical Physics*, eds B. Simon, A. Truman and I.M. Davies (Hilger, Bristol) pp. 498–500.
- Benedicks, M. and L. Carleson, 1991, The dynamics of the Hénon map, *Ann. Math.* 133, 73–169.
- Benettin, G., C. Cercignani, L. Galgani and A. Giorgilli, 1980a, Universal properties in conservative dynamical systems, *Lett. Nuovo Cimento* 28, 1–4.
- Benettin, G., L. Galgani and A. Giorgilli, 1980b, Further results on universal properties in conservative dynamical systems, *Lett. Nuovo Cimento* 29, 163–166.
- Bernussou, J., 1977, *Point Mapping Stability* (Pergamon, Oxford).
- Berry, M.V., 1987, Quantum chaos, *Proc. R. Soc. London A* 413, 183–198.
- Bibikov, Yu.N., 1979, Local theory of nonlinear analytic ordinary differential equations, *Lecture Notes in Mathematics*, Vol. 702 (Springer, Berlin).
- Birkhoff, G.D., 1913, Proof of Poincaré's geometric theorem, *Trans. Am. Math. Soc.* 14, 14–22; reprinted in Birkhoff [1950, Vol. 1, pp. 673–681].
- Birkhoff, G.D., 1915, The restricted problem of three bodies, *Rend. Circ. Mat. Palermo* 39, 265–334; reprinted in Birkhoff [1950, Vol. 1, pp. 682–751].

- Birkhoff, G.D., 1920, Surface transformations and their dynamical applications, *Acta Math.* 43, 1–119; reprinted in Birkhoff [1950, Vol. 2, pp. 111–229].
- Birkhoff, G.D., 1927, On the periodic motions of dynamical systems, *Acta Math.* 50, 359–379; reprinted in Birkhoff [1950, Vol. 2, pp. 333–353], and MacKay and Meiss [1987, pp. 154–174].
- Birkhoff, G.D., 1950, *Collected Mathematical Papers*, Vols. 1, 2 and 3 (Am. Math. Soc., Providence).
- Birkhoff, G.D. and J. Lifshitz, 1945, Ciertas transformaciones en la dinamica sin elementos periodicos, *Publicaciones del Instituto de Mathem.* 6, 1–14; reprinted in Birkhoff [1950, Vol. 2, pp. 718–729].
- Boltzmann, L., 1897a, Über Irreversible Strahlungsvorgänge I, *Berl. Ber.* 660–662.
- Boltzmann, L., 1897b, Über Irreversible Strahlungsvorgänge II, *Berl. Ber.* 1016–1018.
- Boltzmann, L., 1898, Über Vermeintlich Irreversible Strahlungsvorgänge II, *Berl. Ber.* S 182–187.
- Bountis, T.C., 1981, Period doubling bifurcations and universality in conservative systems, *Physica D* 3, 577–589.
- Broer, H.W. and F. Takens, 1989, Formally symmetric normal forms and genericity, *Dyn. Rep.* 2, 39–59.
- Brown, A., 1991, Conditions for local reversibility, *Physica A* 173, 267–280.
- Buck, R.C., 1978, *Advanced Calculus*, 3rd Ed. (McGraw-Hill, New York).
- Bulgac, A. and D. Kusnezov, 1990, Deterministic and time-reversal invariant description of Brownian motion, *Phys. Lett. A* 151, 122–128.
- Bullett, S., 1988, Dynamics of quadratic correspondences, *Nonlinearity* 1, 27–50.
- Bullett, S., 1991, Dynamics of the arithmetic–geometric mean, *Topology* 30, 171–190.
- Bullett, S.R., A.H. Osbaldestin and I.C. Percival, 1986, An iterated implicit complex map, *Physica D* 19, 290–300.
- Cafisch, R.E., C. Lim, J.H.C. Luke and A.S. Sagani, 1988, Periodic solutions for three sedimenting spheres, *Phys. Fluids* 31, 3175–3179.
- Capel, H.W., F.W. Nijhoff and V.G. Papageorgiou, 1991, Complete integrability of Lagrangian mappings and lattices of KdV type, *Phys. Lett. A* 155, 377–387.
- Casdagli, M., 1987, Periodic orbits for dissipative twist maps, *Ergod. Th. Dynam. Sys.* 7, 165–173.
- Casdagli, M., 1988, Rotational chaos in dissipative systems, *Physica D* 29, 365–386.
- Chenciner, A., 1983, Bifurcations de difféomorphismes de \mathbb{R}^2 au voisinage d'un point fixe elliptique, in: *Chaotic Behaviour of Deterministic Systems* (Les Houches, Session XXXVI, 1981) eds G. Iooss, R.H.G. Helleman and R. Stora (North-Holland, Amsterdam) pp. 273–348.
- Chenciner, A., 1987, Resonant elimination of a couple of invariant closed curves in the neighbourhood of a degenerate Hopf bifurcation of difféomorphisms of \mathbb{R}^2 , in: *Dynamical Systems, Lecture Notes in Economics and Mathematical Systems*, Vol. 287, eds A.B. Kurzhanski and K. Sigmund (Springer, Berlin) pp. 3–9.
- Chirikov, B.V., 1979, A universal instability of many-dimensional oscillator systems, *Phys. Rep.* 52, 263–379.
- Chirikov, B.V., 1987, Particle confinement and adiabatic invariance, *Proc. R. Soc. London A* 413, 145–156.
- Collet, P., J.-P. Eckmann and H. Koch, 1981a, Period doubling bifurcations for families of maps on \mathbb{R}^n , *J. Stat. Phys.* 25, 1–14; reprinted in Cvitanovic [1989, pp. 353–366].
- Collet, P., J.-P. Eckmann and H. Koch, 1981b, On universality for area-preserving maps of the plane, *Physica D* 3, 457–467.
- Coveney, R. and R. Highfield, 1990, *The Arrow of Time* (W.H. Allen, London).
- Cvitanovic, P., ed, 1989, *Universality in Chaos*, 2nd Ed. (Hilger, Bristol).
- Cvitanovic, P., G. Gunaratne and I. Procaccia, 1988, Topological and Metric properties of Hénon-type strange attractors, *Phys. Rev. A* 38, 1503–1520.
- Davies, P.C.W., 1974, *The Physics of Time Asymmetry* (Surrey Univ. Press, London).
- de Aguiar, M.A.M. and C.P. Malta, 1988, Isochronous and period doubling bifurcations of periodic solutions of non-integrable Hamiltonian systems with reflexion symmetries, *Physica D* 30, 413–424.
- de Aguiar, M.A.M., C.P. Malta, M. Baranger and K.T.R. Davies, 1987, Bifurcations of periodic trajectories in non-integrable Hamiltonian systems with two degrees of freedom: numerical and analytical results, *Ann. Phys. (NY)* 180, 167–205.
- Derrida, B., A. Gervois and Y. Pomeau, 1979, Universal metric properties of bifurcations of endomorphisms, *J. Phys. A* 12, 269–296.
- Devaney, R.L., 1976, Reversible difféomorphisms and flows, *Trans. Am. Math. Soc.* 218, 89–113.
- Devaney, R.L., 1977, Blue sky catastrophes in reversible and Hamiltonian systems, *Indiana Univ. Math. J.* 26, 247–263.
- Devaney, R.L., 1981, Three area preserving mappings exhibiting stochastic behavior, in: *Classical Mechanics and Dynamical Systems, Lecture Notes in Pure and Applied Mathematics*, Vol. 70, eds R.L. Devaney and Z.H. Nitecki (Marcel Dekker, New York) pp. 39–53.
- Devaney, R.L., 1984, Homoclinic bifurcation and the area-conserving Hénon mapping, *J. Differ. Equations* 51, 254–266.
- Devaney, R.L., 1986, *An Introduction to Chaotic Dynamical Systems* (Benjamin/Cummings, Menlo Park).
- Devaney, R.L., 1988, Reversibility, homoclinic points, and the Hénon map, in: *Dynamical Systems Approaches to Nonlinear Problems in Systems and Circuits*, eds F.M.A. Salam and M.L. Levi (SIAM, Philadelphia) pp. 3–14.
- De Vogelaere, R., 1958, On the structure of symmetric periodic solutions of conservative systems, with applications, in: *Contributions to the Theory of Nonlinear Oscillations*, Vol. 4, ed. S. Lefschetz (Princeton Univ. Press, Princeton) pp. 53–84.
- Dewar, R.L. and J.D. Meiss, 1992, Flux-minimizing curves for reversible area-preserving maps, Preprint, Australian National University.
- Doncel, M.G., 1987, From magnet reversal to time reversal, in: *Symmetries in Physics*, eds M.G. Doncel et al. (Universitat Autònoma de Barcelona, Barcelona) pp. 410–429.
- Eckmann, J.-P., 1981, Roads to turbulence in dissipative dynamical systems, *Rev. Mod. Phys.* 53, 643–654; reprinted in Cvitanovic [1989, pp. 94–105].

- Eckmann, J.-P. and I. Procaccia, 1991a, Onset of defect-mediated turbulence, *Phys. Rev. Lett.* 66, 891–894.
- Eckmann, J.-P. and I. Procaccia, 1991b, The generation of spatio-temporal chaos in large aspect ratio hydrodynamics, *Nonlinearity* 4, 567–581.
- Eckmann, J.-P. and D. Ruelle, 1985, Ergodic theory of chaos and strange attractors, *Rev. Mod. Phys.* 57, 617–656.
- Eckmann, J.-P., H. Koch and P. Wittwer, 1984, A computer-assisted proof of universality for area-preserving maps, *Mem. Am. Math. Soc.* 47(289), 1–122.
- Escande, D.F., 1982, Large scale stochasticity in Hamiltonian systems, *Phys. Scr.* T2/1, 126–141; reprinted in MacKay and Meiss [1987, pp. 446–461].
- Escande, D.F., 1985, Stochasticity in classical Hamiltonian systems: universal aspects, *Phys. Rep.* 121, 165–261.
- Evans, D.J., 1986, Nonequilibrium molecular dynamics, in: *Molecular-Dynamics Simulation of Statistical-Mechanical Systems*, Proc. Inter. School of Physics “Enrico Fermi”, Course 97 (Varena, 1985) eds G. Ciccotti and W.G. Hoover (North-Holland, Amsterdam) pp. 221–240.
- Feigenbaum, M.J., 1978, Quantitative universality for a class of nonlinear transformations, *J. Stat. Phys.* 19, 25–52.
- Feigenbaum, M.J., 1979, The universal metric properties of nonlinear transformations, *J. Stat. Phys.* 21, 669–705.
- Feigenbaum, M.J., 1980, Universal behavior in nonlinear systems, *Los Alamos Science* 1, 4–27; reprinted in Cvitanovic [1989, pp. 49–84].
- Feingold, M., L.P. Kadanoff and O. Piro, 1988, Passive scalars, three-dimensional volume-preserving maps, and chaos, *J. Stat. Phys.* 50, 529–565.
- Feit, S.D., 1978, Characteristic exponents and strange attractors, *Commun. Math. Phys.* 61, 249–260.
- Field, M., M. Golubitsky and I. Stewart, 1991, Bifurcations on hemispheres, *J. Nonlinear Sci.* 1, 201–223.
- Finn, J.M., 1974, Ph.D. Thesis, University of Maryland.
- Fontich, E., 1990, Transversal homoclinic points of a class of conservative diffeomorphisms, *J. Differ. Equations* 87, 1–27.
- Froeschlé, C., 1970, A numerical study of stochasticity of dynamical systems with two degrees of freedom, *Astron. Astrophys.* 9, 15–23.
- Goldstein, H., 1950, *Classical Mechanics* (Addison-Wesley, Reading).
- Golubitsky, M., M. Krupa and C. Lim, 1991, Time-reversibility and particle sedimentation, *SIAM J. Appl. Math.* 51, 49–72.
- Gonchar, V.Yu, P.N. Ostapchuk, A.V. Tur and V.V. Yanovsky, 1991, Dynamics and stochasticity in a reversible system describing interaction of point vortices with a potential wave, *Phys. Lett. A* 152, 287–292.
- Grassberger, P., H. Kantz and U. Moenig, 1989, On the symbolic dynamics of the Hénon map, *J. Phys. A* 22, 5217–5230.
- Grebogi, C. and A.N. Kaufman, 1981, Decay of statistical dependence in chaotic orbits of deterministic mappings, *Phys. Rev. A* 24, 2829–2830.
- Grebogi, C., E. Ott, S. Pelikan and J.A. Yorke, 1984, Strange attractors that are not chaotic, *Physica D* 13, 261–268.
- Greene, J.M., 1978, Unpublished notes.
- Greene, J.M., 1979, A method for determining a stochastic transition, *J. Math. Phys.* 20, 1183–1201; reprinted in MacKay and Meiss [1987, pp. 419–437].
- Greene, J.M., 1986, How a swing behaves, *Physica D* 18, 427–447.
- Greene, J.M., 1990, The status of KAM theory from a physicist’s point of view, preprint of paper presented at Chaos in Australia Conference (February 1990).
- Greene, J.M. and J.-M. Mao, 1990, Higher-order fixed points of the renormalisation operator for invariant circles, *Nonlinearity* 3, 69–78.
- Greene, J.M., R.S. MacKay, F. Vivaldi and M.J. Feigenbaum, 1981, Universal behaviour in families of area-preserving maps, *Physica D* 3, 468–486.
- Greene, J.M., R.S. MacKay and J. Stark, 1986, Boundary circles for area-preserving maps, *Physica D* 21, 267–295.
- Greene, J.M., H. Johannesson, B. Schaub and H. Suhl, 1987, Scaling anomaly at the critical transition of an incommensurate structure, *Phys. Rev. A* 36, 5858–5861.
- Guckenheimer, J. and P. Holmes, 1983, *Nonlinear Oscillations, Dynamical Systems, and Bifurcations of Vector Fields* (Springer, New York).
- Gumowski, I. and C. Mira, 1980, Recurrences and discrete dynamic systems, *Lecture Notes in Mathematics*, Vol. 809 (Springer, Berlin).
- Gunaratne, G.H. and M.J. Feigenbaum, 1985, Trajectory scaling function for bifurcations in area-preserving maps on the plane, *Physica D* 17, 295–307.
- Hawking, S.W., 1987, The direction of time, *New Sci.*, 9 July, pp. 46–49.
- Hawking, S.W., 1988, The arrow of time, in: *A Brief History of Time* (Bantam Books, New York) chapter 9.
- Heagy, J. and J.M. Yuan, 1990, Dynamics of an impulsively driven Morse oscillator, *Phys. Rev. A* 41, 571–581.
- Helleman, R.H.G., 1979, Exact results for some linear and nonlinear beam-beam effects, in: *Nonlinear Dynamics and the Beam-Beam Interaction*, A.I.P. Conf. Proc. No. 57, eds M. Month and J.C. Herrera (Am. Inst. Physics, New York) pp. 236–256.
- Helleman, R.H.G., 1980, Self-generated chaotic behaviour in nonlinear mechanics, in: *Fundamental Problems in Statistical Mechanics*, Vol. 5, ed. E.G.D. Cohen (North-Holland, Amsterdam) pp. 165–233; updated and reprinted in Cvitanovic [1989, pp. 420–488].
- Helleman, R.H.G., 1983, One mechanism for the onsets of large-scale chaos in conservative and dissipative systems, in: *Long-Time Prediction in Dynamics*, eds C.W. Horton, Jr, L.E. Reichl and V.G. Szebehely (Wiley, New York) pp. 95–126.
- Hénon, M., 1969, Numerical study of quadratic area-preserving mappings, *Q. Appl. Math.* 27, 291–312.
- Hénon, M., 1976, A two-dimensional mapping with a strange attractor, *Commun. Math. Phys.* 50, 69–77.
- Hénon, M., 1983, Numerical exploration of Hamiltonian systems, in: *Chaotic Behaviour of Deterministic Systems* (Les Houches, Session XXXVI, 1981), eds G. Iooss, R.H.G. Helleman and R. Stora (North-Holland, Amsterdam) pp. 53–170.
- Herman, M.R., 1983, Sur les courbes invariantes par les difféomorphismes de l’anneau, *Astérisque*, Vol. 1, 103–104.
- Hocking, L.M., 1964, The behaviour of clusters of spheres falling in a viscous fluid, *J. Fluid Mech.* 20, 129–139.

- Holden, A.V. and M.A. Muhamad, 1986, A graphical zoo of strange and peculiar attractors, in: *Chaos*, ed. A.V. Holden (Manchester Univ. Press, Manchester) pp. 15–35.
- Holian, B.L., W.G. Hoover and H.A. Posch, 1987, Resolution of Loschmidt's paradox: the origin of irreversible behaviour in reversible atomistic dynamics, *Phys. Rev. Lett.* 59, 10–13.
- Hoover, W.G., 1985, Canonical dynamics: equilibrium phase-space distributions, *Phys. Rev. A* 31, 1695–1697.
- Hoover, W.G., 1986, *Molecular dynamics*, Lecture Notes in Physics, Vol. 258 (Springer, Berlin).
- Hoover, W.G., 1988, Reversible mechanics and time's arrow, *Phys. Rev. A* 37, 252–257.
- Hoover, W.G., 1989, Generalization of Nosé's isothermal molecular dynamics: non-Hamiltonian dynamics for the canonical ensemble, *Phys. Rev. A* 40, 2814–2815.
- Hoover, W.G., H.A. Posch, B.L. Holian, M.J. Gillan, M. Mareschal and C. Massobrio, 1987, Dissipative irreversibility from Nosé's reversible mechanics, *Mol. Simulation* 1, 79–86.
- Hsu, C.S., 1980, A theory of index for point mapping dynamical systems, *Trans. ASME. J. Appl. Mech.* 47, 185–190.
- Hsu, C.S., 1987, *Cell-to-Cell Mapping* (Springer, New York).
- Hu, B. and J.-M. Mao, 1987, Transitions to chaos in higher dimensions, in: *Directions in Chaos*, Vol. 1, ed. Hao Bai-Lin (World Scientific, Singapore) pp. 206–271.
- Hu, B., J. Shi and S.-Y. Kim, 1991, Recurrence of Kolmogorov–Arnold–Moser tori in nonanalytic twist maps, *J. Stat. Phys.* 62, 631–649.
- Huiszoon, Jr, C., 1983, Break-up of invariant circles for a mapping with a cubic nonlinearity, Graduate research project, Center for Theoretical Physics, Twente University of Technology.
- Ichikawa, Y.H., T. Kamimura, T. Hatori and S.Y. Kim, 1989, Stochasticity and symmetry of the standard map, *Prog. Theor. Phys. Suppl. No. 98*, 1–18.
- Iooss, G. and D.D. Joseph, 1980, *Elementary Stability and Bifurcation Theory* (Springer, New York).
- Iooss, G. and J. Los, 1990, Bifurcation of spatially quasi-periodic solutions in hydrodynamic stability problems, *Nonlinearity* 3, 851–871.
- Janssen, T. and J.A. Tjon, 1983, Bifurcations of lattice structures, *J. Phys. A* 16, 673–696.
- Jellinek, J., 1988, Dynamics for nonconservative systems: ergodicity beyond the microcanonical ensemble, *J. Phys. Chem.* 92, 3163–3173.
- Jellinek, J. and R.S. Berry, 1988, Generalization of Nosé's isothermal molecular dynamics, *Phys. Rev. A* 38, 3069–3072.
- Jellinek, J. and R.S. Berry, 1989, Generalization of Nosé's isothermal molecular dynamics: necessary and sufficient conditions of dynamical simulations of statistical ensembles, *Phys. Rev. A* 40, 2816–2818.
- Johannesson, H., B. Schaub and H. Suhl, 1988, Critical exponents for an incommensurate structure with several length scales, *Phys. Rev. B* 37, 9625–9637.
- Jowett, J.M., M. Month and S. Turner, eds., 1986, *Nonlinear dynamics aspects of particle accelerators*, Lecture Notes in Physics, Vol. 247 (Springer, Berlin).
- Jung, C. and P.H. Richter, 1990, Classical chaotic scattering – periodic orbits, symmetries, multifractal invariant sets, *J. Phys. A* 23, 2847–2866.
- Kazarinoff, N.D. and J.G.G. Yan, 1991, Spatially periodic steady-state solutions of a reversible system at strong and subharmonic resonances, *Physica D* 48, 147–168.
- Keating, J., 1990, Physics and the queen of mathematics, *Physics World*, April, 46–50.
- Kent, P. and J. Elgin, 1991a, A Shilnikov-type analysis in a system with symmetry, *Phys. Lett. A* 152, 28–32.
- Kent, P. and J. Elgin, 1991b, Noose bifurcation of periodic orbits, *Nonlinearity* 4, 1045–1061.
- Ketoja, J.A. and R.S. MacKay, 1989, Fractal boundary for the existence of invariant circles for area-preserving mappings: observations and renormalisation explanation, *Physica D* 35, 318–334.
- Khanin, K.M. and Ya.G. Sinai, 1986, The renormalization group method and Kolmogorov–Arnold–Moser theory, in: *Nonlinear Phenomena in Plasma Physics and Hydrodynamics*, ed. R.Z. Sagdeev (Mir, Moscow) pp. 93–118.
- Kirchgässner, K., 1982, Wave-solutions of reversible systems and applications, *J. Differ. Equations* 45, 113–127.
- Kirchgässner, K., 1983, Homoclinic bifurcation of perturbed reversible systems, in: *Equadiff 82*, Lecture Notes in Mathematics, Vol. 1017, eds H.W. Knobloch and K. Schmitt (Springer, Berlin) pp. 328–363.
- Kohmoto, M., 1987, Electronic states of quasiperiodic systems: Fibonacci and Penrose lattices, *Int. J. Mod. Phys. B* 1, 31–49.
- Kook, H. and J.D. Meiss, 1989, Periodic orbits for reversible, symplectic mappings, *Physica D* 35, 65–86.
- Lahiri, A., 1992, Inverted period-doubling sequences in four-dimensional reversible maps and solutions to the renormalization equations, *Phys. Rev. A* 45, 757–762.
- Lahiri, A. and S.S. Ghosal, 1987, Spatial patterns in a simple reaction–diffusion system, *Phys. Lett. A* 124, 47–52.
- Lahiri, A. and S.S. Ghosal, 1988, Spatially inhomogeneous structures in a one-dimensional array of Brusselators, *J. Chem. Phys.* 88, 7459–7467.
- Lamb, J.S.W., 1992, Reversing symmetries in dynamical systems, *J. Phys. A* 25, 925–937.
- Lamb, J.S.W., J.A.G. Roberts and H.W. Capel, 1992, Conditions for local reversing symmetries in dynamical systems, in preparation.
- Laslett, L.J., 1978, Some illustrations of stochasticity, in: *Topics in Nonlinear Dynamics*, A.I.P. Conf. Proc. No. 46, ed. S. Jorna (Am. Inst. Physics, New York) pp. 221–247.
- Laslett, L.J., 1986, *Nonlinear dynamics: a personal perspective*, in: Jowett et al. [1986, pp. 520–580].
- Lauwerier, H.A., 1986, Two-dimensional iterative maps, in: *Chaos*, ed. A.V. Holden (Manchester Univ. Press, Manchester) pp. 58–95.
- Lenz, G. and F. Haake, 1990, Transitions between universality classes of random matrices, *Phys. Rev. Lett.* 65, 2325–2328.
- Lichtenberg, A.J. and M.A. Lieberman, 1983, *Regular and Stochastic Motion* (Springer, New York).
- Loschmidt, J., 1877, *Wien. Ber.* 75, 67.

- MacKay, R.S., 1982, Renormalisation in area preserving maps, PhD Thesis, Department of Astrophysical Sciences, Princeton University.
- MacKay, R.S., 1983a, Period doubling as a universal route to stochasticity, in: *Long-Time Prediction in Dynamics*, eds C.W. Horton, Jr, L.E. Reichl and V.G. Szebehely (Wiley, New York) pp. 127–134; reprinted in: Cvitanovic [1989, pp. 412–419].
- MacKay, R.S., 1983b, A renormalisation approach to invariant circles in area-preserving maps, *Physica D* 7, 283–300; reprinted in: MacKay and Meiss [1987, pp. 462–479].
- MacKay, R.S., 1984, Equivariant universality classes, *Phys. Lett. A* 106, 99–100.
- MacKay, R.S., 1986, Transition to chaos for area-preserving maps, in: Jowett et al. [1986, pp. 390–454].
- MacKay, R.S., 1987, Instability of vortex streets, *Dyn. Stab. Systems* 2, 55–71.
- MacKay, R.S., 1988, Exact results for an approximate renormalisation scheme and some predictions for the breakup of invariant tori, *Physica D* 33, 240–265.
- MacKay, R.S., 1992, Greene's residue criterion, *Nonlinearity* 5, 161–187.
- MacKay, R.S. and J.D. Meiss, eds, 1987, *Hamiltonian Dynamical Systems: A Reprint Selection* (Hilger, Bristol).
- MacKay, R.S. and J. Stark, 1991, Locally most robust circles and boundary circles for area-preserving maps, preprint, Mathematics Institute, University of Warwick.
- Malomed, B.A. and M.I. Tribelsky, 1984, Bifurcations in distributed kinetic systems with aperiodic instability, *Physica D* 14, 67–87.
- Mao, J.-M., 1988, Period doubling in six-dimensional symmetric volume-preserving maps, *J. Phys. A* 21, 3079–3091.
- Marchal, C., 1990, *The Three-Body Problem* (Elsevier, Amsterdam) chapter 11.
- Margolus, N., 1984, Physics-like models of computation, *Physica D* 10, 81–95.
- Mayer-Kress, G., ed., 1986, *Dimensions and Entropies in Chaotic Systems* (Springer, Berlin).
- McMillan, E.M., 1971, A problem in the stability of periodic systems, in: *Topics in Modern Physics. A Tribute to E.U. Condon*, eds E. Britton and H. Odabasi (Colorado Assoc. Univ. Press, Boulder) pp. 219–244.
- Meiss, J.D., 1986, Class renormalization: islands around islands, *Phys. Rev. A* 34, 2375–2383.
- Mestel, B.D. and A.H. Osbaldestin, 1989, Renormalisation in implicit complex maps, *Physica D* 39, 149–162.
- Meyer, K.R., 1970, Generic Bifurcation of Periodic Points, *Trans. Am. Math. Soc.* 149, 95–107; reprinted in: MacKay and Meiss [1987, pp. 178–190].
- Meyer, K.R., 1981, Hamiltonian systems with a discrete symmetry, *J. Differ. Equations* 41, 228–238.
- Milnor, J., 1985, On the concept of attractor, *Commun. Math. Phys.* 99, 177–195; Erratum: *Commun. Math. Phys.* 102, 517–519.
- Mira, C., 1987, *Chaotic Dynamics* (World Scientific, Singapore).
- Montaldi, J., M. Roberts and I. Stewart, 1990a, Existence of nonlinear normal modes of symmetric Hamiltonian systems, *Nonlinearity* 3, 695–730.
- Montaldi, J., M. Roberts and I. Stewart, 1990b, Stability of nonlinear normal modes of symmetric Hamiltonian systems, *Nonlinearity* 3, 731–772.
- Montgomery, D. and L. Zippin, 1955, *Topological Transformation Groups* (Wiley, New York).
- Moser, J., 1956, The analytic invariants of an area-preserving mapping near a hyperbolic fixed point, *Commun. Pure Appl. Math.* 9, 673–692.
- Moser, J., 1962, On invariant curves of area-preserving mappings of an annulus, *Nachr. Akad. Wiss. Göttingen Math. Phys. Kl.* 2, 1–20.
- Moser, J., 1965, On the volume elements on a manifold, *Trans. Am. Math. Soc.* 120, 286–294.
- Moser, J., 1967, Convergent series expansions for quasi-periodic motions, *Math. Ann.* 169, 136–176.
- Moser, J., 1968, Lectures on Hamiltonian systems, *Mem. Am. Math. Soc.* 81, 1–60; reprinted in MacKay and Meiss [1987 pp., 77–136].
- Moser, J., 1973, *Stable and Random Motions in Dynamical Systems* (Princeton Univ. Press, Princeton).
- Moser, J.K. and S.M. Webster, 1983, Normal forms for real surfaces in C^2 near complex tangents and hyperbolic surface transformations, *Acta Math.* 150, 255–296.
- Nitecki, Z., 1971, *Differentiable Dynamics: An Introduction to the Orbit Structure of Diffeomorphisms* (MIT Press, Cambridge, MA).
- Niven, I., 1956, *Irrational Numbers* (Math. Assoc. of America, Menasha).
- Nosé, S., 1984, A molecular dynamics method for simulations in the canonical ensemble, *Mol. Phys.* 52, 255–268.
- Nosé, S., 1986, An extension of the canonical ensemble molecular dynamics method, *Mol. Phys.* 57, 187–191.
- Ozorio de Almeida, A.M., 1988, *Hamiltonian Systems – Chaos and Quantization* (Cambridge Univ. Press, Cambridge).
- Ozorio de Almeida, A.M. and M.A.M. de Aguiar, 1990, Periodic librations and their effect on the quantum energy spectrum, *Physica D* 41, 391–402.
- Page, D.N., 1992, The arrow of time, preprint, Department of Physics, University of Alberta.
- Painlevé, P., 1904, *Comptes Rendus* 139, 1170–1174.
- Palmer, K.J., 1977, Linearization of reversible systems, *J. Math. Anal. Appl.* 60, 794–808.
- Papageorgiou, V.G., F.W. Nijhoff and H.W. Capel, 1990, Integrable mappings and nonlinear integrable lattice equations, *Phys. Lett. A* 147, 106–114.
- Penrose, R., 1979, Singularities and time-asymmetry, in: *General Relativity*, eds S.W. Hawking and W. Israel (Cambridge Univ. Press, Cambridge) pp. 581–638.
- Penrose, R., 1989, *The Emperor's New Mind* (Oxford Univ. Press, Oxford).
- Percival, I.C., 1979, Variational principles for invariant tori and cantori, in: *Nonlinear Dynamics and the Beam-Beam Interaction*, A.I.P. Conf. Proc. No. 57, eds M. Month and J.C. Herrera (Am. Inst. Physics, New York) pp. 302–310; reprinted in MacKay and Meiss [1987, pp. 367–375].
- Percival, I.C., 1986, Integrable and nonintegrable Hamiltonian systems, in: Jowett et al. [1986, pp. 12–36].
- Piña, E. and E. Cantoral, 1989, Symmetries of the quasi-crystal mapping, *Phys. Lett. A* 135 190–196.
- Piña, E. and L. Jiménez Lara, 1987, On the symmetry lines of the standard mapping, *Physica D* 26, 369–378.

- Pinnow, K.M., 1986, Reversible Strömungen, Master's Thesis, ETH Zurich.
- Poincaré, H., 1912, Sur un théorème de géométrie, *Rend. Circ. Mat. Palermo* 33, 375–407.
- Politi, A., G.L. Oppo and R. Badii, 1985, Conservative-like behaviour and attractors in reversible dynamical systems, in: *Advances in Nonlinear Dynamics and Stochastic Processes*, eds R. Livi and A. Politi (World Scientific, Singapore) pp. 109–118.
- Politi, A., G.L. Oppo and R. Badii, 1986a, Coexistence of attracting and conservative features in reversible dynamical systems, in: *Stochastic Processes in Classical and Quantum Systems, Lecture Notes in Physics*, Vol. 262, eds S. Albeverio, G. Casati and D. Merlini (Springer, Berlin) pp. 486–490.
- Politi, A., G.L. Oppo and R. Badii, 1986b, Coexistence of Conservative and Dissipative Behaviour in Reversible Dynamical Systems, *Phys. Rev. A* 33, 4055–4060.
- Pomeau, Y., 1984, Invariant in cellular automata, *J. Phys. A* 17, L415–L418.
- Post, T., H.W. Capel, G.R.W. Quispel and J.P. van der Weele, 1990a, Bifurcations in two-dimensional reversible maps, *Physica A* 164, 625–662.
- Post, T., H.W. Capel, S.P. Beerens and J.A.G. Roberts, 1990b, Period doublings in two-dimensional reversible maps, preprint ITFA 90-12 (University of Amsterdam); in: *Proc. Seminar on Nonlinear Dynamics* (Twente, The Netherlands, March 1990).
- Quispel, G.R.W., 1985, Analytical crossover results for the Feigenbaum constants: crossover from conservative to dissipative systems, *Phys. Rev. A* 31, 3924–3928.
- Quispel, G.R.W., 1988, Order and chaos in conservative and in reversible systems, in: *Lecture Notes, The Townsville Winter School on Theoretical Physics*.
- Quispel, G.R.W., 1992a, Chaos and time reversal symmetry: an introduction, in: *Nonlinear Dynamics and Chaos, Proc. Fourth Physics Summer School* (Canberra, 1991), eds R.L. Dewar and B.I. Henry (World Scientific, Singapore) pp. 135–151.
- Quispel, G.R.W., 1992b, Reversible integration, in preparation.
- Quispel, G.R.W. and H.W. Capel, 1989, Local reversibility in dynamical systems, *Phys. Lett. A* 142, 112–116.
- Quispel, G.R.W. and F.W. Nijhoff, 1992, Integrable two-dimensional quantum mappings, *Phys. Lett. A* 161, 419–422.
- Quispel, G.R.W. and J.A.G. Roberts, 1988, Reversible mappings of the plane, *Phys. Lett. A* 132, 161–163.
- Quispel, G.R.W. and J.A.G. Roberts, 1989, Conservative and dissipative behaviour in reversible dynamical systems, *Phys. Lett. A* 135, 337–342.
- Quispel, G.R.W., J.A.G. Roberts and C.J. Thompson, 1988, Integrable mappings and soliton equations, *Phys. Lett. A* 126, 419–421.
- Quispel, G.R.W., J.A.G. Roberts and C.J. Thompson, 1989, Integrable mappings and soliton equations II, *Physica D* 34, 183–192.
- Quispel, G.R.W., H.W. Capel, V.G. Papageorgiou and F.W. Nijhoff, 1991, Integrable mappings derived from soliton equations, *Physica A* 173, 243–266.
- Rannou, F., 1974, Numerical study of discrete plane area-preserving mappings, *Astron. Astrophys.* 31, 289–301.
- Renardy, M., 1982, Bifurcation of singular solutions in reversible systems and applications to reaction–diffusion equations, *Adv. Appl. Math.* 3, 384–406.
- Richter, P.H., H.-J. Scholz and A. Wittek, 1990, A breathing chaos, *Nonlinearity* 3, 45–67.
- Rimmer, R.J., 1978, Symmetry and bifurcation of fixed points of area preserving maps, *J. Differ. Equations* 29, 329–344.
- Rimmer, R.J., 1983, Generic bifurcations for involutory area preserving maps, *Mem. Am. Math. Soc.* 41 (272), 1–165.
- Roberts, J.A.G., 1990a, Order and chaos in reversible dynamical systems, PhD Thesis (Mathematics Department, University of Melbourne) [abstract in: *Bull. Aust. Math. Soc.* 42 (1990) 527–528].
- Roberts, J.A.G., 1990b, Conservative and dissipative behaviour can coexist in reversible dynamical systems, *Aust. Math. Soc. Gaz.* 17, 5–9.
- Roberts, J.A.G., 1992, Measure preservation for a class of integrable reversible mappings, in preparation.
- Roberts, J.A.G. and H.W. Capel, 1992a, Area preserving mappings that are not reversible, *Phys. Lett. A* 162, 243–248.
- Roberts, J.A.G. and H.W. Capel, 1992b, Analytical investigation of reversibility in area preserving mappings, in preparation.
- Roberts, J.A.G. and C.J. Thompson, 1988, Dynamics of the classical Heisenberg spin chain, *J. Phys. A* 21, 1769–1780.
- Roberts, J.A.G., T. Post, H.W. Capel and G.R.W. Quispel, 1991, Conservative versus reversible dynamical systems, in: *Solitons and Chaos*, eds I. Antoniou and F.J. Lambert (Springer, Berlin) pp. 218–226.
- Robnik, M. and M.V. Berry, 1985, Classical billiards in magnetic fields, *J. Phys. A* 18, 1361–1378.
- Robnik, M. and M.V. Berry, 1986, False time-reversal violation and energy level statistics: the role of anti-unitary symmetry, *J. Phys. A* 19, 669–682.
- Rom-Kedar, V. and S. Wiggins, 1990, Transport in two-dimensional maps, *Arch. Ration. Mech. Anal.* 109, 239–298.
- Roy, T.K. and A. Lahiri, 1991, Reversible Hopf bifurcation in four-dimensional maps, *Phys. Rev. A* 44, 4937–4944.
- Ruelle, D., 1981, Small random perturbations of dynamical systems and the definition of attractors, *Commun. Math. Phys.* 82, 137.
- Ruelle, D., 1989, *Elements of Differentiable Dynamics and Bifurcation Theory* (Academic Press, Boston).
- Sachs, R.G., 1987, *The Physics of Time Reversal* (Univ. of Chicago Press, Chicago).
- Scheurle, J., 1987, Bifurcation of quasi-periodic solutions from equilibrium points of reversible dynamical systems, *Arch. Ration. Mech. Anal.* 97, 103–139.
- Schmidt, G., 1988, Universality of dissipative systems, in: *Directions in Chaos*, Vol. 2, ed. Hao Bai-Lin (World Scientific, Singapore) pp. 1–15.
- Schmidt, G. and J. Bialek, 1982, Fractal diagrams for Hamiltonian stochasticity, *Physica D* 5, 397–404; reprinted in MacKay and Meiss [1987, pp. 438–461].
- Schmidt, G. and B. Wang, 1983, Alternate routes to chaos in Hamiltonian systems, preprint, Stevens Institute of Technology (Hoboken, N.J.).
- Series, C., 1985, The geometry of Markoff numbers, *Math. Intelligencer* 7, 20–29.
- Sevryuk, M.B., 1986, Reversible systems, *Lecture Notes in Mathematics*, Vol. 1211 (Springer, Berlin).

- Sevryuk, M.B., 1987, On invariant tori of reversible systems in the neighbourhood of an equilibrium position, *Russ. Math. Surv.* 42, 147–148.
- Sevryuk, M.B., 1989, Stationary and nonstationary stability of periodic solutions of reversible systems, *Funct. Anal. Appl.* 23, 116–123.
- Sevryuk, M.B., 1990, Invariant m -tori of reversible systems whose phase space dimension is greater than $2m$, *J. Sov. Math.* 51, 2374–2386.
- Sevryuk, M.B., 1991a, Lower-dimensional tori in reversible systems, *Chaos* 1, 160–167.
- Sevryuk, M.B., 1991b, References on reversible dynamical systems, preprint, Institute of Energy Problems of Chemical Physics, The USSR Academy of Sciences.
- Sevryuk, M.B., 1992, Private communication.
- Sevryuk, M.B. and A. Lahiri, 1991, Bifurcations of families of invariant curves in four-dimensional reversible mappings, *Phys. Lett. A* 154, 104–110.
- Shenker, S.J. and L.P. Kadanoff, 1982, Critical behaviour of a KAM surface: I. empirical results, *J. Stat. Phys.* 27, 631–656.
- Short, T. and J.A. Yorke, 1984, Truncated development and chaotic attractors in a map when the Jacobian is not small, in: *Chaos and Statistical Methods*, ed. Y. Kuramoto (Springer, Berlin) pp. 23–30.
- Siegel, C.L. and J.K. Moser, 1971, *Lectures on Celestial Mechanics* (Springer, Berlin).
- Simó, C., 1979, On the Hénon–Pomeau attractor, *J. Stat. Phys.* 21, 465–494.
- Simó, C., 1980, Invariant curves near parabolic points and regions of stability, in: *Lecture Notes in Mathematics*, Vol. 819 (Springer, Berlin) pp. 418–424.
- Takesue, S., 1987, Reversible cellular automata and statistical mechanics, *Phys. Rev. Lett.* 59, 2499–2502.
- Takesue, S., 1989, Ergodic properties and thermodynamic behavior of elementary reversible cellular automata I, *J. Stat. Phys.* 56, 371–402.
- Takesue, S., 1990a, Fourier's law and the Green–Kubo formula in a cellular-automaton model, *Phys. Rev. Lett.* 64, 252–255.
- Takesue, S., 1990b, Relaxation properties of elementary reversible cellular automata, *Physica D* 45, 278–284.
- Tanikawa, K. and Y. Yamaguchi, 1987, Coexistence of periodic points in reversible dynamical systems on a surface, *J. Math. Phys.* 28, 921–928.
- Tanikawa, K. and Y. Yamaguchi, 1989, Coexistence of symmetric periodic points in the standard map, *J. Math. Phys.* 30, 608–616.
- Taylor, J.B., 1969, Culham Progress Report CLM-PR-12.
- Teixeira, M.A., 1981, Local simultaneous structural stability of certain diffeomorphisms, in: *Dynamical Systems and Turbulence (Warwick 1980)* *Lecture Notes in Mathematics*, Vol. 898, eds D.A. Rand and L.S. Young (Springer, Berlin) pp. 382–390.
- Teixeira, M.A., 1990, Stability conditions for discontinuous vector fields, *J. Differ. Equations* 88, 15–29.
- Thom, R., 1980, Reversibility versus irreversibility in the physical universe, in: *Dynamical Systems and Microphysics*, eds A. Blaquiere, F. Fer and A. Marzollo (Springer, New York) pp. 155–165.
- Thom, R., 1990, On the reversibility (or irreversibility) of time, in: *Proc. Workshop on Dynamical Systems*, eds Z. Coelho and E. Shiels (Longman, Harlow) pp. 59–66.
- Toffoli, T. and N.H. Margolus, 1990, Invertible cellular automata: a review, *Physica D* 45, 229–253.
- Tsang, K.Y., R.E. Mirollo, S.H. Strogatz and K. Wiesenfeld, 1991a, Dynamics of a globally coupled oscillator array, *Physica D* 48, 102–112.
- Tsang, K.Y., S.H. Strogatz and K. Wiesenfeld, 1991b, Reversibility and noise sensitivity of Josephson arrays, *Phys. Rev. Lett.* 66, 1094–1097.
- Turing, A.M., 1952, The chemical basis of morphogenesis, *Philos. Trans. R. Soc. London B* 237, 37–72.
- Turner, G.S. and G.R.W. Quispel, 1992, Reversibility and the ABC -map, in preparation.
- Vanderbauwhede, A., 1986, Bifurcation of subharmonic solutions in time-reversible systems, *J. Appl. Math. Phys. (ZAMP)* 37, 455–478.
- Vanderbauwhede, A., 1990, Subharmonic branching in reversible systems, *SIAM J. Math. Anal.* 21, 954–979.
- Vanderbauwhede, A., 1992, Branching of periodic solutions in time reversible systems, *Geometry and Analysis in Nonlinear Dynamics*, *Research Notes in Mathematics* (Longman Pitman, Boston), to appear.
- Van der Schaft, A.J., 1983, Symmetries, conservation laws, and time reversibility for Hamiltonian systems with external forces, *J. Math. Phys.* 24, 2095–2101.
- Van der Weele, J.P., H.W. Capel and Ch.J. Calkoen, 1985, Crossover from dissipative to conservative systems, *Phys. Lett. A* 111, 5–9.
- Van der Weele, J.P., H.W. Capel, T. Post and Ch.J. Calkoen, 1986, Crossover from dissipative to conservative behaviour in period-doubling systems, *Physica A* 137 1–43.
- Van Saarloos, W. and P.C. Hohenberg, 1991, Fronts, pulses, sources and sinks in generalized complex Ginzburg–Landau equations, preprint, AT & T Bell Laboratories, Murray Hill.
- Vichniac, G.Y., 1984, Simulating physics with cellular automata, *Physica D* 10, 96–116.
- Whittaker, E.T., 1927, *A Treatise on the Analytical Dynamics of Particles and Rigid Bodies*, 3rd Ed. (Cambridge Univ. Press, London).
- Widom, M. and L.P. Kadanoff, 1982, Renormalization group analysis of bifurcations in area-preserving maps, *Physica D* 5, 287–292.
- Wigner, E.P., 1959, Time inversion, in: *Group Theory* (Academic Press, New York) chapter 26.
- Wilbrink, J., 1990, New fixed point of the renormalisation operator associated with the recurrence of invariant circles in generic Hamiltonian maps, *Nonlinearity* 3, 567–584.
- Young, L.S., 1983, Entropy, Lyapunov exponents, and Hausdorff dimension in differentiable dynamical systems, *IEEE Trans. Circuits Syst. CAS-30*, 599–607.
- Zisook, A.B., 1981, Universal effects of dissipation in two-dimensional mappings, *Phys. Rev. A* 24, 1640–1642; reprinted in Cvitanovic [1989, pp. 350–352].
- Zocher, H. and C. Török, 1953, About space–time asymmetry in the realm of classical general and crystal physics, *Proc. Natl. Acad. Sci. USA* 39, 681–686.